

*“-so, verily, with every difficulty, there is relief.*

*verily, with every difficulty there is relief-”*

[Q94:5-6]

**University of Alberta**

Development of Microreactors and Analytical Methods for Lipid  
Transformations

by

Tuan Nurul Sabiqah Tuan Anuar

A thesis submitted to the Faculty of Graduate Studies and Research  
in partial fulfillment of the requirements for the degree of

Doctor of Philosophy

in

Food Science and Technology

Department of Agricultural, Food and Nutritional Science

© Tuan Nurul Sabiqah Binti Tuan Anuar  
Fall 2013  
Edmonton, Alberta

Permission is hereby granted to the University of Alberta Libraries to reproduce single copies of this thesis and to lend or sell such copies for private, scholarly or scientific research purposes only. Where the thesis is converted to, or otherwise made available in digital form, the University of Alberta will advise potential users of the thesis of these terms.

The author reserves all other publication and other rights in association with the copyright in the thesis and, except as herein before provided, neither the thesis nor any substantial portion thereof may be printed or otherwise reproduced in any material form whatsoever without the author's prior written permission.

## **Dedication**

Bismillahirrahmanirrahim, all praise to the God, the Most Gracious, and the Most Compassionate. I would like to dedicate this special journey to my family, supervisors, friends and loved ones. To Ku and Mama, this is for you.

## Abstract

This thesis describes the development of two types of flow-through microreactors containing lipase immobilized onto either a hollow channel support within an optical microstructured fiber capillary (MSF) or onto a silica monolith within a fused silica capillary (SM). The large silica surface area within MSF or SM is suitable for enzyme immobilization. The enzymatic microreactors were used for rapid lipid transformations in small amounts suitable for analytical purposes.

For the SM, the porous monolithic structure was formed based on the sol-gel method involving the reaction of poly(ethylene-glycol) with tetraethyl-orthosilicate at low pH and 40 °C followed by calcination at 200 °C. *Candida antarctica* lipase was immobilized onto both SM and MSF via silanization chemistry using glutaraldehyde-linkages. Successful enzyme immobilization was demonstrated by the FTIR spectra at each step of the immobilization process.

The microreactors were tested by performing analytical scale transformations of triacylglycerols by reaction with ethanol. The effects of reaction temperature, flow rate and type of alcohol on the formation of lipid products were investigated. The data from GC and HPLC analyses indicate that the enzymatic MSF-microreactor was regioselective at 50 °C, producing mainly 2-monooleoylglycerol from the transesterification reaction of trioleoylglycerol, at a flow rate of 1  $\mu\text{L}/\text{min}$ . Using the SM-microreactor at room temperature, trioleoylglycerol and various vegetable oils (canola, sesame, soybean and refined-bleached-deodorized-palm) were quantitatively transformed into ethyl

esters using flow rates of 0.2-0.5  $\mu\text{L}/\text{min}$ . The microreactors were demonstrated to be reusable with minimal loss of activity for >8 runs when operated at room temperature and low flow rates (<1  $\mu\text{L}/\text{min}$ ). The potential use of the SM-microreactor in automated derivatization for the GC analysis of lipids was described. The SM-microreactor was also used to perform online lipid transformations by coupling it with atmospheric-pressure photoionization-mass spectrometry.

An LC/MS method was developed for in-process monitoring of the epoxidation reactions of triacylglycerols. Reaction intermediates were observed allowing the determination of the time required for full or partial epoxidation of the oil.

Overall, this thesis demonstrates a simple approach to the fabrication of enzymatic microreactors for analytical scale oleochemical transformations. Additionally, suitable methods for analyzing lipid transformations were developed.

## **Acknowledgements**

The PhD thesis may never have seen the light without the help of many generous people....

To both of my supervisors, advisors, professors and guiders: Profs. Dr. Jonathan M. Curtis and Dr. Samuel M. Mugo, I cannot thank you both enough. I am grateful for your endless patience and effort in teaching and guiding me all this while; this was a great experience in my life - as a researcher and as a person too. Thank you so much for helping me in revising and editing this thesis, and helping me to go through this journey of finding knowledge.

I would like to thank my Ph.D supervisory committee members: Profs. Dr. Feral Temelli and Dr. David Bressler for their valuable advice and great help throughout my Ph.D years.

I am thankful for research support from Dr. Jonathan Curtis' NSERC Discovery Grant, as well as to the AFNS Department and University of Alberta for giving me this opportunity to learn and gain so much knowledge in this journey. I am grateful to the generous support from Malaysian-MOHE(KPT)/UMT for the award and sponsorship throughout the study, and this thanks goes to all Malaysian taxpayers too. I would also like to thank FGSR for giving me J Gordin Kaplan Graduate Student Award.

To the people in the Lipid Chemistry Group: Dr. Zhao, Dr. Kong, Mr. Kharraz and Dr. Omanov, I am grateful for the great help and assistance in the lab. I am thankful to Carla Villages, Dr. Zhao and Mr. Kharraz for helping me with 2D-GC MS, and GC analyses and discussions. My lovely lab-mates Carla, Brenna, Angela, Metz, Yiran, Lisa, Houssin: thank you so much for creating friendly and enjoyable environment for the lab and good coffee breaks for this 4 and half years. I am also thankful to Ms. Julia Ewaschik for helping me in editing part of the thesis, and to both Mr Geoge Braybrook and Mr. Kupsta from Earth and Atmospheric Sciences Department for assisting me in SEM analysis.

My heartiest and deepest thanks to my parents, my siblings (Azrul, Azwani, Shahida, Aniq, Fathiah, Fasahah, Amir, Amirah) and my big happy family for always supporting me, whenever I needed, and for always loving me.

To my housemates Amirah and Amir, as well as Wan, Fuza, and Izyan, thank you so much, I will never forget this amazing 5 years together. I am thankful to my bestfriends Drs. Azrilawani Ahmad and Alyza Azmi for always listening to me. To my “new family” in Edmonton- Kak Siti, Kak Seri, KakSakinah, “adik-adik” and others, I will be always grateful for our meeting. To all people who are not mentioned here, remember that I will never forget all of you.

And last but not least, To You - for always being there.

THANKING YOU,

SABIQAH

## Table of Contents

<b>CHAPTER 1</b> .....	<b>1</b>
<b>Thesis Introduction</b> .....	<b>1</b>
1.1 Lipid Transformation: General Remarks .....	1
1.2 Microreaction Technology for Lipid Transformations .....	3
1.2.1 General Considerations .....	3
1.2.2 Fabrication and Characterization of the Microreactor .....	5
1.2.3 Enzyme Selection for Use in Microreaction Technology for Lipid Transformations .....	9
1.2.4 Application .....	13
1.3 Analysis of Lipid Transformations .....	14
1.3.1 Liquid Chromatography .....	14
1.3.2 Gas Chromatography .....	19
1.4 Hypothesis and Objectives .....	21
1.5 References .....	22
<b>CHAPTER 2</b> .....	<b>34</b>
<b>The Development of a Microreactor Using Commercial Silica Microstructured Optical Fiber as a Platform for Enzyme Immobilization for Use in Lipid Transformation</b> .....	<b>34</b>
2.1 Introduction .....	34
2.2 Experimental Procedures .....	37
2.2.1 Materials .....	37
2.2.2 MSF Activation .....	38
2.2.3 Lipase Immobilization onto MSF Capillary Support .....	39
2.2.4 Immobilized Lipase Assay .....	40



2.2.5	Lipase Activity Assay .....	40
2.2.6	Specific Activity of Immobilized Lipase .....	41
2.2.7	Lipid Sample Preparation and Transformation .....	42
2.2.8	Instrumentations .....	43
2.2.8.1	NARP-LC/ELSD .....	45
2.2.8.2	GC x GC .....	45
2.2.8.3	Regiospecificity Determination using Normal Phase-LC/ELSD .....	46
2.2.8.4	MSF Morphology Image by Scanning Electron Microscope .....	47
2.3	Results and Discussion .....	47
2.3.1	Lipase-immobilized Microreactor Fabrication .....	47
2.3.2	Enzyme Activity Assay .....	50
2.3.3	Enzymatic-catalyzed Ethanolysis using MSF Microreactor .....	52
2.4	Conclusion .....	62
2.5	References .....	62
<b>CHAPTER 3 .....</b>		<b>66</b>
<b>The Development of a Microreactor Using Silica Monolith Formed within a Fused Silica Capillary as a Platform for Enzyme Immobilization for Use in Lipid Transformation .....</b>		<b>66</b>
3.1	Introduction .....	66
3.2	Experimental Procedures .....	69
3.2.1	Materials .....	69
3.2.2	Preparation of Silica Monolith Capillary .....	70
3.2.3	Lipase Immobilization onto the Monolithic Silica Support .....	71

3.2.4	Evaluation of the Lipase-immobilized Microreactor .....	72
3.2.4.1	Characterization of Microreactor .....	72
3.2.4.2	Immobilized Lipase Assay .....	73
3.2.4.3	Lipase Activity Assay .....	73
3.2.5	Lipid Transformation using the Microreactor .....	74
3.2.6	Reversed Phased Liquid Chromatography / Evaporative Light Scattering Detection (HPLC/ELSD) .....	75
3.2.7	Gas Chromatography / Mass Spectrometry (GC/MS) .....	76
4.2.8	Mass Spectrometry (MS) .....	77
3.3	Results and Discussion .....	77
3.3.1	Characterization of the Microreactor .....	77
3.3.2	Evaluation of the Lipase Activity within the Microreactor .....	83
3.3.3	Formation of Fatty Acid Ethyl Ester using Lipase Immobilized Microreactor .....	87
3.3.4	Direct coupling of the Microreactor to a Mass Spectrometer .....	93
3.4	Conclusion .....	98
3.5	References .....	98
<b>CHAPTER 4 .....</b>		<b>104</b>
<b>A Feasibility Study on the Use of a Laboratory Prepared Bio-Catalyst Microreactor to Derivatize Lipids for Analytical Applications .....</b>		<b>104</b>
4.1	Introduction .....	104
4.2	Experimental Procedures .....	107
4.2.1	Materials .....	107
4.2.2	Fabrication of SM and MSF Microreactors .....	108
4.2.3	Direct Ethylation using the Microreactors .....	110

4.2.4	Batch Ethylation using Commercialized Lipase Beads .....	110
4.2.5	Acid-catalyzed ethylation using H <sub>2</sub> SO <sub>4</sub> .....	111
4.2.6	Reusability of Microreactor for Selected Alcohols .....	111
4.2.7	Instrumentation .....	112
4.2.7.1	GC/MS-NCI .....	112
4.2.7.2	GC/FID .....	112
4.2.7.3	NARP-HPLC/ELSD .....	113
4.3	Results and Discussion .....	114
4.3.1	A Comparison of Procedures for the Ethanolysis of Vegetable Oils .....	114
4.3.2	The Methanolysis of Triolein using SM Microreactor .....	125
4.4	Conclusion .....	128
4.5	References .....	129
<b>CHAPTER 5 .....</b>		<b>134</b>
<b>The Development of an Analytical Method to Characterize the Transformation of Unsaturated Oils into Epoxidised Oil .....</b>		<b>134</b>
5.1	Introduction .....	134
5.2	Experimental Procedures .....	138
5.2.1	Materials .....	138
5.2.2	Epoxidation of Canola Oil .....	138
5.2.3	NARP-LC/MS .....	139
5.2.4	Flow-injection Analysis .....	140
5.3	Results and Discussion .....	140
5.3.1	Monitoring the Epoxidation of Canola Oil by NARP-LC/MS .....	140

5.3.2 Flow-injection Analysis .....	152
5.4 Conclusion .....	156
5.5 References .....	157
<b>CHAPTER 6 .....</b>	<b>160</b>
<b>General Discussion and Conclusion .....</b>	<b>160</b>
<b>PERMISSION FROM PUBLISHER .....</b>	<b>167</b>
<b>APPENDIX .....</b>	<b>179</b>

## List of Tables

<b>Tables</b>		<b>Page No</b>
TABLE 1-1	The role of solvents in lipid transformation in enzymatic reaction media	12
TABLE 2-1	Determination of the amount of lipase immobilized onto the MSF capillary	50
TABLE 2-2	Lipid products formed from canola oil using the lipase immobilized MSF microreactor at various temperatures using a reaction flow rate of 1 $\mu\text{L}/\text{min}$	54
TABLE 3-1	IR bands characteristic of the silica monolith formation and lipase immobilization processes: (a) free lipase from <i>C. antarctica</i> ; (b) silica monolith (SM); (c) SM + APTES; (d) SM + APTES + glutaraldehyde; (e) SM + APTES + glutaraldehyde + lipase	84-85
TABLE 4-1	The major FAEE observed following the transesterification of 4 edible oils and catalyzed by lipase immobilized within SM or MSF microreactors or on commercial enzyme beads or catalyzed by strong acid. The results are expressed as uncorrected GC/FID peak area percentages	115
TABLE 4-2	GC/FID area percentages for FAEE formed by esterification of sesame seed oil using a single SM microreactor for 5 runs. For each run, performed on a separate day, products were collected for 5 h at a flow rate of 0.3 $\mu\text{L}/\text{min}$	124
TABLE 5-1	Exact mass measurements and elemental compositions of the $[\text{M} + \text{NH}_4]^+$ ions taken from the NARP-LC/MS data shown in Figure 2-3 showing the course of a canola epoxidation process.	146

## List of Figures

Figures		Page No
FIG 1-1	Overall thesis construction	2
FIG 1-2	Transesterification reaction of TAG	3
FIG 2-1	Apparatus used with the fabricated MSF microreactor for small scale lipid reactions	42
FIG 2-2	Schematic diagram of GC x GC/FID used for analysis of lipid transformation products	45
FIG 2-3	Scanning Electron Microscope (SEM) image of a Lipase-Immobilized MSF (168 holes) at x300 magnification	48
FIG 2-4	The process of lipase-immobilization onto the silica support of a MSF	49
FIG 2-5	NARP-LC/ELSD separation of (a) a lipid standard mixture containing <i>MO</i> monooleoylglycerol; <i>ME</i> methyl oleate; <i>EE</i> ethyl oleate; <i>DO</i> dioleoylglycerol; <i>TO</i> trioleoylglycerol, (b) canola oil/ethanol (the starting reactant mixture for the MSF microreactor), and c-e the effect of reaction flow rate for a canola oil solution in ethanol passing through the lipase immobilized MSF microreactor at: (c) 1 $\mu\text{L}/\text{min}$ ; (d) 5 $\mu\text{L}/\text{min}$ ; and, (e) 10 $\mu\text{L}/\text{min}$ . All c-e reactions were carried out at 50 $^{\circ}\text{C}$ . The ellipse shows the MSF column carry-over around the TAG peak that could not be resolved	55
FIG 2-6	Chromatograms of a 1-monooleoylglycerol standard and the MAG product of passing canola oil through the microreactor	58
FIG 2-7	GC x GC/FID chromatograms of products from ethanolysis of canola oil using the MSF microreactor. The microreactor bleed ("carry-over") separates from the identified <i>circled</i> lipid products	61

FIG 3-1	Schematic diagram for small scale lipid reaction using fabricated biocatalyst microreactor: (a) offline reaction (b) online coupled with the mass spectrometry system; (c)-(e) SEM image of a cross-section of: (c) a silica monolithic capillary at x1000 magnification, (d) an enzymatic monolithic microreactor at x1000 magnification; (e) an NaOH-treated silica monolithic capillary at x350 magnification; (f) a non-treated silica monolithic capillary at x450 magnification	78
FIG 3-2	Overlapped FTIR spectra for fabrication processes of enzymatic silica monolith microreactor: (a) free lipase from <i>C.antarctica</i> ; (b) silica monolith; (c) silica monolith + APTES; (d) silica monolith + APTES+ glutaraldehyde; (e) silica monolith + APTES+ glutaraldehyde +lipase	81
FIG 3-3	The comparison of: TIC of GCMS for (a) ethyl oleate (EO) standard, (b) product of 0.5 $\mu\text{L}/\text{min}$ RT; extracted ion spectra of MS-EI for GC of (c) EO standard, (d) product of 0.5 $\mu\text{L}/\text{min}$ RT; and LC-ESLD chromatograms for (e) product of 0.5 $\mu\text{L}/\text{min}$ RT, (f) starting material (TO), respectively	88
FIG 3-4	Graph of percentage of conversion of lipid starting materials to fatty acid ethyl ester at different flow rates and conditions for 5 runs each. <i>x</i> -axis represents each number of individual microreactor, and “Run” indicates the infusion of TO solution for 6 h at specified flow rate	89
FIG 3-5	NARP/HPLC-ELSD percentage of molar conversion of substrate trioleoylglycerol (TO) to product ethyl oleate (EO) formation within 12 runs of reaction using the microreactor with 1 $\mu\text{L}/\text{min}$ at the room temperature, respectively	92
FIG 3-6	Extracted mass chromatogram for online direct infusion microreaction for substrate (a) TO in EtOH at 1 $\mu\text{L}/\text{min}$ with compound of interest: (i) TO, <i>m/z</i> 885 (ii) TO fragment/DO, <i>m/z</i> 603; (iii) EO, <i>m/z</i> 311; (iv) MO, <i>m/z</i> 339; (v) mass spectrum (without microreactor); (vi) mass spectrum (with microreactor); and (b) MO in EtOH at 1 $\mu\text{L}/\text{min}$ with compound of interest: (i) MO, <i>m/z</i> 339; (ii) EO, <i>m/z</i> 311; (iii) mass spectrum (without microreactor); (iv) mass spectrum (with microreactor)	96

FIG 4-1	Reaction scheme for the small-scale fabrication of silica monolith (SM) and microstructure fiber (MSF) capillary biocatalyst microreactors	109
FIG 4-2	Comparison of GC/FID chromatograms for (a) ethyl ester FA standards; and the products of canola oil (CanO)+EtOH transesterification using: (b) SM microreactor at 0.3 $\mu\text{L}/\text{min}$ flow-rate; (c) MSF microreactor at 0.3 $\mu\text{L}/\text{min}$ flow-rate; (d) lipase beads after 5 h reaction time; (e) $\text{H}_2\text{SO}_4$ acid catalysis after 12 h reaction time	118
FIG 4-3	NCI-mass spectra from GC/MS separations of the products of sesame seed oil (SSO) and ethanol passing through the SM microreactor. Shown are examples of FAE identified including (a) C16:0 ethyl ester, (b) C18:0 ethyl ester, (c) C18:1 ethyl ester, (d) C18:2 ethyl ester	119
FIG 4-4	Comparison of the GC/MS-NCI total ion current (TIC) and NARP-LC/ELSD traces for the transesterification products of soybean oil (SBO)+EtOH using: i) (a and d) SM microreactor at 0.3 $\mu\text{L}/\text{min}$ ; ii) (b and e) Novozyme 435 lipase beads, 10 min reaction time; iii) (c and f) Novozyme 435 lipase beads, 5 h reaction time; iv) (g): NARP-LC/ELSD of SBO starting oil	121
FIG 4-5	Percent conversion of trioleoylglycerol (TO) in ethanol to ethyl oleate (SM-EtOH) ( $\blacklozenge$ ) and in methanol to methyl oleate (SM-MeOH) ( $\blacksquare$ ) for 5-8 runs, using a single SM microreactor with a flowrate of 0.3 $\mu\text{L}/\text{min}$ at room temperature	125
FIG 4-6	GC/MS traces for C18:1 FAME produced using a single SM microreactor: (a) run 1; (b) run 3; (c) run 5; and (d) NCI spectrum for run 5 extracted from the GC peak in C) showing the presence of methyl oleate ( $[\text{M}-\text{H}]^-$ $m/z$ 295.15)	127
FIG 5-1	The generalized reaction for a hypothetical triglyceride oil consisting of C18:1, C18:2 and C18:3 forming the fully epoxidised product of mono-epoxy C18:0, di-epoxy C18:0, and tri-epoxy C18:0	135



FIG 5-2	The distribution of 54 carbon triglycerides (TAG) in canola oil as a function of the number of double bonds, estimated by NARP-LC/MS	142
FIG 5-3	NARP-LC/ESI-MS chromatograms over the range of $m/z$ 500-1200: (a) canola oil starting material; (b)-(f) formation of intermediates at reaction times of 2-16 hours; and (g) epoxide products after 28 hours of reaction	144
FIG 5-4	The epoxidation of TAG [54:4] from canola oil: relative abundance of the intermediates and final products plotted as a function of reaction time	149
FIG 5-5	The formation of tri-epoxy intermediates and products from TAG (54 carbons) containing 3 to 7 double bonds	150
FIG 5-6	Monitoring the epoxidation of TAG [54:3] from canola oil by either (a) flow-injection analysis (ie without chromatographic separation), or (b) NARP-LC/MS analysis. The plots show the normalized intensities of TAG [54:3], partially epoxidised TAG [54:3] and fully epoxidised TAG [54:3] as a function of reaction time. Each point is a separate LC/MS or flow-injection MS experiment	154
FIG 5-7	ESI mass spectra obtained by flow-injection of (a) the starting TAG oil, (b)-(f) the reaction mixture containing partially epoxidised intermediates at $t=$ 4-16 h, and (g) fully epoxidised oil obtained at $t=$ 28h	155

## List of Symbols, Nomenclature, or Abbreviations

APPI	Atmospheric pressure photoionization
APTES	3-(Aminopropyl)triethoxysilane
C16:0	Palmitic acid
C18:0	Stearic acid
C18:1	Oleic acid
C18:2	Linoleic acid
C18:3	Linolenic acid
DAG	Diacylglycerol
DO	Dioleoylglycerol
EE	Ethyl oleate/ Ethyl ester of C18:1 / Oleic acid ethyl ester
ELSD	Evaporative light scattering detector
EI	Electron impact ionization
<i>epo</i>	Epoxide
ESI	Electrospray ionization
FAAE	Fatty acid alkyl ester
FAEE	Fatty acid ethyl ester
FAME	Fatty acid methyl ester
FFA	Free fatty acid
FID	Flame ionization detector
FTIR	Fourier transform infra-red
GC	Gas chromatography
GC x GC	Comprehensive two-dimensional gas chromatography

GC/MS-NCI	Gas chromatography mass spectrometry – chemical ionization (negative mode)
HPLC	High performance liquid chromatography
MAG	Monoacylglycerol
ME	Methyl oleate / Methyl ester of C18:1 / Oleic acid methyl ester
MO	Monooleoylglycerol
MS	Mass Spectrometry
MSF	Micro structured fiber optic
NARP	Non-aqueous reversed-phased
PCF	Photonic crystal fibers
PDMS	Poly-dimethylsiloxane
PMMA	Poly(methyl-methacrylate)
<i>p</i> NP	<i>p</i> -Nitrophenol
<i>p</i> NPB	<i>p</i> -Nitrophenyl butyrate
SEM	Scanning electron microscope
SM	Silica monolith
TAG	Triacylglycerol
TEOS	Tetraethyl orthosilicate
TIC	Total ion current
TO	Trioleoylglycerol
U	Unit of lipase activity
XIC	Extracted ion chromatogram

## CHAPTER 1

### THESIS INTRODUCTION

---

#### 1.1 Lipid Transformation: General Remarks

Research shows that the market for vegetable oils is expected to grow rapidly partly due to increased demand not only from the food industry, but also for the production of oleochemicals and biofuels (Fry *et al.*, 2010). Many of these processes involve the transformation of fats and oils into other lipid forms such as in the synthesis of structural lipids *via* epoxidation, esterification, ozonolysis, transesterification, hydrogenation (King *et al.*, 2001; Gunstone, 2004; Akoh, 2007) and others. Some of these processes, for example the transesterification of lipids using chemical catalysts, require time-consuming procedures (*i.e.* involving many steps of samples extraction, derivatization, and cleaning-up), and involve of a toxic catalyst (Christie, 1989). Therefore, there is interest in developing a simple approach to perform lipid transformations in a simple, single-step process.

There is a lot of interest in the use of enzymes for lipid transformations such as in the alcoholysis of triacylglycerols to form fatty acid alkyl esters (biodiesel production) (Akoh, 2007) and other lipid products (Irimescu *et al.*, 2002). Enzymatic reactions have been shown to be highly selective, requiring mild reaction conditions and low solvent consumption (Akoh, 2007; Stamenković *et al.*, 2011), thus a much more “green” chemistry. While enzymatic reactions have been extensively used for large scale alcoholysis especially in biodiesel

production, this reaction also can be used for analytical scale applications. For instance, the enzyme can be immobilized over the high surface area of a microplatform; therefore resulting in an efficient microreactor, which is reusable for many process cycles (Ma *et al.*, 2008; Mugo and Ayton, 2012).

This chapter outlines the background to the development of microreactors and analytical methods for lipid transformations (Fig. 1-1):

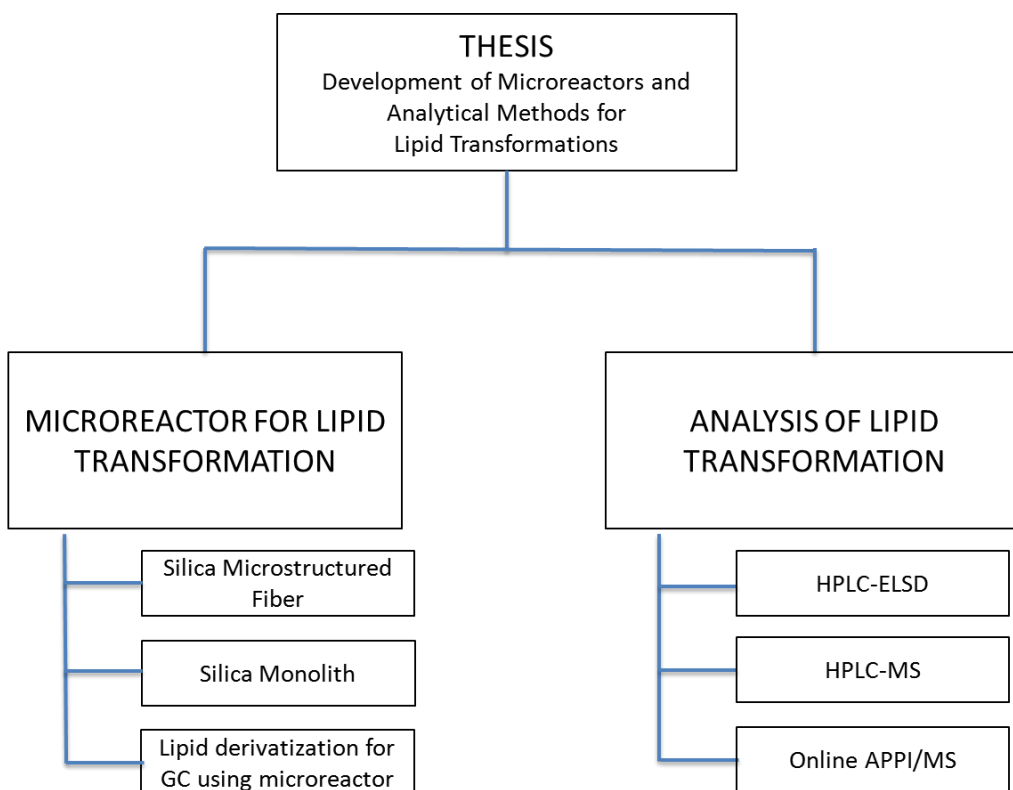


FIG 1-1: Overall thesis construction.

The focus is on the development of a practical approach to transform lipids into lipid products and derivatives. Since lipids can occur as mixtures and derivatives (*i.e.* after the transformations), there is also a need for good methods

for analyzing, quantifying and identifying the lipid products. Therefore, analytical methods involving liquid and gas chromatography that can be used in the analysis of lipids are also developed. This study aims to develop new approaches to fabricating simple flow-through microreactors supporting immobilized lipase.

## 1.2 Microreaction Technology for Lipid Transformations

### 1.2.1 General Considerations

Lipid samples are commonly esterified prior to gas chromatography (GC) analysis, as reported previously (Carrapiso and García, 2000; Christie and Han; 2012). Generally, transesterification reactions occur when fatty acid chains present in a lipid sample (*e.g.* triacylglycerol) react with alcohols, in the presence of a catalyst (Fig. 1-2).

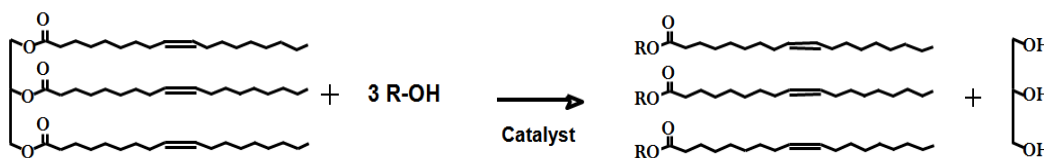


FIG 1-2: Transesterification reaction of triglyceride.

The transesterification process can be alkali-, acid-, or bio-catalyzed. However, most methods require a significant amount of sample for product recovery, are time consuming, and use hazardous chemical reagents. For example, in transesterification reactions involving an acid catalyst, fatty acid alkyl esters are obtained by heating triacylglycerol with excess of methanol in the

presence of a catalyst, such as  $\text{BF}_3$  or  $\text{H}_2\text{SO}_4$  at a high reaction temperature (50 °C to ~100 °C) (Morrison *et al.*, 1964; Christie, 1998). Even though there is no specific amount required for lipid sample prior to the derivatization for some widely used methods, AOCS official method Ce 2-66 suggested that 100-250 mg lipid should be used for the test portion using a minimum amount of methanolic  $\text{BF}_3$  (5 mL), meanwhile AOCS official method Ce 1b-89 suggested using 25 mg of lipid sample for 2 mL methanolic  $\text{BF}_3$  for derivatization. (AOCS, 2012). Therefore, approaches to transesterification requiring short reaction times and minimal sample size for sensitive analytical techniques (*e.g.* GC) where only nanogram to microgram amounts of sample are required. According to AOCS official method Ce 1b-89, GC analysis usually requires injection of no more than 1  $\mu\text{L}$  of a 15 mg/mL FAME solution, *i.e.* <15 $\mu\text{g}$ .

Micro-reaction technology allows the analysis of microscale samples, since all of the chemical transformations occur in a single platform (Ehrfeld *et al.*, 2000; Kaewkool *et al.*, 2009; Mugo and Ayton, 2010; Asanomi *et al.*, 2011). In addition to a small amount of sample and reactant required, some other advantages offered by this technology include: high efficiency in separation and product recovery, reduction of waste, high efficiency with minimal sample manipulation and a sustainable method for carrying out chemical synthesis (Watts and Wiles, 2007; Ispas *et al.*, 2009). Therefore, the focus of the current study was to develop a microreactor containing immobilized catalyst for use in small-volume oleochemical transformations for routine analysis in lipid research; and this will later be explained in detail in Chapters 2, 3 and 4 of this thesis.

### 1.2.2 Fabrication and Characterization of the Microreactor

According to Watts and Wiles (2007), a microreactor was initially designed primarily to integrate various chemical or analytical processes in one platform made up of reaction channels in the micrometer and nanometer ranges (Erhfeld, 2000; Watts and Wiles, 2007). While microreactor technology offers many merits, the fabrication of commercially available microreactors such as photolithographic and wet-etching procedures are often expensive and are generally considered to be complicated processes requiring specialized techniques (McCreedy, 2000). However, some research groups have developed simple and inexpensive approaches to fabricating lab-scale microreactors that could be useful for lipid-based chemical reactions (McCreedy, 2000; Phan *et al.*, 2004; Ma *et al.*, 2008; Sun *et al.*, 2008; Mugo and Ayton, 2010; Mugo and Ayton, 2013). This technology has been developed where various types of catalysts are loaded onto the solid support of microreactors for use in chemical reactions such as in synthetic chemistry and biotechnology (Asanomi *et al.*, 2011; Miyazaki *et al.*, 2013).

In order to develop a catalyst microreactor for use in lipid transformations, the choice of support for immobilization is crucial as it impacts the interaction between the support and the catalyst. According to the IUPAC, immobilization can be defined as “a technique that is used for the physical or chemical fixation of cells, organelles, enzymes, or other proteins onto a solid support, into a solid matrix or retained by a membrane, in order to increase their stability and make possible their repeated or continued use” (IUPAC, 1997). In this case, the



interaction of active functional group(s) in the support medium with the catalyst will create an immobilized device with specific chemical, biochemical, mechanical and kinetic properties (Sheldon, 2007). Some of the solid supports used for catalyst immobilization reported in the literature include hybrid materials especially cross-linked polymer-based supports such as polyurethane, polydimethylsiloxane (PDMS), poly(glycidyl methacrylate-co-ethylene dimethacrylate (PGMA-co-EDMA) and poly(methyl-methacrylate) (PMMA), among others (Henry *et al.*, 2000; Godino *et al.*, 2010; Asanomi *et al.*, 2011; Mugo and Ayton, 2013).

Due to their large surface area and high porosity, mesoporous silica supports have gained attention for greatly increasing the loading capacity of the catalyst (Luckarift *et al.*, 2004; Ispas *et al.*, 2008; Asanomi *et al.*, 2011). The concept involves the use of the active silanol group present in most silica-based supports to provide an amine-based matrix for further enzyme immobilization by covalent attachment of the amine group from the enzyme with the carbonyl group of cross-linkers (Cass and Ligler, 1998; Lee *et al.*, 2006). In addition, the robustness of most silica networks towards a wide range of solvents and temperatures, in addition to easy functionalized catalyst attachment makes it a good candidate as a microreactor support.

Due to the unstable nature of enzymes, the immobilization process will enhance the stability of the enzyme as well as increase the reusability/recyclability of the microreactor, as compared to the free enzyme. In addition, immobilization results in minimized leaching, thereby reducing

contamination of the product with protein (Sheldon, 2007). Enzymes can be covalently immobilized onto the support platform using a cross-linking reagent such as glutaraldehyde (Lee *et al.*, 2006; Ma *et al.* 2008). Other methods that can be used for enzyme immobilization include physical adsorption onto the support and entrapment or encapsulation of enzymes during the synthesis of the immobilization support (Luckarift *et al.*, 2004; Sheldon, 2007). The functional groups that attach to the support surface have been reported to directly affect the interaction of the enzyme and support (Lei *et al.*, 2004).

The incorporation of enzymes onto the support material can be physically revealed by surface morphology by using either transmission or scanning electron microscopy (TEM/SEM) techniques (Lei *et al.*, 2004). However, these techniques are not capable of confirming the presence of functional groups that are chemically activated during various stages of the immobilization processes. Both SEM and TEM, however, are useful in confirming the morphology and geometric structure of the support with or without the immobilized catalyst.

Lei and co-workers (2004) also used powder X-ray diffraction (XRD) to investigate patterns of diffraction peaks of synthesized mesopore materials used for enzyme immobilization. These data were used to predict the structure of support materials before further TEM was conducted. Maria-Chong and Zhao (2003) characterized amine functional groups using a small-angle X-ray scattering detector (SAXS). In addition, the presence of functional groups and immobilized enzymes on the support can also be confirmed by using spectroscopic methods,

such as FTIR (Lendl *et al.*, 1997) or X-ray photoelectron spectroscopy (XPS) (Longo *et al.*, 2006).

FTIR spectroscopy is a qualitative technique that has been used to identify chemical functional groups in a sample. In this technique, when infra-red (IR) radiation is passed through the selected sample, the corresponding molecule can be excited to a higher vibrational state by absorbing IR radiation, thus giving a strong absorbance. This happens when the photon energy coincides with the energy for the vibrational transition of the molecule. Because different molecules absorb radiation at different wavelengths (due to frequencies characteristic of functional group vibration), this produces a unique spectrum that represents characteristic frequencies. Therefore, FTIR is not only used for compound identification but also to provide information regarding structure (Hsu, 1997).

Compared to other techniques such as chromatography, the FTIR technique is also advantageous because it requires only a small amount of sample (1 microliter of sample solution, or microgram if the sample is solid), with minimal sample pre-prep (Peña-Alonso *et al.*, 2007). The incorporation and attachment of some functional groups onto the silica support can be identified by using FTIR (Lendl *et al.*, 1997;; Maria-Chong and Zhao, 2003; Kahraman *et al.*, 2007). For example, Maria-Chong and Zhao (2003) identified the presence of amine groups on the silicate network after treatment of the support with (aminopropyl)triethoxylane (APTES). This observation is important since the amine group from APTES that is grafted onto the monolithic network can be exploited for further immobilization reaction. Later, the carbonyl group from a

bifunctional crosslinker (*e.g.* glutaraldehyde) can react with the primary amine (to form imine), while providing another free carbonyl end for enzyme bonding.

Previous research also used the FTIR method to qualitatively identify the presence of amide groups on the immobilized enzyme (Bajpai and Bhanu, 2003; Kahraman *et al.*, 2007). Therefore, within the scope of the present research, the effectiveness of each stage of the immobilization process could be monitored by the determination and measurement of the presence of active functional groups that bound/incorporate/attach to the surface of the active support material by means of analytical instrumentation including FTIR and the morphology of such support can be observed by SEM technique.

### **1.2.3 Enzyme Selection for Use in Microreaction Technology for Lipid Transformations**

Enzymes, for example lipase, have been widely used in the transesterification of triacylglycerols (commonly vegetable oils) with alcohol to form fatty acid alkyl esters (FAAE) (Nelson *et al.*, 1996; Shimada *et al.*, 2002; Lara and Park, 2004; Leung *et al.*, 2010) and other lipid classes such as diacylglycerol and monoacylglycerol (Arroyo *et al.*, 1996; Irimescu *et al.*, 2002; Stamenkovic *et al.*, 2011). Lipase has also been used in the alcoholysis of structural triacylglycerol consisting of different fatty acid chains of triacylglycerols into monoacylglycerols (Soumanou *et al.*, 1998; Irimescu *et al.*, 2002; Rodriguez and Fernandes-Lafuente, 2010).

Generally, enzyme reactions are preferably performed in aqueous media since free enzyme poses great solubility in water, while immobilized enzyme is efficiently active in ~pH 7 media (Klibanov, 1997). However, in fats and oils modification, concerns of reagent (enzyme solution or substrate with lipids) homogeneity and product recovery have led to the study of optimized reactions in non-aqueous conditions with or without additional organic solvents (Iso *et al.*, 2001; Kilbanov, 2001; Irimescu *et al.*, 2002; Stamenkovic *et al.*, 2011).

The benefit of using enzymes in anhydrous systems is that reactions other than hydrolysis can occur such as transesterification/alcoholysis (depending on the nucleophiles used). Such reactions are useful in preparing structured lipids, for example in the formation alkyl ester of fatty acid (Shimada *et al.*, 2002; Lara and Park, 2004), specific/positional lipid, or other lipid products (mono- and diacylglycerol, glycerol, free fatty acid) (Irimescu *et al.*, 2002; Stamenkovic *et al.*, 2011).

According to Shimada and co-workers (1999), increasing the water content in methanolysis increases the time for completion of the reaction. This is because the interaction of the enzyme with water/oil competes with the reaction of the enzyme with methanol/oil mixtures. However, the same study also reported that when the molar ratio of methanol to oil is more than 1.5:1, loss of enzyme activity was observed (Shimada *et al.*, 1999). Therefore, the use of methanol can be detrimental to enzyme activity and prospect for reusability.

While lipase is widely known to be active in aqueous media (Klibanov, 1997), the reaction of lipase in an oil medium has been studied (Rodriguez and Fernandes-Lafuente, 2010), and it has been demonstrated that alcohol provides a significant role in the reaction. This is because when dealing with an anhydrous system, the solubility of oil in alcohol is an important factor in reaction rate determination (Rodrigues *et al.*, 2008).

In some studies of the alcoholysis of oil by lipase, the addition of an organic solvent was required to allow the homogeneity of the mixture (Fureby *et al.*, 1997; Dossat *et al.*, 2002; Lee *et al.*, 2006; Royon *et al.*, 2007; Liu *et al.*, 2010). Table 1-1 provides information regarding the role of the solvent/media in enzyme-catalyzed lipid transformations.

Many studies have reported that enzymes can still retain their activity in organic media (Lee and Dordick, 2002). According to Iso and co-workers (2001), when a short chain alcohol such as methanol was used in a non-aqueous reaction, the presence of an organic solvent was required, such as 1,4-dioxane, in order to get a homogenous reaction mixture; *tert*-butanol also can be used as a solvent (Li *et al.*, 2006). Moreover, previous studies reported that the use of methanol for lipid transesterification inactivates lipase (Shimada *et al.*, 1999; Li *et al.*, 2006). Longer chain alcohols such as butanol and propanol can also be used, providing greater miscibility in the oil/alcohol mixture (Iso *et al.*, 2001, Kazanceva *et al.*, 2011).

TABLE 1-1: The role of solvents in lipid transformation in enzymatic reaction media.

Oil / TAG	Alcohol	Organic Solvent	Water	Reaction Temp °C	Lipase	Reference
1 mol	3 mol 2-ethyl-1-hexanol		3%	45-50	<i>C.rugosa</i> (3%)	Linko <i>et al.</i> , 1994
1 mol	10 mol EtOH	Diisopropyl ether (DIPE) 3mL		25	<i>P.roquefortii</i> (25 mg)	Fureby <i>et al.</i> , 1997
1 mol	1 mol MeOH		0-2%	30	<i>C.antarctica</i> (400 mg)	Shimada <i>et al.</i> , 1999
1 mol	4 mol MeOH		400 ppm	50	<i>C.antarctica</i> (3000 mg)	Belafi-Bako <i>et al.</i> , 2002
1 mol	5 mol BuOH	<i>n</i> -Hexane		40	<i>T.lanuginosus</i> (10 mg)	Dossat <i>et al.</i> , 2002
1 mol	5 mol BuOH			40	<i>T.lanuginosus</i> (100 mg)	Dossat <i>et al.</i> , 2002
1 mol	77 mol EtOH			25	<i>C.antarctica</i> (50 mg)	Irimescu <i>et al.</i> , 2002
1 mol	4 mol MeOH			50	<i>C.antarctica</i>	Kose <i>et al.</i> , 2002
1 mol	4 mol MeOH	<i>tert</i> -Butanol (1:1 <i>tert</i> -BuOH:Oil, v/v)		35	<i>T.lanuginosus</i> : <i>C.antarctica</i> (1:1)	Li <i>et al.</i> , 2006
1 mol	6 mol MeOH	<i>tert</i> -Butanol (28%)		50	<i>C.antarctica</i> (300 mg)	Royon <i>et al.</i> , 2007
1 mol	6 mol MeOH		0.1 g	40	<i>T.lanuginosus</i> (0.43 mg)	Dizge, 2008
1 mol	5 mol MeOH 7 mol EtOH 9 mol BuOH			30-35	<i>C.antarctica</i> , <i>T.lanuginosus</i> <i>R.miehei</i>	Rodrigues <i>et al.</i> , 2008
1 mol	4 mol MeOH	<i>tert</i> -Butanol		45	5%	Liu <i>et al.</i> , 2010
1 mol	4 mol alcohol			45	5%	Liu <i>et al.</i> , 2010

However, within the scope of this study, a short chain alcohol is preferable since the expected transesterified product will be directly tested using GC, and the resulting short chain ester gives superior chromatographic performance (methanol>ethanol>butanol>isopropanol). Using a short chain alcohol in transesterification will produce a lower molecular weight fatty acid alkyl ester derivative, which can be easily separated and eluted from GC columns using lower GC temperatures compared with higher molecular weight fatty acid alkyl ester.

#### **1.2.4 Application of Microreaction Technology in Lipid Transformations**

Use of microreactors for lipid transformation was studied by Kaewkool *et al.*, (2009) who used a simple base-catalyst microreactor made from NaOH powder packed onto cotton wool within a small syringe to transesterify TAG in methanol in the presence of tetrahydrofuran (THF). The reaction time for producing fatty acid methyl ester using the base-catalyzed microreactor was less than 1 min (Kaewkool *et al.*, 2009). Even though this report of microreactor-based coriander seed oil alcoholysis demonstrated promising data, there was no description of the reusability of the microreactor in that study.

Similarly, Sun and co-workers (2008) reported the synthesis of fatty acid methyl ester from cottonseed oil in KOH-catalyzed capillary microreactors of 0.25 and 0.53 mm sizes. Although high FAME yield was obtained at a shorter time (in range of 3.68 min to 19.73 min), the reaction yield was decreased due to



saponification over time (Sun *et al.*, 2008). On the contrary, an enzymatic polymer monolith microreactor developed for use in the transesterification of castor oil and the synthesis of butyl laurate was successfully employed for several cycles without a major loss of catalyst activity, with a high yield (Mugo and Ayton, 2013).

The use of such microreactors in lipid analysis is still very new; however, in biotechnology and bio-catalysis, enzymatic microreactor technology has been used in order to study enzyme kinetics and proteomics as well as biosensors in glucose measurements (L'Hostis *et al.*, 2000; Seong *et al.*, 2003; Urban *et al.*, 2006, Yang *et al.*, 2010). Previously, Thomsen and co-workers (2007) reported the development of a microfluidic immobilized enzyme reactor for continuous biotransformation, which consists of a functionalized microstructure fabricated from silicone rubber material. Urban and co-workers (2006) have reviewed the role of enzymatic microreactor technology in protein and other chemical analyses, as well as the type of microreactor medium (support) for enzyme immobilization. In that review, they suggested that silicon based supports are the most widely-used supports for enzyme immobilization, especially in protein analysis.

### **1.3 Analysis of Lipid Transformations**

#### **1.3.1 Liquid Chromatography**

Fats and oils are mainly composed of triacylglycerols accompanied by diacylglycerols, monoacylglycerols and free fatty acids; but may also contain

phospholipids, free sterols and sterol esters, tocopherols, triterpene alcohols, hydrocarbons and fat-soluble vitamins (Gunstone, 2004). Because of this wide variety of lipid classes requiring analysis, high resolution chromatographic techniques such as liquid chromatography are mainly being used in the analysis of lipids (Lin, 2007; Christie and Han, 2012).

Usually, high performance liquid chromatography (HPLC) can be used to separate nonvolatile, thermally unstable and high-molecular weight lipids (Aluyor *et al.*, 2009; Christie, 2012), such as for mixtures of non-polar lipids including triacylglycerols, diacylglycerols and monoacylglycerols. The separation of this lipid mixture by HPLC can be carried out using either reversed-phase HPLC or normal-phase HPLC modes. In reversed-phase HPLC, separation is typically carried out using a nonpolar C18 column with the mobile phase consisting of polar solvent such as methanol, water, and/or acetonitrile (Nikolova-Damyanova, 1997). Reversed-phase HPLC can be used for the determination and separation of triacylglycerols species (*i.e.* the degree of unsaturation and chain length), and also to characterize positional isomers (Asshauer and Ullner, 1986; Hinrichsen and Seinhart, 2006); this method will be optimized in this research in order to identify all the reaction products obtained from oleochemical transformations proposed in this thesis.

Previously, a reversed-phase HPLC system was developed to separate fatty acid methyl ester mixtures from biodiesel (Holcapek *et al.*, 1999), where elution was carried out with a two-step gradient solvent system consisting of water-organic and non-aqueous solvents. However, the use of a non-aqueous

gradient is preferable since it can elute non-polar lipids such as triacylglycerols in a shorter time, compared to an aqueous gradient (Türkan and Kalay, 2006). Following this, Nicola and co-workers (2008) proposed the use of a non-aqueous gradient consisting of isopropanol:hexane and methanol:acetonitrile for a reversed-phase HPLC separation for lipid classes. In that study, separation of 47 lipid species consisting of triacylglycerols, diacylglycerols, monoacylglycerols and ethyl esters was achieved in 30 min with UV detection (Nicola *et al.*, 2008).

Even though UV is the most common detection method for HPLC it is often not suitable for lipid detection because of the lack of a UV chromophore group in some lipids that exhibits absorption in the UV region. In addition, the UV cut-off point for many solvents is greater than the absorption range of lipids (200-210nm), thus producing a weak 'end' of absorption. While limited, some solvents do have a lower cut-off point such as hexane, methanol, water, heptane and acetonitrile, and these can be used as solvents for UV detection in lipid analysis (Hinrichsen and Seinhart, 2006).

In contrast, an evaporative light scattering detector (ELSD) can be used in the determination of lipids separated by HPLC (Kittirattanapiboon and Krisnangkura, 2008; Lin, 2007), because it is insensitive to gradient flow compared to refractive index detection (RI), and is universally capable of detecting all lipid classes. ELSD with reversed-phase HPLC has also been reported for the separation of triacylglycerol mixtures from a fat sample (Anklam *et al.*, 1996). With the consideration that the detection of transesterification products and unreacted reactant triacylglycerols (if any) can all be identified in a

single analysis, ELSD will be used for lipid quantification and analyses in the present thesis.

Generally, for ELSD, the mobile phase flowing from the HPLC column (with the analyte of interest) is nebulized (with N<sub>2</sub>) into fine droplets in a nebulizing chamber. These droplets are carried by the gas flow into a heated area where the solvent evaporates, leaving only the solute particles. The sample particles then pass through a flow cell where they interact with the light beam. The amount of the light scattered by the solute is measured and presented as peak intensity (Skoog, 2007). Since ELSD response is greatly affected by analyte volatility, a calibration curve is always needed because the response is not linear for all lipid components (Moreau and Christie, 1999). In order to achieve a better response using an ELSD, the drift tube temperature, nebulizer gas flow as well as the gradient elution from LC separation, all need to be optimized.

Recent studies reported mass spectrometry (MS) as the detector of choice to use with many liquid chromatography systems (Kalo *et al.*, 2004; Liebisch *et al.*, 2004; Hinrichsen and Seinhart, 2006; Christie and Han, 2012). After separation with HPLC, an unknown compound can be identified using a comparable retention time with a known standard and the sample can be characterized by its mass spectrum with MS detection.

Due to the non-polar nature of the triacylglycerol (and also derivatives), atmospheric pressure chemical ionization (APCI) is often the ionization method used, since it was reported to be more compatible with non-polar solvent systems

(Laakso and Voutilainen, 1996; Holcapek *et al.*, 2005; Segall *et al.*, 2005). For example, an earlier report on incomplete methanolysis products from sunflower oil shows the use of LC/MS-APCI to separate and identify the transesterified oil (Türkan and Kalay, 2006). However, APCI gives a much lower response towards fatty acid methyl ester, compared with triacylglycerol, diacylglycerol and monoacylglycerol (Türkan and Kalay, 2006). During the last decade, atmospheric pressure photoionization (APPI) was introduced to lipid analysis and has been reported to give better accuracy and sensitivity in analyzing fatty acid methyl- and ethyl- esters of fish oil, compared to APCI (Cai and Syage, 2006).

On the other hand, the use of electrospray ionization (ESI) was also reported for fats and oils, which gives a better response towards thermally-labile and nonvolatile compounds such as triacylglycerol (Dorschel, 2002, Kalo *et al.*, 2004). In both studies, an adduct ion was used to enhance the ionization of lipid samples. For example, LC-MS-ESI  $[M+NH_4]^+$  was used to characterize triacylglycerols of C<sub>16</sub> to C<sub>26</sub> from peanut oil (Dorschel, 2002). It was shown that ESI ionization was suitable to be used for higher molecular weight compounds such as epoxidised vegetable oil which contains epoxide groups or oxirane rings (Giuffrida *et al.*, 2004). Suman and co-workers (2005) first reported the use of LC-ESI to structurally identify epoxidised soybean oil. Within the scope of this thesis, the optimization of non-aqueous reversed-phase HPLC method with either ELSD or MS detection provides a simple way to analyze oils and fats for triacylglycerols and their derivatives; this will be described in Chapters 2, 3 and 4 of this thesis. Information on the type of fatty acids, including the degree of

unsaturation (based on carbon and double bond numbers), as well as other lipid classes (fatty acid alkyl esters, diacylglycerol, monoacylglycerol) can be obtained directly using this method.

### **1.3.2 Gas Chromatography**

Since it was first developed more than 50 years ago, GC has been widely used in the analysis of lipids and determination of fatty acid composition in a wide range of oils and fats, for example in marine, food and in biological samples (Craig and Murty, 1959; Abel *et al.*, 1963; Tserng, *et al.*, 1981; Lui, 1994; Yang *et al.*, 1996; Kowalski, 2007), due to its sensitivity and convenience. In GC, the analytes in the sample may be separated according to the degree of saturation and chain length such as C16:0, C18:0, C18, C18:1, C18:3, and so on, depending on the choice of the stationary phase. Since then, the use of GC in lipid analysis has been optimized (Christie, 1989; Park and Goins, 1994; Hinrichsen and Seinhart, 2006; Carrasco-Pancorbo *et al.* 2009) for use in various lipid analyses.

In GC analysis, the samples usually need to be derivatized into fatty acid alkyl esters, normally in the form of fatty acid methyl esters prior to the injection because most of the lipids are not suitable (nonvolatile) to be analyzed directly. Methods such as the AOCS official method Ce 2-66 (1997) is widely used for preparing fatty acid methyl esters prior to GC analysis. In this procedure, an amount of methanolic KOH solution is added into the lipid sample, in order to convert the corresponding triacylglycerol into a more volatile fatty acid methyl

ester. In other methods, methanolic NaOH (AOCS, 2012), sodium methoxide, or tetramethylammonium hydroxide (TMAH) also can be used as an alkali-catalyst in the reaction, as previously reported in the derivatization of milk fat and triacylglycerol samples (Metcalf and Wang, 1961; Christoperson and Glass, 1969; Metcalfe and Wang, 1981; Park and Goins, 1994; Ichihara *et al.*, 1996).

Additionally, numerous studies also reported to derivatize the lipid using a Lewis acid such as boron trifluoride (BF<sub>3</sub>) as a catalyst, and this approach has also been widely used in routine lipid analysis (Metcalf and Schmitz, 1961; Morrison and Smith, 1964; Carrapiso and García, 2000). Other acidic methanolic solutions including HCl or H<sub>2</sub>SO<sub>4</sub> acids can also be selected for use in lipid derivatization (Browse *et al.*, 1986; Christie, 1993; Carrapiso and García, 2000; Goff *et al.*, 2004). However, this method requires a higher reaction temperature and longer reaction time. Christie (1989) has simplified the derivatization techniques using a methanol-toluene in acid catalyst to produce fatty acid methyl ester, by proposing a milder reaction temperature (~50 °C) with an extended reaction time.

The most common detector for GC analysis of lipids is the flame ionization detector (FID), however the use of mass spectrometry and FTIR detectors have also been reported (Christie, 1998; Mondello *et al.*, 2004; Hinrichsen and Seinhart, 2006). Within the work presented in this thesis, the GC method is applied in order to analyze derivatized vegetable oils. In addition, the comprehensive two-dimensional GC that was previously reported to have potential in resolving and separating a complex lipid mixture (Tranchida *et al.*, 2008; Villegas *et al.*, 2010), is utilized to analyze the lipid products that eluted

from a microreactor in a collaborative study with another graduate student (Villages C.).

#### **1.4 Hypothesis and Objectives**

It is hypothesized that silica-based capillary microreactors with a very large surface area for enzyme immobilization can be made from either a silica microstructured fiber (MSF) capillary or a fused silica capillary containing a porous silica monolith. These may prove to be effective as flow-through continuous microreactors to perform oleochemical transformations.

In order to test this hypothesis, there are two main areas of study. The first objective of this thesis is to demonstrate the successful fabrication of lipase immobilized microreactors from a silica microstructured fiber and monolithic fused silica capillaries. The combination of microreactor technology with enzymatic reactions is tested for micro-scale lipid conversions and enzyme reusability due to the immobilization process and the reaction parameters such as temperature and flow rates. It is envisioned to use this approach for analytical scale-reactions, such as small-scale lipid derivatization prior to GC analysis, or inline monitoring of lipid transformations.

The second area of study is the development of analytical methods to use with lipid transformations. These include an optimized analytical method consisting of non-aqueous reverse phase liquid chromatography (NARP-HPLC) coupled to electrospray mass spectrometry (ESI-MS) to monitor the formation of



intermediate and final products in the epoxidation of triacylglycerols such as canola oil. Another objective was to optimize the NARP-HPLC method using an evaporative light scattering detector (ELSD) to identify and quantify all reaction products from the lipid transformation.

## 1.5 References

- Abel K, Deschmertz H, Peterson JI (1963) Classification of microorganisms by analysis of chemical composition: Feasibility of utilizing gas chromatography. *J Bacteriol* 85:1039-1044.
- Akoh CC (2007) Enzymatic approach to biodiesel production, *J Agr Food Chem* 55:8995-9005.
- Aluyor EO, Ozigagu CE, Oboh OI, Aluyor P (2009) Chromatographic analysis of vegetable oils: A review. *Sci Res Essay* 4(4):191-197.
- Anklam E, Lipp M, Wagner B (1996) HPLC with light scatter detector and chemometric data evaluation for the analysis of cocoa butter and vegetable fats. *Fett/Lipid* 98:55–59.
- AOCS Ce 1b-89 (2012) AOCS Official Method Ce 1b-89 Fatty Acid Composition of Marine Oils by GLC. *Official Methods and Recommended Practices of the American Oil Chemists' Society*, 6<sup>th</sup> ed. AOCS Press: Champaign, IL, USA.
- AOCS Ce 2-66 (2012) AOCS Official Method Ce 2-66 Preparation of Methyl Esters of Fatty Acids. *Official Methods and Recommended Practices of the American Oil Chemists' Society*, 6<sup>th</sup> ed. AOCS Press: Champaign, IL, USA.
- AOCS Ce 2-66 (1997) AOCS Official Method Ce 2-66 GLC ranges of Fatty acid

composition *Official Methods and Recommended Practices of the American Oil Chemists' Society*. AOCS Press: Champaign, IL, USA.

Arroyo H, Sánchez-Muniz FJ, Cuesta C, Burguillo FJ,, Sánchez-Montero JM (1996) Hydrolysis of used frying palm olein and sunflower oil catalyzed by porcine pancreatic lipase. *Lipids* 31(11):1133-1139.

Asanomi Y, Yamaguchi H, Miyazaki M, Maeda H (2011) Enzyme-immobilized microfluidic process reactors. *Molecules* 16(7):6041-6059.

Asshauer J, Ullner H (1986) Quantitative analysis in HPLC, In: Engelhardt H (Ed): *Practice of High Performance Liquid Chromatography: Chemical Laboratory Practice*. Springer-Verlag: Heidelberg, Germany. p65-108.

Bajpai AK, Bhanu S (2003) Immobilization of alpha-amylase in vinyl-polymer-based interpenetrating polymer networks. *Colld Polym Sci* 282:76–83.

Belafi-Bako KF, Kovacs F, Gubicza L, Hancsok J (2002) Enzymatic biodiesel production from sunflower oil by candida antarctica lipase in a solvent-free system. *Biocatal Biotransform* 20(6):437–439.

Browse J, McCourt PJ, Somerville CR (1986) Fatty-acid composition of leaf lipids determined after combined digestion and fatty-acid methyl-ester formation from fresh tissue. *Anal Biochem* 152:141–145.

Cai S-S, Syage JA (2005) Atmospheric pressure photoionization mass spectrometry for analysis of fatty acid and acylglycerol lipids. *J Chrom A* 1110(1-2):15-26.

Carrapiso AI, García C (2000) Development in lipid analysis: some new extraction techniques and in situ transesterification. *Lipids* 35(11):1167-77.

Carrasco-Pancorbo A, Navas-Iglesias N, Cuadros-Rodríguez L (2009) From lipid

analysis towards lipidomics, a new challenge for the analytical chemistry of the 21st century. Part I: Modern lipid analysis. *TrAC Trends Anal Chem* 28:263-278.

Cass T, Ligler FS (1998) *Immobilized Biomolecules in Analysis: A Practical Approach*, Oxford University Press: Oxford, UK.

Christie WW (1989) *Gas Chromatography and Lipids*, P.J. Barnes & Associates (The Oily Press Ltd): Dundee, UK.

Christie WW (1993) Preparation of ester derivatives of fatty acids for chromatographic analysis, In Christie WW (Ed): *Advances in Lipid Methodology*. The Oily Press Ltd: Dundee, UK. p69-111.

Christie WW (1998) Gas chromatography-mass spectrometry methods for structural analysis of fatty acids. *Lipids* 33:343-353.

Christie W, Han X (2012) *Lipid Analysis. Isolation, Separation, Identification and Lipidomic Analysis*, 4<sup>th</sup> ed. Woodhead Publishing Ltd: Cambridge.

Christopherson SW, Glass RL (1969) Preparation of milk fat methyl esters by alcoholysis in an essentially nonalcoholic solution. *J Dairy Sci* 52:1289-1290

Craig BM, Murty NL (1959) Quantitative fatty acid analysis of vegetable oils by gas-liquid chromatography. *J Am Oil Chem Soc* 36:549-552.

Delmonte P, Yurawecz MP, Mossoba MM, Cruz-Hernandez C, Kramer JK (2004) Improved identification of conjugated linoleic acid isomer using silver-ion HPLC separations. *J Assoc Off Anal Chem Int* 87:563-568.

Dizge N, Keskinler B (2008) Enzymatic production of biodiesel from canola oil using immobilized lipase. *Biomass Bioenergy* 32:1274-1278.

Dorschel CA (2002) Characterization of the TAG of peanut oil by electrospray LC-MS-MS. *J Am Oil Chem Soc* 79:749-753.

- Dossat V, Combes D, Marty A (2002) Lipase-catalysed transesterification of high oleic sunflower oil. *Enzym Microbial Technol* 30:90–94.
- Ehrfeld W, Hessel V, Löwe H (2000). *Microreactors*. Wiley-VCH: Weinheim, Germany.
- Fureby AM, Tian L, Adlercreutz P, Mattiasson B (1997) Preparation of diglycerides by lipase-catalyzed alcoholysis of triglycerides. *Enzym Microbial Technol* 20:196-206.
- Giuffrida F, Destailats F, Skibsted LH, Dionisi F (2004) Structural analysis of hydroperoxy- and epoxy-triacylglycerols by liquid chromatography mass spectrometry. *Chem Phys Lipids* 131:41-49.
- Godino N, Campo FJ, Muñoz FX, Hansen MF, Kutter JP, Snakenborg D (2010) Integration of a zero dead-volume pdms rotary switch valve in a miniaturized (bio) electroanalytical system. *Lab Chip* 10:1841–1847.
- Goff MJ, Bauer NS, Lopes S, Sutterlin WR, Suppes GJ (2004) Acid-catalyzed alcoholysis of soybean oil. *J Am Oil Chem Soc* 81:415-420.
- Gunstone FD (2004) *The Chemistry of Oils and Fats: Sources, Composition, Properties and Uses*. Blackwell Publishing Ltd: Oxford, UK.
- Henry AC, Tutt, TJ, Galloway M, Davidson YY, McWhorter SC, Soper SA, McCarley RL (2000) Surface modification of poly(methylmethacrylate) used in the fabrication of microanalytical devices. *Anal Chem* 72:5331-5337.
- Hinrichsen N, Steinhart H (2006) Techniques and applications in Lipid Analysis, in Massoba, MM *et al* (Eds): *Lipid Analysis and Lipidomics: New Techniques and Applications*. AOCS Press: Champaign, IL.
- Holcapek M, Lída M, Jandera P, Kabátová N (2005) Quantitation of

triacylglycerols in plant oils using HPLC with APCI-MS, evaporative light-scattering, and UV detection. *J Sep Sci* 28:1315-33.

Hsu SC.-P (1997) Ch 15: Infrared spectroscopy, In Settle FA (Ed): *Handbook of Instrumental Techniques for Analytical Chemistry*. Prentice-Hall Inc: Upper Saddle River, NJ, USA.

Irimescu R, Iwasaki Y, Hou CT (2002) Study of TAG ethanolysis to 2-MAG by immobilized *Candida antarctica* lipase and synthesis of symmetrically structured TAG. *J Am Oil Chem Soc* 79:879-883.

Iso M, Chen B, Eguchi M, Kudo T, Shrestha S (2001) Production of biodiesel fuel from triglycerides and alcohol using immobilized lipase. *J Mol Catal B: Enzym* 16:53-58.

Ispas C., Sokolov I, Andreescu S (2009) Enzyme-functionalized mesoporous silica for bioanalytical applications. *Anal Bioanal Chem* 393:543-554.

Kaewkool P, Kittiratanapiboon K, Aryasuk K, Krisnangku K (2009) Micro-reactor for transesterification of plant seed oils. *Eur J Lipid Sci Technol* 111:474-480.

Kahraman MV, Bayramoğlu G, Kayaman-Apohan N, Güngör A (2007)  $\alpha$ -Amylase immobilization on functionalized glass beads by covalent attachment. *Food Chem* 104:1385-1392.

Kalo P, Kempainen A, Ollilainen V, Kuksis A (2004) Regiospecific determination of short-chain triacylglycerols in butterfat by normal-phase HPLC with on-line electrospray-tandem mass spectrometry. *Lipids* 39: 915-928.

Kazanceva I, Makarevičienė V, Kazancev K (2011) Application of biotechnological method to biodiesel fuel production using *n*-butanol. *Env Res Engine Management* 56:35-42.

Kilbanov AM (2001) Improving enzymes by using them in organic solvents. *Nature* 409:241-246.

- King JW, Holliday RL, List GR, Snyder JM (2001) Hydrogenation of vegetable oils using mixtures of supercritical carbon dioxide and hydrogen. *J Am Oil Chem Soc* 78 (2):107-113.
- Kittirattanapiboon K, Krisnangkura K (2008) Separation of acylglycerols, FAME and FFA in biodiesel by size exclusion chromatography. *Eur J Lipid Sci Technol* 110:422-427.
- Kose O, Tuter M, Aksoy HA (2002) Immobilized *Candida antarctica* lipase-catalyzed alcoholysis of cotton seed oil in a solvent-free medium. *Bioresource Technol* 83:125–129.
- Kowalski R (2007) GC analysis of changes in the fatty acid composition of sunflower and olive oils heated with quercetin, caffeic acid, protocatechuic acid, and butylated hydroxyanisole. *Acta Chromatographica* 18:15-23
- Lakso P, Vontilainen P (1996) Analysis of triacylglycerols by silver-ion high performance liquid chromatography-atmospheric pressure chemical ionization mass spectrometer. *Lipids* 31:1311-1322.
- Lara PV, Park EY (2004) Potential application of waste activated bleaching earth on the production of fatty acid alkyl ester using *Candida cylindracea* lipase in organic solvent system. *Enzym Microbial Technol* 34:270-277.
- L'Hostis E, Michel PE, Fiaccabrino GC, Strike DJ, de Rooij NF, Koudelka-Hep M (2000) Microreactor and electrochemical detectors fabricated using Si and EPON SU-8. *Sens Actr B Chem* 64:156–162.
- Lee DH, Park CH, Yeo JM, Kim SW (2006) Lipase immobilization on silica gel using a cross-linking method. *J Ind. Eng. Chem* 12:777–782.
- Lee M-Y, Dordick JS (2002) Enzyme activation for nonaqueous media. *Current Opinion Biotechnol* 13:376–384.

- Lei J, Yu C, Zhang L, Jiang S, Tu B, Zhao D (2004) Immobilization of enzymes in mesoporous materials: controlling the entrance to nanospace. *Micropr Mesopr Mat* 73:121-128.
- Lendl B, Schindler R, Frank J, Kellner R, Drott J, Laurell T (1997) Fourier transform infrared detection in miniaturized total analysis systems for sucrose analysis. *Anal Chem* 69:2877-2881.
- Leung DYC, Wu X, Leung MKH (2010) A review on biodiesel production using catalyzed transesterification. *Applied Energy* 87:1083–1095.
- Li L, Du W, Liu D, Wang L, Li Z (2006) Lipase-catalyzed transesterification of rapeseed oils for biodiesel production with a novel organic solvent as a reaction medium. *J Mol Catal B: Enzym* 43:58-62.
- Lin J-T (2007) HPLC separation of acyl lipid classes. *J Liq Chrom Related Technol* 30:2005-2020.
- Linko Y.-Y, Lamsa M, Huhtala A, Linko P (1994) Lipase-catalyzed transesterification of rapeseed oil and 2-ethyl-1-hexanol. *J Am Oil Chem Soc* 71(12):1411-1414.
- Liu Y, Tan H, Zhang X, Yan Y, Hameed BH (2010) Effect of monohydric alcohols on enzymatic transesterification for biodiesel production. *Chem Eng J* 157:223–229.
- Liu Y, Yan Y, Xu L, Duan X, Tan H, Zhang X (2010) Enzymatic transesterification for biodiesel production from waste baked duck oil. *Mechanic Auto Control Eng (MACE) 2010 International Conference* 3990-3993.
- Longo L, Vasapollo G, Guascito MR, Malitesta C (2006) New insights from X-ray photoelectron spectroscopy into the chemistry of covalent enzyme immobilization, with glutamate dehydrogenase (GDH) on silicon dioxide as an example. *Anal Bioanal Chem* 385:146–152.
- Luckarift HR, Spain JC, Naik RR, Stone MO (2004) Enzyme immobilization in

biomimetic silica support. *Nat Biotech* 22:211-213.

Ma J, Liang Z, Qiao X, Deng Q, Tao D, Zhang L, Zhang Y (2008) Organic-inorganic hybrid silica monolith based immobilized trypsin reactor with high enzymatic activity. *Anal Chem* 80:2949–2956.

Maria-Chong AS, Zhao XS (2003) Functionalization of SBA-15 with APTES and characterization of functionalized materials. *J Phys Chem B* 10: 12650-12657.

McCreedy T (2000) Fabrication techniques and materials commonly used for the production of microreactors and micro total analysis systems. *Trends Anal Chem* 19:396–401.

Metcalf LD, Schmitz AA (1961) The rapid preparation of fatty acid esters for gas chromatographic analysis. *Anal Chem* 33:363-364.

Metcalf LD, Wang CN (1981) Rapid preparation of fatty acid methyl esters using organic base-catalyzed transesterification. *J Chromatogr Sci* 19(10):530-535.

Miyazaki M, Briones-Nagata MP, Honda T, Yamaguchi H (2013) Bioorganic and biocatalytic reactions, In Wirth T (Ed): *Microreactors in Organic Chemistry and Catalysis*, 2<sup>nd</sup> ed. Wiley-VCH Verlag GmbH & Co: Weinheim, Germany.

Mondello L, Casillia A, Tranchida PQ, Costa R, Chiofalo B, Dugo P, Dugo G (2004) Evaluation of fast gas chromatography and gas chromatography-mass spectrometry in the lipid analysis. *J.Chrom A* 1035:237-247.

Moreau RA (2006) An overview of modern mass spectrometry methods in the toolbox of lipid chemists and biochemists, In Massoba MM *et al.* (Eds): *Lipid Analysis and Lipidomics: New Techniques and Applications*, AOCS Press: Champaign, IL, USA.

Moreau RA, Christie WW (1999) The impact of evaporative light-scattering detectors on lipid research. *Inform* 10:471-478.



- Morrison WR, Smith LM (1964). Preparation of fatty acid methyl esters and dimethylacetals from lipids with boron fluoride-methanol. *J Lipid Res* 5:600-608.
- Mugo SM, Ayton K (2010) Lipase immobilized microstructured fiber based flow-through microreactor for facile lipid transformations. *J Mol Catal B Enzym* 67:202–207.
- Mugo SM, Ayton K (2013) Lipase immobilized methacrylate polymer monolith microreactor for lipid transformations and online analytics. *J Am Oil Chem Soc* 90:65–72.
- Nelson JA, Foglia TA, Marmer WN (1996) Lipase-catalyzed production of biodiesel. *J Am Oil Chem Soc* 7(8): 1191-1195.
- Nicola GD, Pacetti M, Polonara F, Santori G, Stryjek R (2008) Development and optimization of a method for analyzing biodiesel mixtures with non-aqueous reversed phase liquid chromatography. *J Chrom A* 1190(1–2):120–126
- Nikolova-Damyanova B (1997) Reversed-phase high-performance liquid chromatography: general principles and application to the analysis of fatty acids and triacylglycerols. In Christie WW (Ed): *Advances in Lipid Methodology – Four*. The Oily Press Ltd: Dundee, UK. p193-251.
- Park PW, Goins RE (1994) In situ preparation of fatty acid methyl esters for analysis of fatty acid composition in foods. *J Food Sci* 59:1262-1266.
- Peña-Alonso R, Rubio F, Rubio J, Oteo JL (2007) Study of the hydrolysis and condensation of  $\gamma$ -Aminopropyltriethoxysilane by FT-IR spectroscopy. *J Mater Sci* 42: 595-60.
- Phan NTS, Brown DH, Styring P (2004) A facile method for catalyst immobilisation on silica: nickel-catalysed Kumada reactions in mini-continuous flow and batch reactors. *Green Chemistry* 6(10):526-532.

- Rodeigues RC, Volpato G, Wada K, Ayub MAZ (2008) Enzymatic synthesis of biodiesel from transesterification reactions of vegetable oils and short chain alcohols. *J Am Oil Chem Soc* 85:925-930.
- Rodrigues R, Fernandez-Lafuente F (2010). Lipase from *Rhizomucor miehei* as an industrial biocatalyst in chemical process. *J Mol Catal B: Enzym* 64:1–22
- Rossell B (1999) *LFRA Oils and Fats Handbook, Volume 1, Vegetable Oils and Fats*. Leatherhead Food RA: Leatherhead UK.
- Royon D, Daz M, Ellenrieder G, Locatelli S (2007) Enzymatic production of biodiesel from cotton seed oil using t-butanol as a solvent. *Bioresource Technol* 98:648–653.
- Segall SD, Artz WE, Raslan DS, Ferraz VP, Takahashi JA (2005) Analysis of triacylglycerol isomers in Malaysian cocoa butter using HPLC–mass spectrometry. *Food Res Inter* 38:167-174
- Seong, GH, Heo J, Crooks RM (2003) Measurement of enzyme kinetics using a continuous-flow microfluidic system. *Anal Chem* 75:3161–3167.
- Sheldon RA (2007) Enzyme immobilization: the quest for optimum performance. *Adv Synth Catal* 349:1289-1307.
- Shimada Y, Watanabe Y, Samukawa T, Sugihara A, Noda H, Fukuda H, Tominaga Y (1999) conversion of vegetable oil to biodiesel using immobilized *Candida antarctica* lipase. *J Am Oil Chem Soc* 76:789-793.
- Shimada Y, Watanabe Y, Sugihara A., Tominaga Y (2002) Enzymatic alcoholysis for biodiesel fuel production and application of the reaction to oil processing. *J Mol Catal B: Enzym* 17:133-142.
- Shimada Y, Ogawa J, Watanabe Y, Nagao T, Kawashima A, Kobayashi T, Shimizu S (2003) Regiospecific analysis by ethanolysis of oil with immobilized *Candida antarctica* lipase. *Lipids* 38:181-186.

- Skoog DA, Holler FJ, Crouch SR (2007). *Principle of Instrumental Analysis* 6<sup>th</sup> ed. Thomson-Brooks/Cole: Belmont, CA, USA.
- Soumanou MM, Bornscheuer UT, Schmid U, Schmid RD (1998) Synthesis of structured triglycerides by lipase catalysis. *Fett/Lipid* 100:156–160.
- Stamenković OS., Veličković AV, Veljković VB (2011) The production of biodiesel from vegetable oils by ethanolysis: current state and perspectives. *Fuel* 90:3141-3155.
- Suman M, La Tegola S, Cayellani D, Bersellini U (2005) Liquid chromatography-electrospray ionization-tandem mass spectrometry method for the determination of epoxidised soybean oil in food products. *J Agri Food Chem* 53:9879-9884.
- Sun J, Ju J, Ji L, Zhang L, Xu N (2008) Synthesis of biodiesel in capillary microreactors. *Ind Eng Chem Res* 47:1398-1403.
- Thomsen MS, Nidetzky B (2008) Microfluidic reactor for continuous flow biotransformations with immobilized enzymes: The example of lactose hydrolysis by a hyperthermophilic  $\beta$ -D-galactosidase. *Eng Life Sci* 8:40-48.
- Tranchida PQ, Giannino A, Mondello M, Sciarrone D, Dugo P, Dugo G, Mondello L. (2008) Elucidation of fatty acid profiles in vegetable oils exploiting group-Type patterning and enhanced sensitivity of comprehensive two-dimensional gas chromatography. *J Sep Sci* 31:1797-1802.
- Tserng, K-Y, Kliegman RM, Miettinen, EI, Kalhan, SC (1981) A rapid, simple, and sensitive procedure for the determination of free fatty acids in plasma using glass capillary column gas-liquid chromatography. *J Lipid Res* 22:852-858.
- Türkan A, Kalay S (2006) Monitoring lipase-catalyzed methanolysis of sunflower oil by reversed-phase high-performance liquid chromatography: elucidation of the mechanisms of lipases. *J Chrom A* 1127(1-2):34-44.

Urban, PL, Goodall DM, Bruce NC (2006) Enzymatic microreactors in chemical analysis and kinetic studies. *Biotech Adv* 24:42-57.

Villegas C, Zhao Y, Curtis JM (2010) Two methods for the separation of monounsaturated octadecenoic acid isomers. *J Chrom A* 1217:775-784.

Watts P, Wiles, C. (2007). Recent advances in synthetic micro reaction technology. *Chem Commun* 5:443–467.

Watts P, Wiles C (2007) Micro reactors: a new tool for the synthetic chemist. *Org. Biomol Chem* 5:727–732.

Yang C, Zhang Z, Shi Z, Xue P, Chang P, Yan R (2010) Development of a novel enzyme reactor and application as a chemiluminescence flow-through biosensor. *Anal Bioanal Chem* 397:2997-3003.

Yang Z, Parrish CC, Helleur RJ (1996) Automated gas chromatographic method for neutral lipid carbon number profiles in marine samples. *J Chrom Sci* 34:556-569.

**CHAPTER 2:**

**THE DEVELOPMENT OF A MICROREACTOR USING COMMERCIAL  
SILICA MICROSTRUCTURED OPTICAL FIBER AS A PLATFORM  
FOR ENZYME IMMOBILIZATION FOR USE IN LIPID  
TRANSFORMATION<sup>1</sup>**

---

## **2.1 Introduction**

Recently, microreactor technologies have gained attention for their application in clinical diagnostics, analytical and synthetic chemistry (Mason *et al.*, 2007; Watts and Wiles, 2007; Watts and Wiles, 2008). For example, Kawaguchi *et al.* (2005) have successfully demonstrated the use of a flow-system microreactor for the Moffatt-Swern oxidation of alcohols into carbonyl compounds.

A microreactor integrates various chemical or analytical processes into a single platform made up of reaction channels in the micrometer (50-1000  $\mu\text{m}$ ) range. In such systems, the chemical reaction takes place under conditions of continuous flow (Watts and Wiles, 2007).

---

<sup>1</sup> A version of this chapter has been published. Anuar *et al.* (2011). *Lipids* 46:545-555. "Springer and Lipids, 46, 2011, 545-555, The Development of Flow-through Bio-Catalyst Microreactors from Silica Micro Structured Fibers for Lipid Transformations , Sabilqah Tuan Anuar, Carla Villegas, Samuel M. Mugo, Jonathan M. Curtis, with kind permission from Springer Science and Business Media".

Supplementary data regarding this chapter are given in Appendix 2.

Whether for analytical or synthetic applications, microreactor technology offers several advantages including: reduced reaction time (Mason *et al.*, 2007; Watts and Wiles, 2008) due to the large surface area to volume ratio in the microchannel; enhanced control over the reaction process (Mason *et al.*, 2007); it is less wasteful since only low volumes of reagent are used (Mason *et al.*, 2007); and rapid optimization of reaction conditions can be achieved (Lu *et al.*, 2004; Kawaguchi *et al.*, 2005; Mason *et al.*, 2007; Watts and Wiles, 2008). The microreactors are also ideally suited for continuous flow processes, a highly desired paradigm in processing.

The fabrication of commercially available microreactors (mainly made from glass, quartz, silica or polymers) is however, generally achieved via expensive photolithographic and wet-etching processes, which are complicated and require specialized clean-room facilities (McCreedy, 2000). Therefore, there is much interest in developing cheaper and more easily accessible approaches to the fabrication of microreactors for laboratory applications (McCreedy, 2000; Phan *et al.*, 2004; Xie *et al.*, 2006; Mason *et al.*, 2007; Watts and Wiles, 2007; Ma *et al.*, 2008; Watts and Wiles, 2008; Carvalho *et al.*, 2009). Amongst the attractive platforms used, are microreactors obtained by means of imprinting on polymers including poly-dimethylsiloxane (PDMS), poly(methyl-methacrylate) (PMMA) (Godino *et al.*, 2010) or polyurethanes. However, the use of silica capillaries is possibly the easiest platform to employ as a flow through microreactor with potential for numerous chemical modifications for use in

enzyme-, organo-, or metal- catalyst immobilization (Phan *et al.*, 2004; Xie *et al.*, 2006; Ma *et al.*, 2008).

There is considerable interest in the use of enzymes for lipid transformations such as in the preparation of structured lipids (Irimescu *et al.*, 2002) as well as in biodiesel production (Akoh *et al.*, 2007). The interest is due to the high yields, minimal side products and mild reaction conditions that can be achieved with enzyme-catalyzed processes. A major impediment to the potential commercialization of enzyme-mediated processes is the cost of enzymes and their unstable nature. However, enzyme immobilized over the high surface area of the capillary walls will result in an efficient flow-through microreactor, which is reusable for many process cycles after which the microreactors can be regenerated with new enzyme.

Microstructured fibers (MSF), also commonly known as photonic crystal fibers (PCF), are silica capillaries that consist of a micro-structured arrangement of air channels within a flexible acrylate polymer-coated silica tube. They are widely used as radiation optical guides and in sensor applications (Holton *et al.*, 2004). Basically, these optical fibers are made from three layers: the core, cladding and the coating. Both the core diameter (an individual air channel, usually in the 8-40  $\mu\text{m}$  range) and the number of channels in the photonic fiber can vary depending on the design of the fiber. In addition, the coating diameter - outer diameter of the fiber - could range from 200-500  $\mu\text{m}$  depending on the requirements of the application (Holton *et al.*, 2004), such as in networking or bio-sensing.

Here, it is proposed that the presence and chemistry of silanol groups within MSFs could be exploited as a platform for enzyme immobilization, as has been widely reported for other silica supports (Ma *et al.*, 2008). MSF contain an array of microchannels and hence an enormous surface is available for enzyme immobilization, and may offer an excellent platform for a flow-through microreactor. In order to demonstrate the performance of such a microreactor in mediating lipid transformations, the lipase from *Candida antarctica* was selected, since it is one of the most widely used enzymes for catalysis in lipid transesterification reactions (Akoh *et al.*, 2007; Marchetti *et al.*, 2007). Overall, the objective of this study is to demonstrate the feasibility of immobilizing enzymes onto microstructured fiber (MSF) capillaries and utilizing the microreactors in lipid transformations. This will combine the advantages of microreactor technology with the green chemistry achievable via enzyme immobilization.

## **2.2 Experimental Procedures**

### **2.2.1 Materials:**

MSF capillary (F-SM20, ID: 4-5  $\mu\text{m}$ , outer diameter: 340  $\mu\text{m}$ , 168 holes) was obtained from Newport Corp. (Irvine, CA, USA). Canola oil was obtained from a local grocery store (with ~50% trioleoylglycerol). Sodium hydroxide powder (reagent grade, 97%), sodium phosphate monobasic monohydrate, 3-(aminopropyl)triethoxylane (APTES, 99%), di-sodium hydrogen phosphate



(bioUltra, Fluka, >99%), glutaraldehyde solution (BioChemika, ~50% in H<sub>2</sub>O), sodium cyanoborohydride (NaCNBH<sub>3</sub>, reagent grade, 95%), lipase from *Candida antarctica* (EC 3.1.1.3, BioChemika), potassium sodium tartrate, copper sulfate, and Folin phenol reagent all were obtained from Sigma-Aldrich Ltd (Oakville, ON, Canada).

Acetic acid (glacial, HPLC) was purchased from Fisher Scientific (New Jersey, USA). C18:1 ethyl ester (EE) and TLC 18-1-A [contains by weight 25% of each of trioleoylglycerol (TO), dioleoylglycerol (DO), monooleoylglycerol (MO), methyl oleate (ME)] standards were purchased from Nu-Chek (Elysian, MN, USA), while 1-monooleoylglycerol standard (98%) was obtained from Sigma Aldrich (Oakville, ON, Canada). All organic solvents were HPLC analytical grade from Sigma-Aldrich (Oakville, ON, Canada). Water was purified by a Milli-Q system (Millipore; Bedford, MA, USA).

### **2.2.2 MSF Activation:**

The MSF capillary (15 cm) was activated by flushing with 1 M NaOH solution for 2 h at a flow rate of 10  $\mu$ L/min. The sodium hydroxide activated the inner surface (silanol groups) of the capillary wall. The residual alkali was flushed by 0.1 M HCl for 2 h at a flow rate of 10  $\mu$ L/min. The activated MSF was then dried under N<sub>2</sub> gas before the lipase enzyme immobilization step.

### **2.2.3 Lipase Immobilization onto MSF Capillary Support:**

*Candida antarctica* lipase was immobilized by introduction of amine functional groups onto the silica wall by a silanization reaction; this was followed by the formation of an imide using glutaraldehyde as a bifunctional reagent; finally immobilization was achieved via a condensation reaction with the lipase. This procedure was adapted with some minor modifications from the method reported by Ma *et al.* (2008).

Briefly, the activated MSF was filled with 20% (v/v) APTES (5:2:3 water: acetic acid: APTES) and left overnight with both capillary ends submerged in the 20% APTES solution to complete the reaction. The MSF was then flushed with 0.1 M sodium phosphate buffer (pH 7), followed by reaction with glutaraldehyde solution (5% glutaraldehyde dissolved in 0.1 M sodium phosphate buffer) and left for 4 h in the solution.

The capillary was then flushed with the buffer again before continuously infusing it with 8 mg/mL lipase from *Candida antarctica* in sodium phosphate buffer (0.1 M, pH 7 with 0.1% NaCNBH<sub>3</sub>) for 24 h at room temperature. The sodium borohydride is used to reduce the Schiff base formation and to stabilize the binding of the enzyme to the support. The enzyme-loaded microreactor was finally flushed with the 0.1 M sodium phosphate buffer at which point it was ready for use.

#### **2.2.4 Immobilized Lipase Assay:**

The amount of lipase immobilized on the MSF was determined using the standard Lowry protein assay (Lowry *et al.*, 1951). This was achieved by determining the difference in protein concentration before and after passing the *Candida antarctica* lipase solution through the MSF during the immobilization process.

The Lowry solution was prepared freshly by mixing solution A (4 mg/mL NaOH and 20 mg/mL Na<sub>2</sub>CO<sub>3</sub> in water) and solution B (10 mg/mL potassium sodium tartrate and 50 mg/mL CuSO<sub>4</sub> in water), prior to use. Solutions of known protein concentration (calibration solutions containing 0, 2.5, 5, 7.5, 10, 12.5, 15, 17.5, 20, 25, 30, and 35 µg protein) and lipase solutions (2 µL) were made up to a total volume of 200 µL with deionized water. One mL of Lowry solution was added to each protein solution then after waiting for 15 min, 100 µL Folin phenol reagent was added. After a further 30 min, an aliquot was sampled in a UV-Vis cuvette (10 mm square cuvette) and their absorbance was measured at 750 nm. The concentration of the enzyme solution before and after passing through the microreactor was determined from the protein calibration curve in order to estimate the amount of enzyme immobilized in the microreactor.

#### **2.2.5 Lipase Activity Assay:**

To determine the lipase (esterase) activity, a 3.5 mM solution of *p*-nitrophenyl butyrate (*p*NPB) was prepared in a 1:1 mixture of acetonitrile (ACN)

and 0.1 mM sodium phosphate buffer). The *p*NPB solution was passed through a 15 cm MSF lipase immobilized microreactor at 1  $\mu$ L/min for 1 h. The hydrolysis products were then collected, their volume measured and then diluted to 2.0 mL in mixture of ACN: sodium phosphate buffer (1:1). The absorbance of the resulting solution of products (absorbing molecule, *p*-nitrophenol) was measured at a wavelength of 410 nm.

A calibration curve was obtained by measuring the absorbance of *p*-nitrophenol (*p*NP) standard solutions prepared in the same solvent mixture of ACN and 0.1 mM sodium phosphate buffer (1:1) at concentrations of 0.5, 1, 3, 5 and 7 mM. The concentration of *p*NP hydrolyzed was determined and lipase enzyme activity calculated. The enzyme activity was expressed as the amount of *p*NP formed on the microreactor under the condition used per minute, *i.e.*  $\mu$ g *p*NP/min. One enzyme unit (U) was the amount of protein liberating 1  $\mu$ g of *p*NP per minute.

#### ***2.2.6 Specific Activity of Immobilized Lipase:***

Based on the amount of protein loaded and lipase activity, a specific activity of lipase immobilized in the MSF was calculated according to Dizge *et al.* (2009):

$$\text{Specific activity} = \frac{\text{activity of immobilized lipase}}{\text{amount of protein loaded}}$$

### 2.2.7 Lipid Sample Preparation and Transformation:

The reactant solution of 5 mg/mL canola oil was prepared in ethanol. The mixture was mixed vigorously using a vortex mixer to dissolve the lipid in ethanol. The parameters affecting the performance of the microreactor including reaction flow rate and temperature were investigated and optimized as follows:

#### a) Temperature

Lipid transformation using the immobilized MSF was carried out at room temperature (24 °C), 30 °C, 40 °C, 50 °C, and 60 °C. A schematic illustrating the experimental setup is shown in Figure 2-1. A syringe pump system (Harvard '11' Plus, Harvard Apparatus, Holliston, MA, USA) was used to infuse the reactant through the MSF microreactor. The products of the reaction were collected in a small capped vial with the microreactor poked through the septum of the vial. The temperature that produced the highest yield was then used to optimize the flow rate for the reaction.

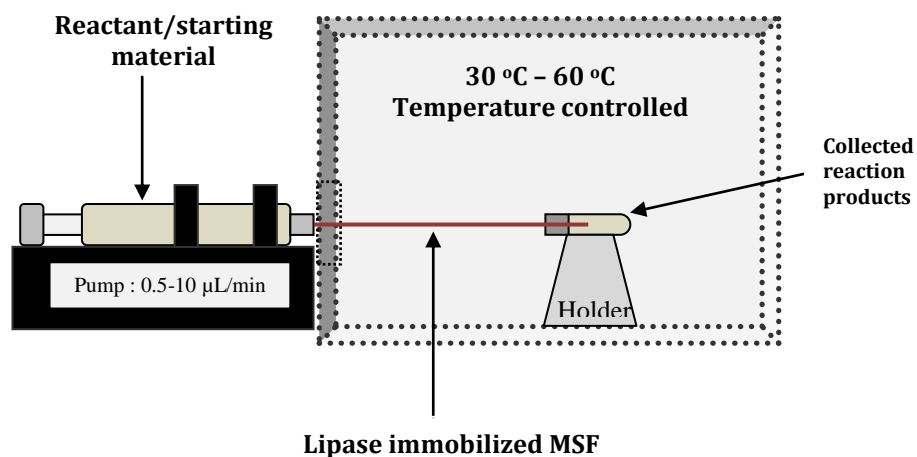


FIG 2-1: Apparatus used with the fabricated MSF microreactor for small scale lipid reactions.

### *b) Flow Rate*

The reactant solution was then pumped through the lipase-immobilized MSF microreactor held at the optimized temperature (50 °C) and using various flow rates (0.5, 1, 5 and 10 µL/min), each held for 3 h. The products were collected into vials for analysis, as described below.

In both the temperature and reaction flow rate optimization experiments, the reaction products collected from the MSF microreactor were diluted 10-25 times in HPLC solvent A (methanol with 0.1% glacial acetic acid) before being analyzed. Standard calibration curves were prepared using 0.05, 0.1, 0.5 and 1.0 mg/mL of total TLC 18-A-1 and 0.05, 0.1, 0.2, 0.5, and 1.0 mg/mL of EE standards. The amount of each compound in the reaction products was determined from the standard calibration curve prepared.

For GC x GC analysis, samples were diluted in dichloromethane and quantified against a calibration curve covering the range of 0.01 to 1 mg/mL of each lipid component.

### **2.2.8 Instrumentation:**

a) A Harvard Model '11' Plus syringe pump (Harvard Apparatus, Holliston, MA, USA) was used to pass all solutions through the MSF both during preparation of the microreactor and for lipid transformations.

b) High-performance liquid chromatography (HPLC) analysis was performed using an Agilent 1200 HPLC system equipped with an evaporative light scattering detector (ELSD) model 1260 Infinity (Agilent Technologies, Santa Clara, CA, USA).

c) Either an Agilent Zorbax HT C18 column (4.6 x 50 mm, 1.8  $\mu\text{m}$ ) (Agilent Technologies; Santa Clara CA, USA) or a Supelco Ascentis Silica column (4.6x150 mm, 3  $\mu\text{m}$ ) (Sigma Aldrich, Oakville, ON, Canada) were used as described below.

d) UV/Visible measurements were made using a Jenway spectrophotometer 6320D series (Bibby Scientific, Staffordshire, UK).

e) <sup>2</sup>A LECO comprehensive 2-dimensional GC  $\times$  GC/FID system (LECO, St. Joseph, MI, USA) was used (Fig. 2-2). It consists of a dual oven GC equipped with flame ionization detector and cryogenic modulator (quadjet) cooled with liquid nitrogen and split–splitless injector. All data was collected by Leco ChromaTOF-GC software v 3.34 optimized for GC  $\times$  GC/FID. The columns used for GCxGC were a DB5HT gas chromatography column (30 m x 0.32 mm x 0.1  $\mu\text{m}$ , bonded and cross-linked 5% phenyl methylpolysiloxane, Agilent technologies; Santa Clara CA, USA) and an RXT65 column (1 m x 0.25 mm x 0.1  $\mu\text{m}$ , crossbond 65% diphenyl-dimethyl polysiloxane, Restek; Bellefonte PA, USA).

---

<sup>2</sup> The 2D-GC analysis was performed by Carla Villages.

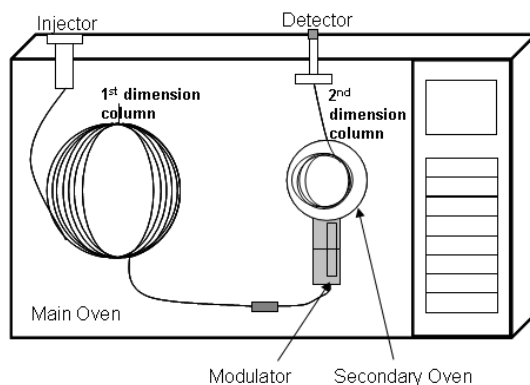


FIG 2-2: Schematic diagram of GC x GC/FID used for analysis of lipid transformation products.

### 2.2.8.1 NARP-LC/ELSD:

Non-aqueous reversed phase (NARP) HPLC with a C18 column was used to speciate the lipid transformation products as well as the starting materials and lipid standards. The ELSD was set to 33 °C and the nitrogen gas flow rate was optimized. All samples were analyzed using an injection volume of 10 µL and a mobile phase flow rate of 1 mL/min. A binary gradient of A, methanol with 0.1% glacial acetic acid; and B, isopropanol/hexane (5:4) was used. The starting condition was 0% B held for 5 min then increased to 66% B in 10 min, held at 66% B for 3.5 min before returning to 0% B (2.5 min) to equilibrate the column.

### 2.2.8.2 GC x GC<sup>3</sup>:

GC x GC was used as a second method to characterize the lipid classes produced by the MSF microreactor and to confirm the LC results. An aliquot of

<sup>3</sup> The 2D-GC analysis was performed by Carla Villages.



the product mixture was dissolved in dichloromethane prior to injection into the LECO GC x GC/FID system. The carrier gas was H<sub>2</sub> at a flow rate of 1.5 mL/min, injection volume 1 µL, split ratio of 15: 1 and He FID make-up gas was used. The inlet and detector temperatures were set to 320 °C and 400 °C, respectively. The temperature program for the first oven was 45 °C (0.5 min) increased at 2 °C/min until 150 °C (0 min) then increased again at 3 °C/min until 375 °C and hold for 10 min. The second oven tracked the first but at a temperature 25 °C higher at all times. The modulator offset was 15 °C.

#### ***2.2.8.3 Regiospecificity Determination using Normal Phase-LC/ELSD:***

Normal phase HPLC with a silica column was used for the regiospecific separation of the MSF microreactor lipid products, following an AOCS standard method Cd 11d-96 (AOCS, 1998). Aliquot of the products formed under the optimized conditions (50 °C, flow rate 1 µL/min) were analyzed by HPLC/ELSD along with a 1-monooleoylglycerol standard.

The method used an injection volume of 10 µL, mobile phase flow rate of 0.5 mL/min, column temperature maintained at 40 °C and the ELSD operating at 90 °C. The mobile phase was a binary gradient of A hexane and B, hexane/isopropanol/ethyl acetate/10% formic acid (80:10:10:1, v/v) (AOCS, 1998). The gradient was 2% B, linear increase to 35% B in 15 min, then linearly increased to 98% in 1 min, and finally held for 10 min at 98% B. The column was allowed to equilibrate at the starting condition for 3 min. Note that all

samples and standards were prepared in hexane/isopropanol (9:1, v/v) prior to analysis.

#### ***2.2.8.4 MSF Morphology Image by Scanning Electron Microscope***

A scanning electron microscope (SEM) (JEOL 6301F; JEOL Ltd., Akishima-Tokyo, Japan) was used for imaging the silica MSF. The MSF was cut to a length of 1-2 mm using a ceramic cutter and mounted on a stub. The mounted MSF sample was then thinly coated with a gold for good electrical conductivity then placed into a holder for transfer to the SEM chamber. The image of the MSF sample was generated by controlling the SEM magnification from 10 to 10 000 times (Fig. 2-3).

### **2.3 Results and Discussion**

#### ***2.3.1 Lipase-immobilized Microreactor Fabrication:***

In this paper, we present the first demonstration of the use of a microreactor, fabricated by immobilizing lipase from *Candida antarctica* onto a silica microstructured fiber (MSF) support, for the ethanolysis of canola oil triacylglycerols. The MSF morphology is shown in the scanning electron microscope image in Figure 2-3.

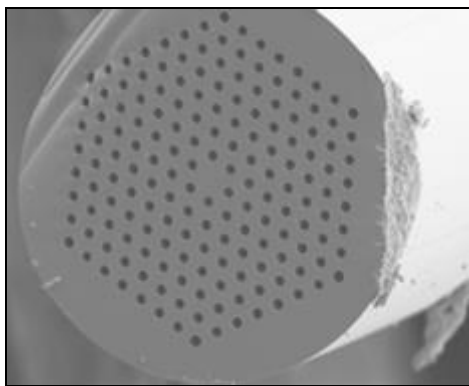


FIG 2-3: Scanning Electron Microscope (SEM) image of a Lipase-Immobilized MSF (168 holes) at x300 magnification.

Although the MSF has been mainly developed for use in light guiding optics, it contains numerous micrometer-sized pores (4-5  $\mu\text{m}$ ) and provides a very large surface area, which makes them ideally suited for immobilizing high amounts of catalysts. Furthermore, the fact that the MSF is made from silica makes it even more attractive for the enzyme immobilization by employing well-known silanization chemistry. In order to ensure the maximum presence of silanol groups at the MSF surface, the use of alkali (NaOH) treatment has been shown to activate the silica wall by increasing the hydrolysis of silanol group (Gibson *et al.*, 2008). The reaction sequence of the immobilization of lipase from *Candida antarctica* onto the silica walls of the MSF is given in Figure 2-4.

Immobilization onto the silica support was achieved by grafting aminopropylethoxilane (APTES) onto the active silanol group (Si-OH) on the MSF wall (Lee *et al.*, 2006). The resultant pendant primary amine group provides

a reactive functionality to form imines when reacted with the bifunctional reagent glutaraldehyde. This in turn results in a pendent carbonyl group from the grafted glutaraldehyde which further reacts with the amino groups of lipase forming a Schiff base, thus covalently attaching the enzyme to the MSF support (Cass and Ligler, 1998; Lee *et al.*, 2006).

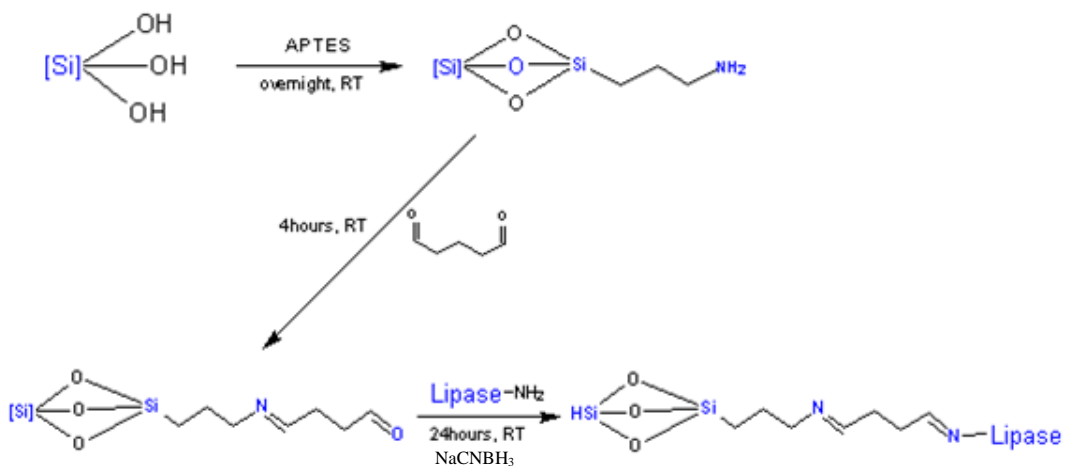


FIG 2-4: The process of lipase-immobilization onto the silica support of a MSF.

It is expected that with such a strong covalent lipase attachment, the probability of enzyme leaching is low and hence the microreactor can potentially be reused multiple times. In contrast, using the simple, commonly used adsorption methods of immobilization, leaching is known to limit reusability (Takahashi *et al.*, 2000; Kim *et al.*, 2007).

### 2.3.2 Enzyme Activity Assay:

Before employing the lipase loaded MSF microreactor it was essential to determine the success of the immobilization method. The total free protein concentration was determined using the widely used Lowry protein assay (Lowry *et al.*, 1951). The amount of protein bound to the MSF microreactor support was estimated by the difference between the amounts of protein in the lipase solution infused through the MSF and the effluent emerging from the MSF. Using this method, the amount of protein loaded on the MSF was determined to be 5.8  $\mu\text{g}/\mu\text{L}$  (Table 2-1).

TABLE 2-1: Determination of the amount of lipase immobilized onto the MSF capillary.

	Protein bound <sup>1</sup> from 1 mL lipase (mg/mL)	Protein bound yield (%)	Lipase activity <sup>2</sup> ( $\mu\text{g pNP}/\text{min}$ ) (U)	Specific activity (U/mg) for 15 cm MSF microreactor	Specific activity for native enzyme (U) before immobilization
Fabricated immobilized MSF	5.83	75.59	4.7	0.81	1.06

<sup>1</sup> 1 mL lipase solution was used to immobilize onto the MSF capillary.

<sup>2</sup> 1U= amount of enzyme to liberate 1  $\mu\text{g pNP}/\text{min}$  under the assay conditions.

It is likely that not all lipase loaded in the MSF is active due to the underlying physicochemical factors associated with the immobilization. As such, it was imperative to also determine the activity of the immobilized lipase. As described in detail in the Experimental Procedures section, the lipase activity of immobilized MSF microreactor was determined by the enzymatic hydrolysis of *p*-nitrophenyl butyrate (*p*NBP) to *p*-nitrophenol, which is quantified

spectrophotometrically. Using this assay, a unit (U) of lipase activity is defined as the amount of enzyme that hydrolyses (liberates) 1  $\mu\text{g}$  of *p*-nitrophenol (*p*NP) from *p*NPB as substrate.

Table 2-1 summarizes the lipase activity assay yield. The enzymatic activity for the immobilized MSF microreactor was determined to be 4.7  $\mu\text{g}$  *p*NP/min (U) for the 15 cm MSF microreactor. Hence, a specific activity of 0.81 U/mg was found for the immobilized lipase from *Candida antarctica* in the MSF microreactor. Data from the manufacturer indicates that the native lipase from *Candida antarctica* has a specific activity of 1.06 U/mg before immobilization (Table 2-1). Therefore, only about 23.6% of the enzyme activity was lost during the proposed immobilization process. This result is comparable with that found in other studies, for example, specific activities of 0.60-0.9 were found using similar methods for lipase immobilized onto styrene-divinylbenzene and styrene-divinylbenzene - polyglutaraldehyde copolymers for biodiesel production (Dizge *et al.*, 2009).

A goal in the development of the lipase immobilized MSF microreactor was to evaluate its performance in lipid transformations. This was done by transesterifying trioleoylglycerol (molecular weight 884) in ethanol in the MSF microreactor. From this reaction, the major transesterified products which were obtained were monooleoylglycerol and ethyl oleate (EE). Since monooleoylglycerol and EE results from the hydrolysis of 2 and 3 ester bonds/molecule respectively, the theoretical conversion rates of trioleoylglycerol can be estimated from the measured lipase activity of 4.7  $\mu\text{g}$  *p*NP/min (U)

assuming that lipase catalysed hydrolysis of triacylglycerol (TAG) ester occurs at the same rate as the lipase catalysed hydrolysis of *p*NBP to give *p*NP. If this assumption is made, then the conversion rate of 5 mg/ml trioleoylglycerol at 1  $\mu$ L/min to monooleoylglycerol and to ethyl oleate would be predicted to be 10 and 6.7  $\mu$ g/min (or 0.0115 and 0.0075 mol/min) respectively. It is apparent that notwithstanding the gross assumptions made, the observed conversion rate (trioleoylglycerol - monooleoylglycerol) is of the same order of magnitude as the rate predicted based on the measured enzyme activity. This implies that to a rough approximation, the enzyme activity assay is quite consistent with the measured results for trioleoylglycerol conversion (described in the next section). It should also be pointed out that canola oil rather than trioleoylglycerol was actually used in the experiments, but this does not change the general arguments used above.

### ***2.3.3 Enzymatic-catalyzed Ethanolysis using MSF Microreactor:***

The ethanolysis of canola oil was performed using the lipase-immobilized MSF microreactor at different temperatures and flow rates, in order to determine the optimal conditions. The selected temperature range was chosen based on the optimized lipase enzyme conditions of other researchers including Köse *et al.* (2001) and Irimescu *et al.* (2002). The former suggested optimal conditions at room temperature, while the latter indicated denaturation of the enzyme at temperatures  $>50$  °C, by decreasing the reaction yield. The products obtained

were then analyzed by NARP-LC/ELSD and Figure 2-5 (a,b) show the chromatograms obtained for both the starting material and pure standards. The conversion of triacylglycerol in canola oil was estimated by means of a calibration curve of a lipid standard consisting of trioleoylglycerol, dioleoylglycerol, monooleoylglycerol and ethyl oleate (Table 2-2).

The data in Table 2-2 show the relative concentrations of reaction products obtained using a flow rate of 1  $\mu\text{L}/\text{min}$  of canola oil TAG in ethanol solution passing through the lipase immobilized MSF microreactor, conditioned at various temperatures. From the LC/ELSD analysis it was found that whilst EE and monoacylglycerols (MAG) products were formed under all conditions, diacylglycerols (DAG) were not observed above the limit of detection, possibly due to the microscale nature of our study. The predominant formation of monooleoylglycerol relative to dioleoylglycerol is consistent with results of others (Irimescu *et al.*, 2002).

In Table 2-2 it is clear that at low temperatures, the conversion of triacylglycerol into other lipid forms was low, and similar result was found at 60  $^{\circ}\text{C}$ . However, at around 50  $^{\circ}\text{C}$  virtually all of the triacylglycerol was consumed indicating a high efficiency of the immobilized lipase microreactor under these conditions.



TABLE 2-2: Lipid products formed from canola oil using the lipase immobilized MSF microreactor at various temperatures using a reaction flow rate of 1  $\mu$ L/min.

Lipid classes	Reaction temperature																				Starting material
	24°C				30°C				40°C				50°C				60°C				
	EE	MAG	DAG	TAG	EE	MAG	DAG	TAG	EE	MAG	DAG	TAG	EE	MAG	DAG	TAG	EE	MAG	DAG	TAG	TAG
Analytical method																					
LC/ELSD (mol %)	9%	9%	nd	82%	3%	14%	nd	84%	3%	24%	nd	73%	5%	95%	nd	nd	2%	3%	nd	96%	100%
GCxGC/FID (mol %)	22%	5%	21%	53%	nt	nt	nt	nt	nt	nt	nt	nt	37%	59%	nd	3%	nt	nt	nt	nt	nt

Result of NARP-HPLC/ELSD analysis are compared to GCxGC/FID data for selected samples. Mole percentages were estimated based on the response of trioleoylglycerol, dioleoylglycerol, monooleoylglycerol and ethyl oleate standards.

*nd* not detected.

*nt* not tested.

The effect of the reaction flow rate on the lipid conversion was then investigated with the temperature fixed at 50 °C (Figs. 2-5 c-e).

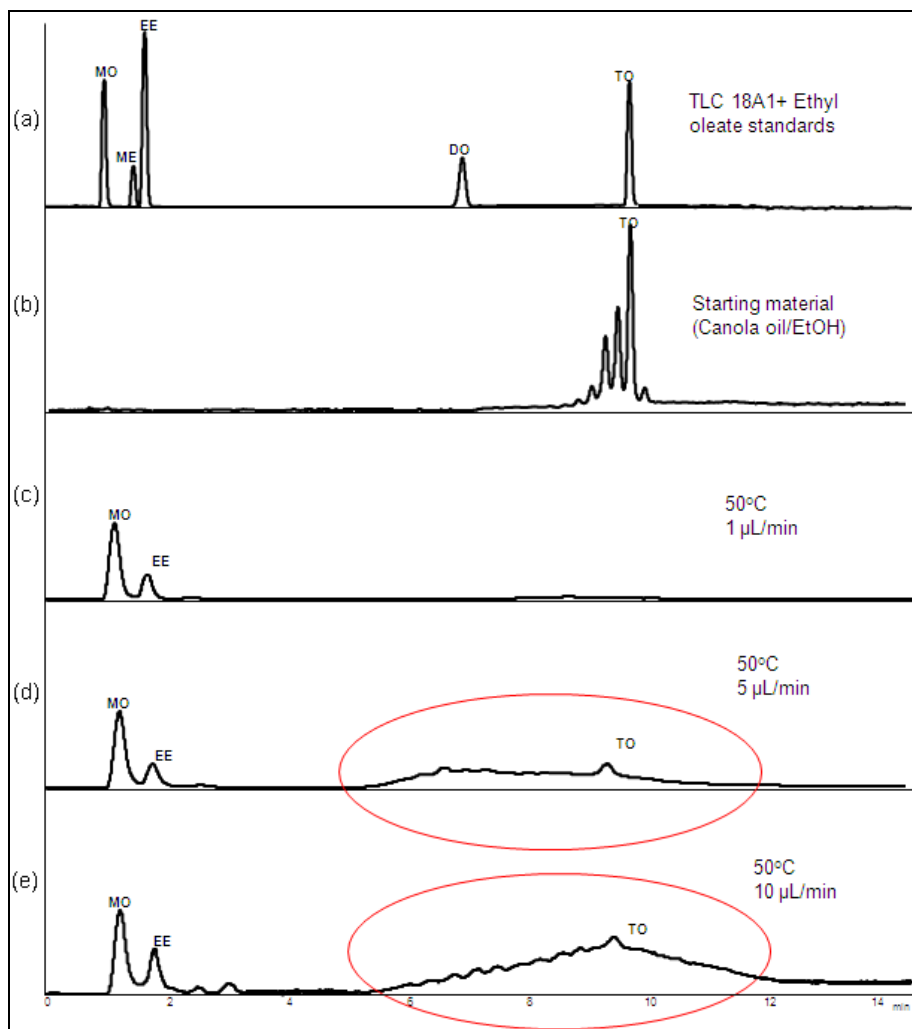


FIG 2-5: NARP-LC/ELSD separation of (a) a lipid standard mixture containing *MO* monooleoylglycerol; *ME* methyl oleate; *EE* ethyl oleate; *DO* dioleoylglycerol; *TO* trioleoylglycerol, (b) canola oil/ethanol (the starting reactant mixture for the MSF microreactor), and c-e the effect of reaction flow rate for a canola oil solution in ethanol passing through the lipase immobilized MSF microreactor at: (c) 1 μL/min; (d) 5 μL/min; and, (e) 10 μL/min. All c-e reactions were carried out at 50 °C. The ellipse shows the MSF column carry-over around the TAG peak that could not be resolved.

As indicated in Figures 2-5 c-e, the microreactor flow rates investigated included 1, 5 and 10  $\mu\text{L}/\text{min}$ . The narrow flow rate range evaluated was due to the achievable linear force of the syringe pump utilized (Harvard'11' Plus). The results show that the optimal flow rate for the enzymatic MSF microreactor reaction is at 1  $\mu\text{L}/\text{min}$ , where complete disappearance of the TAG starting material was evident along with the formation of MAG and EE.

As the flow rate increased above 1  $\mu\text{L}/\text{min}$ , a broad 'hump' is seen in the chromatogram, co-eluting with unreacted starting material (Figs. 2-5 d, e). This is likely due to removal of oligomeric glutaraldehyde material from the walls of the microreactor attributable to the high pressures ( $\sim 21$  psi) that occur with higher flow rates through the small channels in the MSF reactor. However, since the flow rate of 1  $\mu\text{L}/\text{min}$  (which corresponds to a residence time of 28.5 s in the 15 cm MSF) allows sufficient contact time between the starting material and the lipase immobilized in the microreactors, these destructive conditions can be avoided. As demonstrated in Figure 2-5, the lipid transformation performance reduces as flow rate increases due to the lower contact time of the substrates with the immobilized lipase. At 10  $\mu\text{L}/\text{min}$  the calculated MSF residence time was 3 s.

Recently, there have been several reports describing how ethanolysis of TAG using immobilized lipase from *Candida antarctica* can, under certain conditions, become 1,3 regiospecific (Irimescu *et al.*, 2002; Shimada *et al.*, 2003). Furthermore, the reaction in excess ethanol can also promote the formation of the 2-MAG, compared to other products (Watanabe *et al.*, 2009). For example, using an ethanol/trioleoylglycerol molar ratio of 77:1 at 25°C, Novozyme 435 beads and

a reaction time of 4 h, Irimescu *et al.* (2002) achieved an ~88% reaction yield of which >98% of the acylglycerol content was 2-monooleoylglycerol. The actual molar ratio of ethanol:TAG has also been shown to be important in order to achieve regiospecificity and high reaction rates (Muñío *et al.*, 2008). In systems where long reaction times are possible, it has been proposed (Irimescu *et al.*, 2002; Shimada *et al.*, 2003) that although 2-MAG is formed exclusively at low ethanolysis times, longer times (>7 h under the conditions used in that study) result in acyl migration forming some 1[3]-MAG. However, in the present experiment, reaction times range from seconds to a few minutes, so acyl migration is unlikely to occur.

To confirm the regiospecificity of the ethanolysis reaction in the microreactor, a sample of canola oil that passed through the reactor under the optimized conditions for maximum conversion of TAG to MAG (1  $\mu$ L/min, 50  $^{\circ}$ C) was collected. The regiospecificity was then determined by normal phase HPLC following AOCS official method Cd 11d-96 (AOCS, 1998), as described in the Materials and Methods section. This confirmed that >96% of the MAG produced was indeed 2-MAG. Figure 2-6 illustrates the addition of a 1-monooleoylglycerol standard to the MAG product; before the addition there was no peak at the retention time of the 1-monooleoylglycerol standard (data not presented) confirming that the product is the 2-MAG isomer.

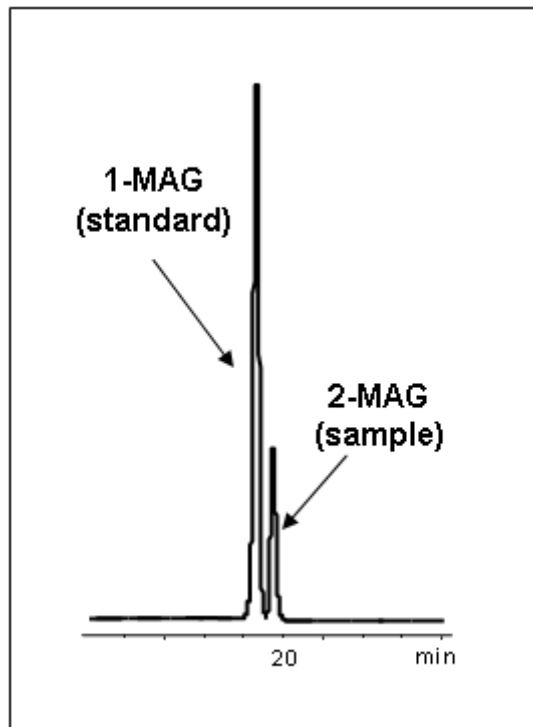


FIG 2-6: Chromatograms of a 1-monooleoylglycerol standard and the MAG product of passing canola oil through the microreactor<sup>4</sup>.

It should be noted that Table 2-2 presents qualitative data, which serves to illustrate the performance of the microreactor, rather than rigorous quantitative results. These shortcomings are in part due to the difficulties associated with collecting and manipulating small volumes of solution eluting from a prototype device. Also, there are several disadvantages of performing analysis using LC/ELSD, one which is that the ELSD response is not the same towards all compounds, being greatly affected by analyte volatility, and non-linearity<sup>5</sup>. As a

---

<sup>4</sup> Supplementary data are given in Appendix A2-3.

<sup>5</sup> Supplementary data are given in Appendix A2-1 to A2-2.

result, the measured EE concentration in particular, is less reliable. Another drawback of the LC/ELSD analysis is that it did not separate the microreactor column bleed from the DAG and TAG peaks, when operating at high reactant flow rates (Figs. 2-5 d, e). Therefore, a second independent analytical method was carried out to support the findings of the LC/ELSD results. The method chosen uses comprehensive two-dimensional gas chromatography (GC x GC/FID) to separate neutral lipid microreactor products.

GC x GC (Figure 2-2) is a multidimensional technique that consists of orthogonal hyphenation (*via* a cryogenic modulator) of two columns of different stationary phases, each housed in its own temperature programmable oven. Upon injection of the sample chromatography takes place conventionally on the first column but subsequently the modulator collect the effluent and periodically re-injects it into the second column for further separation (Dalluge *et al.*, 2003; Górecki *et al.*, 2004).

The sampling frequency is high enough so that each peak eluting from the first column is sampled at least multiple times, thus preserving the primary separation in addition to the separation in the second column (Dalluge *et al.*, 2003; Górecki *et al.*, 2004; Semard *et al.*, 2009). Thus, GC x GC is essentially multiple sequential heart-cuts. The raw data have to be converted from the conventional linear form to a 2D representation using special software algorithms (Górecki *et al.*, 2004; Semard *et al.*, 2009).

The GC x GC results obtained for the MSF reaction products at room temperature and 50 °C are presented in Figure 2-7 and in Table 2-2. In both cases, the optimal flow rate, 1  $\mu$ L/min was used. Note that the tandem high temperature columns used in the GC x GC experiments preclude the need for the typical silylation derivatizations of lipids to increase their volatility in order to enable their GC analysis.

What is notable in Figure 2-7 is the complete separation of EE, MAG, DAG and TAG along with the relatively higher response of EE compared to that seen by LC/ELSD. In addition, the presumably oligomeric material (carry-over) discharged from the microreactor especially at high flow rates does not interfere with the separation of lipid peaks (Fig. 2-7), further giving credence to the use of GC x GC. Using the GC x GC method, the compounds with lower molecular weight (EE) elute first, followed by MAG, DAG and TAG. Also, the response for the volatile EE is higher than for the other lipid classes in contrast to the LC/ELSD method where the opposite is observed. This discrepancy in product yields (seen in Table 2-2) may be a consequence of the nonlinear nature of HPLC/ELSD, especially for compounds differing in volatility. In general, the GC x GC/FID results support the conclusions of the LC/ELSD data described above, but the estimated ethyl ester concentrations are considerably higher and likely much more realistic (Table 2-2).

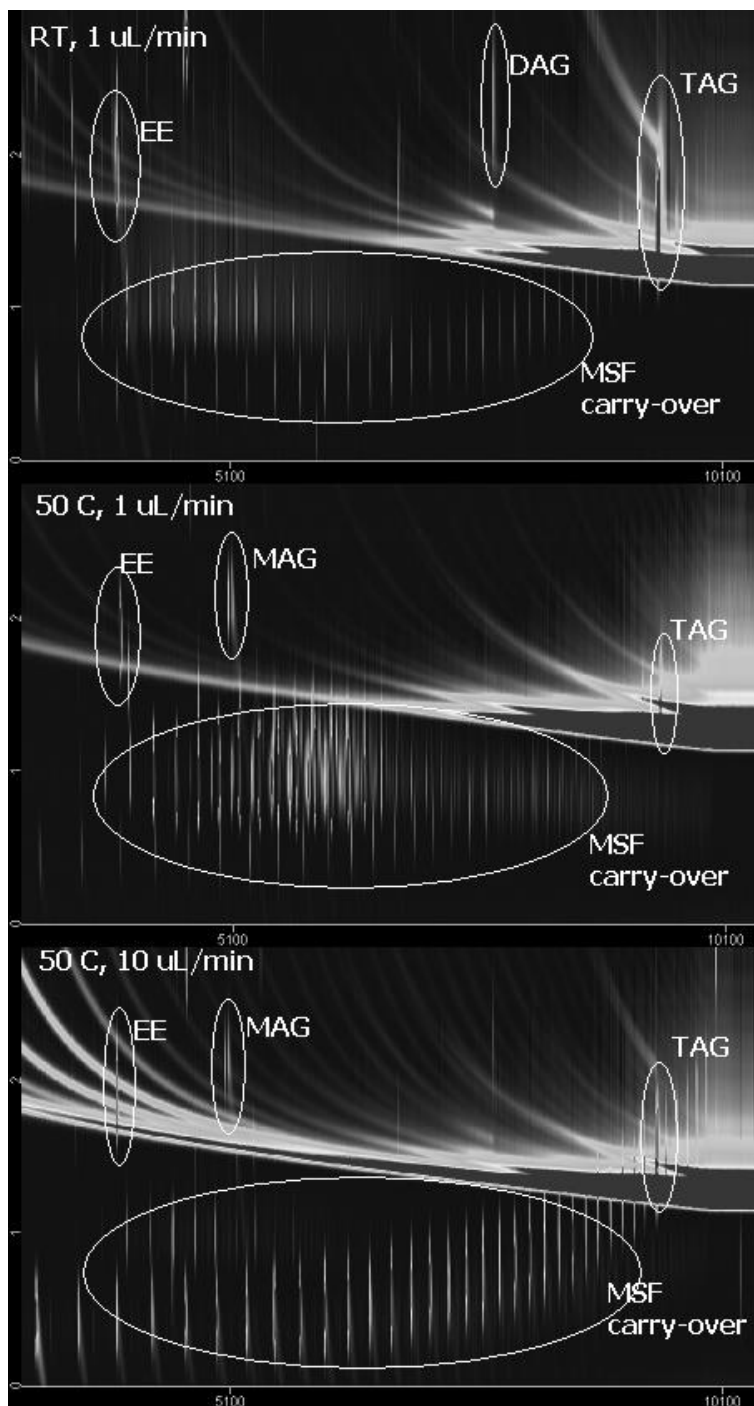


FIG 2-7: GC x GC/FID<sup>6</sup> chromatograms of products from ethanolsis of canola oil using the MSF microreactor. The microreactor bleed (“carry-over”) separates from the identified *circled* lipid products.

<sup>6</sup> The 2D-GC analysis was performed by Carla Villages. Supplementary data are given in Appendix A2-5 to A3-7.



## 2.4 Conclusion

In conclusion, the results clearly demonstrate the successful lipase immobilization on silica microstructure fibers and the use of the resulting microreactor for the ethanolysis of a vegetable oil under conditions of continuous flow. A high degree of regiospecificity was observed in the reaction under optimized conditions, with almost complete conversion to 2-monoacylglycerol. This is consistent with earlier reports for ethanolysis using the same lipase (Irimescu *et al.*, 2002; Shimada *et al.*, 2003), although under quite different reaction conditions and at much lower reaction rates. Although not yet robust, the MSF microreactors have been reused several times, and future work will aim to produce microreactors with longer lifetimes. It is envisioned that on-line enzyme immobilize MSF microreactors will prove to be valuable in analytical lipid profiling applications.

## 2.5 References

- Akoh CC, Chang SW, Lee GC, Shaw JF (2007) Enzymatic approach to biodiesel production. *J Agric Food Chem* 55:8995–9005.
- American Oil Chemists' Society (1998) Official method Cd 11d-96 mono- and diglycerides determination by HPLC-ELSD In: Firestone D (ed) *Official Methods and Recommended Practices of the AOCS, 5<sup>th</sup> edn*. American Oil Chemists' Society: Champaign, IL, USA.
- Carvalho AT, Lima RR, Silva LM, Simoões EW, Silva MLP (2009) Three-dimensional microchannels as a simple microreactor. *Sens Actuat B* 137:393–402.

- Cass T, Ligler FS (1998) *Immobilized Biomolecules in Analysis: A Practical Approach*. Oxford University Press: Oxford, UK.
- Dalluge J, Beens J, Brinkman UAT (2003) Comprehensive two dimensional gas chromatography: a powerful and versatile analytical tool. *J Chrom A* 1000:69–108.
- Dizge N, Keskinler B, Tanriseven A (2009) Biodiesel production from canola oil by using lipase immobilized onto hydrophobic microporous styrene-divinylbenzene copolymer. *Biochem Eng J* 44:220–225.
- Gibson GTT, Mugo SM, Oleschuk RD (2008) Surface mediated effects on porous polymer monolith formation within capillaries. *Polymer* 49:3084–3090.
- Godino N, Campo FJ, Muñoz FX, Hansen MF, Kutter JP, Snakenborg D (2010) Integration of a zero dead-volume pdms rotary switch valve in a miniaturized (bio) electroanalytical system. *Lab Chip* 10:1841–1847.
- Gońrecki T, Harynuk J, Panic O (2004) The evolution of comprehensive two-dimensional gas chromatography. *J Sep Sci* 27:359–379.
- Holton C, Meissner K, Herz E, Kominsky D, Pickrell G (2004) Colloidal quantum dots entrained in micro-structured optical fiber In: Durvasula LN (ed) *Fiber Lasers: Technology, Systems, and Applications*. 2004 Proceedings SPIE: Bellingham, WA, USA. 5335:258–265.
- Irimescu R, Iwasaki Y, Hou CT (2002) Study of tag ethanolysis to 2-MAG by immobilized *Candida antarctica* lipase and synthesis of symmetrically structured TAG. *J Am Oil Chem Soc* 79:879–883.
- Kawaguchi T, Miyata H, Ataka K, Mae K, Yoshida J (2005) Room-temperature Swern oxidations by using a microscale flow system. *Angew Chem Int Ed* 44:2413–2416.

- Kim MI, Kim J, Lee J, Jia H, Na HB, Youn JK, Kwak JH, Dohnalkova A, Grate JW, Wang P, Hyeon T, Park HG, Chang HN (2007) Crosslinked enzyme aggregates in hierarchically ordered mesoporous silica: a simple and effective method for enzyme stabilization. *Biotech Bioeng* 96:210–218.
- Koçse O , Tuğter M, Ays,e Aksoy H (2001) Immobilized *Candida antarctica* lipase-catalyzed alcoholysis of cotton seed oil in a solvent-free medium. *Biores Tech* 83:125–129.
- Lee DH, Park CH, Yeo JM, Kim SW (2006) Lipase immobilization on silica gel using a cross-linking method. *J Ind Eng Chem* 12:777–782.
- Lowry OH, Rosebrough NJ, Farr AL, Randall RJ (1951) Protein measurement with the Folin phenol reagent. *J Biol Chem* 193:265–275.
- Lu SY, Watts P, Chin FT, Hong J, Musachio JL, Briard E, Pike VW (2004) Syntheses of <sup>11</sup>C- and <sup>18</sup>F - labeled carboxylic esters within a hydrodynamically driven micro-reactor. *Lab Chip* 4:523–525.
- Ma J, Liang Z, Qiao X, Deng Q, Tao D, Zhang L, Zhang Y (2008) Organic-inorganic hybrid silica monolith based immobilized trypsin reactor with high enzymatic activity. *Anal Chem* 80:2949–2956.
- Marchetti JM, Miguel VU, Errazu AF (2007) Possible methods for biodiesel production. *Renew Sust Energy Rev* 11:1300–1311.
- Mason BP, Price KE, Steinbacher JL, Bogdan AR, McQuade DT (2007) Greener approaches to organic synthesis using microreactor technology. *Chem Rev* 107:2300–2318.
- McCreeedy T (2000) Fabrication techniques and materials commonly used for the production of microreactors and micro total analysis systems. *Trends Anal Chem* 19:396–401.

- Muñoz MM, Esteban L, Robles A, Hita E, Jiménez MJ, González PA, Camacho B, Molina E (2008) Synthesis of 2-monoacylglycerols rich in polyunsaturated fatty acids by ethanolysis of fish oil catalyzed by 1, 3 specific lipases. *Process Biochem* 43:1033–1039.
- Phan NTS, Brown DH, Styring P (2004) A facile method for catalyst immobilisation on silica: nickel-catalysed Kumada reactions in mini-continuous flow and batch reactors. *Green Chem* 6:526–532.
- Semard G, Adahchour M, Focant JF (2009) Chapter 2 basic instrumentation for GC. *Compr Anal Chem* 55:15–48.
- Shimada Y, Ogawa J, Watanabe Y, Nagao T, Kawashima A, Kobayashi T, Shimizu S (2003) Regiospecific analysis by ethanolysis of oil with immobilized *Candida antarctica* lipase. *Lipids* 38:1281–1286.
- Takahashi H, Li B, Sasaki T, Miyazaki C, Kajino T, Inagaki S (2000) Catalytic activity in organic solvents and stability of immobilized enzymes depend on the pore size and surface characteristics of mesoporous silica. *Chem Mater* 12:3301–3305.
- Xie C, Ye M, Jiang X, Jin W, Zou H (2006) Octadecylated silica monolith capillary column with integrated nanoelectrospray ionization emitter for highly efficient proteome analysis. *Molec Cell Proteom* 5:454–461.
- Watanabe Y, Nagao T, Shimada Y (2009) Control of the regiospecificity of *Candida antarctica* lipase by polarity. *New Biotech* 26:23–28.
- Watts P, Wiles C (2007) Recent advances in synthetic microreaction technology. *Chem Commun* 5:443–467.
- Watts P, Wiles C (2007) Micro reactors: a new tool for the synthetic chemist. *Org Biomol Chem* 5:727–732.

## CHAPTER 3:

# THE DEVELOPMENT OF A MICROREACTOR USING SILICA MONOLITH FORMED WITHIN A FUSED SILICA CAPILLARY AS A PLATFORM FOR ENZYME IMMOBILIZATION FOR USE IN LIPID TRANSFORMATION<sup>7</sup>

---

### 3.1 Introduction

A microreactor is a device that consists of microstructured components in which chemical reactions can take place in continuous flow (Watts and Wiles, 2007). New technologies for producing microreactors have been employed both in organic synthesis and more recently in biotechnology (Bolivar *et al.*, 2011). Microreaction devices were initially designed primarily for integrating different analytical or chemical processes including sample preparation, derivatization, separation and detection into a single platform.

Most of the microreactors currently made enable the use of micro- and sometimes nano-litre process volumes, hence the terms ‘microfluidic’ and ‘nanofluidic’ are often applied (Ehrfeld *et al.*, 2000). Microreactors can be used as an efficient and sustainable way of doing chemical synthesis (Ehrfeld *et al.*,

---

<sup>7</sup> A version of this chapter has been published. Anuar *et al.* (2013). *Journal of Molecular Catalysis B: Enzymatic* 92: 62-70.

“Reprinted from *Journal of Molecular Catalysis B: Enzymatic* , 92, Sabiqah Tuan Anuar, Yuan-Yuan Zhao, Samuel M. Mugo, Jonathan M. Curtis, The Development of a Capillary Microreactor for Transesterification Reactions using Lipase Immobilized onto a Silica Monolith, 62-70, Copyright (2013), with permission from Elsevier”.

Supplementary regarding this chapter are given in Appendix 3.

2000; Watts and Wiles, 2007; Watts and Wiles, 2007; Bolivar *et al.*, 2011) that achieve high separation efficiencies and use small reagent volumes, thereby reducing waste. Other reported applications of microreactor technologies include their integration on-line with mass spectrometry for real-time proteomic analysis (Brivio *et al.*, 2002; Zhou *et al.* 2012), as emitters in electrospray (Xie *et al.*, 2006) and atmospheric pressure photoionization (Kauppila *et al.*, 2004) mass spectrometry and in chromatography and electrophoresis (Ishizuka *et al.*, 2000; Klepárník, 2013).

Commercially available microreactors can be expensive due to the complex methods that are required for their manufacture (McCreeedy, 2000). These fabrication methods are varied based on the end purpose of the microreactor, choice of the support (e.g. silica, quartz, metal, glass or polymer supports) (Athens *et al.*, 2009; Carvalho *et al.*, 2009; Kataoka *et al.*, 2010; Mugo and Ayton, 2010; Chapter 2) and the catalyst that is immobilized (Phan *et al.*, 2004; Ma *et al.*, 2008; Athens *et al.*, 2009; Kataoka *et al.*, 2010; Mugo and Ayton, 2010).

The objective of this work is to create and test a flow-through lipase immobilized silica monolithic microreactor for small-scale lipid transformations. The use of a lipase-mediated approach for lipid transformations is of major interest in biodiesel, structural lipids synthesis and in lipidomics (Soumanou *et al.*, 1998; Irimescu *et al.*, 2002; Shimada *et al.*, 2002; Lara and Park, 2004; Akoh *et al.*, 2007; Chopra *et al.*, 2008; Kataoka *et al.*, 2010). A commonly used enzyme in lipid catalysis is the commercially available lipase isolated from

*Candida antarctica* (Akoh *et al.*, 2007). Immobilized *C.antarctica* lipase has been used by others for the conversion of triacylglycerols (TAG) to fatty acid alkyl esters, diacylglycerols and monoacylglycerols (Irimescu *et al.*, 2002; Shimada *et al.*, 2002; Chapter 2). It has also been employed for synthesis of flavor compounds such as butyl laurate (Mugo and Ayton, 2010) or isoamyl acetate (Pohar *et al.*, 2009) and in hydrolysis of nitrophenyl butyrate (He *et al.*, 2010). Since enzymes are generally expensive, their immobilization is desirable to promote its recovery and reusability (Ehrfeld *et al.*, 2000; Thomsen *et al.*, 2007; Watts and Wiles, 2007; Ma *et al.*, 2008; Athens *et al.*, 2009; He *et al.*, 2010; He *et al.*, 2010; Kataoka *et al.*, 2010; Mugo and Ayton, 2010; Bolivar *et al.*, 2011; Chapter 2).

In this chapter, the use of a silica monolith support for lipase immobilization *via* silanol chemistry has been investigated. A silica monolith should be a favorable substrate for enzyme immobilization since it can provide a large surface area while maintaining a good flow-through characteristic with minimal back-pressure (Ishizuka *et al.*, 2000; Xie *et al.*, 2006; Thomsen *et al.*, 2007; Ma *et al.*, 2008; Kawakami *et al.*, 2009; He *et al.*, 2010). The structure of the silica scaffold also allows a high loading capacity for the immobilized lipase.

The fabricated silica monolith microreactor has been employed for small-scale (microlitre volumes) transesterification targeted to analytical lipid applications. Previously, the product was collected off-line and then injected into a mass spectrometer for analysis (Kauppila *et al.*, 2004; Xie *et al.*, 2006). Here, it is demonstrated how transesterification products eluting from the microreactor

can flow directly into an atmospheric pressure photoionization-mass spectrometer (APPI-MS) ion source, allowing real-time monitoring of the reaction. Although there are some reports of in-line coupling mass spectrometry (especially using ESI and MALDI) with enzymatic microfluidic devices (Bolivar et al., 2011; Brivio *et al.*, 2002; Xie *et al.*, 2006; Zhou *et al.* 2012) the technology is still in its infancy. Furthermore, while ESI is the ionization method of choice in proteomics, it is not suitable for the analysis of lipids such as fatty acid alkyl esters due to its poor response towards these low polarity compounds. For this reason, in this work have used a photoionization source, which is better suited to the analysis of many lipids compared to ESI. The integration of APPI-MS with enzymatic microreactor has not been reported before.

## **3.2 Experimental Procedures**

### **3.2.1 Materials:**

Fused silica capillary (ID: 320  $\mu\text{m}$ ) was obtained from Polymicro Technologies (Phoenix, AZ, USA). All the PEEK tubing (ID: 0.005 in), PTFE fittings (F-110), sleeves and ferrules were obtained from Upchurch Scientific (Oak Harbor, WA, USA). Tetraethyl orthosilicate (TEOS, 98%), 3-(aminopropyl)triethoxysilane (APTES, 99%), polyethylene glycol (PEG, MW: 10 000), sodium hydroxide powder (reagent grade, 97%), sodium phosphate monobasic monohydrate, disodium hydrogen phosphate (bioUltra, Fluka, 99%), glutaraldehyde solution (BioChemika, 50% in  $\text{H}_2\text{O}$ ), sodium cyanoborohydride



(NaCNBH<sub>3</sub>, reagent grade, 95%), lipase from *Candida antarctica* (EC 3.1.1.3, BioChemika), potassium sodium tartrate, copper sulfate, and Folin phenol reagent all were obtained from Sigma-Aldrich Ltd (Oakville, ON, Canada).

Acetic acid (glacial, HPLC) was purchased from Fisher Scientific (Bridgewater, NJ, USA). Pure trioleoylglycerol (TO) together with ethyl oleate (EE) and TLC 18-1-A (contains by weight 25% of each of trioleoylglycerol (TO), dioleoylglycerol (DO), monooleoylglycerol (MO), methyl oleate (ME)) standards were purchased from Nu-Chek (Elysian, MN, USA). Acetonitrile, ethanol, dichloromethane, hexane, isopropanol and methanol were all HPLC analytical grade from Sigma-Aldrich (Oakville, ON, Canada).

### **3.2.2 Preparation of Silica Monolith Capillary:**

The silica monolith capillary was prepared following the procedure reported elsewhere (Ishizuka *et al.*, 2000; Xie *et al.*, 2006), but with some modification. Briefly, fused silica capillary (15 cm) was prepared by activating the surface with 1 M NaOH solution for 2 h at a flow rate of 10  $\mu$ L/min. The residual alkali was washed with 0.1 M HCl for 2 h at a flow rate of 10  $\mu$ L/min, and then the silica capillary was dried by a flow of air.

The prepolymer sol-gel was prepared by mixing 0.1 g PEG with 0.45 mL TEOS and 1 mL 0.01 M acetic acid in ice for 45 min. The silica capillary was then filled with the prepolymer sol-gel at a flow rate of 5  $\mu$ L/min for 2 h. Both ends of the capillary were then sealed before it was immersed into a water bath at

40 °C for 24 h. Finally, the resulting monolith was calcined to degrade all organic moieties by heating the capillary in an oven at 200 °C for a further 24 h. After this, the monolith was ready for lipase immobilization.<sup>8</sup>

### ***3.2.3 Lipase Immobilization onto the Monolithic Silica Support:***

The lipase from *C. antarctica* was immobilized onto the monolithic supports using the glutaraldehyde as a cross linking agent, as previously reported (Mugo and Ayton, 2010; Chapter 2, Fig.2-4).

To prepare the silica monolith capillary for immobilization, it was flushed with 0.1 mM sodium phosphate buffer (at pH 7.2). The capillary was filled with APTES solution containing 2:3:5 (v/v/v) parts of APTES: CH<sub>3</sub>CH<sub>2</sub>COOH: H<sub>2</sub>O and left overnight at room temperature in order to ensure that the APTES had been fully grafted onto the silica monolith. This results in a surface containing free primary amines available for reaction with the cross-linker. The capillary was then washed with the 0.1 mM phosphate buffer for 1 h at 5 µL/min, followed by 5% glutaraldehyde solution in 0.1 mM sodium phosphate buffer for 4 h at the same flow rate. The capillary was again washed with a flow of phosphate buffer followed by loading with an 8 mg/mL lipase solution in sodium phosphate buffer containing 0.1% NaCNBH<sub>3</sub> for 24 h at room temperature and a flow rate of 1 µL/min. The lipase-immobilized microreactor was ready for use after a final flush with sodium phosphate buffer.

---

<sup>8</sup> Supplementary data are given in Appendix A3-1 to A3-2.

### **3.2.4 Evaluation of the Lipase-immobilized Microreactor:**

#### **3.2.4.1 Characterization of Microreactor:**

A scanning electron microscope (SEM) (JEOL 6301F; JEOL Ltd., Akishima-Tokyo, Japan) was used for imaging the silica monolith. Sample was prepared as previously stated in Chapter 2, Section 2.2.8.4. Attenuated-total reflection (ATR) Fourier transform infrared (FTIR) spectroscopy (TENSOR 27 FTIR Spectroscopy with Diamond ATR A225/Q, Bruker Optics GmbH, Ettlingen, Germany) equipped with OPUS 6.5 spectroscopy software (Bruker Optics GmbH, Ettlingen, Germany) was used to characterize the changes in the surface functional groups during the multiple steps of lipase immobilization.

Before the analysis, the diamond ATR crystal was solvent washed, dried and an infrared background was collected. The sample was loaded onto the ATR crystal and scanned in the mid infra-red region of 4000-400  $\text{cm}^{-1}$ ; 8 scans were averaged over 20 sec for each spectrum. For each step of microreactor fabrication (i.e. **(a)** silica monolith formation, **(b)** APTES treatment, **(c)** glutaraldehyde crosslinking, and **(d)** enzyme immobilization), 3 cm of the capillary was cut and crushed using a small grinder so the outer layer of capillary could be removed. Then, a small amount of each sample of monolith was taken out from the capillary respectively, and IR spectra acquired.

The porosity of the fabricated silica monolith capillary is described as a volume fraction (He *et al.*, 2010):

$$Porosity = \frac{(M_{MW} - M_M) / \rho}{(M_{TW} - M_T) / \rho}$$

where  $M_{MW}$  is the weight of the microreactor with water loaded,  $M_M$  is the weight of the microreactor alone;  $M_{TW}$  is the weight of empty capillary (i.e. without the silica monolith) with water loaded;  $M_T$  is the weight of empty capillary and  $\rho$  is the density of water.

#### **3.2.4.2 Immobilized Lipase Assay:**

The concentration of the lipase solution introduced into the capillary and the concentration of lipase eluting from the capillary during the immobilization process were determined. Then from the mass balance, the amount of immobilized lipase on the silica monolithic based microreactor could then be determined. The Lowry protein assay, as described elsewhere (Lowry *et al.*, 1951; Dizge *et al.*, 2009; Mugo and Ayton, 2010) was used to measure the lipase concentrations.

#### **3.2.4.3 Lipase Activity Assay:**

Lipase activity was determined spectroscopically by measuring the concentration of *p*-nitrophenol (*p*NP) obtained from the lipase catalyzed hydrolysis of *p*-nitrophenyl butyrate (*p*NPB) solution (Dizge *et al.*, 2009; Mugo and Ayton, 2010; Chapter 2). All reagents, sample and standard solutions were

prepared in a solvent mixture of 1:1 of acetonitrile (ACN): 0.1 mM sodium phosphate buffer. Briefly, a known amount of 3.5 mM *p*NPB solution was flushed through a 15 cm enzymatic silica monolith microreactor at 0.5  $\mu$ L/min and the hydrolysis products were then collected and diluted to 2 mL. GC/MS analysis of this solution confirmed that none of the *p*NPB reactant remained whereas *p*NP was the only significant peak observed. For quantification of the *p*NP product, its UV absorbance was measured at a wavelength of 410 nm using a UV-Vis spectrophotometer (Jenway 6340D; Bibby Scientific, Staffordshire, UK).

A calibration curve of *p*NP standard solution with concentrations: 0.5, 1, 3, 5 and 7 mM was obtained, then the concentration of *p*NP hydrolyzed was determined and lipase activity was calculated. One enzyme unit (U) was the amount of protein liberating 1  $\mu$ mol of *p*NP per minute. Based on the amount of enzyme loaded and lipase activity calculated, a specific activity of lipase immobilized on the monolithic support was calculated (Dizge *et al.*, 2009).

### ***3.2.5 Lipid Transformation using the Microreactor:***

The biocatalyst microreactor was evaluated for its performance both offline (Fig. 3-1 a) and online (Fig. 3-1 b). Two reaction mixture of: (i) 0.5 mg/mL trioleoylglycerol (TO), and (ii) 0.5 mg/mL monooleoylglycerol (MO) were both prepared in ethanol and vortexed vigorously to dissolve the lipids in ethanol. The substrate solution was infused through the lipase immobilized microreactor at room temperature and at flow rates of 0.2, 0.3, 0.5 and 1  $\mu$ L/min

using a Harvard Model '11 Plus syringe pump (Harvard Apparatus, Holliston, MA, USA). The reusability of an SM microreactor was tested over 12 repeat runs at a flow rate of 1  $\mu\text{L}/\text{min}$  (room temperature) using 0.5 mg/mL trioleoylglycerol (TO) as the substrate. The reproducibility of the microreactor fabrication process was tested by preparing 5 identical microreactors and measuring the degree of substrate conversion at flow rates of 0.2, 0.3, 0.5 and 1  $\mu\text{L}/\text{min}$  at room temperature, and 1  $\mu\text{L}/\text{min}$  at 35 °C.

The reaction products collected were analyzed by reversed phased liquid chromatography with an evaporative light scattering detector (HPLC/ELSD). The possibility of using the microreactor connected on-line to a mass spectrometer in order to directly monitor the reaction product was also tested, as described below.

### ***3.2.6 Reversed Phased Liquid Chromatography / Evaporative Light Scattering Detection (HPLC/ELSD):***

Non-aqueous reversed phased high-performance liquid chromatography (HPLC) analysis was performed using an Agilent 1200 HPLC system equipped with an evaporative light scattering detector (ELSD) model 1260 Infinity (Agilent Technologies, Santa Clara, CA, USA) in order to determine the lipid classes present following enzymatic reactions. The same procedure as reported previously (Chapter 2) was used with slight modification. An Agilent Zorbax HT C18 column (4.6 x 50 mm, 1.8  $\mu\text{m}$ , Agilent Technologies, Santa Clara, CA, USA) with a gradient of A, 100% methanol and B, isopropanol: hexane (5:4) was used.

The starting condition was 25% B then increased to 90% B in 5 min, before returning to 25% B at 5.1 min and hold for 2.9 min (t=8 min) in this condition to re-equilibrate the column. Throughout the analysis, the ELSD temperature was set to 33 °C, with computer-controlled N<sub>2</sub> gas flow of 3 L/min at pressure of 3.5 bars.

### ***3.2.7 Gas Chromatography / Mass Spectrometry (GC/MS):***

An Agilent GC/MS system with electron impact (EI) ionization (Agilent Technologies, Santa Clara, CA, USA) was used. All data were collected by Agilent Chemstation software. The column used for the separation was a J&W HP-5 (30 m x 0.32 mm x 0.25 µm) gas chromatography column (Agilent Technologies; Santa Clara, CA, USA).

A series of ethyl oleate standards were prepared in the range of 0.005, 0.01, 0.05, 0.1, 0.25 and 0.5 mg/mL in dichloromethane (DCM) to construct a standard calibration curve. Reaction product samples were dissolved in DCM prior to injection. The carrier gas was H<sub>2</sub> at a flow rate of 1.0 mL/min, with injection volume of 1 µL, and the inlet injector temperature was set at 300 °C. The optimized temperature program started at an oven temperature of 100 °C (6 min), then increased at 10 °C/min until reaching 285 °C (0 min) before increasing again at 15 °C/min to 300 °C (hold 3 min).

### **3.2.8 Mass Spectrometry (MS):**

A QStar Elite Mass spectrometer (Applied Biosystems/Sciex, Concord, ON, Canada) with Analyst software (Applied Biosystems/Sciex, Concord, ON, Canada) was used to observe the online performance of the microreactor without chromatographic separation (Fig. 4-1 b). For this purpose, the lipase-immobilized microreactor effluent was directly coupled to APPI-MS to monitor the lipid reactions.

The substrate was infused from a 1 mL Hamilton syringe through the microreactor using a syringe pump operating at 1  $\mu\text{L}/\text{min}$ . The silica microreactor was connected to the APPI ion source using PEEK tubing (0.0127 cm ID) connected using Upchurch sleeves and ferrules. A 200  $\mu\text{L}/\text{min}$  make-up flow of hexane joined the microreactor eluent via a tee-piece prior to the APPI ion source. The APPI source parameters used were as follow: gas (GAS 1) at 10; nebulizing gas (GAS 2) at 65; declustering potential (DP) at 40 V; focus potential (FP) at 150 V; declustering potential 2 (DP 2) at 15 V; ionspray voltage (IS) at 1,300 V; and the ion source temperature was 375  $^{\circ}\text{C}$ .

## **3.3 Results and Discussion**

### **3.3.1 Characterization of the Microreactor:**

This chapter demonstrates the preparation and performance of a 15 cm lipase immobilized silica monolith microreactor for triacylglycerol alcoholysis. In



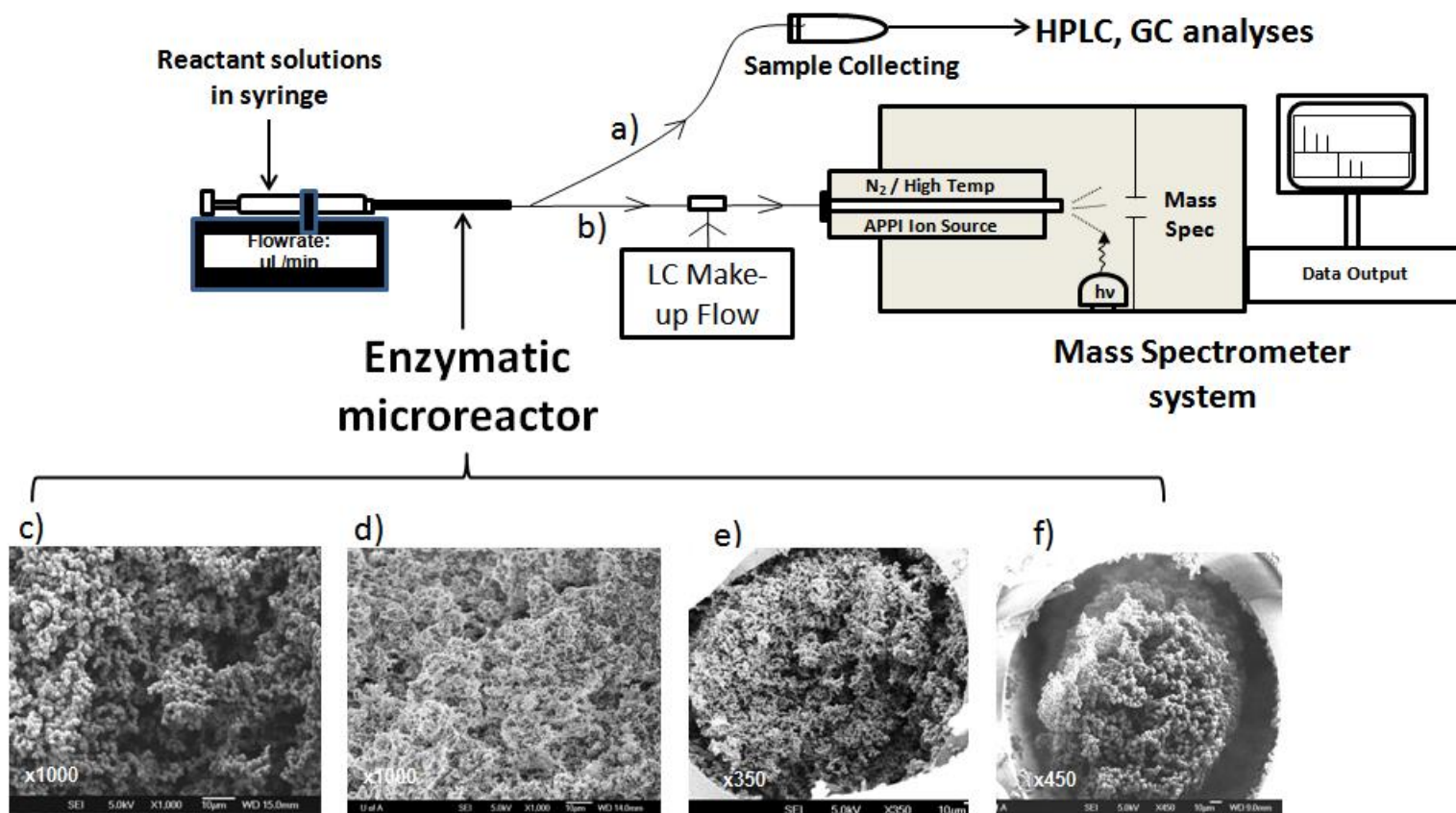


FIG 3-1: Schematic diagram for small scale lipid reaction using fabricated biocatalyst microreactor: (a) offline reaction (b) online coupled with the mass spectrometry system; (c)-(e) SEM image of a cross-section of: (c) a silica monolithic capillary at x1000 magnification, (d) an enzymatic monolithic microreactor at x1000 magnification; (e) an NaOH-treated silica monolithic capillary at x350 magnification; (f) a non-treated silica monolithic capillary at x450 magnification. Larger SEM images are given in Appendix 3.

order to demonstrate that the stages of microreactor fabrication were successful, SEM and FTIR characterizations of the morphology and chemical substitution of the monolith surface were conducted. As can be seen in Figures 3-1 c and e, the cross section of the silica monolith capillary consists of a micro-porous structure and monolithic network. Such a structure clearly has a large surface area and it would be expected that this surface would have a good enzyme loading capacity. Figure 3-1 d shows the SEM image after lipase immobilization onto the silica monolith. By comparison with Figure 3-1 c, it can be seen that the microreactor still maintains much of the porosity and the monolithic structure that is present prior to introduction of the enzyme.

According to IUPAC nomenclature (IUPAC, 1994), pores can be differentiated according to their diameters: macropores have diameter more than 50 nm, mesopores are between 2 to 50 nm, while the pores with free diameter less than 2 nm are defined as micropores. Hence, both macropores and mesopores were seen in the SEM images of the monolith microreactor. In addition, SEM images can be used to observe the homogeneity of the silica monolithic network and any shrinkage of the monolith from the silica capillary wall or other void volume (Lei *et al.*, 2004; Xie *et al.*, 2006). It is known that separation of the silica monolith from the capillary wall (Fig. 3-1 f) can be prevented by the use of alkali to activate the silica wall as illustrated in Figure 3-1e (Ishizuka *et al.*, 2000; Xie *et al.*, 2006).<sup>9</sup>

---

<sup>9</sup> Supplementary data are given in Appendix A3-3 to A3-6.

The porosity of the enzymatic microreactor is an important factor in estimating the surface area of the monolithic networks. Porosity can be defined as the ratio of the total pore volume ( $M_{MW}/\rho$ ) to the apparent volume of the material ( $M_{TW}/\rho$ ) (IUPAC, 1994; He *et al.*, 2010). Here, the porosity of a 15 cm silica monolith within a 320  $\mu\text{m}$  ID capillary was determined from the weight of water that fills the monolith capillary ( $M_{MW}-M_M$ ) and the weight of water that fills an identical length of empty capillary (i.e. without the monolith) ( $M_{TW}-M_T$ ). In this way, the silica monolith was estimated to have a porosity of 0.70 which is comparable to the porosity of 0.67 reported for a TEOS-methyl trimethoxysilane based silica monolith (He *et al.*, 2010). The morphology of the silica must influence the porosity of the column, the surface area available for enzyme loading and ultimately the capacity of the column to perform reactions (Cabrera, 2004; Ishizuka *et al.*, 2000; Xie *et al.*, 2006). Clearly, the high porosity achieved is desirable in order to minimize back-pressure when pumping fluid through the capillary monolith.

FTIR spectroscopy was used to observe the presence of the functional groups involved in the immobilization process steps (Maria Chong and Zhao, 2003; Lendl *et al.*, 2006; Kahraman *et al.*, 2007). Figure 3-2 shows the IR spectra recorded for pieces of the monolith removed from the capillary at various stages throughout the fabrication and enzyme immobilization process. The silica monolith (Fig. 3-2 b) shows strong absorption for both Si-O-Si asymmetric and symmetric stretching vibrations at around  $1050\text{ cm}^{-1}$  and  $798\text{ cm}^{-1}$ , respectively. In addition, it can be seen that there is a small band at  $960\text{ cm}^{-1}$  that could be

attributed to the bending vibration of the Si-H bond (Battisha *et al.*, 2007) or an Si-O(H) stretching mode (Nocuñ *et al.*, 2005).

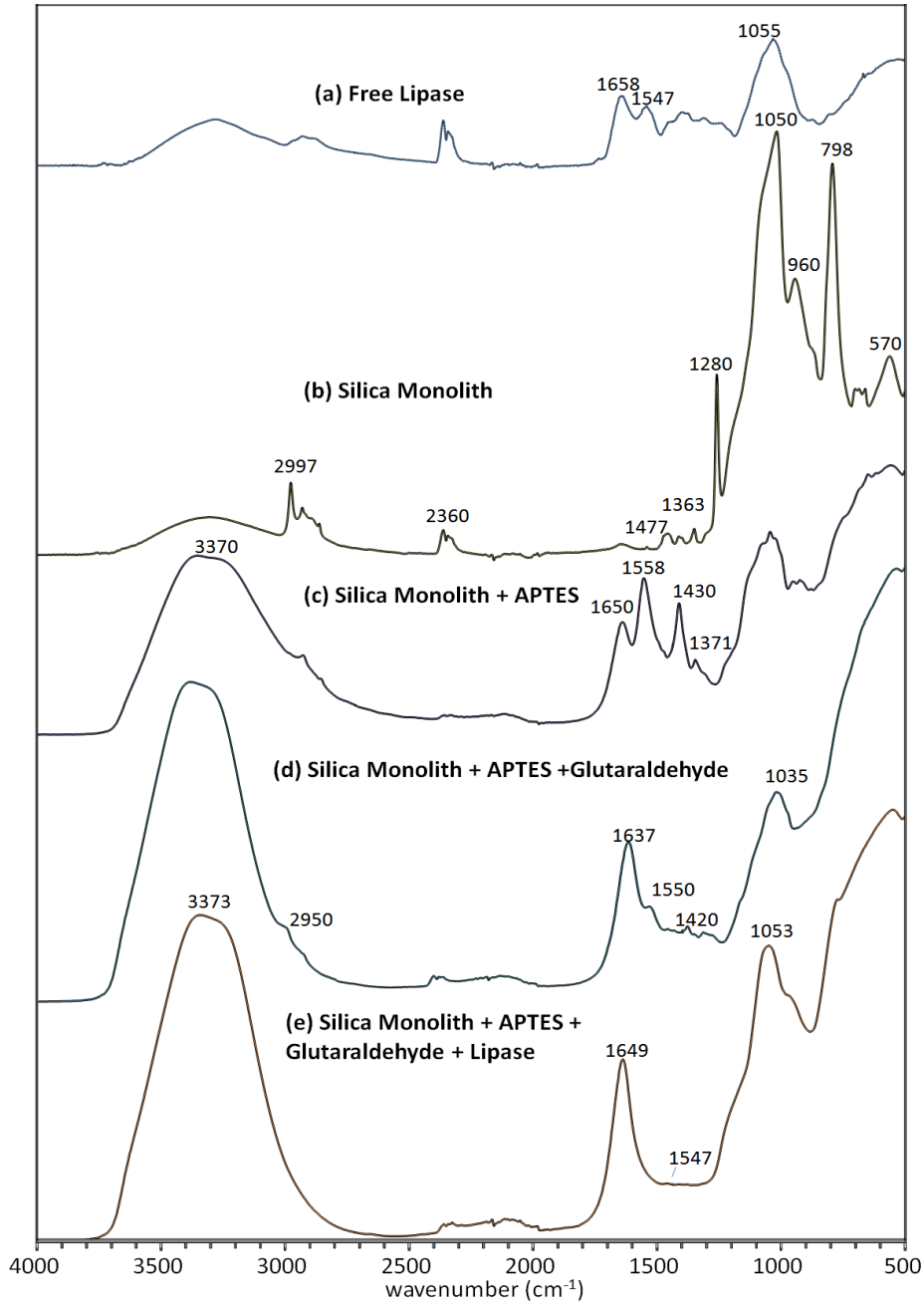


FIG 3-2: Overlapped FTIR spectra for fabrication processes of enzymatic silica monolith microreactor: (a) free lipase from *C.antarctica*; (b) silica monolith; (c) silica monolith + APTES; (d) silica monolith + APTES+ glutaraldehyde; (e) silica monolith + APTES+ glutaraldehyde +lipase.

In summary, these characteristic absorptions indicate the formation of the bonds between silica as a result of the polymerization of TEOS (Nocuñ *et al.*, 2005) during the formation of the monolith. A strong band at around  $1200\text{ cm}^{-1}$  reported previously for a pure silica powder sample (Haan *et al.*, 1986) was not observed.

Small bands at around  $1477\text{ cm}^{-1}$ ,  $1442\text{ cm}^{-1}$ , and  $1363\text{ cm}^{-1}$  are related to the  $\text{CH}_3$  bending vibration of the ethoxy group (Nocuñ *et al.*, 2005; Battisha *et al.*, 2007). Bands at  $2997$ ,  $2930$  and  $2883\text{ cm}^{-1}$  all correspond to the C-H absorption and vibration from  $\text{CH}_3$  and  $\text{CH}_2$ . These indications of the residual presence of small amounts of ethoxy groups in the monolith even after calcination have also been reported in other studies (Peña-Alonso *et al.*, 2005).

Note that in Figure 3-2 b there is absorption at around  $3500$  to  $3300\text{ cm}^{-1}$  due to the presence of adsorbed water (Battisha *et al.*, 2007); the intensity is small since most of the water is removed during monolith fabrication at  $200\text{ }^\circ\text{C}$ . During enzyme immobilization, the broad absorption at around  $3500$ - $3300\text{ cm}^{-1}$  sequentially becomes much stronger (Figs. 3-2 c-e). This is due to the O-H stretching bond from the adsorption of the water used in the immobilization process (buffer) onto the monolith.

After reaction with APTES (Fig. 3-2 c), the FTIR spectrum of the monolith changes considerably (Table 3-1). A medium intensity band corresponding to the primary amine  $\text{NH}_2$  stretching and bending becomes pronounced at around  $1558\text{ cm}^{-1}$ . This, together with the appearance of C-N group

around  $1370\text{ cm}^{-1}$  (Pavia *et al.*, 2001) is consistent with the presence of APTES in the silica monolith.

Introduction of glutaraldehyde results in the complete disappearance of the primary amine absorption at  $1558\text{ cm}^{-1}$  (Fig. 3-2 d). A strong absorption at  $1637\text{ cm}^{-1}$  appears that was previously assigned to the N=C vibration (Tlili *et al.*, 2005; Hiraoui *et al.*, 2011) formed by the reaction of glutaraldehyde with the APTES free amine group. The shoulder at  $1550\text{ cm}^{-1}$  is also consistent with the reported spectrum following this reaction (Hiraoui *et al.*, 2011). A weak absorption at  $1420\text{ cm}^{-1}$  is due to C=O vibration on the free end of the glutaraldehyde (Tlili *et al.*, 2005).

The subsequent immobilization of the enzyme to the monolith *via* the glutaraldehyde crosslinker (Fig. 3-2 e) results in a shift in the N=C vibration band (amide I band) from  $1637\text{ cm}^{-1}$  to  $1649\text{ cm}^{-1}$ , which is similar to a previous report for the immobilization of bovine serum albumin (Hiraoui *et al.*, 2011). The weak amide II band at  $1547\text{ cm}^{-1}$  is also observed due to the combination of C-N stretching and N-H bending in the lipase backbone (Mei *et al.*, 2003; Hiraoui *et al.*, 2011). All of these characteristic bands are listed in Table 3-1.

### ***3.3.2 Evaluation of the Lipase Activity within the Microreactor:***

In order to evaluate the enzyme activity within the microreactor it is necessary to measure the amount of protein immobilized. This was achieved

TABLE 3-1: IR bands characteristic of the silica monolith formation and lipase immobilization processes: (a) free lipase from *C.antarctica*; (b) silica monolith (SM); (c) SM + APTES; (d) SM + APTES+ glutaraldehyde; (e) SM + APTES+ glutaraldehyde +lipase.

Wavenumber (cm <sup>-1</sup> )	(a)	(b)	(c)	(d)	(e)
790, 1050		Si-O-Si asymmetric and symmetric str. Silica characteristic (Nocuñ <i>et al.</i> , 2005; Battisha <i>et al.</i> , 2007)			
960		Si-H Bond (Battisha <i>et al.</i> , 2007) Si-OH bending mode (Nocuñ <i>et al.</i> , 2005)			
1055		Si-O stretching (Battisha <i>et al.</i> , 2007)			
1363, 1442, 1477		CH <sub>3</sub> bending vibration ethoxy group (Nocuñ <i>et al.</i> , 2005; Battisha <i>et al.</i> , 2007)			
1370			C-N group formation (Pavia <i>et al.</i> , 2001)		
1420				C=O vibration free end glutaraldehyde (Tlili <i>et al.</i> , 2005)	
1547	Amide II from C-N str. N-H bend (Hiraoui <i>et al.</i> , 2011; Mei <i>et al.</i> , 2003)				C-N str. and N-H bending (amide II) (Mei <i>et al.</i> , 2003; Hiraoui <i>et al.</i> , 2011)

TABLE 3-1: (Continued) IR bands characteristic of the silica monolith formation and lipase immobilization processes: (a) free lipase from *C.antarctica*; (b) silica monolith (SM); (c) SM + APTES; (d) SM + APTES+ glutaraldehyde; (e) SM + APTES+ glutaraldehyde +lipase.

Wavenumber (cm <sup>-1</sup> )	(a)	(b)	(c)	(d)	(e)
1558			NH <sub>2</sub> stretching (Pavia <i>et al.</i> , 2001)		
1637				C=N vibration (Hiraoui <i>et al.</i> , 2011; Tlili <i>et al.</i> , 2005)	
1649					C=N vibration band (amide I) (Hiraoui <i>et al.</i> , 2011)
2883, 2930, 2997		C-H absorption and vibration CH <sub>3</sub> and CH <sub>2</sub> (Peña-Alonso <i>et al.</i> , 2007)			
3300-3500	OH stretching water (Battisha <i>et al.</i> , 2007)		OH stretching water (Battisha <i>et al.</i> , 2007)	OH stretching water (Battisha <i>et al.</i> , 2007)	OH stretching water (Battisha <i>et al.</i> , 2007)



by measuring the protein concentration before and after passing the lipase solution through the capillary in the final immobilization step. To do this, the well-known Lowry method for measuring protein concentrations was used (Lowry *et al.*, 1951). In this way it was found that from 1 mL of an 8 mg/mL solution of lipase from *Candida antarctica*, 6.34 mg or 79.3% of the protein was bound to the silica monolith support by the immobilization process, which is comparable to the amount found in other studies (Dizge *et al.*, 2009; He *et al.*, 2010; He *et al.*, 2010).

The overall efficiency of the immobilization also was determined by measuring the activity of the lipase immobilized (Dizge *et al.*, 2009). In most of the protein activity studies, a unit (U) of lipase activity is defined as the amount of any enzyme that hydrolyses 1  $\mu\text{g}$  of *p*-nitrophenol (*p*NP) from a *p*-nitrophenyl butyrate (*p*NPB) substrate (Dizge *et al.*, 2009; Mugo and Ayton, 2010; Chapter 2). Using this reaction, it was determined that a lipase immobilized on a 15 cm silica monolith microreactor had enzymatic activity of 5.04  $\mu\text{g}$  *p*NP/min (U). This represents about 17% loss compared to the specific lipase activity of the 6.34 mg of lipase that were immobilized based on the measurement of native lipase activity specified by the supplier (0.88 U/mg vs. 1.06 U/mg specified). This modest loss is easily offset by the benefits of immobilization, such as greater reusability compared to free enzyme. Furthermore, this result is comparable to other work using various supports that report specific activities for immobilized lipases of around 0.6-0.91 U/mg (Dizge *et al.*, 2009; Mugo and Ayton, 2010; Chapter 2).

### ***3.3.3 Formation of Fatty Acid Ethyl Ester using Lipase Immobilized Microreactor:***

A major industrial application of lipase is to catalyze lipid transformations such as the transesterification of triacylglycerol (TAG) with alcohols to produce fatty acid alkyl esters (FAAE), also known as alcoholysis (Soumanou *et al.*, 1998; Shimada *et al.*, 2002; Lara and Park, 2004; Akoh *et al.*, 2007; Stamenković *et al.*, 2011). In general, the products of ethanolysis are ethyl esters although under specific conditions of excess ethanol and low reaction times with some presence of water, regiospecific hydrolysis to form 2-monoacylglycerol (2-MAG) has been reported (Irimescu *et al.*, 2002; Shimada *et al.*, 2003; Asanomi *et al.*, 2011). In the present work, the microreactor was shown to transform infused trioleoylglycerol completely into ethyl oleate at room temperature and using a flow rate of  $\geq 0.5$   $\mu\text{L}/\text{min}$  (Figs. 3-3 and 3-4).

GC/MS with electron impact ionization (EI) was used as a method to definitively identify and quantify the FAAE reaction products from the microreactor (Figs. 3-3 a-d ) using both retention times and mass spectral data. Figure 3-3a shows the GC/MS total ion current (TIC) trace for an ethyl oleate standard; the same retention time was observed for the reaction product for a 0.5  $\mu\text{L}/\text{min}$  flow rate of trioleoylglycerol in ethanol through the microreactor (Fig. 3-3b). The identity of this peak is further confirmed by the EI mass spectra (Fig. 3-3 c and d) which show the molecular ions at  $m/z$  310 and characteristic fragment ions at  $m/z$  180, 207, 264, 280 in both cases.

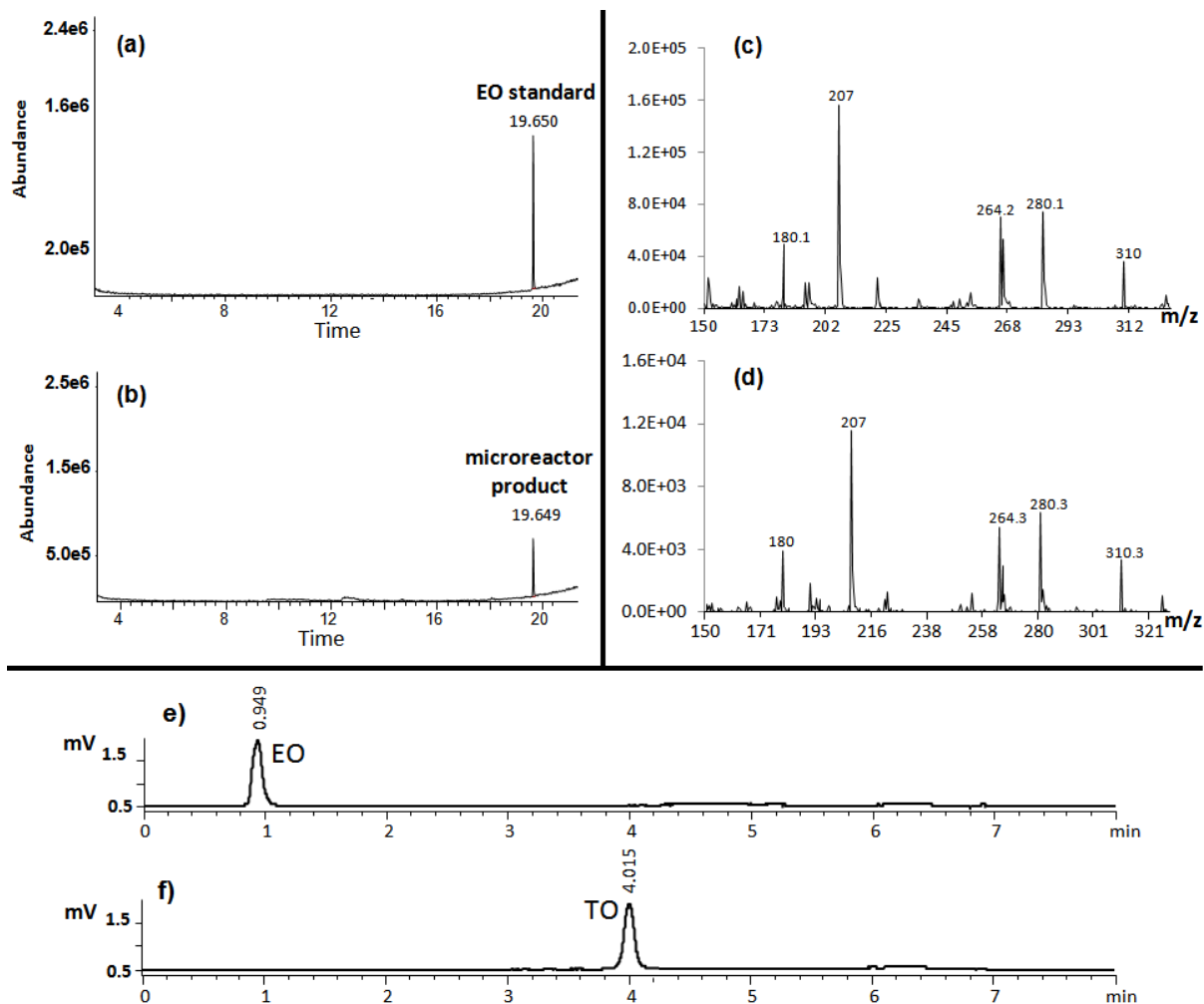


FIG 3-3: The comparison of: TIC of GCMS for (a) ethyl oleate (EO) standard, (b) product of 0.5  $\mu\text{L}/\text{min}$  RT; extracted ion spectra of MS-EI for GC of (c) EO standard, (d) product of 0.5  $\mu\text{L}/\text{min}$  RT; and LC-ESLD chromatograms for (e) product of 0.5  $\mu\text{L}/\text{min}$  RT, (f) starting material (trioleoylglycerol, TO), respectively.

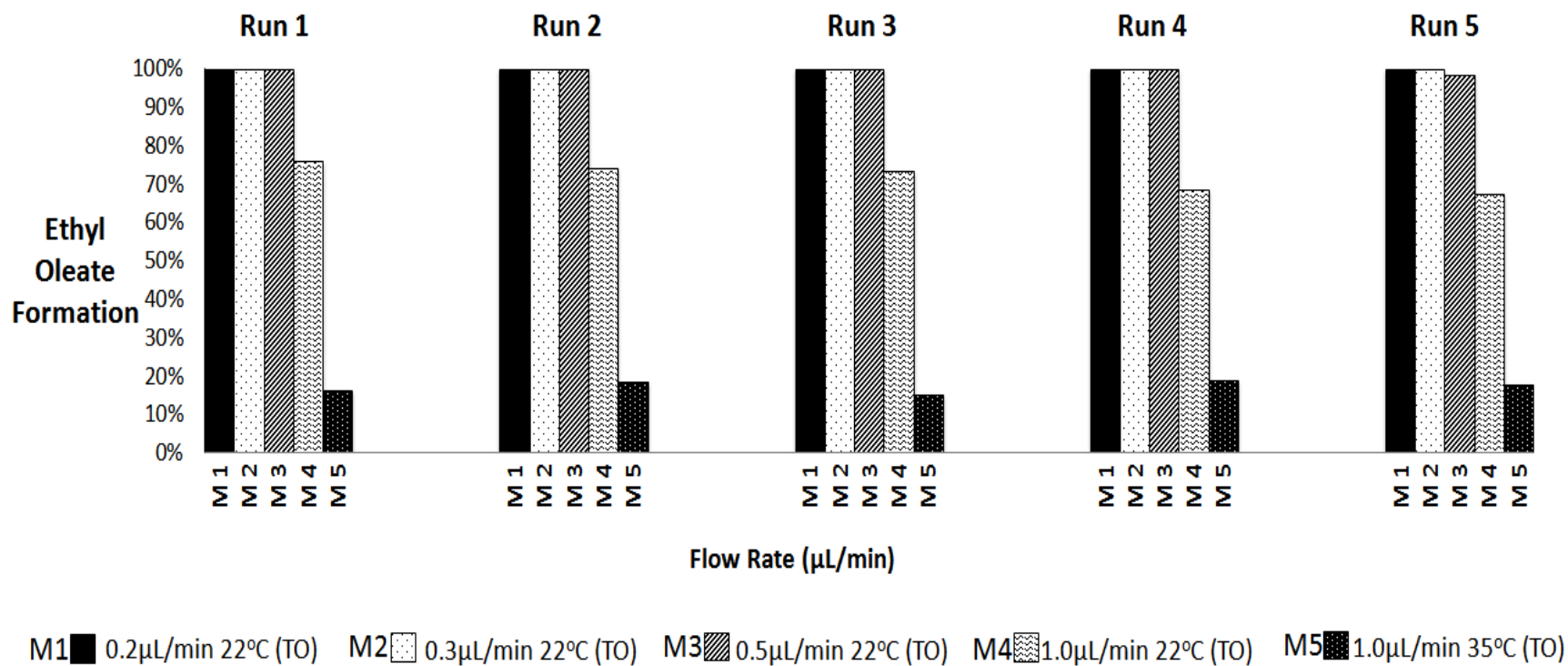


FIG 3-4: Graph of percentage of conversion of lipid starting materials to fatty acid ethyl ester at different flow rates and conditions for 5 runs each. *x*-axis represents each number of individual microreactor, and “Run” indicates the infusion of trioleoylglycerol (TO) solution for 6 h at specified flow rate.

The degree of conversion of trioleoylglycerol to ethyl oleate was then determined by quantifying both compounds by GC/MS, using external calibration curves. For this experiment, 5 identical microreactors were prepared using the same fabrication and immobilization conditions. A trioleoylglycerol standard solution was then infused into each microreactor under various conditions of flow rate and temperature.

Each condition was repeated on the same microreactor 5 x (Fig. 3- 4). It was found that at flow rates through the microreactor of 0.2  $\mu\text{L}/\text{min}$ , 0.3  $\mu\text{L}/\text{min}$  and 0.5  $\mu\text{L}/\text{min}$  and at room temperature ( $\sim 22\text{ }^\circ\text{C}$ ), trioleoylglycerol is quantitatively converted to ethyl oleate (Fig. 3-4, M1-M3). Furthermore, it was shown that complete conversion of trioleoylglycerol to ethyl oleate was achieved for each of 5 consecutive runs, demonstrating that the enzyme activity remained undiminished over 5 uses. At higher flow rates ( $\geq 1.0\text{ } \mu\text{L}/\text{min}$ ), lower yields of ethyl esters were observed, presumably due to insufficient residence time within the microreactor. However, the yields of ethyl oleate remained constant over the 5 repeat runs (Fig. 3-4, M4).

Notably, increasing the temperature of the microreactor to  $35\text{ }^\circ\text{C}$  did not result in an increased yield of ethyl oleate (Fig. 3-4, M5) but rather decreased the yield from  $\sim 72\%$  to  $<20\%$  at  $1.0\text{ } \mu\text{L}/\text{min}$ . This is consistent with previous studies employing a lipase immobilized microstructured fiber, which showed that as the reaction temperature is increased, TAG is regiospecifically converted to 2-monoacylglycerol (2-MAG) (Chapter 2). In that work, TAG were converted to MAG with 9% yield at  $24^\circ\text{C}$  rising to 90% at  $50\text{ }^\circ\text{C}$ . Hence, the lower yield of

ethyl oleate observed in the 35 °C condition of the present experiment is to be expected due the competitive formation of MAG. In summary, the formation of ethyl esters from TAG occurs optimally at about room temperature with flow rates of 0.5  $\mu\text{L}/\text{min}$  or lower through the silica monolith lipase microreactor.

The products collected from the microreactor were also analyzed by a non-aqueous reversed phase liquid chromatography (NARP-HPLC) with an evaporative light scattering (ELSD) detection. Figure 3-3 e shows the chromatogram obtained for the reaction products at 0.5  $\mu\text{L}/\text{min}$  flow rate, compared to the starting material (Fig. 3-3 f). Since the LC/ELSD method allows for the separation and universal detection of the trioleoylglycerol ethylation products present in the microreactor eluent, it was used as a second method to analyze the microreactor performance.

In order to investigate the reusability of the microreactor, the alcoholysis of trioleoylglycerol was carried out at room temperature at a flow-rate of 1  $\mu\text{L}/\text{min}$  (Fig. 3-5). Figure 3-5 shows the performance of the same microreactor over 12 consecutive runs. It was found that under these conditions, the molar conversion of trioleoylglycerol to ethyl oleate is ~70%; the remainder was largely monooleoylglycerol.

Figure 3-5 indicates that the conversion of trioleoylglycerol to ethyl oleate at this flow-rate is constant for the first 5 runs. After the 6<sup>th</sup> run, the conversion to ethyl oleate starts to decrease with a corresponding increase in remaining unconverted trioleoylglycerol substrate.

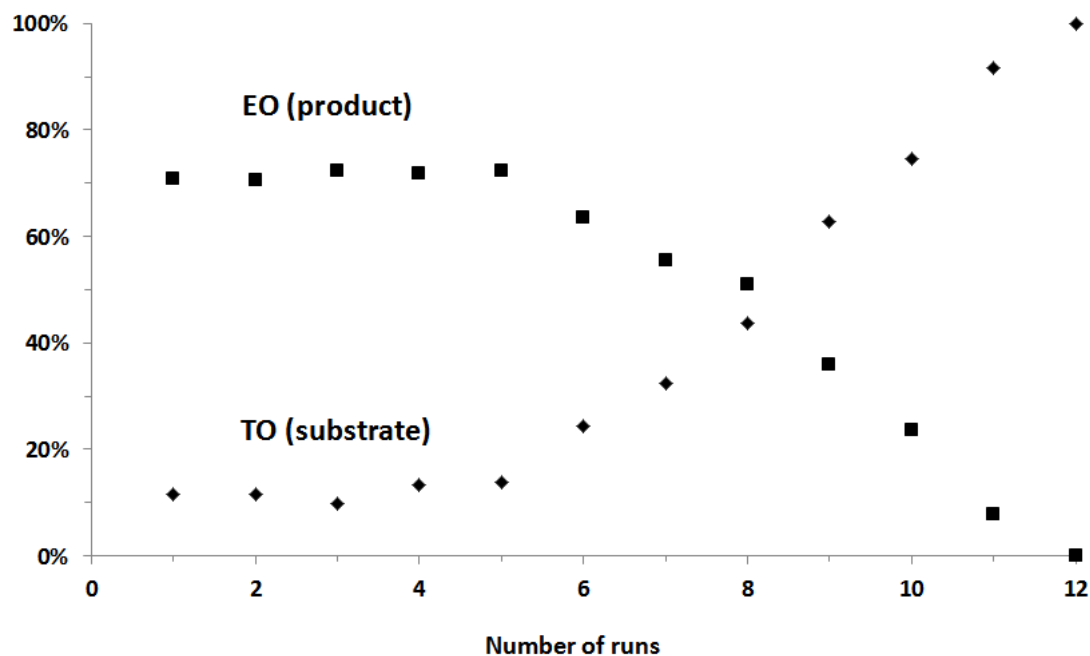


FIG 3-5: NARP/HPLC-ELSD percentage of molar conversion of substrate trioleoylglycerol (TO) to product ethyl oleate (EO) formation within 12 runs of reaction using the microreactor with 1  $\mu\text{L}/\text{min}$  at the room temperature, respectively.

After the 9<sup>th</sup> run, the microreactor had lost about 50% of its transformation efficiency and completely lost its efficiency by the 12<sup>th</sup> run. It was predicted that when using the more optimal flow rates of 0.2-0.5  $\mu\text{L}/\text{min}$  where complete conversion of trioleoylglycerol to ethyl oleate was observed, the lifetime of the microreactor would be extended due to the lower volume of lipid/ethanol solution passing through the reactor and the lower backpressure generated. Hence it is reasonable to assume that a similar microreactor operated at 0.5  $\mu\text{L}/\text{min}$  could be reused up to 10 times without loss of activity. Furthermore, the data presented in

Figures 3-4 and 3-5 demonstrate that microreactors can be produced with very consistent performance, which is essential for their future use in more routine and practical applications.<sup>10</sup>

#### ***3.3.4 Direct coupling of the Microreactor to a Mass Spectrometer:***

As described above, the microreactor operates optimally at low flow rates so that only microliter volumes of solutions containing the products elute. At these small volumes, sample collection and subsequent manipulation become somewhat difficult. Hence it would be desirable to directly monitor the products of the enzymatic lipid transformation in real-time.

The present study demonstrates how this can be achieved by coupling the microreactor to a mass spectrometer (MS) (Fig. 3-1 b) *via* the atmospheric pressure photoionization source, thus allowing real-time monitoring of the products. In this experiment, the microreactor flow rate was set to 1  $\mu\text{L}/\text{min}$  but the effluent was augmented by a 200  $\mu\text{L}/\text{min}$  make-up flow of hexane through a mixing tee. The make-up flow brings the total flow rate into the range for optimal operation of the APPI source. Hexane was chosen as the make-up solvent since this can participate in the photoionization process and avoids the need for an additional dopant and is a suitable solvent for lipids. APPI was chosen as the ionization method rather than electrospray ionization since it gives far superior

---

<sup>10</sup> Supplementary data are given in Appendix A3-7 to A3-8.



response for low polarity compounds and in particular ethyl esters, which is the product of interest in this experiment.

The results of this experiment are shown in Figure 3-6, which shows 4 extracted ion chromatograms of (a) trioleoylglycerol  $[\text{MH}]^+$  ions ( $m/z$  885), (b) the dioleoylglycerol fragment ion seen in the APPI mass spectrum of trioleoylglycerol ( $m/z$  603), (c) ethyl oleate  $[\text{MH}]^+$  ions ( $m/z$  311) and (d) an ion that indicates the presence of monooleoylglycerol – the fragment ion due to loss of water  $[\text{MH}-\text{H}_2\text{O}]^+$  ( $m/z$  339). The figure shows these extracted ion traces over 3 time periods labeled as time zones A, B and C. In zone A (Fig. 3-6 a), a 1  $\mu\text{L}/\text{min}$  infusion of a trioleoylglycerol standard solution bypasses the microreactor and flows directly to the ion-source. During zone A, the intact trioleoylglycerol reactant ( $m/z$  885) (Fig. 3-6 a-i) was observed along with  $m/z$  603, which is an intense fragment ion of trioleoylglycerol attributed to the loss of one acyl chain, as is common under APPI conditions (Figs. 3-6 a-ii and v).

At the start of time zone B, the 1  $\mu\text{L}/\text{min}$  flow of the trioleoylglycerol standard solution passes through the microreactor and into the mass spectrometer. Unfortunately, under the conditions used in the prototype arrangement, there is a large dead-time (zone B) due to the significant tubing volume at such a low flow rate. At the start of time zone C the reaction products reach the ion-source. The formation of ethyl oleate is clearly indicated by the mass spectrum (Figs. 3-6 a-vi) and by the extracted ion chromatogram of the EO  $[\text{MH}]^+$  ion at  $m/z$  311 (Fig. 3-6 a-iii). This observation is consistent with the LC and GC data described above.

Remarkably, the intensity of the ethyl oleate product from the microreactor is constant over a 35 min infusion time period as seen in Figure 3-6 a-iii, zone C. This is indicative of both reaching a steady state reaction in the enzymatic microreactor, and of the stability of the APPI ion-source for hexane mobile phase, as reported previously (Villegas *et al.*, 2010). In contrast, the extracted ion chromatogram seen for the monooleoylglycerol fragment ion ( $m/z$  339) in zone C decreases by more than 50% over the first 20 minutes (Fig. 3-6 a-iv). This may be due to the nature of the reaction – monooleoylglycerol is formed by hydrolysis of trioleoylglycerol and so requires some water to proceed. Presumably the immobilized enzyme traps water during the flow of buffer which is subsequently removed as the reaction proceeds in a flow of ethanol.

It should be noted that the absolute intensities of the extracted ion current traces shown in Figure 3-6 cannot be used directly to compare the yields of the reaction products since the response factors for these ions vary widely, with the mass spectrometer being considerably less responsive towards ethyl oleate than trioleoylglycerol. In fact, the relative response factor for trioleoylglycerol and ethyl oleate, measured using C19:1 FAME as an internal standard, is 0.43 for ethyl oleate compared to 1.6 for trioleoylglycerol. Hence, although the uncorrected intensity of trioleoylglycerol trace appears to be higher than that of ethyl oleate, both GC and LC data indicate the conversion of ~60-70% of trioleoylglycerol into ethyl oleate.

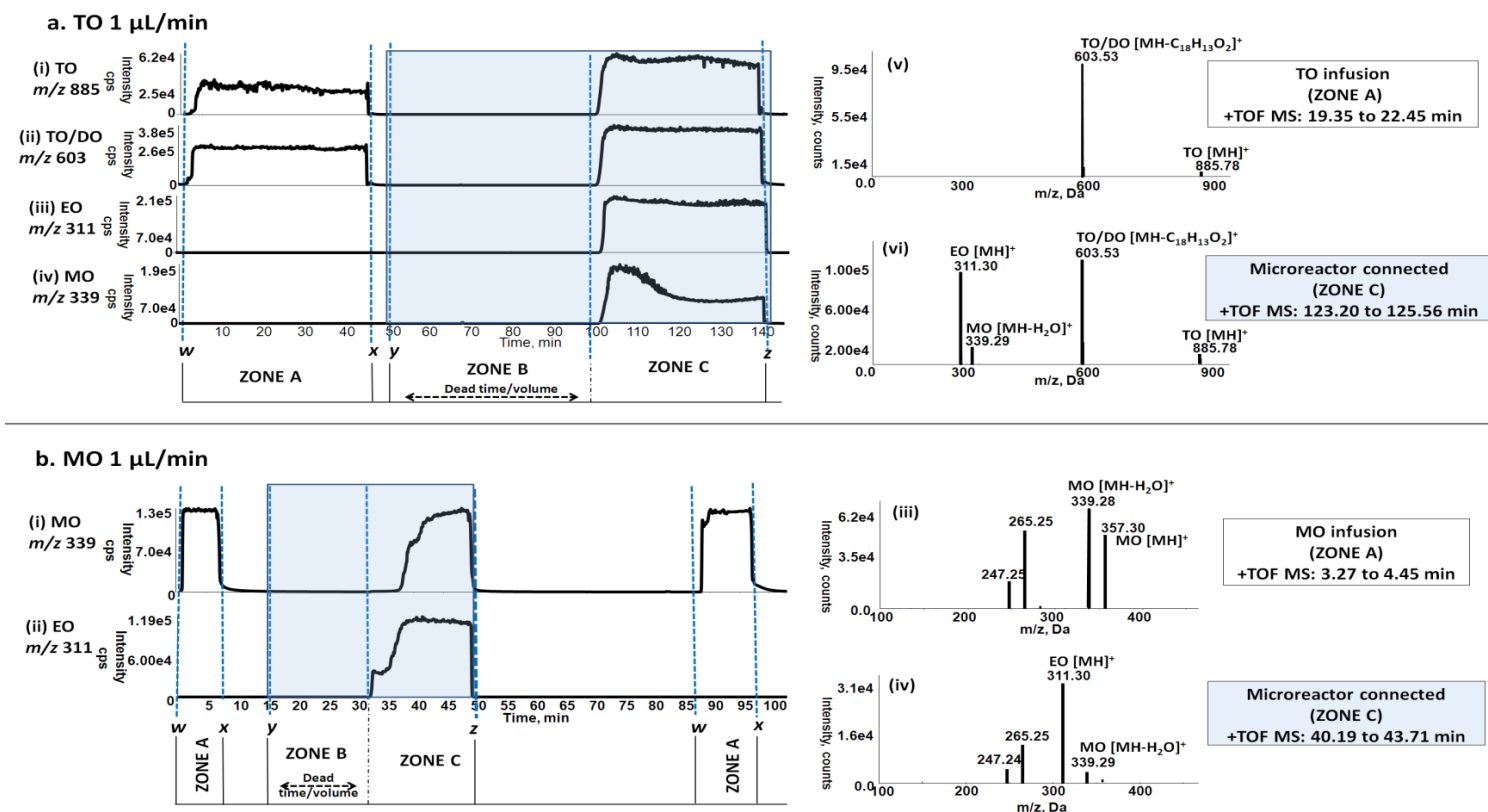


FIG 3-6: Extracted mass chromatogram for online direct infusion microreaction for substrate (a) trioleoylglycerol (TO) in EtOH at 1  $\mu\text{L}/\text{min}$  with compound of interest: (i) TO,  $m/z$  885 (ii) TO fragment/dioleoylglycerol (DO),  $m/z$  603; (iii) ethyl oleate (EO),  $m/z$  311; (iv) monooleoylglycerol (MO),  $m/z$  339; (v) mass spectrum (without microreactor); (vi) mass spectrum (with microreactor); and (b) MO in EtOH at 1  $\mu\text{L}/\text{min}$  with compound of interest: (i) MO,  $m/z$  339; (ii) EO,  $m/z$  311; (iii) mass spectrum (without microreactor); (iv) mass spectrum (with microreactor). \*Zone A, B and C represent the period of direct infusion without microreactor, infusion with microreactor started, and signal yielded from microreactor infusion, respectively. \*\*w, x, y, and z represent direct infusion ON with microreactor disconnected; direct Infusion OFF; microreactor connected with pump ON; and pump OFF, respectively.

To further assess the effectiveness of the lipase immobilized microreactor for direct coupling to the APPI-MS, the transesterification of monooleoylglycerol in ethanol to ethyl oleate was evaluated (Fig. 3-6 b). The extracted ion traces in Figure 3-6b-i indicate the existence of the monooleoylglycerol substrate when it was directly infused into the APPI-MS system (zone A). This was confirmed both by the presence of monooleoylglycerol  $[MH]^+$  ion at  $m/z$  357 and the  $[MH-H_2O]^+$  fragment ion at  $m/z$  339 due to loss of water, as seen in Figure 3-6 b-iii.

When the microreactor was connected to the APPI-MS system, the formation of product ethyl oleate was observed in Zone C (Fig. 3-6 b-ii), as shown by the observation of  $[MH]^+$  ions at  $m/z$  311 for ethyl oleate (Fig. 3-6b-iv). The ethyl oleate peak was found to disappear when the microreactor was disconnected (Fig. 3-6b-ii, pump off) but later MO reappeared with the flow on but bypassing the microreactor (Fig. 4-6b-i at  $t=90$  min). As is evident in Figure 3-6 b, monooleoylglycerol was substantially converted to ethyl oleate by passage through the microreactor, as was the case with trioleoylglycerol as starting material.

Overall, coupling the microreactor online to APPI/MS clearly demonstrates that triacylglycerols and monoacylglycerols in ethanol can be efficiently transformed into ethyl esters. This technology could in future be adapted for online lipid derivatization with analytical applications.<sup>11</sup>

---

<sup>11</sup> Supplementary data are given in Appendix A3-9 to A3-10.

### 3.4 Conclusion

Silica monolith capillaries containing immobilized *Candida antarctica* lipase have been successfully prepared in a reproducible manner maintaining a high degree of enzyme activity. The production of the monoliths and subsequent enzyme immobilization was demonstrated by FTIR spectroscopy. The microreactors were reusable multiple times without loss of enzyme activity, which demonstrates the success of covalent attachment of the lipase onto this silica structure that possesses an extremely high surface area. At room temperature, the microreactor was shown to convert triolein to ethyl oleate, or ethyl oleate and monoacylglycerols, depending on flow rate. Furthermore, the microreactor was successfully coupled to APPI mass spectrometry resulting in stable signals for both the reactants and products. Overall, the immobilization of enzymes onto silica monolith capillaries is a promising approach for micro-scale applications.

### 3.5 References

Akoh CC, Chang SW, Lee GC, Shaw JF (2007) Enzymatic approach to biodiesel production. *J Agric Food Chem* 55:8995–9005.

Asanomi Y, Yamaguch Y, Miyazaki M, Maeda H (2011) Enzyme-immobilized microfluidic process reactors. *Molecules* 16:6041-6059.

Athens GL, Shayib RM, Chmelka BF (2009) Functionalization of mesostructured inorganic–organic and porous inorganic materials. *Cur Opin Coll Inter Sci* 14:281-292.

- Battisha JK, El Beyally A, Abd El Mongy S, Nahrawi AM (2007) Development of the FTIR properties of nano-structure silica gel doped with different rare earth elements, prepared by sol-gel route J Sol-Gel Sci Techn 41:129-137.
- Bolivar JM, Wiesbauer J, Nidetzky B (2011) Biotransformations in microstructured reactors: More than flowing with the stream?. Trends Biotechnol 29:333-342.
- Brivio M, Fokkens RH, Verboom W, Reinhoudt DN, Tas NR, Goedbloed M, van der Berg A (2002) Integrated microfluidic system enabling (bio)chemical reactions with on-line MALDI-TOF mass spectrometry. Anal Chem 74:3972-3976.
- Cabrera K (2004) Applications of silica-based monolithic HPLC columns. J Sep Sci 27:843-852.
- Carvalho AT, Lima RR, Silva LM, Simoães EW, Silva MLP (2009) Three-dimensional microchannels as a simple microreactor. Sens Actuat B 137:393-402.
- Chopra R, Reddy SRY, Sambaiah K, (2008) Structured lipids from rice bran oil and stearic acid using immobilized lipase from *Rhizomucor miehei*. Eur J Lipid Sci Technol 110:32-39.
- De Haan JW, Van Den Bogaert HM, Ponjee JJ, Van De Ven LJM (1986) Characterization of modified silica powders by fourier transform infrared spectroscopy and cross-polarization magic angle spinning NMR. J Coll Inter Sci 110:591-597.
- Dizge N, Keskinler B, Tanriseven A (2009) Biodiesel production from canola oil by using lipase immobilized onto hydrophobic microporous styrene-divinylbenzene copolymer. Biochem Eng J 44:220-225.
- Ehrfeld W, Hessel V, Löwe H (2000). *Microreactors*. Wiley-VCH: Weinheim, Germany.

- He P, Greenway G, Haswell SJ (2010) Development of a monolith based immobilized lipase micro-reactor for biocatalytic reactions in a biphasic mobile system. *Process Biochem* 45:593-597.
- He P, Greenway G, Haswell SJ, (2010) Development of enzyme immobilized monolith micro-reactors integrated with microfluidic electrochemical cell for the evaluation of enzyme kinetics *Microfluid. Nanofluid* 8:565-573.
- Hiraoui M, Guendouz M, Lorrain N, Moadhen A, Haji L, Oueslati M (2011) Spectroscopy studies of functionalized oxidized porous silicon surface for biosensing applications *Mat Chem Physic* 128:151-156.
- Irimescu R, Iwasaki Y, Hou CT (2002) Study of tag ethanolsis to 2-MAG by immobilized *Candida antarctica* lipase and synthesis of symmetrically structured TAG. *J Am Oil Chem Soc* 79:879–883.
- Ishizuka N, Minakuchi H, Nakanishi K, Soga N, Nagayama H, Hosoya K, Tanaka N, (2000) Performance of a Monolithic Silica Column in a Capillary under Pressure-Driven and Electrodriven Conditions. *Anal Chem* 72:1275-1280.
- IUPAC (1994) Recommendations for the characterization of porous solids: Technical report. *Pure Appl Chem* 66:1739-1758.
- Kahraman MV, Bayramoğlu G, Kayaman-Apohan N, Güngör A (2007)  $\alpha$ -Amylase immobilization on functionalized glass beads by covalent attachment. *Food Chem*, 104:1385-1392.
- Kataoka S, Takeuchi Y, Harada A, Yamada M, Endo A (2010) Microreactor with mesoporous silica support layer for lipase catalyzed enantioselective transesterification. *Green Chem* 12:331-337.
- Kaupilla TJ, Östman P, Marttila S, Ketola RA, Kotiaho T, Franssila S, Kostianen R (2004) Atmospheric pressure photoionization-mass spectrometry with a microchip heated nebulizer. *Anal Chem* 76:6797-6801.

- Kawakami K, Takahashi R, Shakeri M, Sakai S (2009) Application of a lipase-immobilized silica monolith bioreactor to the production of fatty acid methyl esters. *J Mol Catal. B: Enzym* 57:194-197.
- Klepárník K (2013) Recent advances in the combination of capillary electrophoresis with mass spectrometry: From element to single-cell analysis. *Electrophoresis* 34:70-85.
- Lara PV, Park EY (2004) Potential application of waste activated bleaching earth on the production of fatty acid alkyl ester using *Candida cylindracea* lipase in organic solvent system. *Enzym Microbial Technol* 34:270-277.
- Lei J, Yu C, Zhang L, Jiang S, Tu B, Zhao D (2004) Immobilization of enzymes in mesoporous materials: controlling the entrance to nanospace. *Micropr Mesopr Mat* 73:121-128.
- Lendl B, Schindler R, Frank J, Kellner R, Drott J, Laurell T (1997) Fourier transform infrared detection in miniaturized total analysis systems for sucrose analysis. *Anal Chem* 69:2877-2881.
- Lowry OH, Rosebrough NJ, Farr AL, Randall RJ (1951) Protein measurement with the Folin phenol reagent. *J Biol Chem* 193:265-275.
- Ma J, Liang Z, Qiao X, Deng Q, Tao D, Zhang L, Zhang Y (2008) Organic-inorganic hybrid silica monolith based immobilized trypsin reactor with high enzymatic activity. *Anal Chem* 80:2949-2956.
- Maria Chong AS, Zhao XS (2003) Functionalization of SBA-15 with APTES and characterization of functionalized materials. *J Phys Chem B* 10: 12650-12657.
- McCreedy T (2000) Fabrication techniques and materials commonly used for the production of microreactors and micro total analysis systems. *Trends Anal Chem* 19:396-401.
- Mei Y, Miller L, Gao W, Gross RA (2003) Imaging the distribution and



secondary structure of immobilized enzymes using infrared microspectroscopy. *Biomacromol* 4:70-74.

Mugo SM, Ayton K (2010) Lipase immobilized microstructured fiber based flow-through microreactor for facile lipid transformations. *J Mol Catal B Enzym* 67:202–207

Nocuñ M, Siwulski S, Leja E, Jedliński J, (2005) Structural studies of TEOS-tetraethoxytitanate based hybrids. *Optic Mat* 27:1523-1528.

Pavia DL, Lampman GM, Kriz GS, Vyvyan JA (2009) *Introduction to Spectroscopy*, 4<sup>th</sup> ed. Brooks/Cole: Belmont, CA, USA.

Peña-Alonso R, Rubio F, Rubio J, Oteo JL (2007) Study of the hydrolysis and condensation of  $\gamma$ -Aminopropyltriethoxysilane by FT-IR spectroscopy. *J Mater Sci* 42:595-603.

Phan NTS, Brown DH, Styring P (2004) A facile method for catalyst immobilisation on silica: nickel catalysed Kumada reactions in mini-continuous flow and batch reactors. *Green Chem.* 6:526-532.

Pohar A, Plazl I, Žnidaršič-Plazl P (2009) Lipase-catalyzed synthesis of isoamyl acetate in an ionic liquid/n-heptane two-phase system at the microreactor scale. *Lab Chip* 9:3385-339.

Shimada Y, Ogawa J, Watanabe Y, Nagao T, Kawashima A, Kobayashi T, Shimizu S (2003) Regiospecific analysis by ethanolysis of oil with immobilized *Candida antarctica* lipase. *Lipids* 38:1281–1286.

Shimada Y, Watanabe Y, Sugihara A, Tominaga Y (2002) Enzymatic alcoholysis for biodiesel fuel production and application of the reaction to oil processing. *J Mol Catal B: Enzym* 17:133-142.

Soumanou MM, Bornscheuer UT, Schmid U, Schmid RD (1998) Synthesis of structured triglycerides by lipase catalysis. *Fett/Lipid* 100:156-160.

- Stamenković OS, Veličković AV, Veljković VB (2011) The production of biodiesel from vegetable oils by ethanolysis: Current state and perspectives. *Fuel* 90:3141-3155.
- Thomsen MS, Pölt P, Nidetzky B (2007) Development of a microfluidic immobilised enzyme reactor. *Chem Comm* 24:2527-2529.
- Tlili A, Ali Jarboui M, Abdelghani A, Fathala DM, Maaref MA (2005) A novel silicon nitride biosensor for specific antibody–antigen interaction. *Mat Sci Eng C* 25:490-495.
- Villegas C, Zhao Y, Curtis JM (2010) Two methods for the separation of monounsaturated octadecenoic acid isomers. *J Chrom A* 1217:775-784.
- Watts P, Wiles C (2007) Micro reactors: a new tool for the synthetic chemist. *Org Biomol Chem* 5:727–732.
- Watts P, Wiles C (2007) Recent advances in synthetic microreaction technology. *Chem Commun* 5:443–467.
- Xie C, Ye M, Jiang X, Jin W, Zou H (2006) Octadecylated silica monolith capillary column with integrated nanoelectrospray ionization emitter for highly efficient proteome analysis. *Molec Cell Proteom* 5:454–461.
- Zhou Z, Yang Y, Zhang J, Zhang Z, Bai Y, Liao Y, Liu H (2012) Ion-exchange-membrane-based enzyme micro-reactor coupled online with liquid chromatography–mass spectrometry for protein analysis *Anal Bioanal Chem* 403:239-246.

## CHAPTER 4:

# A FEASIBILITY STUDY ON THE USE OF A LABORATORY PREPARED BIO-CATALYST MICROREACTOR TO DERIVATIZE LIPIDS FOR ANALYTICAL APPLICATIONS<sup>12</sup>

---

### 4.1 Introduction

For at least 5 decades, gas chromatography (GC) has been the most widely used method to characterize the fatty acid composition of fats and oils as their methyl ester derivatives (FAME) (Craig and Murty, 1959; Sheppard and Iverson, 1975; Ichihara *et al.*, 1996; Aichholz and Lorbeer, 1998; Gunstone, 2004; Christie and Han, 2012). During this period of time there have been many developments in both GC technology and in derivatization techniques (Carrapiso and Carmen, 2000; Indarti *et al.*, 2005; Christie and Han, 2012).

The transesterification of animal or vegetable triacylglycerol (TAG) by methanol involves the use of either an alkaline or acid catalyst and the reaction conditions have been optimized for temperatures, amounts and times (Craig and Murty, 1959; Sheppard and Iverson, 1975; Carrapiso and Carmen, 2000; Goff *et al.*, 2004; Igarashi *et al.*, 2004; Indarti *et al.*, 2005; AOCS, 2012; Christie and Han, 2012;) leading to the development of a number of widely used official methods. For instance, both of the AOCS official methods Ce 2-66 and Ce 1b-89

---

<sup>12</sup> A version of this chapter has been submitted to *Journal of the American Oil Chemist Society* (2013) as Anuar *et al.*

Supplementary data regarding this chapter are given in Appendix 4.

include the use of a boron trifluoride/methanol ( $\text{BF}_3/\text{MeOH}$ ) solution to convert the lipid sample into FAME prior to GC analysis (AOCS, 2012). In addition, there are several other standard methods for preparing FAME including AOCS Ce 1k-09 and AOAC 965.49 (AOAC, 2000; AOCS, 2012). These methods have been shown to produce quantitative amounts of fatty acid methyl ester but usually involve multiple steps of sample derivatization and workup prior to obtaining the final solution for GC analysis. Another disadvantage is the time and cost of these procedures as well as the need for handling chemical reagents including  $\text{BF}_3$ , strong acids or bases and various organic solvents. Hence, a move towards enzyme catalyzed transesterification reactions for analytical applications could be advantageous. It should be noted that although most methods use fatty acid methyl ester derivatives, comparable separation of fatty acid ethyl esters (FAEE) by GC is readily achieved. Thus, some official methods for the analysis of oils already in the fatty acid ethyl esters form do not require conversion to fatty acid methyl ester prior to GC analysis, such as Ph.Eur.2063 for omega-3-acid ethyl esters (European Pharmacopoeia, 2012).

Recently, considerable advances have been made in industrial production of biodiesel and food grade ethyl esters using enzyme mediated approaches (Iso *et al.*, 2001; Dossat *et al.*, 2002; Akoh, 2007; Leung *et al.*, 2010; Stamenković *et al.*, 2011). The use of lipases is advantageous since it benefits from milder conditions, avoids the need for strong acids and bases and can result in high yields of fatty acid alkyl esters (FAAE) with few side products (Arroyo *et al.*, 1996; Iso *et al.*, 2001; Dossat *et al.*, 2002; Akoh, 2007; Leung *et al.*, 2010; Stamenković *et al.*,

2011). A challenge to the success of a biocatalytic process is the cost of the enzyme and ensuring its reusability under the reaction conditions. However, enzymes can be immobilized onto high surface area supports which can both facilitate the catalysis and aid in enzyme re-use.

In this research, it was proposed to immobilize enzymes within a 'microreactor', a structure containing channels or networks in the  $\mu\text{m}$  range (Watts and Wiles, 2007). This provides a high internal surface area for enzyme support and ultimately for efficient small-scale reactions. In the microreactor systems considered here, chemical reactions can take place under conditions of continuous flow. The substrate can be passed through the microreactor for as many cycles as the enzyme remains active, so that the microreactor is both versatile and reusable.

Commercially, some types of microreactors for chemical synthesis are made by photolithographic and wet-etching techniques (McCreeley, 2000). However, in order to develop a process amenable to laboratory fabrication, other approaches are required. This thesis proposes the use of silica support, a platform with great potential for chemical modifications to allow the immobilization of catalysts including enzymes, organometallics or metals (McCreeley, 2000; Phan *et al.*, 2004; Xie *et al.*, 2006; Ma *et al.*, 2008; Mugo and Ayton, 2010; Mugo and Ayton, 2013). Previously, the use of microreactors in which lipase was immobilized onto either a silica monolith (SM) within a fused-silica capillary or immobilized within a fused silica microstructured fiber (photonic fibre, MSF) has been discussed (Chapters 2 and 3). These studies demonstrated the effectiveness

of the prototype devices in transforming triacylglycerols into fatty acid ethyl esters and into 2-monoacylglycerols, depending on the experimental conditions. Lipase from *Candida antarctica* was chosen since it is a widely used and commercially produced enzyme for lipid transesterification (Shimada *et al.*, 1999; Dossat *et al.*, 2002; Irimescu *et al.*, 2002; Akoh, 2007; Mugo and Ayton, 2010; Leung *et al.*, 2010; Stamenković *et al.*, 2011; Mugo and Ayton, 2013; Chapters 2 and 3).

This chapter investigates the possibility that lipase microreactors could be used for the transesterification of triacylglycerols into fatty acid alkyl esters for GC analyses as an alternative to the widely used chemical procedures for derivatization to fatty acid methyl ester.

## **4.2 Experimental Procedures**

### ***4.2.1 Materials:***

Fused silica (ID: 320  $\mu\text{m}$ , 8cm) and microstructured fiber optic (MSF) (F-SM35, ID: 12-13  $\mu\text{m}$ , outer diameter: 480  $\mu\text{m}$ , 90 holes, 8 cm) capillaries were obtained from Polymicro Technologies (Phoenix, AZ, USA) and Newport Corp. (Irvine, CA, USA), respectively.

A Harvard Model '11 Plus syringe pump was from Harvard Apparatus (Holliston, MA, USA). All food grade canola (CanO), sesame seed (SSO) and soybean (SBO) oils were purchased from a local grocery store. Refined-bleached-

deodorized palm oil (RBD-PO) was obtained from Malaysian Palm Oil Board. 3-(Aminopropyl)triethoxylane (APTES, 99%), sodium sulfate, sodium carbonate, sodium chloride, glutaraldehyde solution (BioChemika, ~50% in H<sub>2</sub>O), sodium cyanoborohydride (reagent grade, 95%), Novozyme 435 lipase beads and lipase from *Candida antarctica* (EC 3.1.1.3, BioChemika) were obtained from Sigma-Aldrich Ltd (Oakville, ON, Canada). Sulphuric acid and acetic acid (glacial, HPLC) were purchased from Fisher Scientific (Bridgewater, NJ, USA). Pure triolein (>99%) and all C16:0, C18:0, C18:1, C18:2 and C18:3 ethyl ester (FAEE) standards were purchased from Nu-Chek (Elysian, MN, USA). All organic solvents were HPLC analytical grade from Sigma-Aldrich (Oakville, ON, Canada).

#### ***4.2.2 Fabrication of SM and MSF Microreactors***

The silica monolith (SM) was made following the procedure described in detail earlier (Chapter 3, Section 3.2.2) and outlined in Figure 4-1. The procedure for the immobilization of the free lipase onto either the SM or within a silica microstructured fibre (MSF) involves the coupling of a linker molecule, aminopropyl ethoxysilane (APTES) onto the silica surface (Fig. 4-1).

The lipase is then immobilized onto the active site by means of glutaraldehyde (Mugo and Ayton, 2010; Mugo and Ayton, 2013; Chapter 2-3). Using these procedures, a number of identical SM and MSF microreactors were prepared for this study.

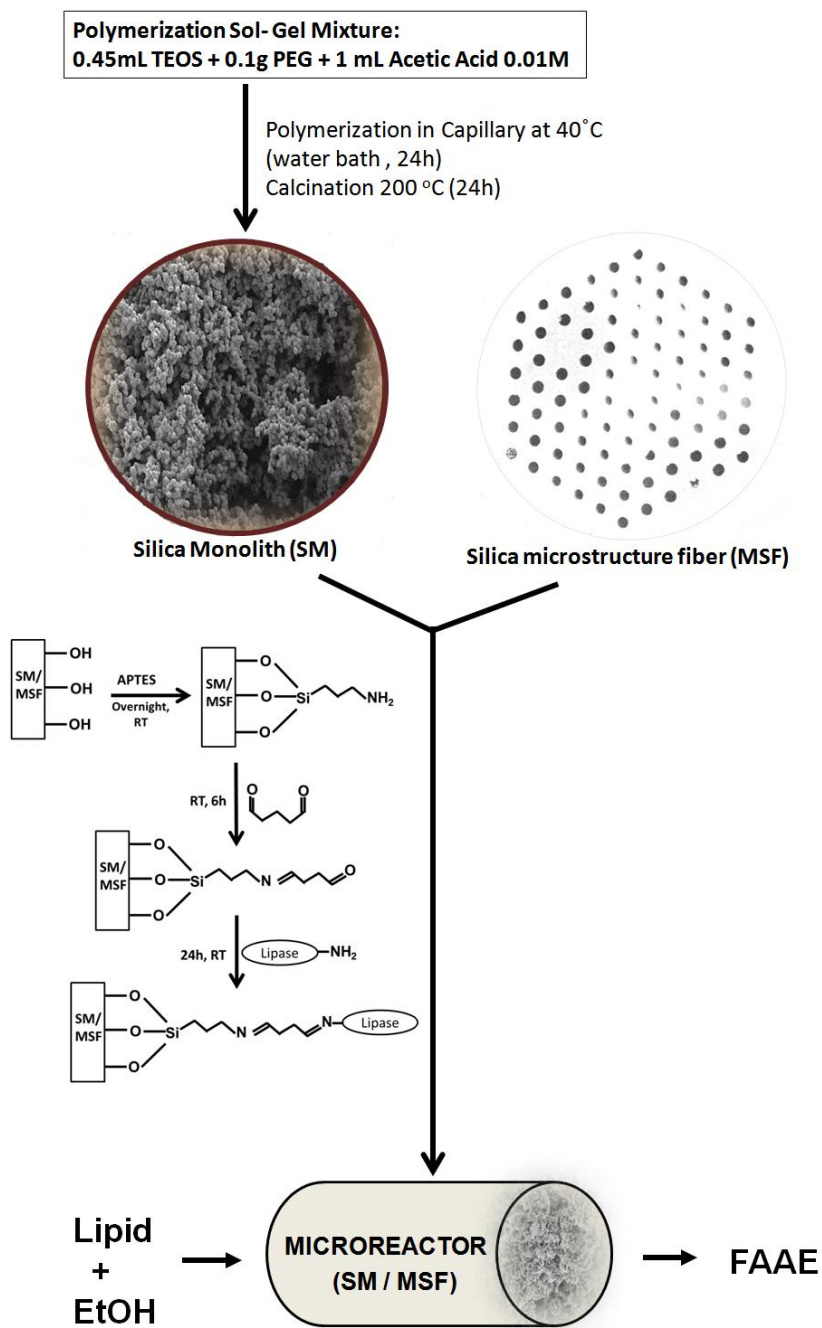


FIG 4-1: Reaction scheme for the small-scale fabrication of silica monolith (SM) and microstructure fiber (MSF) capillary biocatalyst microreactors.



#### ***4.2.3 Direct Ethylation using the Microreactors***

Selected reaction mixtures of: (i) 0.5 mg/mL canola oil, (ii) 0.5 mg/mL sesame seed oil and (iii) 0.5 mg/mL soybean oil were prepared in ethanol (EtOH) and vortexed vigorously to dissolve the lipids in ethanol. 0.5 mg/mL refined-bleached-deodorized palm oil was prepared in ethanol with excess of hexane (ethanol:hexane, 1:2, v/v).

Each substrate solution was infused through the enzymatic microreactors at room temperature at 0.3  $\mu\text{L}/\text{min}$  for 5 h using a Harvard Model '11 Plus syringe pump. The eluent was collected and prepared in dichloromethane (DCM) prior to GC/FID and GC/MS injection.

#### ***4.2.4 Batch Ethylation using Commercial Lipase Beads***

The same reaction mixtures of ethanolic canola oil, sesame seed oil, soybean oil, and refined-bleached-deodorized palm oil were each stirred at 80 rpm in the presence of 3 mg of commercialized lipase beads (Novozyme 435) in a small vial for 5 h at room temperature. Aliquots of the ethylation reaction mixture (~100  $\mu\text{L}$ ) were collected (**i**) after 10 min; and (**ii**) after 5 h of reaction. Samples were filtered through a syringe filter and diluted 5 times in DCM for GC/MS and GC/FID analyses.

#### ***4.2.5 Acid-catalyzed ethylation using H<sub>2</sub>SO<sub>4</sub>***

The ethylation of triacylglycerols (TAG) in canola oil, sesame seed oil, soybean oil, and palm oil using an acid-catalyzed method followed a procedure described by Christie (1989). Briefly, 1 mg of each vegetable oil was mixed with 1% H<sub>2</sub>SO<sub>4</sub> in 2 mL EtOH. One mL toluene was added to the reaction mixtures before they were left overnight at 50 °C. Then, the samples were washed with 5 mL of 5% NaCl in H<sub>2</sub>O before adding 5 mL hexane to extract the ethyl esters. The extraction with hexane was performed twice to ensure that all of the fatty acid ethyl esters were extracted. The hexane layer was then washed with 2% NaHCO<sub>3</sub> solution (2 mL) then dried with 2 g anhydrous sodium sulphate (Na<sub>2</sub>SO<sub>4</sub>). The solution was filtered and the lipid was concentrated under N<sub>2</sub> gas. Prior to GC analyses, all samples were weighed and diluted with DCM.

#### ***4.2.6 Reusability of Microreactor for Selected Alcohols***

To test the robustness and reusability of the microreactor in performing alcoholysis, 2 identical SM microreactors were tested using (i) 0.2 mg/mL trioleoylglycerol in EtOH, and (ii) 0.2 mg/mL trioleoylglycerol in methanol:toluene (1:2, v/v), both at 0.3 μL/min at room temperature. Each condition was repeated on the same microreactor 5-8 times, and the transesterification products that eluted from the microreactors were collected, identified and quantified by GC/MS with negative ion chemical ionization mode

(NCI) and GC/FID. The uncorrected GC/FID peak areas were expressed as a percentage of the total peak area for fatty acid ethyl ester or fatty acid methyl esters. The reusability of the microreactor was further tested using sesame seed oil, a natural oil sample. GC/FID peak areas of the resulting fatty acid ethyl ester products were expressed as uncorrected area percentages. For each component, the overall precision was estimated by calculating the standard deviations over the 5 runs.

#### **4.2.7 Instrumentation**

##### **4.2.7.1 GC/MS-NCI**

An Agilent GC/MS system (GC/MS 5975C, Agilent Technologies, Santa Clara, CA, USA) operating in negative ion chemical ionization mode (NCI) was used with ammonia as reagent gas. All data was collected by Agilent Chemstation software (version G1701EA). The GC column used for separation was an HP-5MS 5% phenyl methyl siloxane (30 m x 0.25 mm x 0.25  $\mu$ m) column (Agilent Technologies; Santa Clara, CA, USA). The make-up gas was He at a flow rate of 1 mL/min, with split mode at 20:1. Reaction product samples were dissolved in DCM (1 mL) prior to injection. The injection volume of 2  $\mu$ L and the split/splitless injector temperature was set at 275  $^{\circ}$ C. The oven program started at a temperature of 80  $^{\circ}$ C (0 min), then increased at 15  $^{\circ}$ C/min until reaching 150  $^{\circ}$ C (0 min) before increasing again at 10  $^{\circ}$ C/min to 260  $^{\circ}$ C (15 min). A mass spectrometer scan range of  $m/z$  35 to 600 was used.

#### **4.2.7.2 GC/FID**

An Agilent 7890 GC system (Agilent Technologies, Santa Clara, CA, USA) equipped with a flame ionization detector (FID), autosampler and split/splitless injector was used to run samples and standards on a BPX-70 column 110 m x 0.25 mm x 0.25  $\mu\text{m}$  (Agilent Technologies; Santa Clara, CA, USA) and all data were collected by Agilent Chemstation software (version G1701EA). The GC parameters were: 2  $\mu\text{L}$  injection volume, split ratio 20:1, FID carrier gas:  $\text{H}_2$ , flow rate 2 mL/min, inlet temperature 250  $^\circ\text{C}$ , detector temperature 250  $^\circ\text{C}$ , make-up gas: He. Temperature program: 140  $^\circ\text{C}$  (hold 5 min); 8  $^\circ\text{C}/\text{min}$  to 180  $^\circ\text{C}$  (0 min); 4  $^\circ\text{C}/\text{min}$  to 210  $^\circ\text{C}$  (0 min); 20  $^\circ\text{C}/\text{min}$  to 270  $^\circ\text{C}$  (hold 7 min). All reaction product samples were dissolved in DCM prior to injection.

#### **4.2.7.3 NARP-HPLC/ELSD**

In order to confirm the disappearance of TAG from starting oil after the reaction, a non-aqueous reversed phased high-performance liquid chromatography (NARP-HPLC) analysis was performed using an Agilent 1200 HPLC system equipped with an evaporative light scattering detector (ELSD 1260 Infinity, Agilent Technologies, Santa Clara, CA, USA). Separations were achieved using an Agilent Zorbax HT C18 column (4.6 x 50 mm, 1.8  $\mu\text{m}$ , Agilent Tech, Santa Clara CA USA) with a gradient of solvent A, acetonitrile:methanol (1:4, v/v) and solvent B, hexane:isopropanol (5:4, v/v) was used .

The starting condition was 0% B and held for 5 min, then increased to 70% B in 13.5 min, and held for another 5.5 min, before returning to 0% B at 19.1 min. This condition was held for 1 min ( $t = 20.1$  min) in order to equilibrate the column. The ELSD temperature was set to 33 °C, with N<sub>2</sub> gas flow of 3 L/min at pressure of 3.5 bar, and all data were collected by Agilent Chemstation software (version G2180BA).

## **4.3 Results and Discussion**

### ***4.3.1 A Comparison of Procedures for the Ethanolysis of Vegetable Oils***

Usually, the analysis of fatty acids by GC is preceded by their conversion into fatty acid alkyl esters. Previously, the potential use of microreactors for such simple lipid conversions was discussed (Mugo and Ayton, 2010; Mugo and Ayton, 2013; Chapter 2 and 3). Here, this chapter describes the conversion of triacylglycerol mixtures from edible oils into their fatty acid ethyl ester derivatives using two types of laboratory prepared enzymatic capillary microreactors (SM and MSF) that were optimized for use at a low flow rates (0.3  $\mu\text{L}/\text{min}$ ) and at room temperature. Under these conditions the microreactors produce fatty acid ethyl ester in amounts that are suitable for GC analyses. The conversions of canola, sesame, soybean and RBD-palm oils into fatty acid ethyl esters were tested to evaluate the performance of the microreactors, as shown in Table 4-1.

TABLE 4-1: The major FAEE observed following the transesterification of 4 edible oils catalyzed by lipase immobilized within SM or MSF microreactors; by commercially immobilized lipase on beads; or catalyzed by strong acid. The results are expressed as uncorrected GC/FID peak area percentages.

	FAEE Composition (%)				
	C16:0	C18:0	C18:1	C18:2	C18:3
<b>Canola Oil (CanO)</b>					
SM Microreactor <sup>a</sup>	4.2	1.1	69.7	18.2	5.9
MSF Microreactor <sup>b</sup>	4.3	1.2	68.5	17.2	6.2
Novozyme 435 <sup>c</sup>	4.2	1.1	69.9	17.0	5.7
H <sub>2</sub> SO <sub>4</sub> catalyst <sup>d</sup>	4.4	1.1	68.4	17.1	5.1
<b>Sesame Seeds Oil (SSO)</b>					
SM Microreactor <sup>a</sup>	9.3	5.3	40.2	43.2	1.2
MSF Microreactor <sup>b</sup>	9.7	6.3	39.5	42.9	1.0
Novozyme 435 <sup>c</sup>	9.2	5.6	40.4	43.1	1.2
H <sub>2</sub> SO <sub>4</sub> catalyst <sup>d</sup>	9.2	5.2	39.6	42.6	1.3
<b>Soybean Oil (SBO)</b>					
SM Microreactor <sup>a</sup>	10.0	1.0	22.8	56.4	9.6
MSF Microreactor <sup>b</sup>	9.7	1.0	22.5	56.6	9.2
Novozyme 435 <sup>c</sup>	9.3	1.0	21.9	56.4	9.8
H <sub>2</sub> SO <sub>4</sub> catalyst <sup>d</sup>	8.9	1.2	21.1	53.8	8.9
<b>RBD Palm Oil (RBD-PO)</b>					
SM Microreactor <sup>a</sup>	43.8	8.9	36.7	9.5	0.4
MSF Microreactor <sup>b</sup>	43.6	8.9	36.6	9.2	0.4
Novozyme 435 <sup>c</sup>	42.1	8.4	35.4	9.4	0.4
H <sub>2</sub> SO <sub>4</sub> catalyst <sup>d</sup>	40.8	8.5	33.2	9.3	0.4

<sup>a</sup> Collected from Silica Monolith Microreactor at 0.3 μL/min (constant continuous conversion over >5 h).

<sup>b</sup> Collected from Silica MSF Microreactor at 0.3 μL/min (constant continuous conversion over >5 h).

<sup>c</sup> Collected by vortexed reactants with Novozyme 435 at 100 rpm after 5 h.

<sup>d</sup> Collected from transesterification of reactant using acid catalyst after 12 h.

The transesterification of canola oil in ethanol using the SM and MSF microreactors resulted in virtually identical fatty acid ethyl esters peak areas in the GC/FID trace, as indicated in Table 4-1. Furthermore, NARP-LC/ELSD analysis of the microreactor product indicated complete conversion from the triacylglycerol to the ethyl oleate form of the lipid (data not shown). Quantitative conversion into fatty acid ethyl ester was expected based on a previous study in which a lipase immobilized silica monolith succeeded in converting a pure standard of trioleoylglycerol (C18:1) completely into ethyl oleate when at room temperature and with flow rates through the microreactor of 0.2-0.5  $\mu\text{L}/\text{min}$  (Chapter 3, Section 3.3.3).

In the case of conversion of RBD-palm oil, which has a high level of palmitic acid, the solubility in ethanol was very sparing and so hexane was added (1:2 *v/v* ethanol/hexane) in order to make a solution. However, under the same conditions of flow rate and temperature the presence of hexane did not affect the conversion of triacylglycerol to fatty acid ethyl ester and complete conversion to ethyl esters was achieved.

Previous studies have also shown that addition of modest amounts of organic solvents such as *n*-hexane, di-ethyl- and di-isopropyl-ether (DIPE) to enzymatic reactions in lipid transformations does not result in enzyme deactivation (Fureby *et al.*, 1997; Linko *et al.*, 1998; Dossat *et al.*, 2002). The fatty acid distributions measured by GC/FID for the fatty acid ethyl ester of each of the 4 oils following transesterification catalyzed within the MSF or SM

microreactors were all consistent with literature reports (Lee *et al.*, 1998; Hammond, 2003).

The MSF and SM catalyzed ethanolysis was then compared to ethanolysis of identical oils using commercial immobilized lipase beads (Novozyme 435, lipase immobilized on acrylic resin) as well as to a conventional acid catalysis using sulphuric acid (Christie, 1989). The fatty acid ethyl ester compositions from both methods were consistent with the distribution of fatty acid ethyl esters that were produced from MSF and SM microreactors (Table 4-1), within experimental error. Examples of GC/FID chromatograms for transesterification of canola oil in ethanol are shown in Figure 4-2. Figures 4-2b and c show the ethylation products that eluted from the SM and MSF microreactors. These products had retention times that matched those of the corresponding standards (Fig. 4-2a). In addition, the fatty acid ethyl ester distribution and retention times obtained using commercial immobilized lipase (Fig. 4-2d) and the acid catalyst (Fig. 4-2e) were consistent with results from MSF and SM microreactors.

All of the reaction products were also identified by GC/MS using negative ion chemical ionization (GC/MS-NCI). In all four cases, the GC/MS-NCI traces (not shown) closely resembled the GC/FID traces seen in Figure 4-2. Furthermore, the NCI mass spectra of the major peaks confirm the presence of fatty acid ethyl ester for both the MSF and SM; this is shown in Figure 5-3 for the example of conversion of sesame seed oil in the SM.



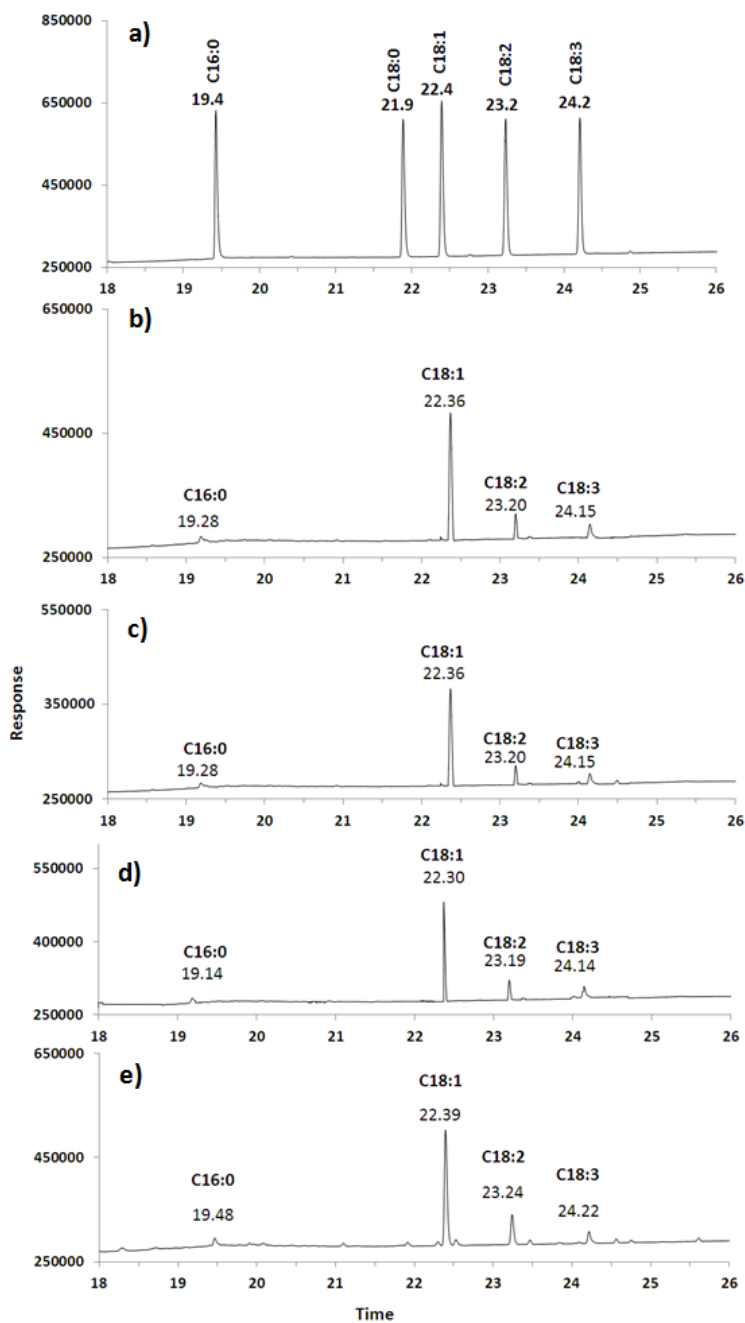


FIG 4-2: Comparison of GC/FID chromatograms for (a) fatty acid ethyl ester standards; and the products of canola oil (CanO)+EtOH transesterification using: (b) SM microreactor at 0.3  $\mu\text{L}/\text{min}$  flow-rate ; (c) MSF microreactor at 0.3  $\mu\text{L}/\text{min}$  flow-rate; (d) lipase beads after 5 h reaction time; (e) H<sub>2</sub>SO<sub>4</sub> acid catalysis after 12 h reaction time.<sup>13</sup>

<sup>13</sup> Supplementary data are given in Appendix A4-3 to A4-6.

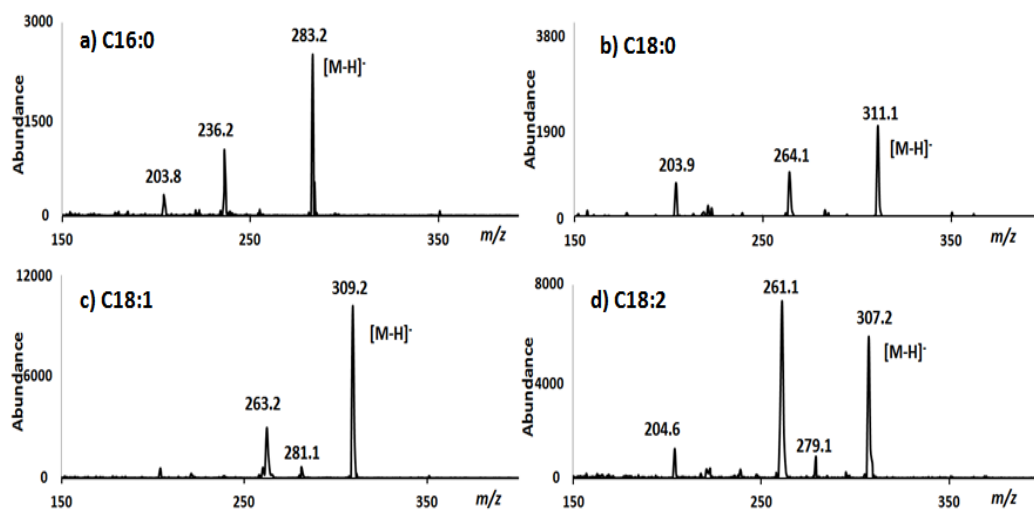


FIG 4-3: NCI-mass spectra from GC/MS separations of the products of sesame seed oil (SSO) and ethanol passing through the SM microreactor. Shown are examples of FAEE identified including (a) C16:0 ethyl ester, (b) C18:0 ethyl ester, (c) C18:1 ethyl ester, (d) C18:2 ethyl ester.

Specifically, the presence of ethyl oleate (C18:1) and ethyl linoleate (C18:2) was confirmed by their [M-H]<sup>-</sup> ions at  $m/z$  309.1 and  $m/z$  307.1 (Figs. 4-3 c and 3d) as well as the characteristic fragment ions due to loss of ethanol. Similarly, the [M-H]<sup>-</sup> ions for both fatty acid ethyl ester of palmitic and stearic acid GC peaks were observed (Figs.4-3 a and b).

It is of importance to demonstrate the performance of the enzymatic microreactor in comparison to the use of the same lipase that is available commercially immobilized onto 0.3 – 1 mm sized beads since it might be possible to perform the transesterification using these, albeit with a considerably larger

quantity of starting oil. Figure 4-4 shows examples of the results for the transesterification of soybean oil in ethanol for several conditions: a) SM microreactor at 0.3  $\mu\text{L}/\text{min}$ , b) lipase beads (Novozyme 435, stirred for 10 min), c) lipase beads (Novozyme 435, stirred for 5 h).

The degree of conversion from triacylglycerol to fatty acid ethyl ester was demonstrated by the NARP-LC/ELSD traces for the same experiments shown in Figures 4-4 d, e and f respectively (Fig. 4-4 g is the starting material given for comparison). This gives an indication of the relative reaction rates catalyzed by the same lipase either immobilized onto the monolithic microreactor (SM) support or onto beads. Comparing the manufacturer specified enzyme activity for the beads to the measured enzyme activity in the SM (Chapter 3) would predict a somewhat higher activity in the beads based on the conditions used here. However, what was found was that after 10 min reaction using lipase beads stirred in a vial (1 mL ethanol, 0.5 mg oil, 3 mg Novozyme 435 beads, see Figs. 4-4b and e) the starting soybean oil was only partially converted to fatty acid ethyl ester and the diacylglycerol intermediates were also present.

After 5 h of stirred reaction at room temperature, there is complete conversion to fatty acid ethyl ester as seen in Figures 4-4 c and f. In contrast, using the flow-through microreactor rapid ethanolysis of soybean oil was achieved (Fig. 4-4a and d) resulting in complete conversion of triacylglycerol during the residence time of approximately 336 s (for 8 cm SM). This greatly enhanced rate of ethanolysis (336 s vs up to 5 h) can be partly explained by the

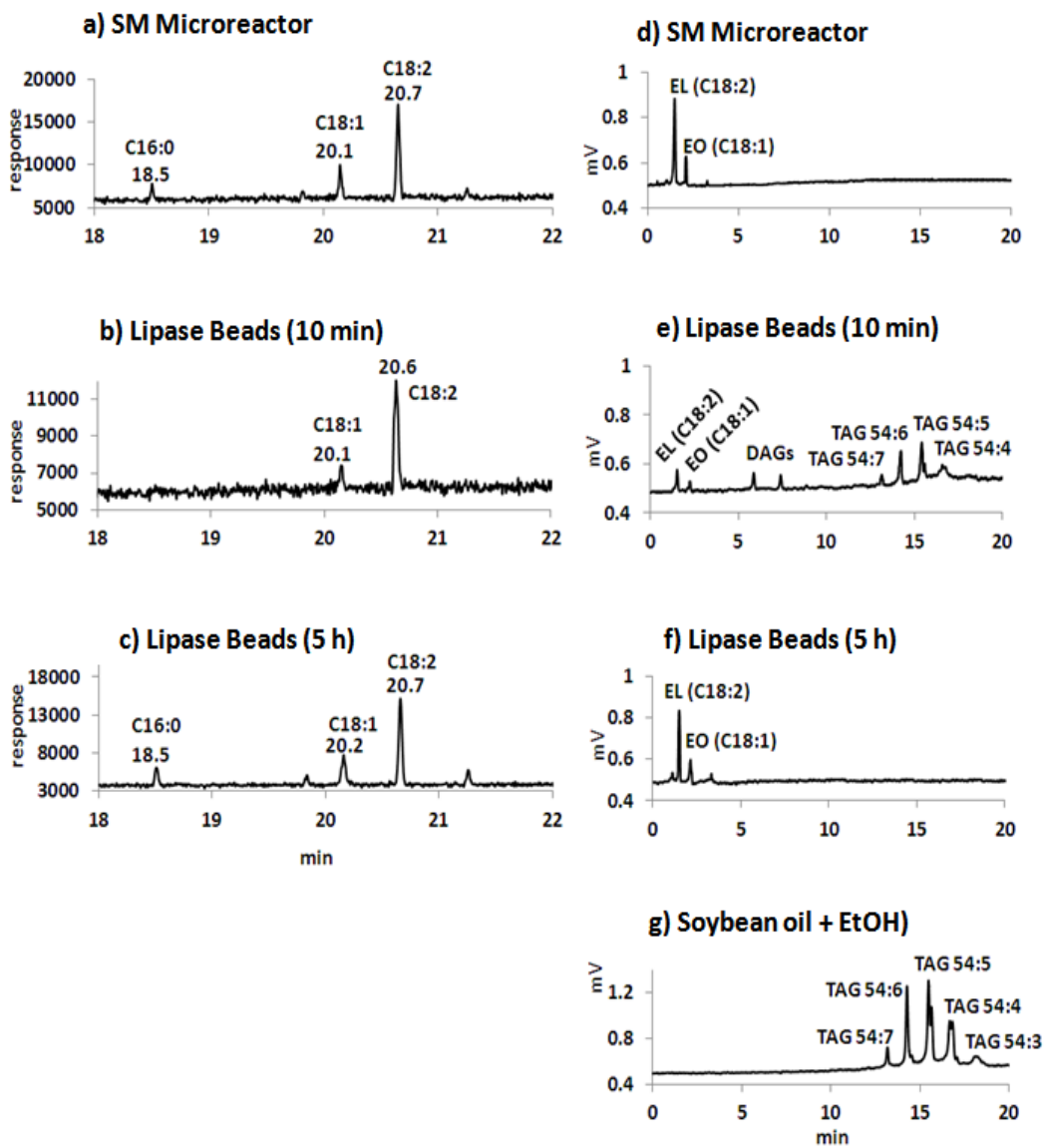


FIG 4-4: Comparison of the GC/MS-NCI total ion current (TIC) and NARP-LC/ELSD traces for the transesterification products of soybean oil (SBO)+EtOH using: i) **(a and d)** SM microreactor at 0.3  $\mu\text{L}/\text{min}$ ; ii) **(b and e)** Novozyme 435 lipase beads, 10 min reaction time; iii) **(c and f)** Novozyme 435 lipase beads, 5 h reaction time; iv) **(g)**: NARP-LC/ELSD of SBO starting oil.

vastly increased surface area available for reaction as the solution passes through the monolithic structure (Fig. 4-1), which may be particularly important due to the formation of a biphasic system as glycerol and water are liberated. In addition, over time the enzymatic action on complex lipid mixtures such as in soybean oil may also result in acyl migrations (*i.e.* interesterification reactions) that compete with ethanolysis (Irimescu *et al.*, 2002). These processes, especially the much lower catalytic surface area, may be responsible for the much lower rate of ethanolysis with the lipase immobilized onto beads.

In summary, it was shown that at room temperature and low flow rates, the SM microreactor is a flow-through system that is able to achieve quantitative conversion of oils into fatty acid ethyl ester derivatives. In order to demonstrate the reusability of SM microreactors, transesterification was performed by passing a 0.2 mg/mL solution of trioleoylglycerol in ethanol at a flow rate of 0.3  $\mu\text{L}/\text{min}$  through a single microreactor at room temperature. Eight consecutive experiments were performed, separated by a sodium phosphate buffer (pH 7.23) flush between each run.

It was found that 6 repeat ethanolysis reactions could be performed without any loss of conversion efficiency (see Fig. 4-5). Over these 6 runs, the average GC/FID peak area for ethyl oleate, normalized to that of run 1, was 0.997 with an RSD of 0.19%. Complete conversion to ethyl oleate was also seen by NARP-LC/ELSD so that for runs 1 to 6 no residual TAG peak observed. At runs 7 and 8 triacylglycerol was present at an estimated concentration of 0.6% and 2.5% of total lipid. The corresponding normalized GC/FID peak areas for

trioleoylglycerol were 0.993 and 0.948 respectively indicating <1% and < 5% reduction in fatty acid ethyl ester yield for runs 7 and 8 compared to run 1. Hence, a single SM microreactor could be used for 7 times whilst maintaining >99% conversion of trioleoylglycerol to fatty acid ethyl ester (Fig. 4-5).

A similar result was also achieved for the conversion sesame seed oil triacylglycerols into fatty acid ethyl ester using a single SM microreactor. It can be seen in Table 4-2, that the RSD's of the GC/FID peak areas for 5 runs were <1.5% for the 3 most abundant fatty acid ethyl ester; for less abundant fatty acid ethyl ester the standard deviations were similar but resulting in RSDs of ~7%. Hence, the SM microreactor was reused 5 times for the direct conversion of a natural vegetable oil to fatty acid ethyl ester, without loss of efficiency.

It should be noted that in the above experiments, fatty acid ethyl ester were collected continuously over a period of 5 h and samples of the collected fraction were used for GC/FID or LC/ELSD analyses<sup>14</sup>. This long period of collection (>25 h total for the sesame seed oil data shown in Table 4-2) was chosen in order to demonstrate the longevity of the microreactor; in practice only a few minutes of collection time is required to produce a sample for GC analysis. Hence, it is reasonable to estimate that if used in a flow-injection mode, even with only 1 sample per hour the microreactor could be reused 25 times or more, if similar conditions are maintained.

---

<sup>14</sup> Supplementary data are given in Appendix A4-1 and A4-2.

TABLE 4-2 GC/FID area percentages for fatty acid ethyl ester (FAEE) formed by esterification of sesame seed oil using a single SM microreactor for 5 runs. For each run, performed on a separate day, products were collected for 5 h at a flow rate of 0.3  $\mu$ L/min.

GC/FID <sup>a</sup> (%)							
FAEE	Run 1	Run 2	Run 3	Run 4	Run 5	STDEV	%RSD
C18:2	43.1	43.5	42.4	42.5	43.0	0.47	1.1
C18:1	40.3	39.7	39.7	40.0	39.3	0.38	1.0
C18:0	5.8	5.9	6.7	6.4	6.9	0.48	7.5
C16:0	9.1	9.3	9.5	9.4	9.4	0.14	1.5
C18:3	1.1	1.0	1.2	1.1	1.0	0.08	7.1
TAG <sup>b, c</sup>	n/d	n/d	n/d	n/d	0.17 <sup>b</sup>	-	-

<sup>a</sup>the GC/FID was expressed by normalizing individual peak area to the total peak area.

<sup>b</sup>TAG was quantified using % NARP-LC/ELSD as described in Section 4.2.7.3. Note that the normalized response factor of ELSD was higher for TAG (1) compared to that for FAEE (0.5).

<sup>c</sup>n/d not detectable.

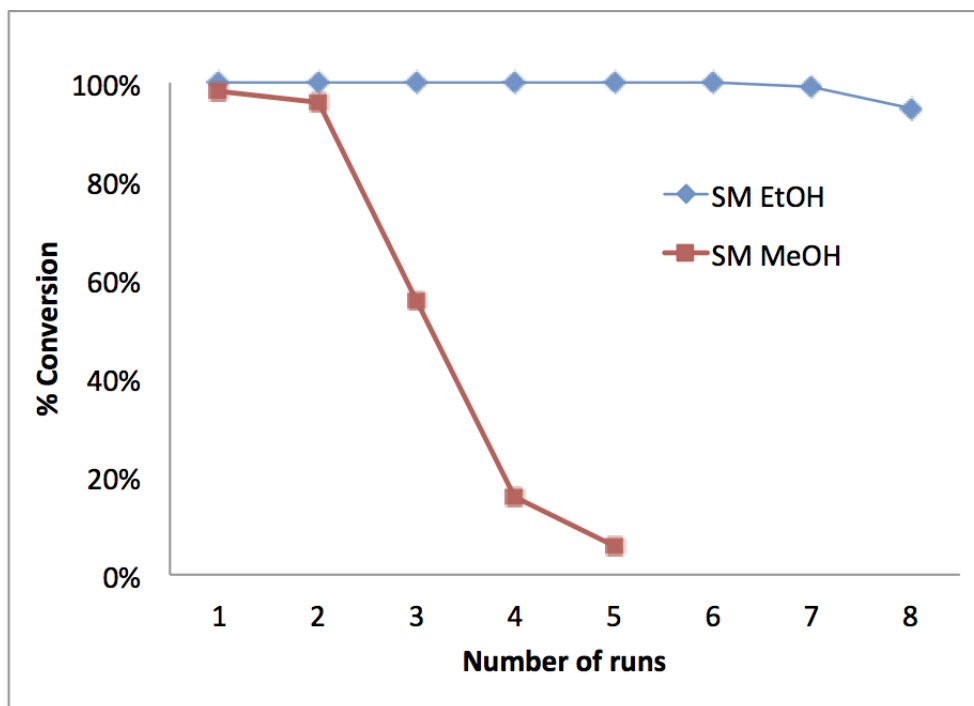


FIG 4-5: Percent conversion of trioleoylglycerol (TO) in ethanol to ethyl oleate (SM-EtOH) (◆) and in methanol to methyl oleate (SM-MeOH) (■) for 5-8 runs, using a single SM microreactor with a flow rate of 0.3  $\mu\text{L}/\text{min}$  at room temperature.

#### 4.3.2 The Methanolysis of Triolein using SM Microreactor

In oil derivatization for GC analysis using chemical catalysts, methanol is typically the alcohol used, producing fatty acid methyl ester. However, concerns over the miscibility of the reaction mixture and product recovery may favor the use of longer chain alcohols such as ethanol and butanol (Mittelbach, 1990; Li *et al.*, 2006; Rodeigues *et al.*, 2008; Kazanceva *et al.*, 2011; Stamenković *et al.*, 2011). Furthermore, high concentrations of methanol can reduce the enzyme



activity (Mittelbach, 1990; Irimescu *et al.*, 2002; Rodeigues *et al.*, 2008; Kazanceva *et al.*, 2011) and therefore here initially used ethanol in the alcoholysis reaction. Following this, experiments were performed in order to test the compatibility and reusability of the microreactor in a methanol environment (Figs. 4-5 and 4-6).

Using the same conditions as described above for the formation of fatty acid ethyl ester, transesterification was performed using a 0.2 mg/mL solution of trioleoylglycerol in methanol. However, since methanol does not completely dissolve trioleoylglycerol, toluene was added into the system at a ratio of 1:2  $v/v$  (methanol: toluene). The conversion of triolein into C18:1 fatty acid methyl ester was confirmed by GC/MS-NCI by the observation of the molecular ion at  $m/z$  295.15  $[M-H]^-$  after the reaction (Fig. 4-6d).

Complete methanolysis of triolein was achieved for 2 repeated runs as shown in Figure 4-5 which compares the methanolysis to ethanolysis on a similar SM. Figure 4-6a shows the chromatogram of methyl oleate (run 1) from a GC/MS-NCI experiment. However, on the third run, the conversion efficiency of the SM decreased to about 50% of the expected methyl oleate (Fig.4-5 and Fig. 4-6b). In comparison, the formation of fatty acid ethyl ester remained quantitative for over 5 runs under the same reaction conditions (Fig. 4-5). After 5 runs, the SM microreactor used for methanolysis resulted in minimal conversion (~5%) to fatty acid methyl ester (Fig 4-5, Fig 4-6c and 4-6d). This is likely due to partial denaturation of the lipase in the high methanol environment within the

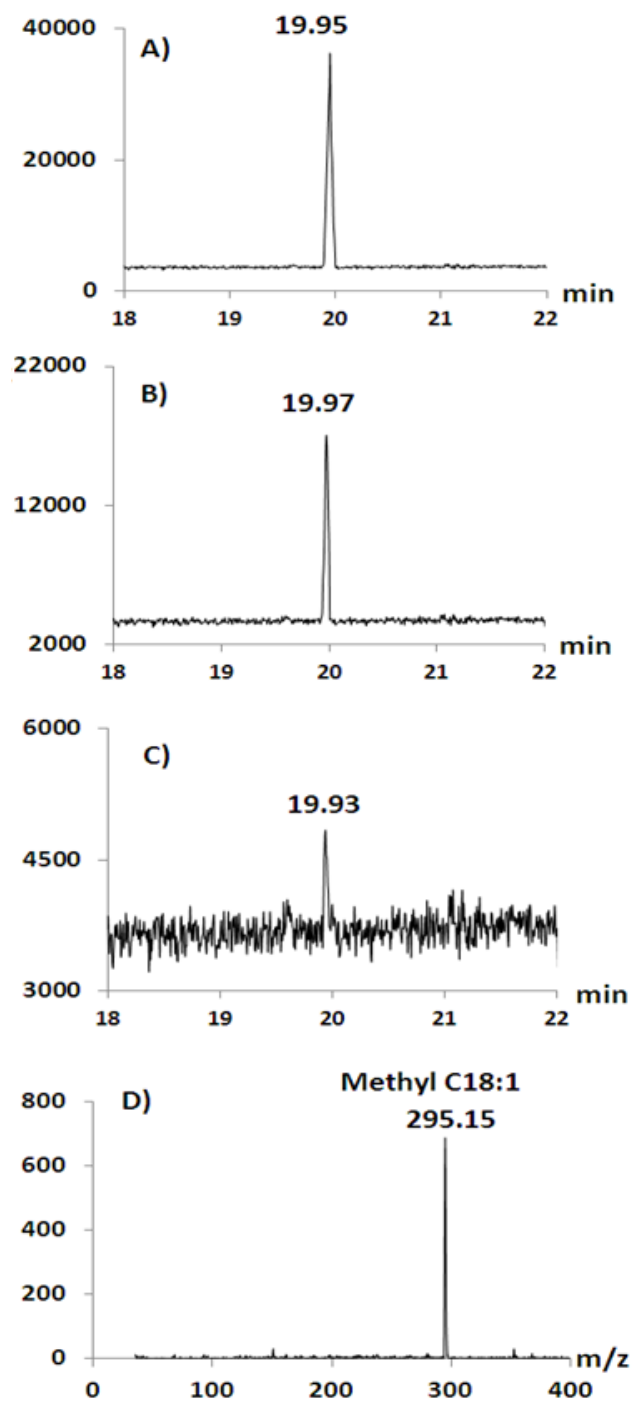


FIG 4-6: GC/MS traces for C18:1 FAME produced using a single SM microreactor: (a) run 1; (b) run 3; (c) run 5; and (d) NCI spectrum for run 5 extracted from the GC peak in C) showing the presence of methyl oleate ( $[M-H]^-$   $m/z$  295.15).

microreactor. Because of the low tolerance of lipase to methanol, previous studies have suggested that the stepwise addition of methanol into the system is preferable to obtain a high yield of fatty acid methyl ester (Watanabe *et al.*, 2000; Deng *et al.*, 2003; Turkan and Kalay, 2006). It is also possible that the inclusion of toluene negatively affects the SM performance. However, the experiment has demonstrated the possibility of forming fatty acid methyl ester using the SM, although further work is required to optimize conditions.

#### **4.4 Conclusion**

In conclusion, the enzymatic microreactor technology employed in this study provides the ability to carry out the transesterification of TAG in a simple and rapid manner, which will benefit the analysis of fats and oils. The products obtained from both the SM and MSF microreactors were consistently similar to the ethylation products obtained using both commercial immobilized lipase and conventional acid catalysts. This not only proves the success of the lipase immobilization within the microreactor but also demonstrates that plant oils can be directly converted to fatty acid methyl ester or fatty acid ethyl ester using the prototype SM device with no prior sample preparation and only using alcohol in the reaction.

The reusability of the microreactor provides an additional advantage that minimizes the cost of analysis and increases the potential for use in automation. The preliminary results presented here need to be followed by a quantitative

validation of the fatty acid conversions achieved using similar microreactors. However, since the analysis of fatty acid composition by GC is so widely used, this approach to lipid derivatization could be of significant benefit.

#### 4.5 References

- Aichholz R, Lorbeer E (1998) Separation of triacylglycerols by high temperature gas chromatography on seven different stationary phases. *J High Resol Chromatogr* 21:363-367.
- Akoh CC (2007) Enzymatic approach to biodiesel production. *J Agr Food Chem* 55:8995-9005.
- Anuar ST, Zhao Y-Y, Mugo SM, Curtis JM (2013) The development of a capillary microreactor for transesterification reactions using lipase immobilized onto a silica monolith. *J Mol Catal B: Enzym* 92:67-70.
- Anuar ST, Villegas C, Mugo SM, Curtis JM (2011) The development of flow-through bio-catalyst microreactors from silica microstructured fibers for lipid transformations. *Lipids* 46:545-555.
- AOAC (2000) AOAC Official Methods 965.49. Preparation of Methyl Esters (Final Action 1984). In: *AOAC Official Methods for Fatty Acids in Oils and Fats*. AOAC International: Urbana, IL, USA.
- AOCS (2012) Official Method Ce 2-66. Preparation Methyl Ester of Fatty Acids (Reapproved 2009). In Firestone D (ed): *Official Methods and Recommended Practices of the American Oil Chemists' Society*, 6<sup>th</sup> ed, 2<sup>nd</sup> printing. AOCS Press: Urbana, IL, USA.
- AOCS (2012) Official Method Ce 1b-89. Fatty Acid Composition of Marine Oils by GLC (Reapproved 2009). In Firestone D (ed): *Official Methods and Recommended Practices of the American Oil Chemists' Society*, 6<sup>th</sup> ed, 2<sup>nd</sup> printing. AOCS Press: Urbana, IL, USA.

AOCS (2012) Official Method Ce 1k-09. Direct Methylation of Lipids in Foods for the Determination of Total Fat, Saturated *cis*-Monounsaturated, *cis*-Polyunsaturated and Trans Fatty Acid by GC (Reapproved 2009). In Firestone D (ed): *Official Methods and Recommended Practices of the American Oil Chemists' Society*, 6<sup>th</sup> ed, 2<sup>nd</sup> printing AOCS Press: Urbana, IL, USA.

Arroyo H, Sanchez-Muniz FJ, Cuesta C, Burguillo FJ, Sanchez-Montero JM (1996) Hydrolysis of used frying palm olein and sunflower oil catalyzed by porcine pancreatic lipase. *Lipids* 31:1133-1139.

Carrapiso AI, Carmen G (2000) Development in lipid analysis: some extraction techniques and in situ transesterification. *Lipids* 35:1167-1177.

Christie WW (1989) The Preparation of Derivatives of Fatty Acids. In: *Gas Chromatography and Lipids- A Practical Guide*, 1<sup>st</sup> ed. The Oily Press: Scotland, UK.

Christie W, Han X (2012) *Lipid Analysis: Isolation, Separation, Identification and Lipidomic Analysis*, 4<sup>th</sup> ed. Woodhead Publishing Ltd: Cambridge, UK.

Craig BM, Murty NL (1959) Quantitative fatty acid analysis of vegetable oils by gas-liquid chromatography. *J Am Oil Chem Soc* 36: 549-552.

Deng L, Tan T, Wang F, Xu X (2003) Enzymatic production of fatty acid alkyl esters with a lipase preparation from *Candida sp.* 99-125. *Eur J Lipid Sci Technol* 105:727-734.

Dossat V, Combes D, Marty A (2002) Lipase-catalysed transesterification of high oleic sunflower oil. *Enzym Microbial Tech* 30:90-94.

European Pharmacopoeia (2012) Ph. Eur. Monograph number 2063. Omega-3-Acid Ethyl Esters 60. In: *Pharmacopoeia* 7<sup>th</sup> edn, *Supplement 7.5, Pharmeuropa 22.4*. European Pharmacopoeia: Strasbourg, France.

- Fureby AM, Tian L, Adlercreutz P, Mattiasson B (1997) Preparation of diglycerides by lipase-catalyzed alcoholysis of triglycerides. *Enzym Microbial Tech* 20:196-206.
- Goff MJ, Bauer NS, Lopes S, Sutterlin WR, Suppes GJ (2004) Acid-catalyzed alcoholysis of soybean oil. *J Am Oil Chem Soc* 81:415-420.
- Gunstone FD (2004) *The Chemistry of Oils and Fats: Sources, Composition, Properties and Uses*. Blackwell Publishing Ltd: Oxford, UK.
- Hammond EW (2003) Vegetable oils- Types and Properties. In: Caballero B, Trugo LC, Finglas PM (eds) *Encyclopedia of Food Sciences and Nutrition*. Elsevier Science Ltd: Amsterdam, Netherlands. pp5899-5904.
- Ichihara K, Shibara A, Yamamoto K, Nakayama T (1996) An improved method for rapid analysis of the fatty acid glycerolipids. *Lipids* 31:535-539.
- Igarashi M, Tsuzuki T, Kambe T, Miyazawa T (2004) Recommended methods of fatty acid methylester preparation for conjugated and trienes in food and biological samples. *J Nutr Sci Vitaminol* 50:121-128.
- Indarti E, Majid MISA, Hashim R, Chong A (2005) Direct FAME synthesis for rapid total analysis from fish oil and cod liver oil. *J Food Comp Anal* 18: 161-170.
- Irimescu R, Iwasaki Y, Hou CT (2002) Study of TAG ethanolysis to 2-MAG by immobilized *Candida antarctica* lipase and synthesis of symmetrically structured TAG. *J Am Oil Chem Soc* 79:879-883.
- Iso M, Chen B, Eguchi M, Kudo T, Shrestha S (2001) Production of biodiesel fuel from triglycerides and alcohol using immobilized lipase. *J Mol Catal B: Enzym* 16:53-58.
- Kazanceva I, Makarevičienė V, Kazancev K (2011) Application of biotechnological method to biodiesel fuel production using *n*-butanol. *Environmt Res Eng Manage* 56:35-42.

- Lee D-S, Noh B-S, Bae S-Y, Kim K (1998) Characterization of fatty acids compositions in vegetable oils by gas chromatography and chemometrics. *Anal Chimica Acta* 358:163-175.
- Leung DYC, Wu X, Leung MKH (2010) A Review on biodiesel production using catalyzed transesterification. *Applied Energy* 87:1083–1095.
- Li L, Du W, Liu D, Wang L, Li Z (2006) Lipase-catalyzed transesterification of rapeseed oils for biodiesel production with a novel organic solvent as a reaction medium. *J Mol Catal B: Enzym* 43:58-62.
- Linko Y-Y, Lamsa M, Wu X, Uosakainen E, Seppala J, Linko P (1998) Biodegradable products by lipase biocatalysis. *J Biotech* 66:41-50.
- Ma J, Liang Z, Qiao X, Deng Q, Tao D, Zhang L, Zhang Y (2008) Organic-inorganic hybrid silica monolith based immobilized trypsin reactor with high enzymatic activity. *Anal Chem* 80:2949-2956.
- McCreeedy T (2000) Fabrication techniques and materials commonly used for the production of microreactors and micro total analytical systems. *Trends Anal Chem* 19:396-401.
- Mittelbach M (1990) Lipase catalyzed alcoholysis of sunflower oil. *J Am Oil Chem Soc* 67:168-170.
- Mugo SM, Ayton K (2013) Lipase immobilized methacrylate polymer monolith microreactor for lipid transformations and online analytics. *J Am Oil Chem Soc* 90:65-72.
- Mugo SM, Ayton K (2010) Lipase immobilized microstructured fiber based flow-through microreactor for facile lipid transformations. *J Mol Catal B: Enzym* 67:202-207
- Phan NTS, Brown DH, Styring P (2004) A facile method for catalyst immobilisation on silica: nickel catalysed Kumada reactions in mini-continuous flow and batch reactors. *Green Chem* 6:526-532.

- Rodeigues RC, Volpato G, Wada K Ayub MAZ (2008) Enzymatic synthesis of biodiesel from transesterification reactions of vegetable oils and short chain alcohols. *J Am Oil Chem Soc* 85:925-930.
- Sheppard AJ, Iverson JL (1975) Esterification of fatty acids for gas-liquid chromatographic analysis. *J Chromatogr Sci* 13:448-452.
- Shimada Y, Watanabe Y, Samukawa T, Sugihara A, Noda H, Fukuda H, Tominaga Y (1999) Conversion of vegetable oil to biodiesel using immobilized *Candida antarctica* lipase. *J Am Oil Chem Soc* 76:789-793.
- Stamenković OS, Veličković AV, Veljković VB (2011) The production of biodiesel from vegetable oils by ethanolysis: current state and perspectives. *Fuel* 90:3141-3155.
- Türkan A, Kalay S (2006) Monitoring lipase-catalyzed methanolysis of sunflower oil by reversed-phase high-performance liquid chromatography: elucidation of the mechanisms of lipases. *J Chrom A* 1127:34-44.
- Watanabe Y, Shimada Y, Sugihara A, Noda H, Fukuda H, Tominaga Y (2000) Continuous production of biodiesel fuel from vegetable oil using immobilized *Candida antarctica* lipase. *J Am Oil Chem Soc* 77:355-360.
- Watts P, Wiles C (2007) Recent advances in micro reaction technology. *Chem Commun* 5:443-467.
- Xie C, Ye M, Jiang X, Jin W, Zou H (2006) octadecylated silica monolith capillary column with integrated nanoelectrospray ionization emitter for highly efficient proteome analysis. *Moll Cell Proteom* 5:454-461.



**CHAPTER 5:**

**THE DEVELOPMENT OF AN ANALYTICAL METHOD TO  
CHARACTERIZE THE TRANSFORMATION OF UNSATURATED OILS  
INTO EPOXIDISED OIL<sup>15</sup>**

---

### **5.1 Introduction**

Epoxidized vegetable oils (EVO) are formed when oxygen is added across the double bonds of the fatty acid chains in plant oils, forming the reactive oxirane groups. These oxiranes then can act as intermediates in the formation of other industrially useful fatty acid derivatives (Goud *et al.*, 2006). EVOs have been used as a starting material for a wide variety of products such as alcohols, glycols, alkanolamines, and polymers such as polyurethanes (PU), and for epoxy resin production (Tan and Chow, 2002). They have also been used in preparing plasticizers and stabilizers for the production of polyvinyl chloride (PVC). Thus, the process of vegetable oil epoxidation is of significant industrial importance. There are several methods that can be used to prepare EVO (Klaas and Warwel, 1999; La Scala and Wool, 2002; Meyer *et al.*, 2008; Mungroo *et al.*, 2008; Abdullah and Salimon, 2010; Milchert *et al.*, 2010), the most common of which

---

<sup>15</sup> A version of this chapter has been published. Anuar *et al.* (2012). *Journal of the American Oil Chemist Society*. 89:1951-1960.

"Springer and Journal of American Oil Chemist Society, 89, 2012, 1951-1960, Monitoring the Epoxidation of Canola Oil by Non-aqueous Reversed Phase Liquid Chromatography/Mass Spectrometry for Process Optimization and Control, Sabiqah Tuan Anuar, Yuan-Yuan Zhao, Samuel M. Mugo, Jonathan M. Curtis, with kind permission from Springer Science and Business Media".

Supplementary data regarding this chapter are given in Appendix 5.

uses the oxidation by peroxy acids (peracids) formed by reaction of formic or acetic acid with hydrogen peroxide (Fig. 5-1).

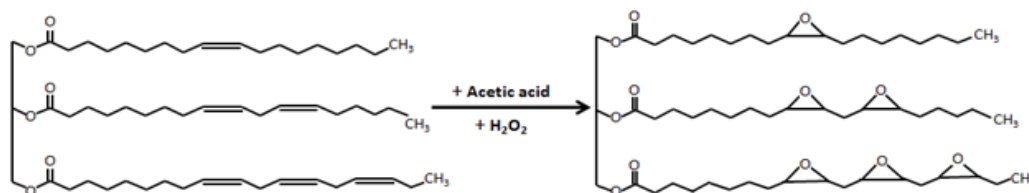


FIG5-1: The generalized reaction for a hypothetical triglyceride oil consisting of C18:1, C18:2 and C18:3 forming the fully epoxidised product of mono-epoxy C18:0, di-epoxy C18:0, and tri-epoxy C18:0.

At laboratory scale, it can also be more convenient to make use of commercially available *m*-chloroperbenzoic acid (MCPBA), a more stable peroxy acid (Klaas and Warwel, 1999). Another method describes the epoxidation of oleic acid occurring via reaction with molecular oxygen in the presence of a catalyst comprised of cobalt acetate in benzaldehyde (Kuo and Chou, 1987). A chemo-enzymatic method of forming epoxides of unsaturated free fatty acids has been reported that proceeds via the formation of long-chain peroxy acids by reaction with hydrogen peroxide in the presence of lipase (Klaas and Warwel, 1999; Orellana-Coca *et al.*, 2005; Vlček and Petrović, 2006). However, the preparation of EVO by the reaction of vegetable oils with hydrogen peroxide and formic or acetic acid is the most attractive for both technical and economic reasons (Goud *et al.*, 2006; Goud *et al.*, 2007). In this process, in addition to the formation of epoxides, certain side reactions can occur, including decomposition

of the peroxy acid or opening of oxirane rings via acid addition. Since vegetable oils often contain multiple sites of unsaturation per triglyceride and per fatty acid chain, the reaction with peroxy acids does not result directly in the formation of fully epoxidised oil but rather proceeds via the formation of partially epoxidised intermediates. It is hypothesized that understanding the formation of these partially epoxidised intermediates will help to control the reaction conditions and decrease the side reactions.

Canola oil (CO) is a good candidate for epoxide production since it contains a high abundance of unsaturated fatty acids, especially oleic acid (~62%), linoleic acid (~22%) and linolenic acid (~10%) (Dubois *et al.*, 2007). Thus, since >90% of the fatty acid content of canola oil is unsaturated, fully epoxidised canola oil should contain high percentages of triacylglycerols (TAG) with 3 or more epoxide groups.

The epoxidation process can be monitored by means of titrimetric methods that determine the iodine value and oxirane number (Gunstone, 2004). In these tests, the iodine value indicates the number of double bonds remaining whilst the oxirane number indicates the degree of epoxidation that has occurred. Thus, as the epoxidation reaction progresses, the iodine value will decrease and the oxirane number will increase so that these two values can be used to calculate the conversion of C=C double bonds to oxiranes. Fourier transform infra-red (FTIR) spectroscopy (Pérez *et al.*, 2008), and nuclear magnetic resonance (NMR) have also been used to monitor the epoxidation process (Aerts and Jacobs, 2004). For FTIR, the intensities of a C-H stretching band at  $3009\text{ cm}^{-1}$  from C=C-H and the

C-O-C (oxirane)  $3463\text{ cm}^{-1}$  band are used as indicators. Similarly, in  $^1\text{H-NMR}$  (Farias *et al.*, 2010) changes in the intensity of resonances for CH=CH and the formation of the resonance characteristic for oxiranes have been monitored.

Overall, while all of these methods provide information on the C=C double bond and oxirane abundance, they do not differentiate between, or identify, the individual epoxy products formed. Gas chromatography (GC) (Rothenbacher and Schwack, 2007; Farias *et al.*, 2010) coupled with a flame ionization detector (FID) and/or mass spectrometry (MS) has also recently been used to study the vegetable oil epoxidation products. However, this method requires derivatization of the EVO prior to analysis and the information on intact triacylglycerol (TAG) structure is lost. Suman *et al.* (2005) used LC/MS for the identification of epoxidised soybean oil but limited their study to food products. Thus, there is very limited literature on analytical methods to directly determine of the degree of epoxidation in triacylglycerols structures and to elucidate the structures of the partially epoxidised triacylglycerols intermediates.

This section describes the development of a method using non-aqueous reversed phased liquid chromatography / electrospray - mass spectrometry (NARP-LC/ESI-MS) to monitor the epoxidation of canola oil. Using this method, both the intermediates and products produced during the epoxidation of canola oil could be monitored thereby providing insight into the overall reaction kinetics. In addition, the flow-injection MS analysis of the epoxidised oil is tested as a rapid method to monitor the progress of the epoxidation reaction.

## 5.2 Experimental Procedures

### 5.2.1 Materials:

Food-grade canola oil was purchased from a local grocery store. Formic acid, hydrogen peroxide, sodium sulfate and sodium carbonate were all purchased from Sigma-Aldrich (Oakville, ON, Canada), while analytical grade ethyl acetate and dichloromethane were obtained from Fluka Analytical-Sigma Aldrich, (Oakville, ON, Canada).

### 5.2.2 Epoxidation of Canola Oil:

The epoxidation process was performed by mixing 30 g of canola oil with 18.5M formic acid (85% in water) and 10.3M hydrogen peroxide (35% in water) to give a final molar ratio of 1:3:8 respectively. The oil and acid were placed in a round bottom flask, which was immersed in an oil bath maintained at 35°C. The hydrogen peroxide was added drop-wise into the mixture of oil and acid in order to minimize the rise in reaction temperature. The reactants were continuously stirred at 180 rpm and the epoxidation intermediates monitored by sampling the products after 30 min, 1 h and subsequently every hour up to 28 h, when the reaction was determined to be complete.

At every sampling interval, a 3 g aliquot was taken and diluted with 10 mL ethyl acetate immediately followed by washing with about 15 mL of brine (saturated sodium chloride) solution. The mixture was left to separate into 2

layers and the upper layer was collected and washed with 15 mL 1M sodium bicarbonate (NaHCO<sub>3</sub>) solution. After phase separation the aqueous layer was discarded while the oily upper layer was retained. This was washed with 5 mL of brine and finally the upper organic layer was dried with 2 g of anhydrous sodium sulfate. The oil was concentrated using a rotary evaporator, weighed and diluted to 0.1 mg/mL in dichloromethane prior to LC/MS and flow-injection MS analyses.

### ***5.2.3 NARP-LC/MS:***

An Agilent 1200 liquid chromatograph (Agilent Technologies; Palo Alto, CA, USA) was coupled to an AB/Sciex QStar Elite mass spectrometer (Applied Biosystems/ Sciex; Concord, ON, Canada) equipped with an electrospray-ion source. A Supelco Ascentis C18 column (15x2.1 mm, 3 µm) (Sigma Aldrich,, Oakville, ON, Canada) was used with the following linear gradient at a flow rate was 200 µL/min with an injection volume of 1 µL: Solvent A = isopropanol (IPA); Solvent B = Acetonitrile (ACN); t=0, 20% A, hold 0.1 min; t=25min 90%A. Data were acquired using ESI in positive ion mode, with the following instrumental parameters: declustering potential (DP) at 45V; focus potential (FP) at 150V; declustering potential 2 (DP 2) at 10V; gas (GAS 1) at 20; nebulizing gas (GAS 2) at 60; and an ionspray voltage (IS) of 5200V. A post column addition of 40 mM ammonium acetate in methanol at a flow rate of 20 µL/min was used to enhance ionization efficiency. Analyst QS software (Applied

Biosystems/ Sciex; Concord, ON, Canada) was used for data acquisition and analysis.

#### ***5.2.4 Flow-injection Analysis:***

Direct flow-injection analysis ESI-MS was performed in order to investigate whether this rapid method provides enough information for reaction monitoring without the need to use chromatography. One  $\mu\text{L}$  injections of 0.1 mg/mL solutions of the extracted epoxides in DCM were introduced into mass spectrometer through HPLC auto-sampler with a mobile phase of 20% IPA/80% ACN at a flow rate of 200  $\mu\text{L}/\text{min}$ . The mass spectrometer operated in the positive ion electrospray mode with a post column addition of 40 mM ammonium acetate in methanol, and all parameters were set at the same conditions described above in the NARP-LC/MS section.

### **5.3 Results and Discussion**

#### ***5.3.1 Monitoring the Epoxidation of Canola Oil by NARP-LC/MS:***

NARP-liquid chromatography has been widely used for the separation of TAG species in natural oils (Holčapek *et al.*, 2003). In this study, a gradient of acetonitrile and isopropanol was used with a low-bleed C18 column. Since non-aqueous chromatography was used, atmospheric pressure photoionization (APPI)

and atmospheric pressure chemical ionization (APCI) were initially investigated as possible ionization methods for use in NARP-LC/MS experiments.

However, it was found that in using these techniques it was difficult to obtain intact molecular species which are required to identify the epoxidised or partially epoxidised triacylglycerols molecules. This problem was overcome by using electrospray ionization (ESI) with a post-column addition of ammonium acetate resulting in the formation of abundant  $[M+NH_4]^+$  ions, as described previously (Andrikopoulos, 2002). The distribution of triacylglycerols in canola oil bearing 2-, 3-, 4-, 5-, 6- and 7-double bonds was estimated from the relative abundance of the corresponding triacylglycerols peaks in the NARP-LC/MS data (Fig. 5-2 and 5-3a), showing that triacylglycerols species with 3 double bonds have the highest relative abundance at around 45% (Fig 5-3).

These triacylglycerols with 54 carbons and 3 double bonds can consist of many isomeric structures. For example, combinations containing 3 oleic acid moieties, or the combination of 1 oleic (18:1) plus 1 linoleic (18:2) plus 1 stearic (18:0) acid moiety, are both 54:3 triacylglycerols. In this report, for the sake of clarity we focus only on those triacylglycerols with 54 carbon structures but any number of double bonds, these making up >93% of the total triacylglycerols (Dubois *et al.*, 2007). However, the NARP-LC/MS methods described provide data on all triacylglycerols chain lengths of significant intensity.



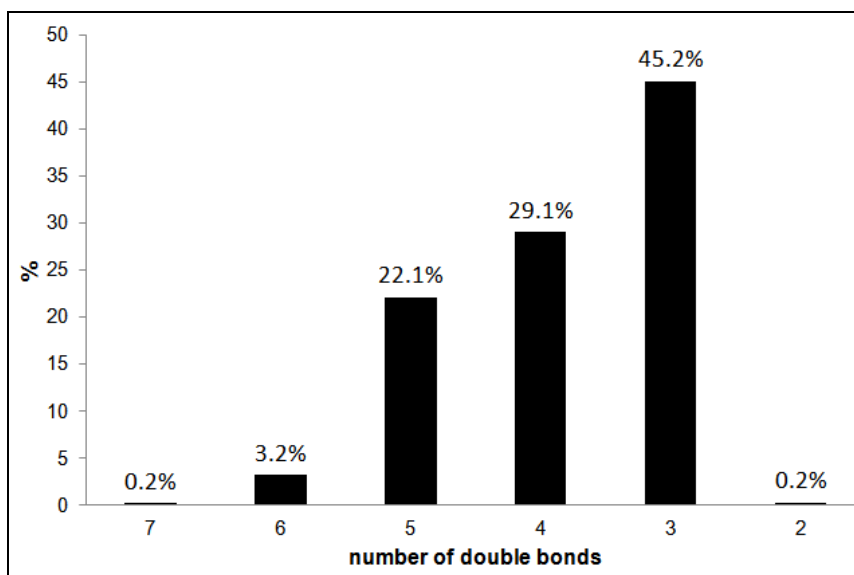


FIG 5-2: The distribution of 54 carbon triacylglycerols (TAG) in canola oil as a function of the number of double bonds, estimated by NARP-LC/MS.

The epoxidation of vegetable oils can be accompanied by side reactions including the ring-opening reaction of epoxide groups by the acid reagent (Milchert *et al.*, 2010), resulting in a lower final yield of epoxides. In the present experiment, the molar ratio of 1:3:8 of canola oil: formic acid: hydrogen peroxide used provides an excess of hydrogen peroxide that ensures all of the formic acid is converted to the peroxy acid that is used to introduce the epoxy group at the site of TAG double bonds (Suman *et al.*, 2005). Under these conditions, NARP-LC/MS data indicated that none of the ring-opened products were formed whereas this could be clearly observed in other experiments. After 0.5 h, 1.0 h and at every subsequent hour up to 28 h of reaction time, a small aliquot of the reaction mixture was collected in order to determine the changes in the profile of

unsaturated triacylglycerols and the degree of epoxide formation<sup>16</sup>. Each sample collected was immediately extracted into ether and neutralized to quench the epoxidation reaction which otherwise can continue at room temperature, as reported previously (La Scala and Wool, 2002).

In this section, an epoxide is symbolized as ‘*epo*’ while the chain length and degree of unsaturation are given in the conventional way. For instance, the most abundant triacylglycerols species is TAG [54:3] with 45% relative abundance (Fig. 5-2), about half of which is trioleoylglycerol, one of the main components of canola oil (Przybylski *et al.*, 2005). The next most abundant triacylglycerols are TAGs [54:4], [54:5] and [54:6] with 29%, 22% and 3.2% relative abundance, respectively. The abundance of TAG structures with 2 or 7 double bonds is rather low at only ~0.2%.

Figure 5-3 shows the NARP-LC/ESI-MS total ion current chromatograms over the  $m/z$  range of 500-1200 for the reaction products sampled at different time points throughout the course of the reaction. In this experiment, both the fully epoxidised products and partially epoxidised intermediates from the epoxidation of canola oil can be identified by the  $[M + NH_4]^+$  seen in their ESI-mass spectra (Table 5-1).

---

<sup>16</sup> Supplementary data are given in Appendix A5-1 and A5-2.

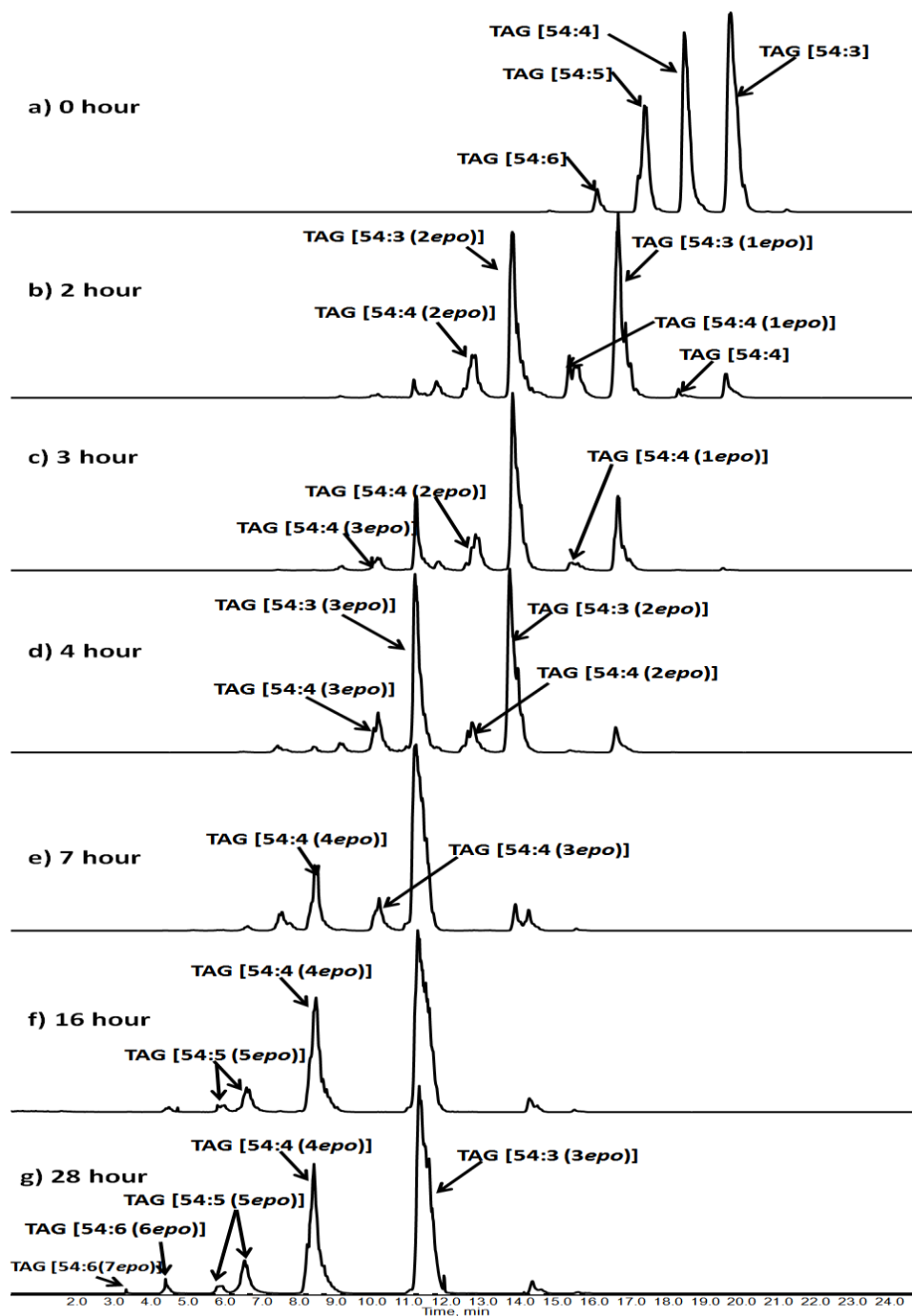


FIG 5-3: NARP-LC/ESI-MS chromatograms over the range of  $m/z$  500-1200: (a) canola oil starting material; (b)-(f) formation of intermediates at reaction times of 2-16 hours; and (g) epoxide products after 28 hours of reaction.

Furthermore, the elemental compositions of  $[M + NH_4]^+$  ions, which uniquely identify the reaction products and intermediates, were determined from exact  $m/z$  measurements. These are listed in Table 5-1 for all of the molecular species present in the NARP-LC/MS traces shown in Figure 5-3. For example, the measured  $m/z$   $[M + NH_4]^+$  ion of triacylglycerols isomers (54 carbons) with 4 double bond is 900.8026 ( $C_{57}H_{102}O_6 + NH_4^+$ ;  $\Delta=1.3$  ppm). The observed  $[M + NH_4]^+$  ion of the first intermediate formed once one of the double bonds had been epoxidised, was at  $m/z$  916.7960 ( $C_{57}H_{102}O_7 + NH_4^+$ ;  $\Delta=0.4$  ppm) for triacylglycerols isomers (54 carbons) having 1 epoxy group and 3 double bonds left unreacted. As mentioned above, ring opened products were not observed under the experimental conditions used.

It is clear from Figure 5-3 that as unsaturated triacylglycerols are converted to epoxides, they shift to earlier elution times in the non-aqueous reversed phase chromatography used. After 28 h, when the epoxidation is complete (Fig. 5-3g,  $t=28$  h), the epoxide products are completely resolved from the starting oil (Fig. 5-3a,  $t=0$  h). Between these two extremes, intermediates were observed which contained both residual double bonds and the newly formed epoxide groups and are described as in the following example. The epoxidation of TAG [54:3] may proceed *via* intermediates with 1 or 2 epoxide groups before forming the fully epoxidised species. Here refer to these intermediates as TAG [54:3 ( $1_{epo}$ )] and TAG [54:3 ( $2_{epo}$ )], respectively, and the fully epoxidised species as TAG [54:3 ( $3_{epo}$ )]. The nomenclature TAG [54: $x$  ( $y_{epo}$ )] thus describes a

TABLE 5-1 Exact mass measurements and elemental compositions of the  $[M + NH_4]^+$  ions taken from the NARP-LC/MS data presented in Figure 2-3 showing the course of a canola epoxidation process.

Double Bond	Epoxy							
	0	1	2	3	4	5	6	7
2	904.8347 (+2.1) $C_{57}H_{106}O_6 + NH_4^+$	920.8313 (+3.9) $C_{57}H_{106}O_7 + NH_4^+$	936.8269 (+4.6) $C_{57}H_{106}O_8 + NH_4^+$					
3	902.8156 (-1.7) $C_{57}H_{104}O_6 + NH_4^+$	918.8122 (+0.2) $C_{57}H_{104}O_7 + NH_4^+$	934.8069 (0) $C_{57}H_{104}O_8 + NH_4^+$	950.8025 (+0.7) $C_{57}H_{104}O_9 + NH_4^+$				
4	900.8026 (+1.3) $C_{57}H_{102}O_6 + NH_4^+$	916.7960 (-0.4) $C_{57}H_{102}O_7 + NH_4^+$	932.7947 (+3.6) $C_{57}H_{102}O_8 + NH_4^+$	948.7848 (-1.5) $C_{57}H_{102}O_9 + NH_4^+$	964.7802 (-0.9) $C_{57}H_{102}O_{10} + NH_4^+$			
5	898.7851 (-0.8) $C_{57}H_{100}O_6 + NH_4^+$	914.7798 (-1.0) $C_{57}H_{100}O_7 + NH_4^+$	930.7803 (-5.0) $C_{57}H_{100}O_8 + NH_4^+$	946.7751 (+4.8) $C_{57}H_{100}O_9 + NH_4^+$	962.7673 (+1.9) $C_{57}H_{100}O_{10} + NH_4^+$	978.7628 (+2.5) $C_{57}H_{100}O_{11} + NH_4^+$		
6	896.7713 (+1.3) $C_{57}H_{98}O_6 + NH_4^+$	912.7686 (+3.8) $C_{57}H_{98}O_7 + NH_4^+$	928.7625 (+2.7) $C_{57}H_{98}O_8 + NH_4^+$	944.7597 (+5.1) $C_{57}H_{98}O_9 + NH_4^+$	960.7544 (+4.7) $C_{57}H_{98}O_{10} + NH_4^+$	976.7502 (+5.6) $C_{57}H_{98}O_{11} + NH_4^+$	992.7446 (+5.0) $C_{57}H_{98}O_{12} + NH_4^+$	
7	894.7568 (+2.6) $C_{57}H_{96}O_6 + NH_4^+$	910.7546 (+5.6) $C_{57}H_{96}O_7 + NH_4^+$	926.7403 (-4.4) $C_{57}H_{96}O_8 + NH_4^+$	942.7403 (+1.1) $C_{57}H_{96}O_9 + NH_4^+$	958.7394 (+5.5) $C_{57}H_{96}O_{10} + NH_4^+$	974.7339 (+4.9) $C_{57}H_{96}O_{11} + NH_4^+$	990.7274 (+3.4) $C_{57}H_{96}O_{12} + NH_4^+$	1006.7175 (-1.4) $C_{57}H_{96}O_{13} + NH_4^+$

The  $\Delta$  value (in parenthesis) refers to the difference (in ppm) between the measured and exact mass for the elemental composition given.

product originating from any 54-carbon TAG isomer with x-double bonds in the starting oil where y-double bonds have been converted into epoxide groups.

At t=0 h, the NARP-LC/MS trace shows a triacylglycerol profile dominated by TAG [54:3], [54:4] and [54:5] that closely matches that predicted from the fatty acid distribution, as shown in Figure 5-2. Similarly, the final products at t=28 h show a distribution dominated by TAG [54:3(3<sub>epo</sub>)], [54:4(4<sub>epo</sub>)], [54:5(5<sub>epo</sub>)]. In this case, the apparently lower relative abundance of [54:5(5<sub>epo</sub>)] can be explained by the splitting of this peak into 2 or more isomeric forms (Fig. 5-3g) as well as the fact that there may be differences in response factors in the experiment, especially at different points in the LC gradient. Despite this, it is evident from this data that at t=28h all of the starting triacylglycerol has been converted to epoxides.

In this study, it was found that TAG [54:3] molecules were converted to their fully epoxidised form TAG [54:3(3<sub>epo</sub>)] more quickly than the other abundant TAG molecules which contain more unsaturations. This can be clearly seen in Figure 5-3d where at t=4 h the TAG [54:3(3<sub>epo</sub>)] peak is the base peak (although note that this species does not reach maximum abundance until t=8 h, as described below). In contrast, at t=4 h the TAG [54:4(4<sub>epo</sub>)] peak is very minor. In a similar way, the fully epoxidised species TAG [54:4(4<sub>epo</sub>)] is abundant at t=7 h (Fig. 3e) whereas TAG [54:5(5<sub>epo</sub>)] doesn't become abundant until t=16 h or above. In summary, it is confirmed that the time required for the full epoxidation of triacylglycerol molecules increases considerably with the number of double bonds, as might be expected. Hence, if the epoxidation reaction

is stopped before completion, the remaining unsaturations are on epoxidised triacylglycerol molecules, which initially had the highest number of double bonds.

The intermediates in the reaction have been highlighted in Figure 5-3 for the case of TAG [54:4]. After 2 h of reaction (Fig 5-3b) the formation of the partially-epoxidised products TAG [54:4(1<sub>epo</sub>)] and TAG [54:4(2<sub>epo</sub>)] was observed whereas the starting TAG [54:4] peak had virtually disappeared. At t=3 h the TAG [54:4(1<sub>epo</sub>)] peak had almost disappeared and the TAG [54:4(3<sub>epo</sub>)] peak appears. At t=7 h, only TAG [54:4(3<sub>epo</sub>)] and TAG [54:4(4<sub>epo</sub>)] are seen (Fig. 5-3e); complete conversion to TAG [54:4(4<sub>epo</sub>)] occurs by t=16 h (Fig. 5-3f). Thus, the data demonstrate the stepwise nature of the epoxidation of unsaturated triacylglycerol molecules with the conversion of the third and fourth double bonds proceeding at a slower rate than the conversion of the first and second double bonds as the overall concentration of double bonds available for epoxidation decreases. This can be seen most clearly in Figure 5-4 in which the normalized extracted ion chromatograms (XIC) of all partially-epoxidised products from a single triacylglycerol structure (TAG [54:4] in this case) are plotted as a function of reaction time.

The data clearly indicate how each partial epoxide intermediate peaks in relative abundance as the preceding species with one fewer epoxide group rapidly declines. For instance the mono-epoxide starts to form at t>0 h, peaks in intensity at ~t=1 h and is completely consumed by t=5 h; in contrast the di-epoxide starts to form at t=1 h, peaks in intensity at t=2-3 h and is consumed by t=7 h. Earlier (Dubois *et al.*, 2007) it was determined, based on measurements of

total oxirane formation kinetics from triacylglycerols and fatty acid methyl esters using  $^1\text{H}$  NMR, that the epoxidation rate constants vary with fatty acid composition.

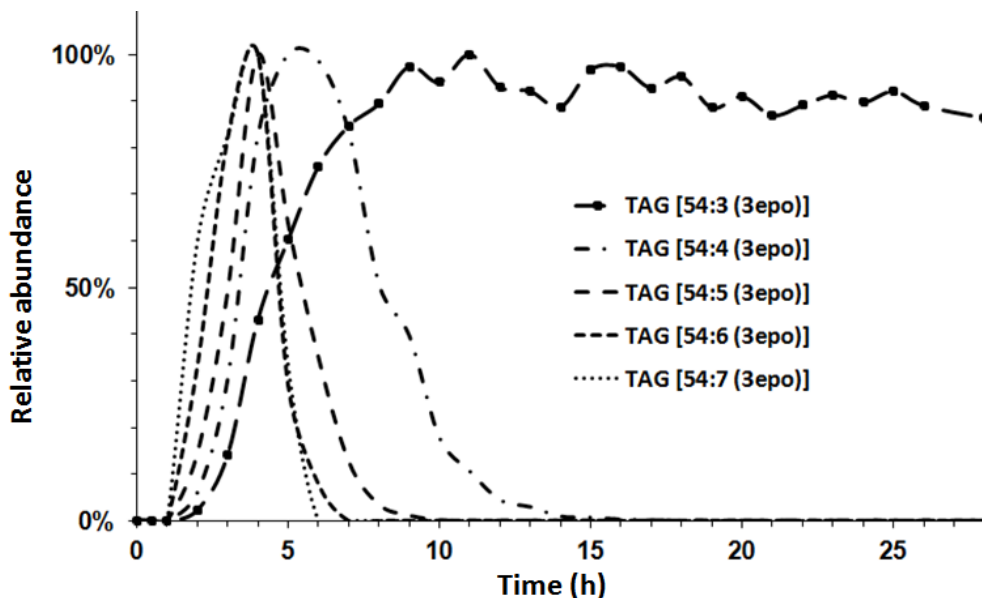


FIG 5-4: The epoxidation of TAG [54:4] from canola oil: relative abundance of the intermediates and final products plotted as a function of reaction time.<sup>17</sup>

The suggestion (Dubois *et al.*, 2007) was that this was either due to steric effects, such as distance from the glycerol backbone, or due to greater reactivity as a result of higher electron density with more double bonds. However, from the results it appears that the situation is more complex than can be revealed when considering only the overall formation of epoxide groups. Indeed, there are unique rates of formation of individual partial epoxide intermediates, as discussed further below.

<sup>17</sup> Supplementary data are given in Appendix A5-3 to A5-7.



These individual rates could only be studied using the relevant pure triacylglycerol reactants, rather than the triacylglycerol mixture found in natural oils, as studied here. It can also be seen from Figure 5-4 that full epoxidation of TAG [54:4] occurs at around  $t=15$  h when the plot of the abundance of 54:4 ( $4_{epo}$ ) reaches its maximum and the precursor intermediate 54:4( $3_{epo}$ ) is fully consumed.

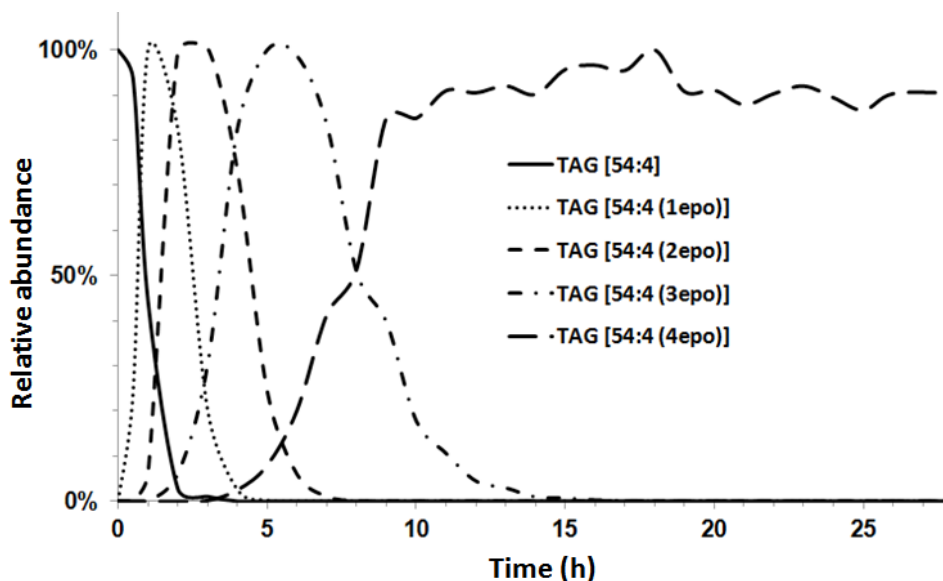


FIG 5-5: The formation of tri-epoxy intermediates and products from TAG (54 carbons) containing 3 to 7 double bonds.<sup>18</sup>

It should be noted that a limitation of this approach is that the NARP-LC/MS method does not readily distinguish between isomers so does not indicate which positions are preferentially epoxidised. On the other hand, its ability to monitor the progress of the reaction and to identify the times for complete or some level of partial epoxidation, make it potentially useful in optimizing reaction conditions.

<sup>18</sup> Supplementary data are given in Appendix A5-8 to A5-11.

In order to further explore the relative rates of reaction of different triacylglycerol species, Figure 5-5 illustrates the formation all 54-carbon triacylglycerol products and intermediates containing 3 epoxide groups produced during the epoxidation of canola oil from starting structures ranging from TAG [54:3] to TAG [54:7].

This reveals that the two most unsaturated TAGs [54:7] and [54:6] form their respective tri-epoxy compounds 54:7(3<sub>epo</sub>) and 54:6(3<sub>epo</sub>) the most rapidly, with maximum intensity occurring at about 4 h reaction time. These two intermediates are completely consumed by 6 and 7 h, respectively (Fig. 5-5) to form compounds with 4 or more epoxide groups. The intermediate 54:5 (3<sub>epo</sub>) lags slightly behind the latter two compounds in its rate of formation and disappearance, lasting until about 9-10 h.

As seen in both Figures 5-4 and 5-5, the species 54:4(3<sub>epo</sub>) exists over a broader range of reaction times than the above-mentioned species that originate from more highly unsaturated triacylglycerols. In fact, the intermediates 54:7(3<sub>epo</sub>), 54:6(3<sub>epo</sub>) and 54:5(3<sub>epo</sub>) exist for 4-5 h at above 10% of their maximum abundance whereas the equivalent is around 9 h for 54:4(3<sub>epo</sub>) and its maximum intensity occurs 2 h later in the reaction. The latter point is understandable from Figure 5-4, which indicates that how its formation is synchronous with the disappearance of its precursor for 54:4(2<sub>epo</sub>) so must reach a maximum intensity at a later time than 54:4(2<sub>epo</sub>). The longevity of the 54:4(3<sub>epo</sub>) species is presumably a result of the slow rate at which further epoxidation occurs

under the experimental conditions and leading to the fully epoxidised product for 54:4(4<sub>epo</sub>).

The above discussion is for the case of forming a tri-epoxide, from which it can be concluded that the rate of epoxidation of a triacylglycerol is dependent on the starting degree of unsaturation, being the fastest for the most unsaturated species. Similar conclusions are reached when examining plots of species having different levels of epoxidation. This is in agreement with a previous study (La Scala and Wool, 2002) that proposed rate constants for the epoxidation of fatty acid methyl ester and triacylglycerol in the order linolenic acid > linoleic acid > oleic acid. In the present case of canola oil, some of the most reactive unsaturated TAGs 54:7 and 54:6 isomers must contain higher proportions of linoleic or linolenic acid.

Most of the epoxidation is complete after 15 h of reaction (Figs 5-3 – 5-5) but it takes up to 28 h for the slowest process, the formation of 54:7(7<sub>epo</sub>) and 54:6(6<sub>epo</sub>), and to go to completion as seen by comparing Figures 5-3f and 5-3g. However, since this represents such a small proportion of canola oil with triacylglycerols 54:7 and 54:6 totalling <4% of the oil (Fig. 5-2), there is little benefit in prolonging the reaction beyond 15 h.

### **5.3.2 Flow-injection Analysis:**

An aim of this study was to develop a fast method to monitor and characterize the formation of epoxide intermediates. Therefore, with the above

knowledge, all of the samples were also tested without liquid chromatographic separation, by flow-injection ESI/MS analysis. In Figure 5-6a, the flow-injection analysis data has been used to extract the intensities of TAG [54:3] and its epoxidised intermediates and products as a function of reaction time.

Figure 5-6b shows the data for the same species but obtained with chromatographic separation by NARP-LC/ESI-MS. It is apparent that the data presented in Figures 5-6a and 6b are substantially equivalent, demonstrating that the data extracted from the flow-injection analyses can provide similar information on the epoxidation reaction to that obtained by NARP-LC/MS. Similar conclusions were drawn for other unsaturated triacylglycerol species undergoing epoxidation. However, although the results do show that the relative responses for epoxidised species seen in either analysis were similar, there was a significant difference between their absolute responses. This discrepancy is at least partly due to ion suppression (King *et al.*, 2000; Miller *et al.*, 2002) since in flow-injection ESI/MS analyses, the ions of all species including the sample matrix are present in the ion source simultaneously since there is no prior separation.

This results in competitive ionisation and hence lower ion intensities in general. For both flow-injection and NARP-LC/MS analysis there is agreement on the time for complete epoxidation. This appears to be close to 11 h, when all of the 54:3(2<sub>epo</sub>) has been consumed and the end product 54:3(3<sub>epo</sub>) has reached its maximum abundance.

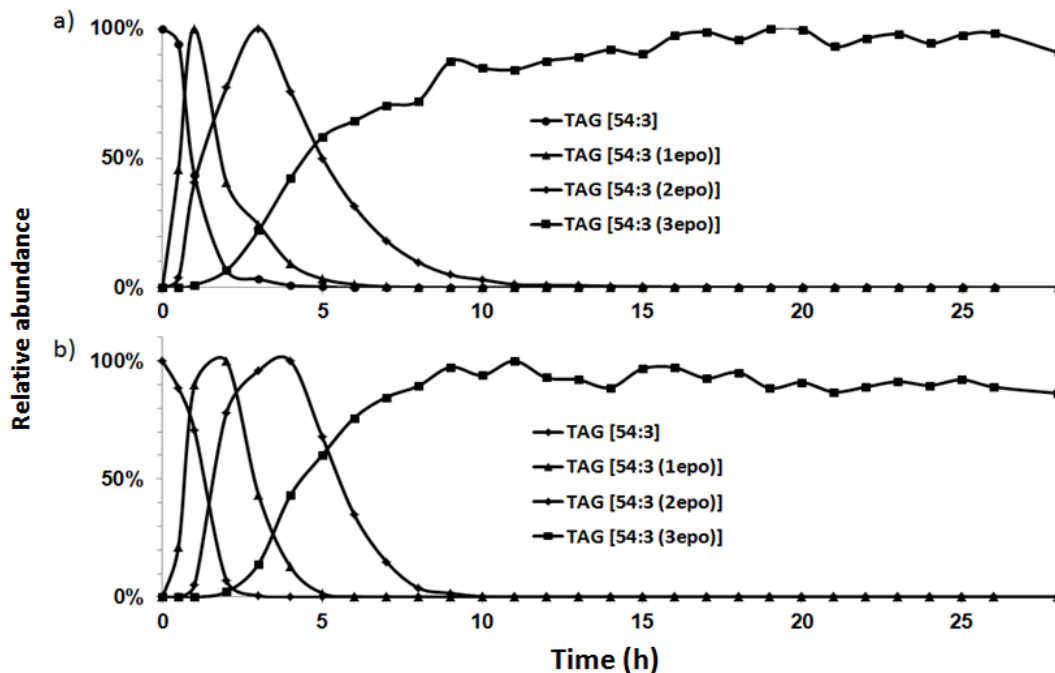


FIG 5-6: Monitoring the epoxidation of TAG [54:3] from canola oil by either (a) flow-injection analysis (ie without chromatographic separation), or (b) NARP-LC/MS analysis. The plots show the normalized intensities of TAG [54:3], partially epoxidised TAG [54:3] and fully epoxidised TAG [54:3] as a function of reaction time. Each point is a separate LC/MS or flow-injection MS experiment.

Figure 5-7 shows the mass spectra obtained by flow-injection of the epoxidised oils sampled at  $t = 0$  h (starting material),  $t = 4$  h and  $t = 28$  h. The mass spectra at these 3 time-points are clearly quite distinct with, for instance, the unreacted 54 carbon triacylglycerols all bunched at around  $m/z$  900 and spaced by  $2 m/z$  units whereas the fully epoxidised oils appear at  $m/z$  950 and above and are spaced  $14 m/z$  units apart.

From these, and similar spectra, it was found that the  $[M + NH_4]^+$  ions observed for each triacylglycerol compound provide the information required in

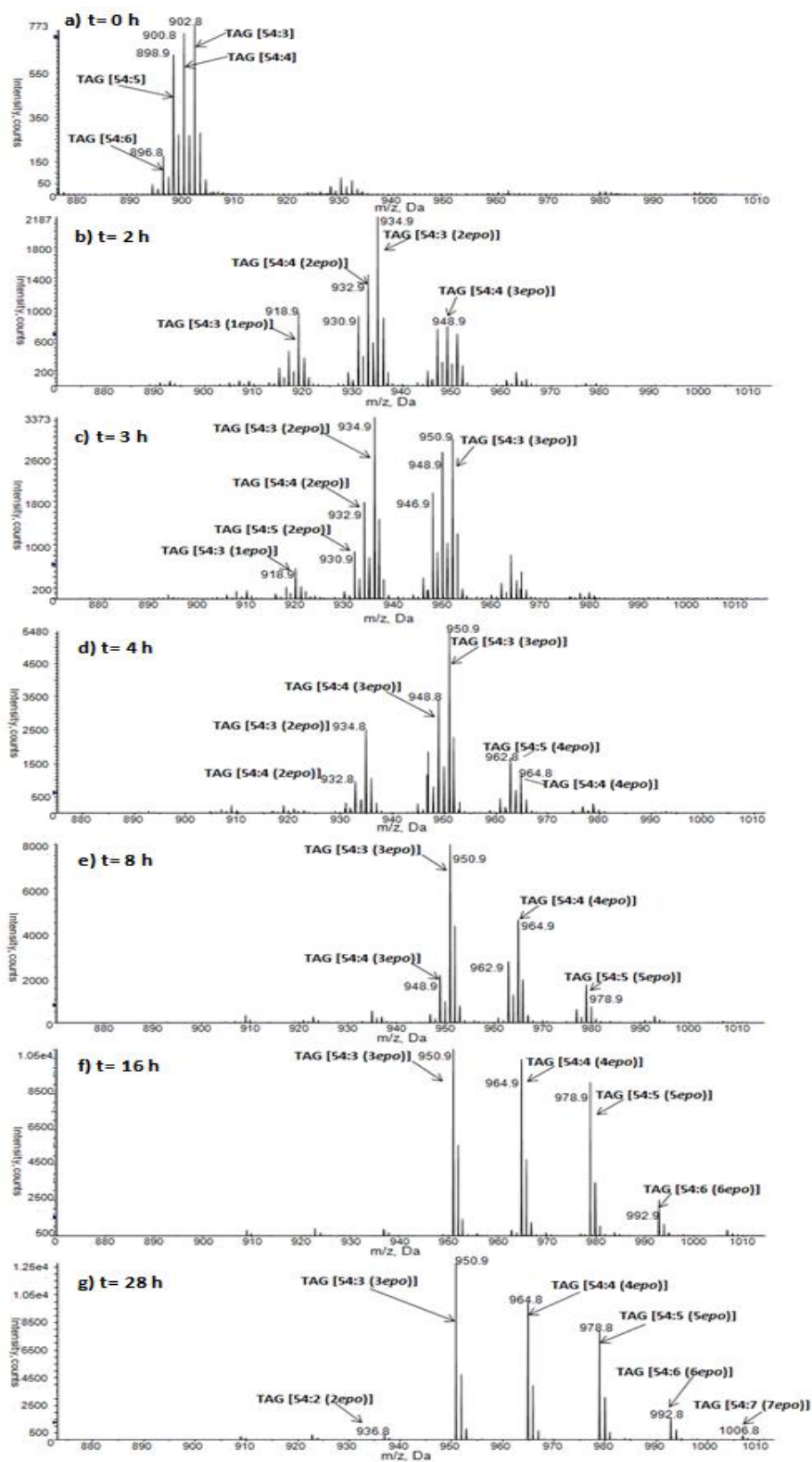


FIG 5-7: ESI mass spectra obtained by flow-injection of (a) the starting TAG oil, (b)-(f) the reaction mixture containing partially epoxidised intermediates at t= 4-16 h, and (g) fully epoxidised oil obtained at t=28h.

order to determine the degree of epoxidation at any given sampling time. Hence, Figures 5-6 and 5-7 demonstrate that flow-injection ESI/MS analyses can be used to monitor epoxidation reactions and determine their end-points. This avoids the need to spend further time performing chromatography, which is less compatible with reaction monitoring. Furthermore, more closely monitoring the reaction would allow the epoxidation to be stopped once a predetermined degree of conversion has been reached.<sup>19</sup>

#### **5.4 Conclusion**

The NARP-LC/ESI-MS method described here has been shown to be useful for monitoring the intermediates and final products formed in the epoxidation of a vegetable oil. A particular advantage is that the formation and disappearance of all of the partially epoxidised intermediates can be followed by this method in contrast to other analytical methods that can only show the overall degree of oxirane formation or loss of unsaturation.

This information would be useful to optimize reaction conditions and to determine an appropriate end point for the epoxidation reaction. We have shown that rapid assessment of the epoxidation reaction is possible by means of a simple flow-injection mass spectrometry experiment to test for completion or near completion of the epoxidation reaction. This could be adopted for in-process measurements of epoxidation reactions. Although in this work we have focused

---

<sup>19</sup> Supplementary data is given in Appendix A5-12.

on a qualitative description of the epoxidation process, the method would be amenable to use in a more quantitative study of the reaction kinetics including that relating to the formation of selected intermediates.

## 5.5 References

- Abdullah BM, Salimon J (2010) Epoxidation of vegetable oils and fatty acids: catalysts, methods and advantages. *J Applied Sci* 10(15):1545-1553.
- Aerts HAJ, Jacobs PA (2004) Epoxide yield determination of oils and fatty acid methyl ester using  $^1\text{H}$  NMR. *J Am Oil Chem Soc* 82(9):841-846.
- Andrikopoulos NK (2002) Chromatographic and spectroscopic methods in the analysis of triacylglycerol species and regiospecific isomers of oils and fats. *Critical Review Food Sci Nutr* 42(5):473-505.
- Dubois V, Breton S, Linder M, Fanni J, Parmentier M (2007) Fatty acid profiles of 80 vegetable oils with regard to their nutritional potential. *Eur J Lipid Sci Technol* 109:710-732.
- Farias M, Martinelli M, Bottega DP (2010) Epoxidation of soybean oil using homogeneous catalytic system based on a molybdenum (VI) complex. *Appl Catal A: General* 384:213-219.
- Goud VV, Patwardhan AV, Pradhan NC (2006) Studies on the epoxidation of mahua oil (*Modhumica Indica*) by hydrogen peroxide. *Bioresource Technol* 97(12):1365-1371.
- Goud VV, Patwardhan AV, Dinda S, Pradhan S (2007) Epoxidation of karanja (*Pongamia glabra*) oil catalyzed by acidic ion exchange resin. *Eur J Lipid Sci Tech* 109:575-584.
- Gunstone FD (2004) Rapeseed and Canola Oil, Production, Processing, Properties and Uses. Oxford-Blackwell Publishing: Oxford, UK.



- Holčapek M, Jandera P, Zderadička, Hrubá L (2003) Characterization of triacylglycerol and diacylglycerol composition of plant oil using high-performance liquid chromatography-atmospheric pressure chemical ionization mass spectrometry. *J Chrom A* 1010:195-215.
- Klaas MRG Warwel S (1999) New oxidation methods for unsaturated fatty acids, esters, and triglycerides. In Gerhard K, Johannes TPD (eds) *Recent Developments in the Synthesis of Fatty Acid Derivatives*. AOCS Press: Champaign, IL, USA. pp157.
- King R, Bonfiglio R, Fernandez-Metzler C, Miller-Stein C, Timothy O (2000) Mechanistic investigation of ionization suppression in electrospray ionization. *J Am Soc Mass Spectrom* 11:942-950.
- Kuo M-C., Chou T-C (1987) Kinetics and mechanism of the catalyzed epoxidation of oleic acid with oxygen in the presence of benzaldehyde. *Ind Eng Chem Res* 26(2):277-284.
- La Scala J, Wool RP (2002) Effect of FA Composition on Epoxidation Kinetics of TAG. *J Am Oil Chem Soc* 79(4):373-378.
- Meyer PP, Techaphattana N, Manundawee S, Sangkeaw S, Junlakan W, Tongurai C (2008) Epoxidation of soybean oil and jatropha oil. *Thammasat Int J Sci Tech* 13:1-5.
- Milchert M, Smagowicz A, Lewandowski G (2010) Optimization of the reaction parameters of epoxidation of rapeseed oil with peracetic acid. *J Chem Technol Biotechnol* 85:1099-1107.
- Müller C, Schäfer P, Störtzel M, Vogt S, Weinmann W (2002) Ion suppression effects in liquid chromatography-electrospray-ionization transport-region collision induced dissociation mass spectrometry with different serum extraction methods for systematic toxicological analysis with mass spectra libraries. *J Chrom B* 773:47-52.
- Mungroo R, Pradhan NC, Goud VV, Dalai AK (2008) Epoxidation of canola oil

with hydrogen peroxide catalyzed by acidic ion exchange resin. *J Am Oil Chem Soc* 85:887-896.

Orellana-Coca C, Törnvall U, Adlercreutz D, Mattiasson B, Hatti-Kaul R (2005) Chemo-enzymatic epoxidation of oleic acid and methyl oleate in solvent-free medium. *Biocatal Biotrans* 23(6):431-437.

Pérez JDE, Wiesenborn DP, Haagenson DM, Ulven CA (2008) Study of the process parameters of the canola oil epoxidation. *ASABE Paper No 08*. 2008 ASABE Annual International Meeting: St. Joseph, MI, USA.

Przybylski R, Mag T, Eskin NAM, McDonald BE (2005) Canola oil. In Shahidi F (ed) *Bailey's Industrial Oil and Fat products, Vol 2, Edible Oil and Fat Products: Edible Oil*. John Wiley & Sons: New York, NY, USA. pp66.

Rothenbacher T, Schwack W (2007) Determination of epoxidized soybean oil by gas chromatography/single quadrupole and tandem mass spectrometry stable isotope dilution assay. *Rapid Comm Mass Spec* 21:1937-1943.

Suman M, La Tegola S, Catellani D, Bersellini U (2005) Liquid chromatography - electrospray ionization-tandem mass spectrometry method for the determination of epoxidized soybean oil in food products. *J Agric Food Chem* 53:9879-9884.

Tan SG, Chow WS (2010) Biobased epoxidised vegetable oils and its greener epoxy blends: A review. *Polymer-Plastic Tech Eng* 49:1581-1590.

Vlček T, Petrović ZS (2006) Optimization of the chemoenzymatic epoxidation of soybean oil. *J Am Oil Chem Soc* 83:247-252.

## CHAPTER 6:

### GENERAL DISCUSSION AND CONCLUSION

---

Microreactors have been primarily designed to integrate different analytical processes including sample preparation, derivatization, extraction and separation, into a single platform, in a continuous flow system. The present thesis research proved that this technology is indeed suitable for use in lipid derivatization for analysis where the enzyme-catalyzed microreactor can be used to produce a high yield of derivative while the use of reagents and chemicals is reduced (Chapters 2 to 4).

Commercially available microreactors are usually produced by complicated processes which require specialized and costly equipment, for instance the photolithographic and wet-etching techniques. Moreover, these procedures usually require a flat surface to start with (*i.e.* for industrial production of chip-based microreactor). However, both chip-type and microcapillary-type microreactors can be also made in small batches using simple laboratory setups. In the present study, the latter was chosen because it allows for simpler fabrication and provides abundant microchannel spaces that can be utilized to give a large surface area for catalyst entrapment and here for reactions to take place. The goal of this thesis is to develop simple methods for fabricating microreactors and to investigate the use of these microreactors in lipid transformation. During the study, there were a few factors that determined the efficient performance of the microreactors. First is the surface area of the

microreactor for catalyst immobilization; second is the contact time between the microreactor and the reactant/substrate; and third is the microreactor temperature. The present study clearly shows that optimizing all of these conditions will result in a consistently high yield of transesterification products. Even though many processes of transesterification fats and oils into other lipid forms involve the use of alkali and acid catalyst, as discussed in Chapter 1, in this thesis, enzyme catalyst is used, which provide milder reaction conditions and by immobilizing the enzyme onto a support, increases its reusability.

This present study exploited the use of silica capillary as a support for the immobilization of lipase using covalent attachment by means of a cross-linker reagent. Two types of silica capillary were employed - silica monolithic (SM) and silica microstructured fiber (MSF) capillaries, since it was hypothesized that they would each provide high surface area for enzyme immobilization.

For the SM, the monolith network was fabricated within a fused silica capillary and the process was optimized to achieve a high surface area of porous monolith, as demonstrated by SEM images. One significant finding was a method to activate the internal wall of the fused silica capillary prior to the monolith formation in order to avoid the detachment of monolith from the fused silica wall (Chapter 3 and supplementary data in Appendices A3-3 to A3-6). The monolith formation was also found to be temperature and time dependent, so maintaining a stable temperature in the water bath and oven for a period of time (24 h) was needed to form the monolith from the sol-gel solution and in the drying process. Since the reproducible fabrication of the microreactor was an essential step, it is

correspondingly important that all of the monolith formation and further enzyme immobilization processes were fully successful. Results from SEM and porosity tests clearly demonstrated that the morphology of the microreactor was indeed a very high surface area porous monolithic structure suitable for further enzyme immobilization. The presence or disappearance of key functional groups (*e.g.* –N–H) during each step in the immobilization process was confirmed by FTIR analysis.

The applicability of novel microstructured platform, commonly known as microstructured fiber (MSF) and used as a photonic fiber in guiding light, was also studied as a potential microreactor support. The microstructured fibers used were made of silica which was demonstrated to be a good support for lipase immobilization, exploiting the silanol group for enzyme attachment *via* a cross-linking process.

It was intended to use the microreactors to perform small-scale lipid transesterification to produce the low amount of derivative that is necessary for GC analysis. In fact, the amounts of products from microreactors were also sufficient for other type of analysis such as LC-ELSD.

The effects of temperature and flow rate on the microreactor performance were studied and the optimized. In the presence of ethanol, using a MSF microreactor it was found that triglyceride were converted specifically to sn-2 monoacylglycerol in a very short timeframe when using the optimized reaction flow rate of 1  $\mu\text{L}/\text{min}$  and at a temperature of 50  $^{\circ}\text{C}$ .

Consequently, it was also shown that higher temperatures could affect the microreactor performance, presumably since the enzyme was deactivated. Moreover, since the MSF used consisted of very small hollow channels (4-5  $\mu\text{m}$  to 9-11  $\mu\text{m}$ ) the back pressure was found to be a disadvantage, as compared to the SM. Hence, the SM microreactor was used for more complex lipid derivatization.

Using the SM microreactor, the main products of alcoholysis of triolein and ethanol were identified as fatty acid ethyl esters. This occurred when the SM microreactor was used at both room temperature and a flow rate of  $< 0.5 \mu\text{L}/\text{min}$ . When the flow rate was increased, a decrease in fatty acid ethyl esters formation was observed, together with the appearance of monoacylglycerol. Similarly, a decreased fatty acid ethyl esters yield was also observed when the reaction temperature was increased. This result clearly indicates that in order to achieve complete transesterification, the reaction time needs to be longer (slower flow rate) because in the flow-through system the reactant needs to have enough contact time with the immobilized enzyme within the microreactor. Nevertheless, the reaction time was still short when considering that the estimated contact time was about 100-300 s (depending on the reaction flow rate and microreactor length that was used). Overall, successful immobilization of lipase onto both silica monolith and MSF capillaries was achieved, along with a high degree of reusability especially for the SM microreactor.

The flow-through enzymatic microreactor system was envisioned for use in analytical applications. Therefore, in this present study, the SM microreactor was coupled with mass spectrometry (MS), in order to observe and measure

online lipid transformations of triolein and monooleoylglycerol in the presence of ethanol. It was shown that the formation of ethyl oleate was still observed even though a high flow rate of 1  $\mu\text{L}/\text{min}$  was used. This higher than optimum flow rate was chosen for use in online SM microreactor-MS reaction due to the limitations in the instrumentation setup, including the size of the T-piece and large tubing ID. Hence, the formation of incomplete transesterification products such as mono- and di-oleoylglycerols was also observed (Chapter 3 and Appendices A3-9). However, this study proved that the enzymatic silica monolith microreactor can be adapted to couple with mass spectrometry, and this can be improved by using tubing and connectors designed for  $\text{nL}/\text{min}$  flow rates, or nano-spray ionization emitter, for future consideration.

Since it was successful in transesterifying lipid standards such as trioleoylglycerol and monooleoylglycerol, the microreactors were later used with more complicated lipid mixtures. Microreactors were employed to convert various plant/edible oils into their fatty acid ethyl ester constituents (Chapter 4). As reported in Chapter 4, this microreaction system succeeded in rapidly transesterifying oils such as canola, sesame seed, soybean and refined-bleached-deodorized palm oils under mild reaction conditions. Moreover, results attained from lipase-microreactor studies were comparable with observations from control studies (derivatization of triacylglycerol with acid catalysis and transesterification of triacylglycerol with commercial lipase Novozyme 435 beads), yet allowed the reaction to take place using  $<1$  mg quantities of lipid in a simple and rapid manner that will be of benefit in analytical applications. The use of a

microreactor decreased the number of chemical derivatization steps required for oil (and fatty acid) analysis prior to the GC injection. With the microreactor, the oil was transesterified with minimal use of chemical reagent/solvent since only ethanol (or methanol with co-solvent) was used. This avoids the use of toxic chemical catalyst and solvents used in standard procedures. Furthermore, minimal sample preparation is required - the collected product was simply diluted with a compatible solvent prior to analysis.

Fatty acid ethyl ester derivatives were collected directly from small lipid sample sizes in amounts compatible with GC analyses. However, fatty acid methyl ester derivatives are more commonly used in GC analysis, so methanolysis of triglycerides was attempted in order to investigate the compatibility of the prototype microreactor in a methanolic environment. In the enzyme-mediated reaction, there was concern about the solubility of lipid and the effect of methanol on the enzyme. However, it was found that the micro-transesterification reaction was successful in performing quantitative methanolysis for at least 2 times using a single microreactor. This promising preliminary result can be used for future optimization in micro-derivatization technology involving methanol using the enzymatic microreactors.

Furthermore, this thesis research also demonstrates the utilization of several analytical methods for use in lipid analysis. These include non-aqueous reversed-phase LC and LC/MS used for analyzing products and intermediates from both transesterification (Chapter 3 to 4) and epoxidation (Chapter 5)



reactions of vegetable oils. The methods developed provide practical and routine separations for the detection of oleochemical products.

Overall, the research presented in this thesis provides a proof of concept for the development of more advanced technology for micro-scale lipid and oleochemical transformations including the transesterification of lipids. Microreactor technology provides an alternative method for lipid derivatization, especially applicable to small sample amounts. The development of the prototype enzymatic microreactors paves the way for future research into analytical applications, including rigorous method validation. The possibility of in-line automation for GC derivatization, manipulating the microreactors using robotics prior to GC injection, is suggested for future development. The use of methanol to produce fatty acid methyl ester derivatives using the microreactor should also be considered for future optimization in order to comply with conventional GC methods. In addition, the research could be expanded by exploring the use of different types of enzyme for other types of lipid transformations, for example the use of lipoxygenase in forming hydroxyl fatty acids.

## PERMISSION FROM PUBLISHER

### (APPENDIX 1)

---

In this paper-format thesis, three chapters were already published (Chapter 2,3 and 5). These publications were reused in the thesis with permission from the publishers. The author(s) and page numbers with regards to the publication are mentioned with the permission letter.

#### SPRINGER LICENSE TERMS AND CONDITIONS

May 22, 2013

This is a License Agreement between Sabiqah Tuan Anuar ("You") and Springer ("Springer") provided by Copyright Clearance Center ("CCC"). The license consists of your order details, the terms and conditions provided by Springer, and the payment terms and conditions.

License Number	3153740169448
License date	May 21, 2013
Licensed content publisher	Springer
Licensed content publication	Lipids
Licensed content title	The Development of Flow-through Bio-Catalyst Microreactors from Silica Micro Structured Fibers for Lipid Transformations
Licensed content author	Sabiqah Tuan Anuar
Licensed content date	Jan 1, 2011
Volume number	46
Issue number	6
Type of Use	Thesis/Dissertation
Portion	Full text

Number of copies	1
Author of this Springer article	Yes and you are the sole author of the new work
Order reference number	1
Title of your thesis / dissertation	Development of Microreactors and Analytical Methods for Lipid Transformations
Expected completion date	Jul 2013
Estimated size(pages)	186
Total	0.00 USD

Terms and Conditions

Limited License  
 With reference to your request to reprint in your thesis material on which Springer Science and Business Media control the copyright, permission is granted, free of charge, for the use indicated in your enquiry.

Licenses are for one-time use only with a maximum distribution equal to the number that you identified in the licensing process.

This License includes use in an electronic form, provided its password protected or on the university's intranet or repository, including UMI (according to the definition at the Sherpa website: <http://www.sherpa.ac.uk/romeo/>). For any other electronic use, please contact Springer at ([permissions.dordrecht@springer.com](mailto:permissions.dordrecht@springer.com) or [permissions.heidelberg@springer.com](mailto:permissions.heidelberg@springer.com)).

The material can only be used for the purpose of defending your thesis, and with a maximum of 100 extra copies in paper.

Although Springer holds copyright to the material and is entitled to negotiate on rights, this license is only valid, subject to a courtesy information to the author (address is given with the article/chapter) and provided it concerns original material which does not carry references to other sources (if material in question appears with credit to another source, authorization from that source is required as well).

Permission free of charge on this occasion does not prejudice any rights we might have to charge for reproduction of our copyrighted material in the future.

Altering/Modifying Material: Not Permitted  
 You may not alter or modify the material in any manner. Abbreviations, additions, deletions and/or any other alterations shall be made only with prior written authorization of the author(s) and/or Springer Science + Business Media. (Please contact Springer at ([permissions.dordrecht@springer.com](mailto:permissions.dordrecht@springer.com) or [permissions.heidelberg@springer.com](mailto:permissions.heidelberg@springer.com)))

Reservation of Rights

Springer Science + Business Media reserves all rights not specifically granted in the combination of (i) the license details provided by you and accepted in the course of this licensing transaction, (ii) these terms and conditions and (iii) CCC's Billing and Payment terms and conditions.

#### Copyright

#### Notice:Disclaimer

You must include the following copyright and permission notice in connection with any reproduction of the licensed material: "Springer and the original publisher /journal title, volume, year of publication, page, chapter/article title, name(s) of author(s), figure number(s), original copyright notice) is given to the publication in which the material was originally published, by adding; with kind permission from Springer Science and Business Media"

#### Warranties: None

Example 1: Springer Science + Business Media makes no representations or warranties with respect to the licensed material.

Example 2: Springer Science + Business Media makes no representations or warranties with respect to the licensed material and adopts on its own behalf the limitations and disclaimers established by CCC on its behalf in its Billing and Payment terms and conditions for this licensing transaction.

#### Indemnity

You hereby indemnify and agree to hold harmless Springer Science + Business Media and CCC, and their respective officers, directors, employees and agents, from and against any and all claims arising out of your use of the licensed material other than as specifically authorized pursuant to this license.

No Transfer of License  
This license is personal to you and may not be sublicensed, assigned, or transferred by you to any other person without Springer Science + Business Media's written permission.

No Amendment Except in Writing  
This license may not be amended except in a writing signed by both parties (or, in the case of Springer Science + Business Media, by CCC on Springer Science + Business Media's behalf).

Objection to Contrary Terms  
Springer Science + Business Media hereby objects to any terms contained in any purchase order, acknowledgment, check endorsement or other writing prepared by you, which terms are inconsistent with these terms and conditions or CCC's Billing and Payment terms and conditions. These terms and conditions, together with CCC's Billing and Payment terms and conditions (which are incorporated herein), comprise the entire agreement between you and Springer Science + Business Media (and CCC) concerning this licensing transaction. In the event of any conflict between your obligations established by these terms and conditions and those established by

CCC's Billing and Payment terms and conditions, these terms and conditions shall control.

#### Jurisdiction

All disputes that may arise in connection with this present License, or the breach thereof, shall be settled exclusively by arbitration, to be held in The Netherlands, in accordance with Dutch law, and to be conducted under the Rules of the 'Netherlands Arbitrage Instituut' (Netherlands Institute of Arbitration).*OR:*

All disputes that may arise in connection with this present License, or the breach thereof, shall be settled exclusively by arbitration, to be held in the Federal Republic of Germany, in accordance with German law.

**ELSEVIER LICENSE  
TERMS AND CONDITIONS**

May 22, 2013

This is a License Agreement between Sabiqah Tuan Anuar ("You") and Elsevier ("Elsevier") provided by Copyright Clearance Center ("CCC"). The license consists of your order details, the terms and conditions provided by Elsevier, and the payment terms and conditions.

Supplier	Elsevier Limited The Boulevard, Langford Lane Kidlington, Oxford, OX5 1GB, UK
Registered Company Number	1982084
Customer name	Sabiqah Tuan Anuar
Customer address	Lipid Chemistry Group, AFNS Department Edmonton, AB T6G2P5
License number	3153740806647
License date	May 21, 2013
Licensed content publisher	Elsevier
Licensed content publication	Journal of Molecular Catalysis B: Enzymatic
Licensed content title	The development of a capillary microreactor for transesterification reactions using lipase immobilized onto a silica monolith
Licensed content author	Sabiqah Tuan Anuar, Yuan-Yuan Zhao, Samuel M. Mugo, Jonathan M. Curtis
Licensed content date	August 2013
Licensed content volume number	92
Licensed content issue number	
Number of pages	9
Start Page	62
End Page	70

Type of Use	reuse in a thesis/dissertation
Intended publisher of new work	other
Portion	full article
Format	both print and electronic
Are you the author of this Elsevier article?	Yes
Will you be translating?	No
Order reference number	3
Title of your thesis/dissertation	Development of Microreactors and Analytical Methods for Lipid Transformations
Expected completion date	Jul 2013
Estimated size (number of pages)	186
Elsevier VAT number	GB 494 6272 12
Permissions price	0.00 USD
VAT/Local Sales Tax	0.0 USD / 0.0 GBP
Total	0.00 USD
Terms and Conditions	

#### GENERAL TERMS

2. Elsevier hereby grants you permission to reproduce the aforementioned material subject to the terms and conditions indicated.

3. Acknowledgement: If any part of the material to be used (for example, figures) has appeared in our publication with credit or acknowledgement to another source, permission must also be sought from that source. If such permission is not obtained then that material may not be included in your publication/copies. Suitable acknowledgement to the source must be made, either as a footnote or in a reference list at the end of your publication, as follows:

“Reprinted from Publication title, Vol /edition number, Author(s), Title of article / title of chapter, Pages No., Copyright (Year), with permission from Elsevier [OR APPLICABLE SOCIETY COPYRIGHT OWNER].” Also Lancet special credit - “Reprinted from The Lancet, Vol. number, Author(s), Title of article, Pages No., Copyright (Year), with permission from Elsevier.”

4. Reproduction of this material is confined to the purpose and/or media for which

permission is hereby given.

5. **Altering/Modifying Material: Not Permitted.** However figures and illustrations may be altered/adapted minimally to serve your work. Any other abbreviations, additions, deletions and/or any other alterations shall be made only with prior written authorization of Elsevier Ltd. (Please contact Elsevier at [permissions@elsevier.com](mailto:permissions@elsevier.com))

6. If the permission fee for the requested use of our material is waived in this instance, please be advised that your future requests for Elsevier materials may attract a fee.

7. **Reservation of Rights:** Publisher reserves all rights not specifically granted in the combination of (i) the license details provided by you and accepted in the course of this licensing transaction, (ii) these terms and conditions and (iii) CCC's Billing and Payment terms and conditions.

8. **License Contingent Upon Payment:** While you may exercise the rights licensed immediately upon issuance of the license at the end of the licensing process for the transaction, provided that you have disclosed complete and accurate details of your proposed use, no license is finally effective unless and until full payment is received from you (either by publisher or by CCC) as provided in CCC's Billing and Payment terms and conditions. If full payment is not received on a timely basis, then any license preliminarily granted shall be deemed automatically revoked and shall be void as if never granted. Further, in the event that you breach any of these terms and conditions or any of CCC's Billing and Payment terms and conditions, the license is automatically revoked and shall be void as if never granted. Use of materials as described in a revoked license, as well as any use of the materials beyond the scope of an unrevoked license, may constitute copyright infringement and publisher reserves the right to take any and all action to protect its copyright in the materials.

9. **Warranties:** Publisher makes no representations or warranties with respect to the licensed material.

10. **Indemnity:** You hereby indemnify and agree to hold harmless publisher and CCC, and their respective officers, directors, employees and agents, from and against any and all claims arising out of your use of the licensed material other than as specifically authorized pursuant to this license.

11. **No Transfer of License:** This license is personal to you and may not be sublicensed, assigned, or transferred by you to any other person without publisher's written permission.

12. **No Amendment Except in Writing:** This license may not be amended except in a writing signed by both parties (or, in the case of publisher, by CCC on publisher's behalf).



13. **Objection to Contrary Terms:** Publisher hereby objects to any terms contained in any purchase order, acknowledgment, check endorsement or other writing prepared by you, which terms are inconsistent with these terms and conditions or CCC's Billing and Payment terms and conditions. These terms and conditions, together with CCC's Billing and Payment terms and conditions (which are incorporated herein), comprise the entire agreement between you and publisher (and CCC) concerning this licensing transaction. In the event of any conflict between your obligations established by these terms and conditions and those established by CCC's Billing and Payment terms and conditions, these terms and conditions shall control.

14. **Revocation:** Elsevier or Copyright Clearance Center may deny the permissions described in this License at their sole discretion, for any reason or no reason, with a full refund payable to you. Notice of such denial will be made using the contact information provided by you. Failure to receive such notice will not alter or invalidate the denial. In no event will Elsevier or Copyright Clearance Center be responsible or liable for any costs, expenses or damage incurred by you as a result of a denial of your permission request, other than a refund of the amount(s) paid by you to Elsevier and/or Copyright Clearance Center for denied permissions.

#### LIMITED LICENSE

The following terms and conditions apply only to specific license types:

15. **Translation:** This permission is granted for non-exclusive world **English** rights only unless your license was granted for translation rights. If you licensed translation rights you may only translate this content into the languages you requested. A professional translator must perform all translations and reproduce the content word for word preserving the integrity of the article. If this license is to re-use 1 or 2 figures then permission is granted for non-exclusive world rights in all languages.

16. **Website:** The following terms and conditions apply to electronic reserve and author websites:

**Electronic reserve:** If licensed material is to be posted to website, the web site is to be password-protected and made available only to bona fide students registered on a relevant course if: This license was made in connection with a course, This permission is granted for 1 year only. You may obtain a license for future website posting, All content posted to the web site must maintain the copyright information line on the bottom of each image, A hyper-text must be included to the Homepage of the journal from which you are licensing at <http://www.sciencedirect.com/science/journal/xxxxx> or the Elsevier homepage for books at <http://www.elsevier.com> , and

Central Storage: This license does not include permission for a scanned version of the material to be stored in a central repository such as that provided by Heron/XanEdu.

17. **Author website** for journals with the following additional clauses:

All content posted to the web site must maintain the copyright information line on the bottom of each image, and the permission granted is limited to the personal version of your paper. You are not allowed to download and post the published electronic version of your article (whether PDF or HTML, proof or final version), nor may you scan the printed edition to create an electronic version. A hyper-text must be included to the Homepage of the journal from which you are licensing at <http://www.sciencedirect.com/science/journal/xxxxx> . As part of our normal production process, you will receive an e-mail notice when your article appears on Elsevier's online service ScienceDirect ([www.sciencedirect.com](http://www.sciencedirect.com)). That e-mail will include the article's Digital Object Identifier (DOI). This number provides the electronic link to the published article and should be included in the posting of your personal version. We ask that you wait until you receive this e-mail and have the DOI to do any posting.

Central Storage: This license does not include permission for a scanned version of the material to be stored in a central repository such as that provided by Heron/XanEdu.

18. **Author website** for books with the following additional clauses: Authors are permitted to place a brief summary of their work online only. A hyper-text must be included to the Elsevier homepage at <http://www.elsevier.com> . All content posted to the web site must maintain the copyright information line on the bottom of each image. You are not allowed to download and post the published electronic version of your chapter, nor may you scan the printed edition to create an electronic version.

Central Storage: This license does not include permission for a scanned version of the material to be stored in a central repository such as that provided by Heron/XanEdu.

19. **Website** (regular and for author): A hyper-text must be included to the Homepage of the journal from which you are licensing at <http://www.sciencedirect.com/science/journal/xxxxx>. or for books to the Elsevier homepage at <http://www.elsevier.com>

20. **Thesis/Dissertation**: If your license is for use in a thesis/dissertation your thesis may be submitted to your institution in either print or electronic form. Should your thesis be published commercially, please reapply for permission. These requirements include permission for the Library and Archives of Canada to supply single copies, on demand, of the complete thesis and include permission for UMI to supply single copies, on demand, of the complete thesis. Should your thesis be published commercially, please reapply for permission.

**SPRINGER LICENSE  
TERMS AND CONDITIONS**

May 22, 2013

This is a License Agreement between Sabiqah Tuan Anuar ("You") and Springer ("Springer") provided by Copyright Clearance Center ("CCC"). The license consists of your order details, the terms and conditions provided by Springer, and the payment terms and conditions.

License Number	3153740516460
License date	May 21, 2013
Licensed content publisher	Springer
Licensed content publication	Journal of the American Oil Chemists' Society
Licensed content title	Monitoring the Epoxidation of Canola Oil by Non-aqueous Reversed Phase Liquid Chromatography/Mass Spectrometry for Process Optimization and Control
Licensed content author	Sabiqah Tuan Anuar
Licensed content date	Jan 1, 2012
Volume number	89
Issue number	11
Type of Use	Thesis/Dissertation
Portion	Full text
Number of copies	1
Author of this Springer article	Yes and you are the sole author of the new work
Order reference number	2
Title of your thesis / dissertation	Development of Microreactors and Analytical Methods for Lipid Transformations
Expected completion date	Jul 2013
Estimated size(pages)	186
Total	0.00 USD

## Terms and Conditions

### Limited

### License

With reference to your request to reprint in your thesis material on which Springer Science and Business Media control the copyright, permission is granted, free of charge, for the use indicated in your enquiry.

Licenses are for one-time use only with a maximum distribution equal to the number that you identified in the licensing process.

This License includes use in an electronic form, provided its password protected or on the university's intranet or repository, including UMI (according to the definition at the Sherpa website: <http://www.sherpa.ac.uk/romeo/>). For any other electronic use, please contact Springer at ([permissions.dordrecht@springer.com](mailto:permissions.dordrecht@springer.com) or [permissions.heidelberg@springer.com](mailto:permissions.heidelberg@springer.com)).

The material can only be used for the purpose of defending your thesis, and with a maximum of 100 extra copies in paper.

Although Springer holds copyright to the material and is entitled to negotiate on rights, this license is only valid, subject to a courtesy information to the author (address is given with the article/chapter) and provided it concerns original material which does not carry references to other sources (if material in question appears with credit to another source, authorization from that source is required as well).

Permission free of charge on this occasion does not prejudice any rights we might have to charge for reproduction of our copyrighted material in the future.

### Altering/Modifying

### Material:

### Not

### Permitted

You may not alter or modify the material in any manner. Abbreviations, additions, deletions and/or any other alterations shall be made only with prior written authorization of the author(s) and/or Springer Science + Business Media. (Please contact Springer at ([permissions.dordrecht@springer.com](mailto:permissions.dordrecht@springer.com) or [permissions.heidelberg@springer.com](mailto:permissions.heidelberg@springer.com)))

### Reservation

### of

### Rights

Springer Science + Business Media reserves all rights not specifically granted in the combination of (i) the license details provided by you and accepted in the course of this licensing transaction, (ii) these terms and conditions and (iii) CCC's Billing and Payment terms and conditions.

### Copyright

### Notice:Disclaimer

You must include the following copyright and permission notice in connection with any reproduction of the licensed material: "Springer and the original publisher /journal title, volume, year of publication, page, chapter/article title, name(s) of author(s), figure number(s), original copyright notice) is given to the publication in which the material was originally published, by adding; with kind permission from Springer Science and Business Media"

Warranties: None

Example 1: Springer Science + Business Media makes no representations or warranties with respect to the licensed material.

Example 2: Springer Science + Business Media makes no representations or warranties with respect to the licensed material and adopts on its own behalf the limitations and disclaimers established by CCC on its behalf in its Billing and Payment terms and conditions for this licensing transaction.

#### Indemnity

You hereby indemnify and agree to hold harmless Springer Science + Business Media and CCC, and their respective officers, directors, employees and agents, from and against any and all claims arising out of your use of the licensed material other than as specifically authorized pursuant to this license.

No Transfer of License  
This license is personal to you and may not be sublicensed, assigned, or transferred by you to any other person without Springer Science + Business Media's written permission.

No Amendment Except in Writing  
This license may not be amended except in a writing signed by both parties (or, in the case of Springer Science + Business Media, by CCC on Springer Science + Business Media's behalf).

Objection to Contrary Terms  
Springer Science + Business Media hereby objects to any terms contained in any purchase order, acknowledgment, check endorsement or other writing prepared by you, which terms are inconsistent with these terms and conditions or CCC's Billing and Payment terms and conditions. These terms and conditions, together with CCC's Billing and Payment terms and conditions (which are incorporated herein), comprise the entire agreement between you and Springer Science + Business Media (and CCC) concerning this licensing transaction. In the event of any conflict between your obligations established by these terms and conditions and those established by CCC's Billing and Payment terms and conditions, these terms and conditions shall control.

#### Jurisdiction

All disputes that may arise in connection with this present License, or the breach thereof, shall be settled exclusively by arbitration, to be held in The Netherlands, in accordance with Dutch law, and to be conducted under the Rules of the 'Netherlands Arbitrage Instituut' (Netherlands Institute of Arbitration).**OR:**

All disputes that may arise in connection with this present License, or the breach thereof, shall be settled exclusively by arbitration, to be held in the Federal Republic of Germany, in accordance with German law.

## APPENDIX 2

Analyte	Normalized Average Response Factor in LC/ELSD
EO	0.5
MO	0.8
DO	0.7
TO	1

**FIG A2-1** Response factors (RF) of the analytes in LC/ELSD (relative to TO) that achieved at 33 °C.

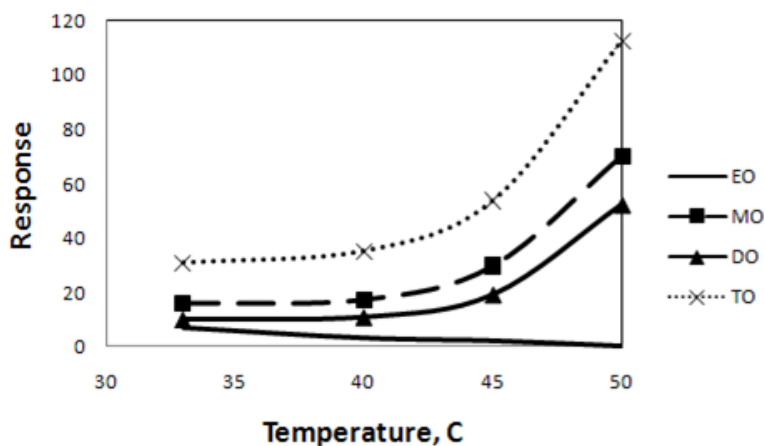


**FIG A2-2** LC/ELSD response for EO, MO, DO and TO (0.125 mg/mL each) at different temperatures. Higher temperatures result in greatly increased responses for glycerides but almost no response for ethyl esters. At higher ELSD temperatures, which might be more optimal for TO for example, this difference can become even higher and little or no response is seen for EO.

## APPENDIX 2

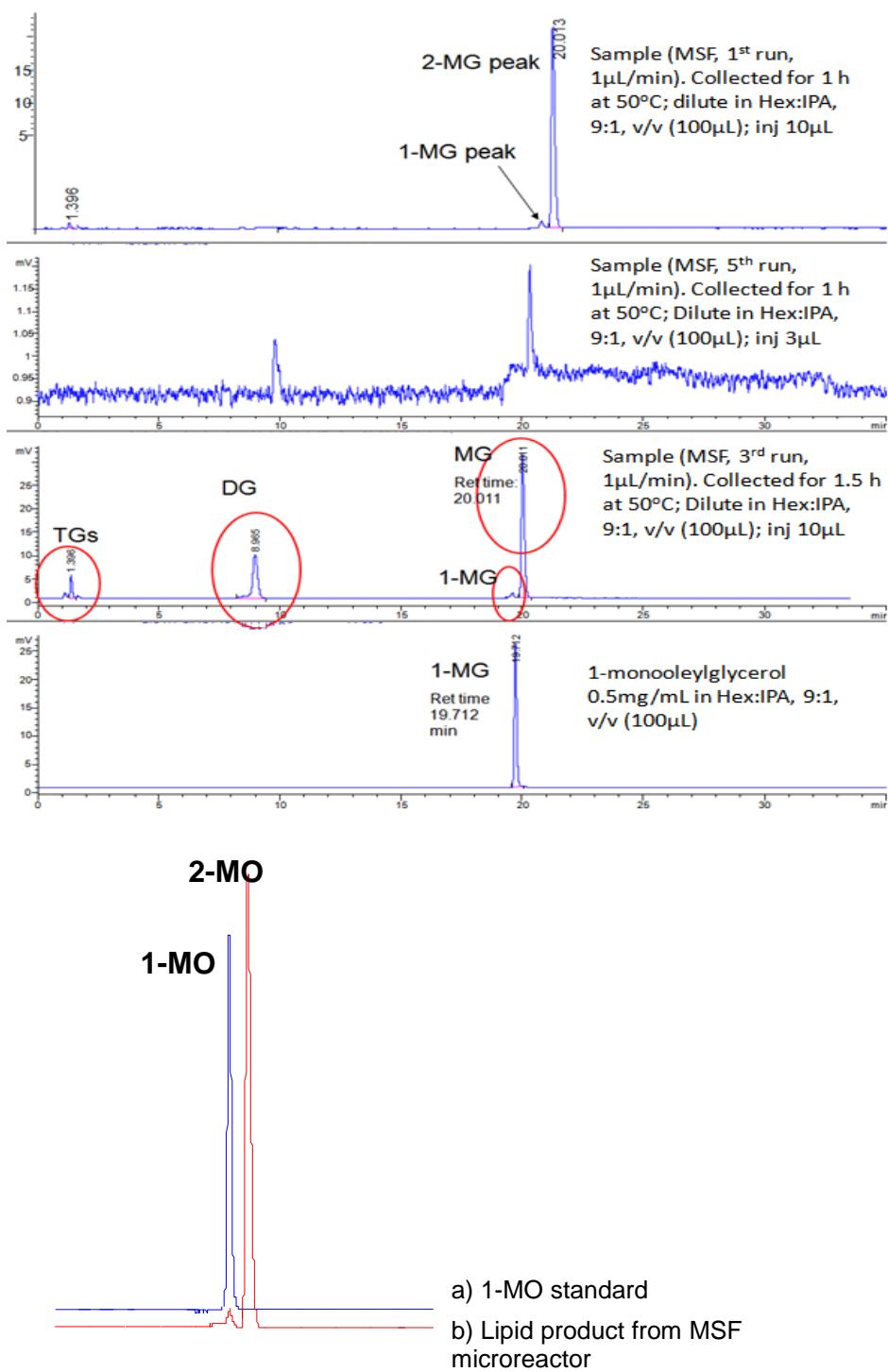


**FIG A2-3** Normal Phase LC/ELSD (AOCS method) for MSF trial at 50°C.

## APPENDIX 2

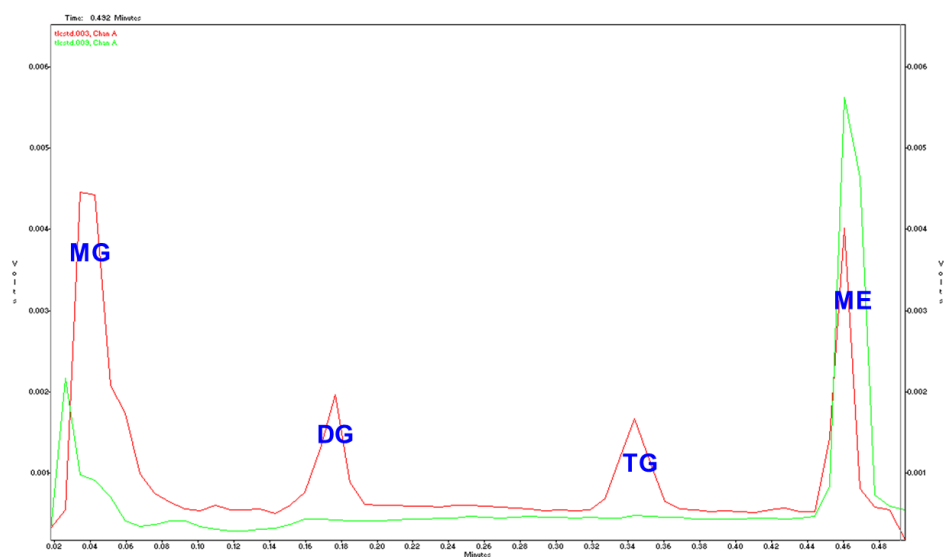


**FIG A2-4** TLC/Iatroscan-FID for MSF trial at 50°C

Red: TLC standard 5µg/mL; Green: Ethanolic tristearin (transesterified in the lipase-immobilized MSF column) 1mg tristearin in 9:11 (ethanol: hexane) mL; TLC developing solvents: hexane/diethyl ether/formic acid.

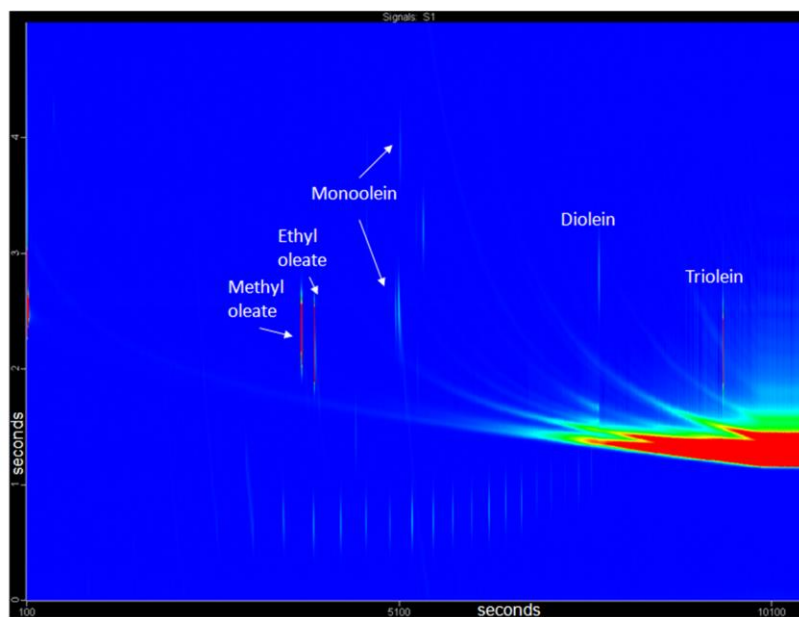


**FIG A2-5** GCxGC chromatogram for standards: TLC-18A+Ethyl oleate (0.18mg/mL –each TLC – 0.29 mg/mL EE). The 2D-GC analysis was performed by Carla Villages.



## APPENDIX 2

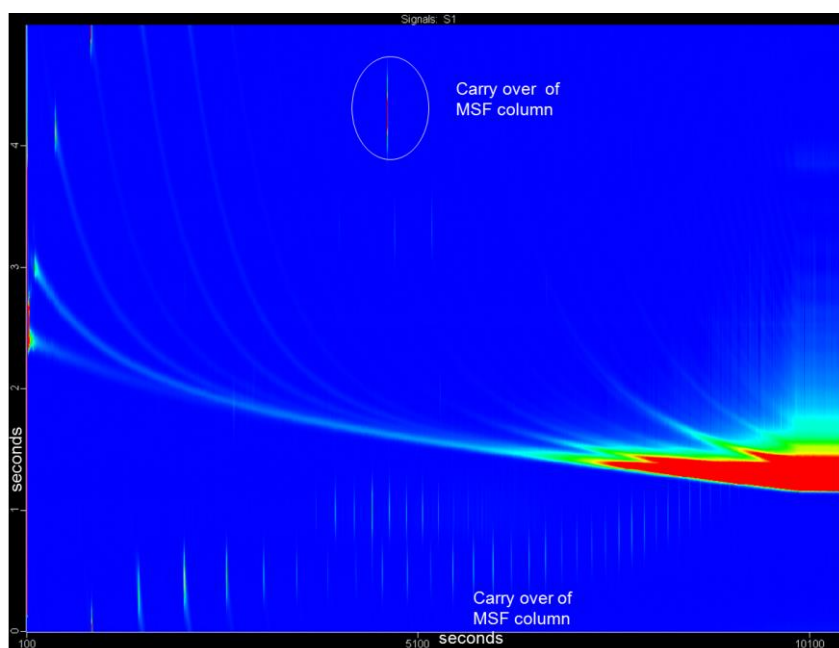


**FIG A2-6** GCxGC chromatogram for MSF microreactor without sample at 1  $\mu\text{L}/\text{min}$  flow rate of ethanol blank.

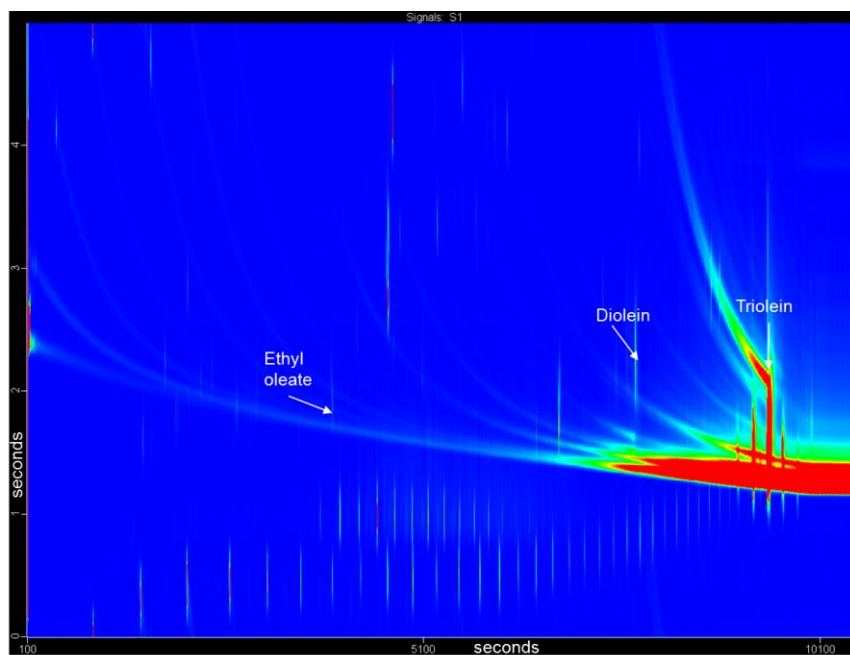


**FIG A2-7** Ethanol washout of MSF microreactor after run with triolein sample.

### APPENDIX 3

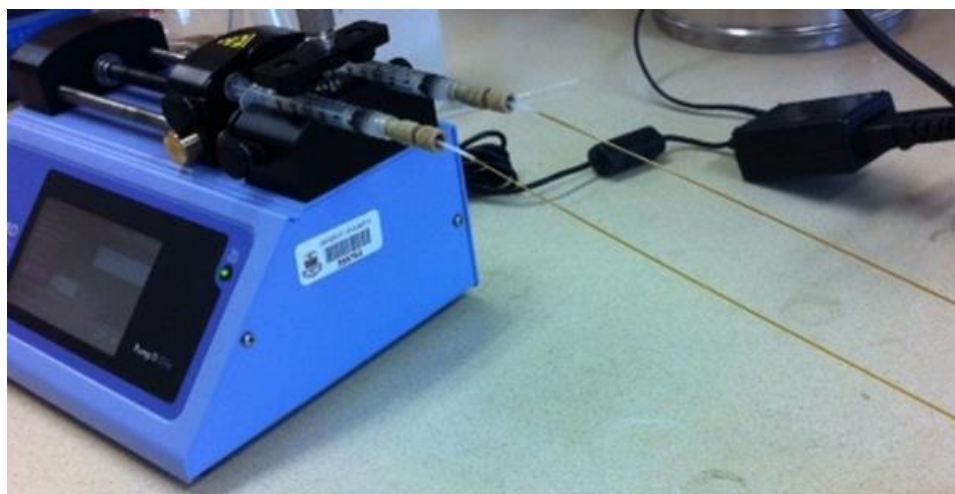


**FIG A3-1** Experimental setup: Microreaction was carried out using a syringe pump (Harvard Plus '11).

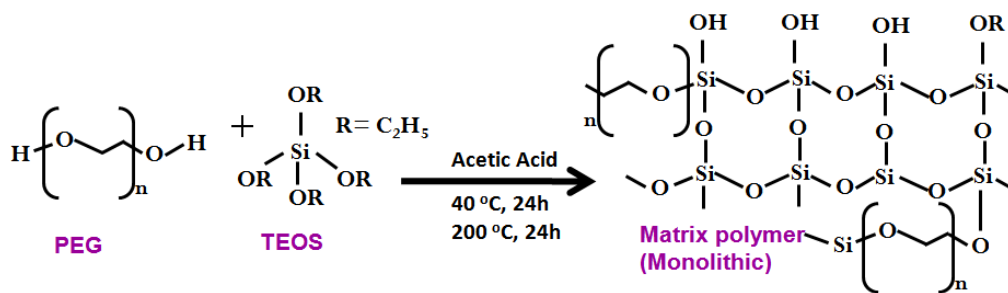


**FIG A3-2** Schematic diagrams of monolith formation by reaction of polyethylene(glycol) and tetraethylorthosilicate in acetic acid.

### APPENDIX 3

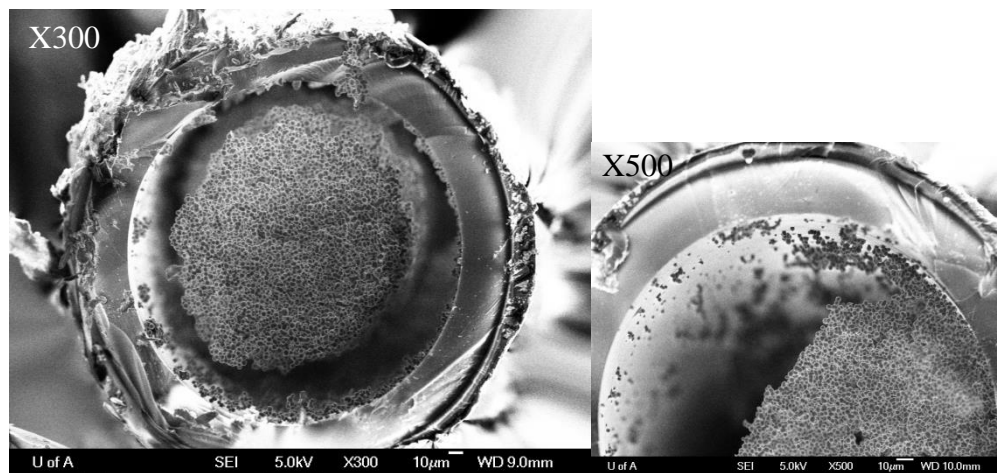


**FIG A3-3** Preparation of silica monolith: Effect of Non-treated silica capillary wall. The silica monolith network was found separated from the silica wall resulted from non-treated capillary.

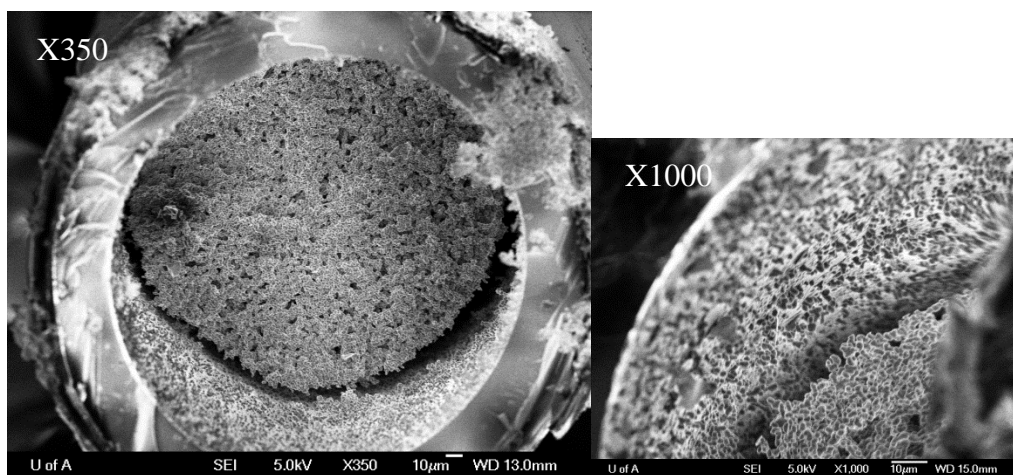


**FIG A3-4** Effect of 0.5M NaOH-treated silica capillary wall shows some of the silica monolith networks bounded to the wall.

### APPENDIX 3

---

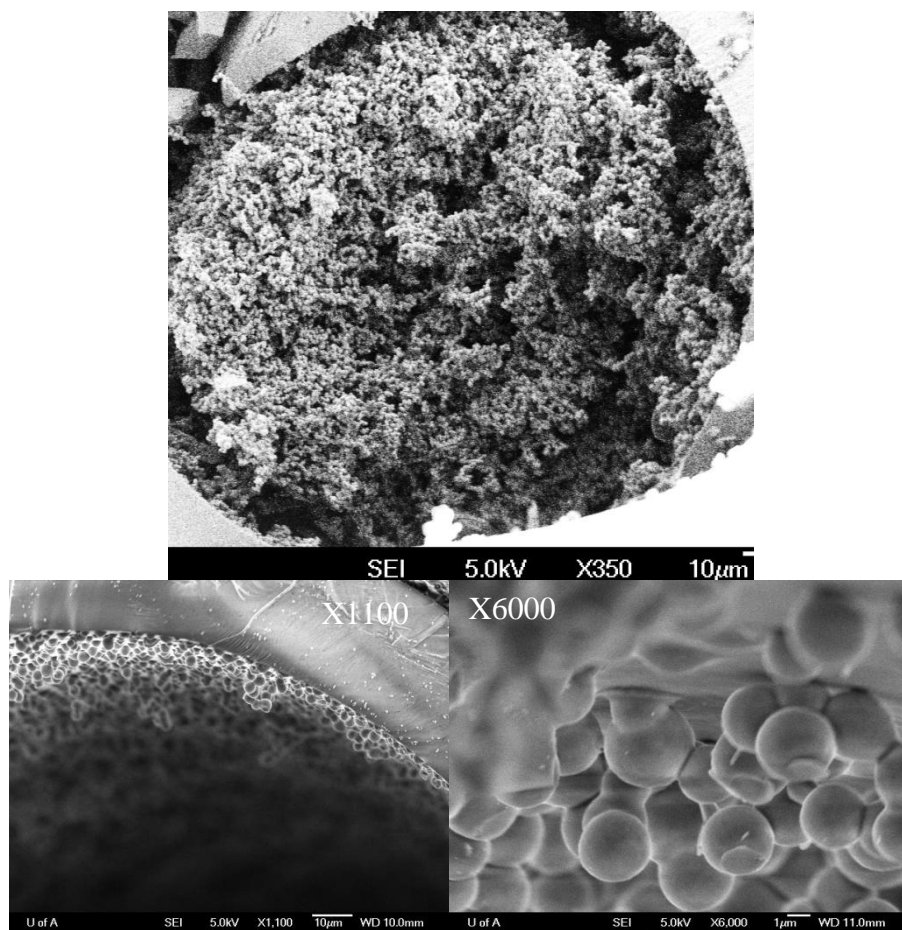


**FIG A3-5** Effect of 1.0 M NaOH-treated silica capillary wall: The silica wall was fully activated and readily attached with silica monolith networks.

## APPENDIX 3

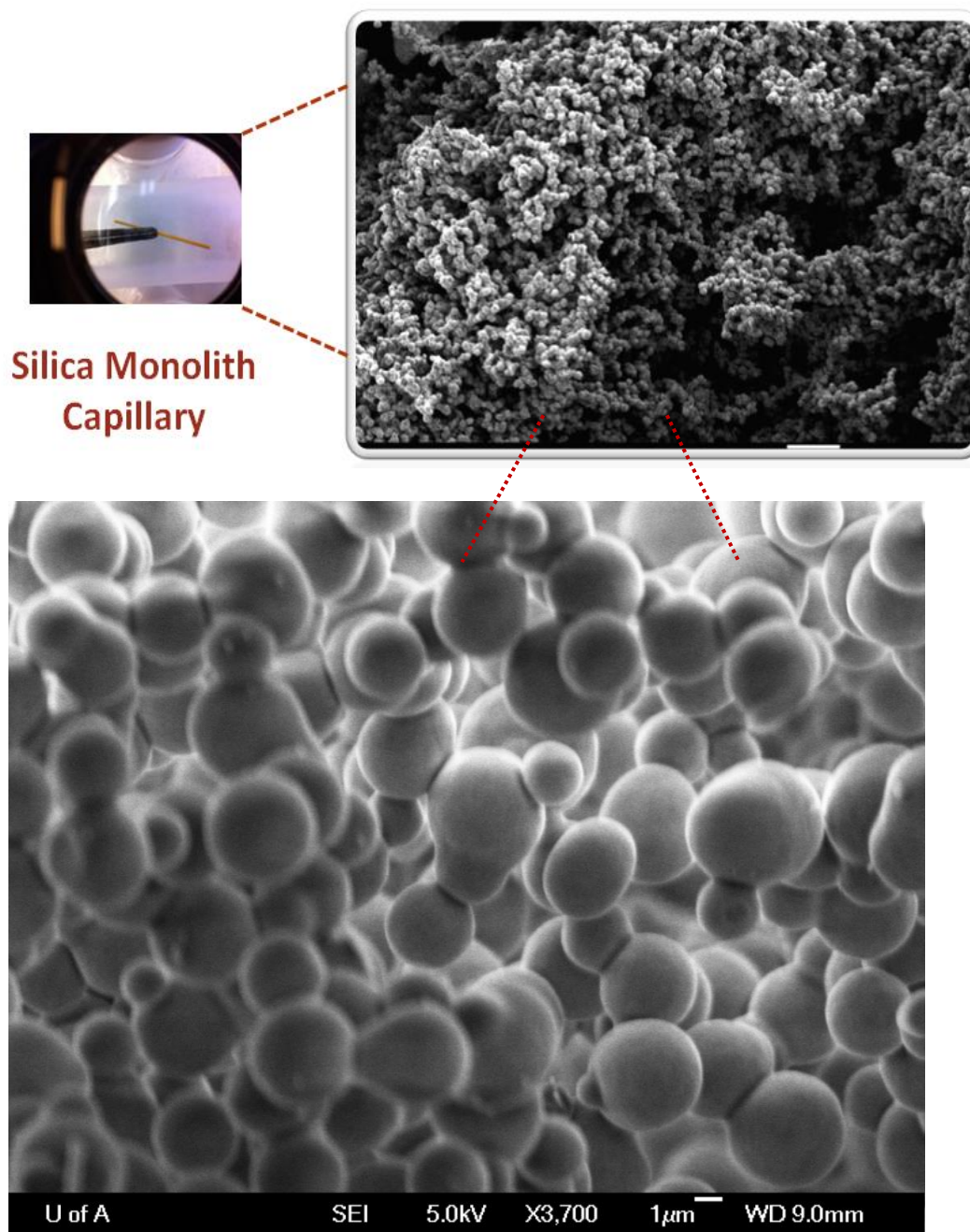


**FIG A3-6** Porous Silica Monolith inside silica capillary prepared from 0.1 g PEG + 0.45 mL TEOS + 1 mL  $\text{CH}_3\text{CH}_2\text{COOH}$  (0.01 M) (cold, mixing, 45 min). Refer Chapter 4.

### APPENDIX 3

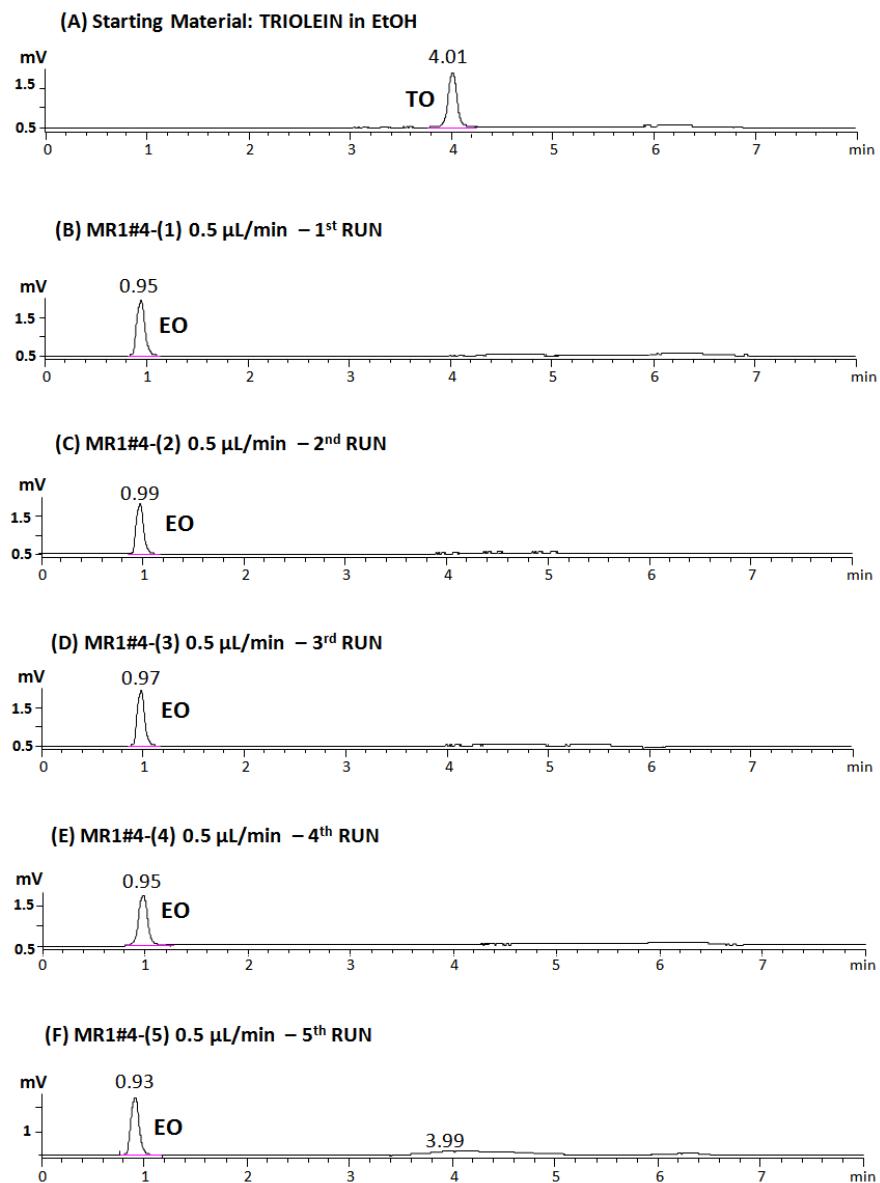


**FIG A3-7** LC/ELSD traces for TO starting oil and EO products for reaction with SM for 5 times at room temperature and flow rate of 0.5  $\mu$ L/min.

### APPENDIX 3

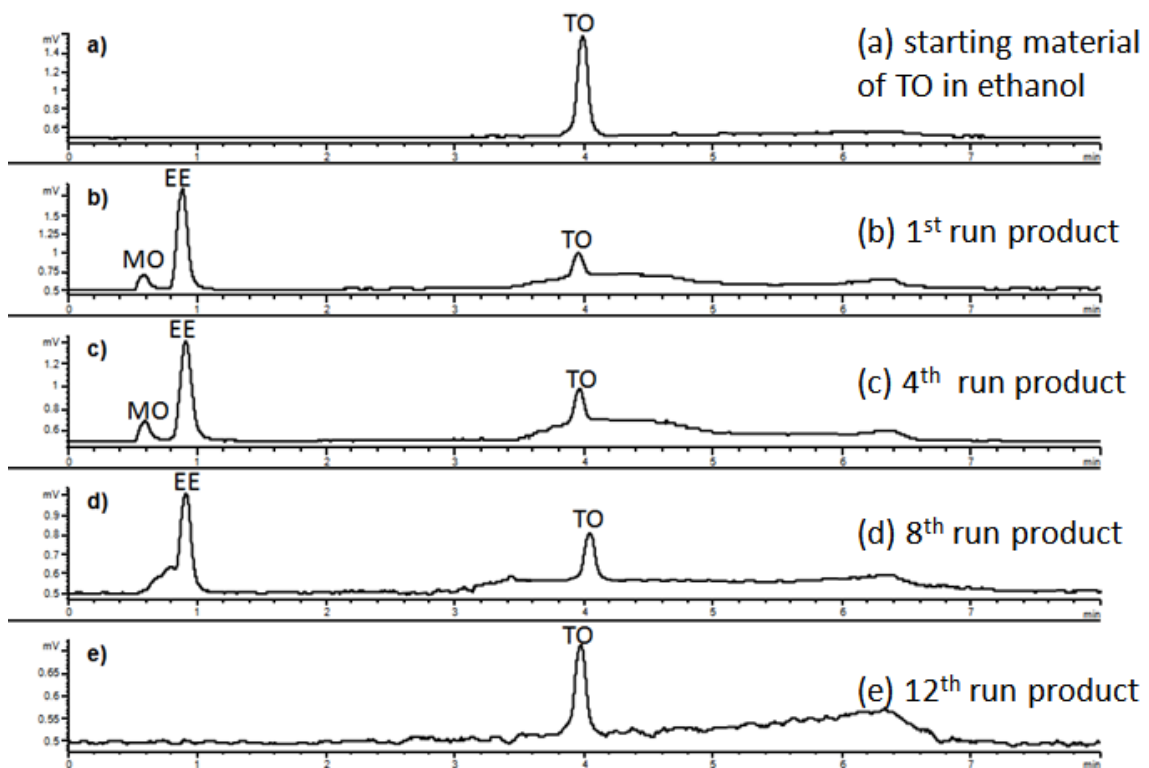


**FIG A3-8** LC/ELSD traces for TO starting oil and ethylation products for reaction with SM at room temperature and flow rate of 1.0  $\mu\text{L}/\text{min}$ .

### APPENDIX 3

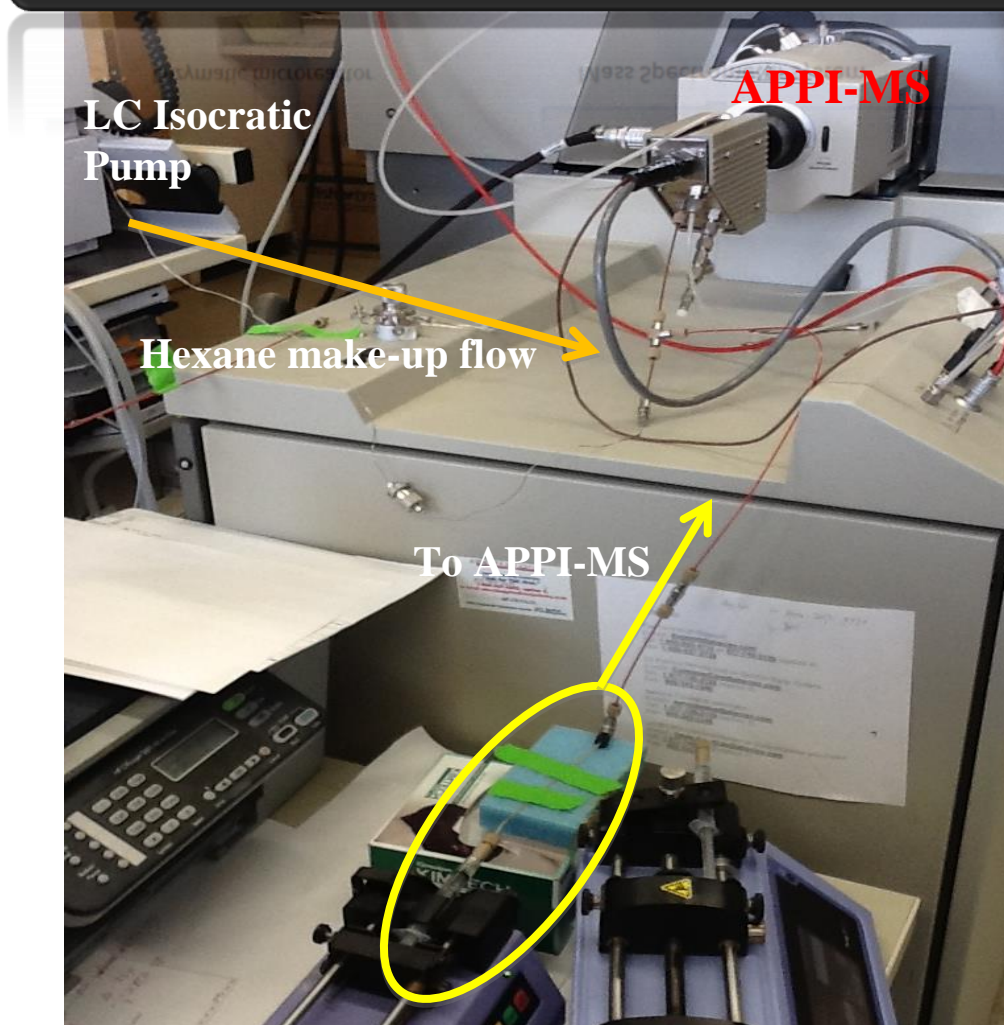
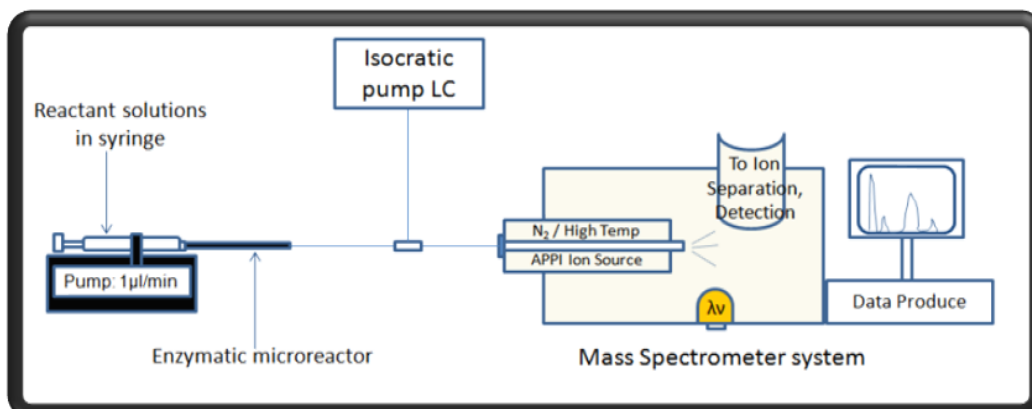
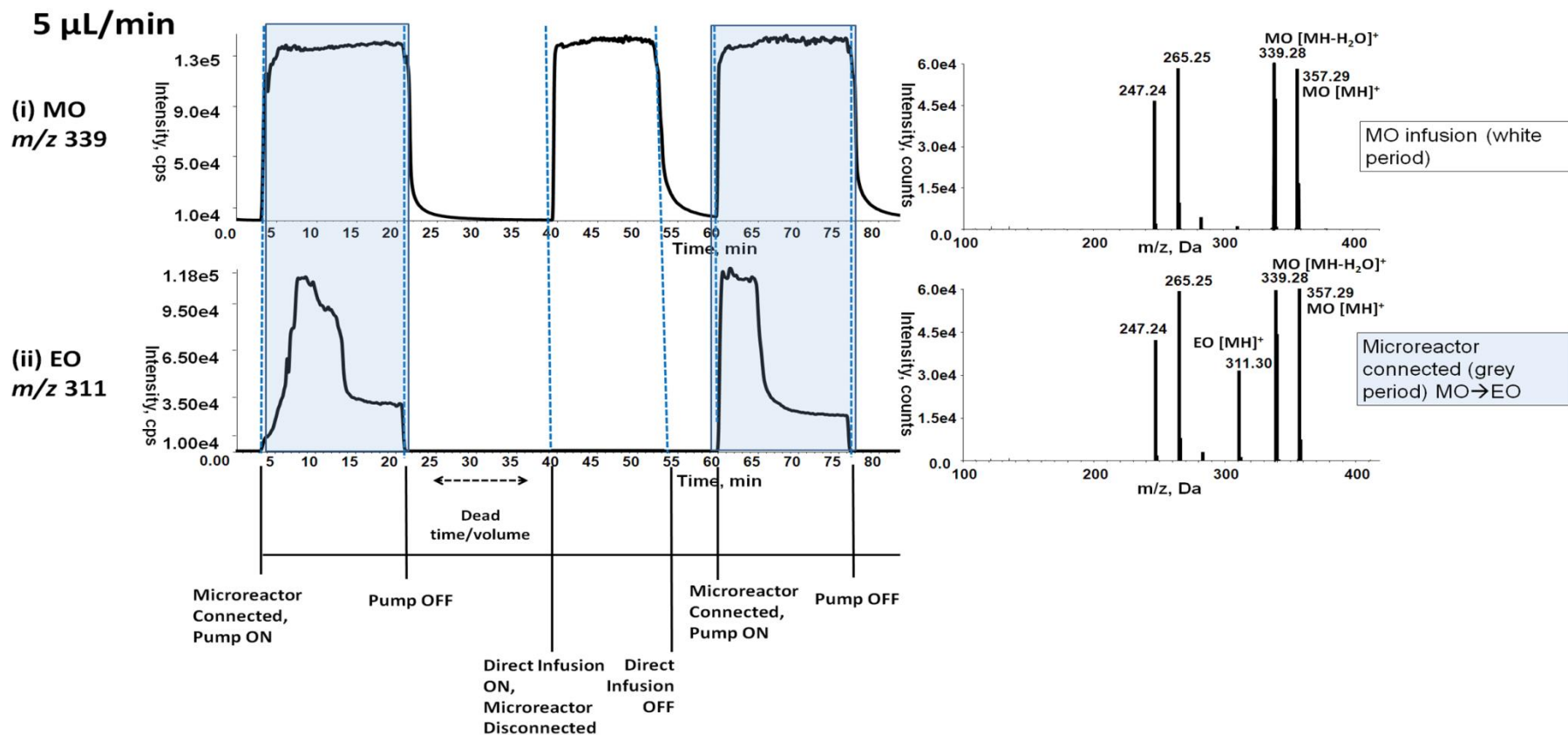


FIG A3-9 Instrumentation setup for online SM Microreactor – MS.



APPENDIX 3



**FIG A3-10** Online SM Microreactor – MS ; Substrate: Monoolein+EtOH (0.5mg/mL); Flowrate: 5µL/min. Refer Chapter 4 for MS conditions. The substrate was infused through the microreactor using an automatic syringe pump method at 5µL/min, with the make-up flow (isocratic LC pump): 100% hexane at 200 µL/min.

### APPENDIX 3

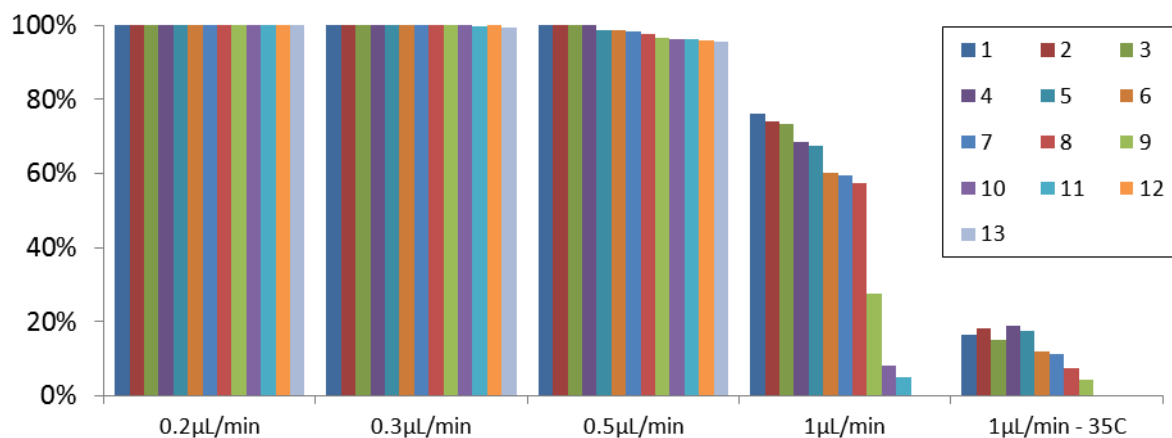


**FIG A3-11** Percentage of conversion of lipid starting materials (TO) to FAEE at different flow rates at room temperature (22°C) and 35°C for 13 consecutive runs, using GC/MS.

## APPENDIX 4

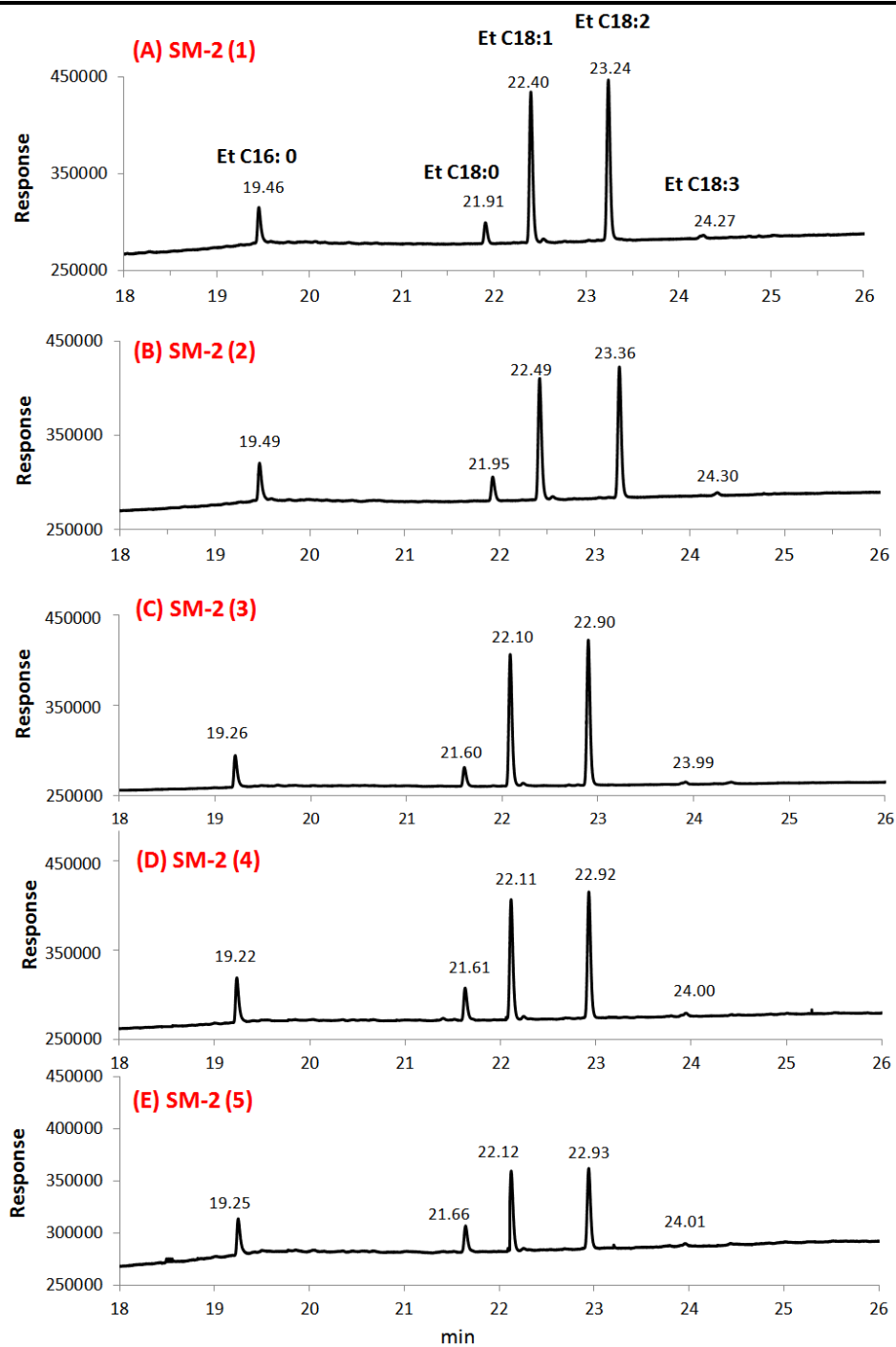


**FIG A4-1** The reusability of the microreactor for transesterification of sesame seeds oil were tested for 5 consecutive runs at RT and at 0.3  $\mu\text{L}/\text{min}$  infusion. GC/FID.

## APPENDIX 4

**TABLE A4-2** The transesterification of triolein in ethanol using the SM microreactor repeated 8 times. For each run, products were collected for 5 h at a flow rate of 0.3  $\mu\text{L}/\text{min}$ . The GC/FID peak area was normalized to the Run 1.

	GC/FID <sup>a</sup> (%)								Mean	%RSD
	Run 1	Run 2	Run 3	Run 4	Run 5	Run 6	Run 7	Run 8		
FAEE	100.0	99.8	99.6	99.8	99.4	99.7	99.3	94.8	99.0	1.76
TAG <sup>b, c</sup>	n/d	n/d	n/d	n/d	n/d	n/d	1.2 <sup>b</sup>	5.0 <sup>b</sup>	-	-

<sup>a</sup>the GC/FID was expressed by normalizing individual peak area to Run 1

<sup>b</sup>TAG was quantified using % NARP-LC/ELSD as describes in Material and Method. Note that the normalized response factor of ELSD was higher for TAG (1) compared for FAEE (0.5).

<sup>c</sup>n/d not detectable.

## APPENDIX 4

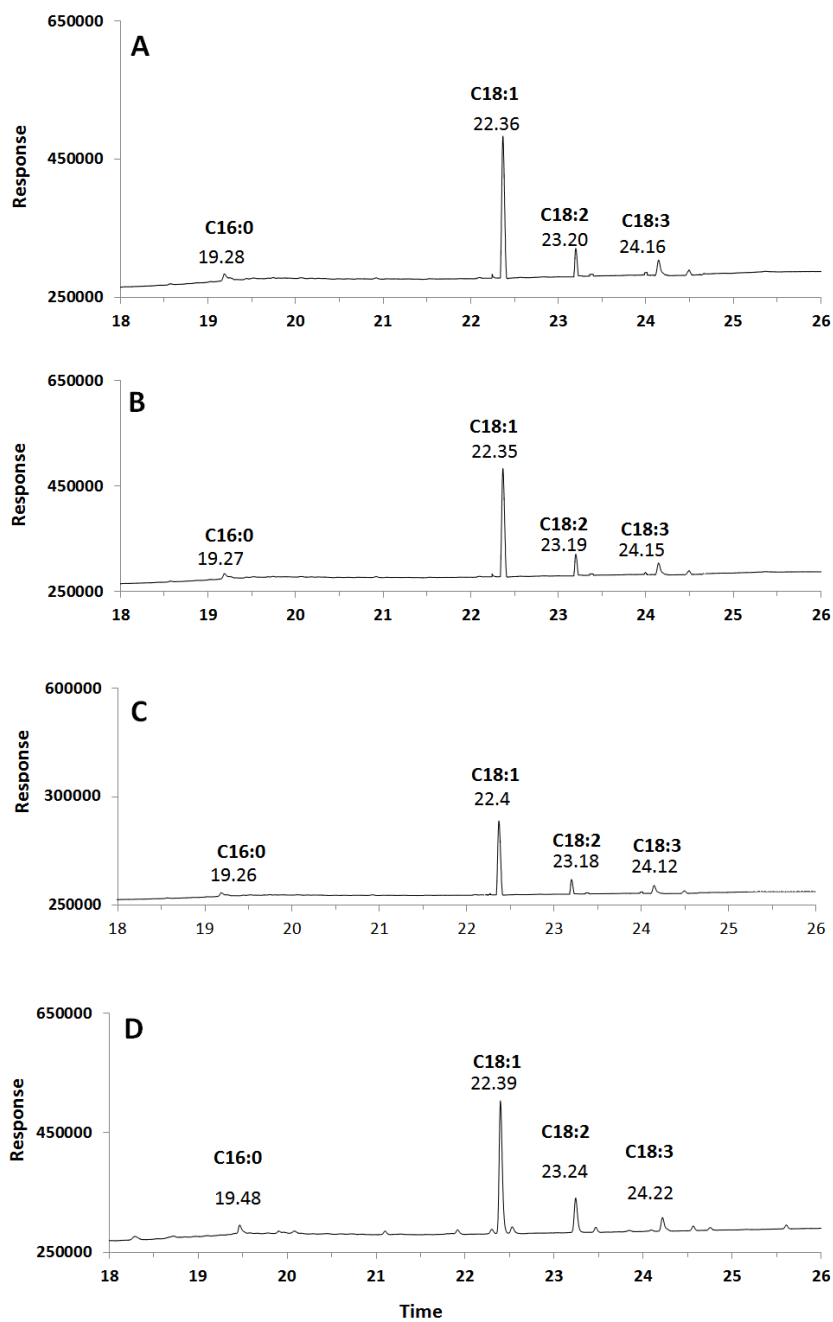


**FIG A4-3** GC/FID traces for FAEE products for transesterification reaction of canola oil at room temperature and conditions using: (A) SM at flow rate of 0.3  $\mu\text{L}/\text{min}$ , (B) MSF at flow rate of 0.3  $\mu\text{L}/\text{min}$ , (C) commercial lipase beads (Novozyme 435) for 5 h in stirring-reactor, (D)  $\text{H}_2\text{SO}_4$  acid catalyst for overnight.

## APPENDIX 4

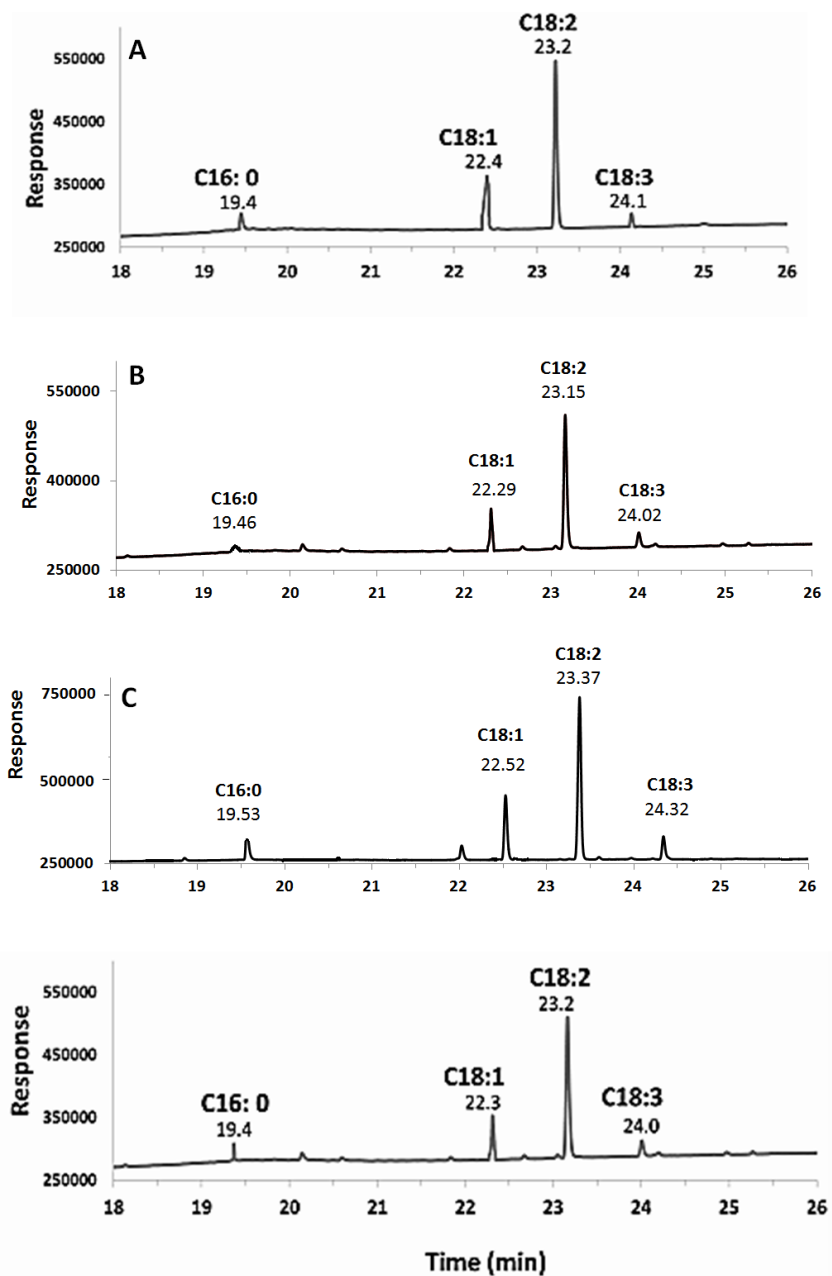


**FIG A4-4** GC/FID traces for FAEE products for transesterification reaction of soybean oil at room temperature and conditions using: (A) SM at flow rate of 0.3  $\mu\text{L}/\text{min}$ , (B) MSF at flow rate of 0.3  $\mu\text{L}/\text{min}$ , (C) commercial lipase beads (Novozyme 435) for 5 h in stirring-reactor, (D) H<sub>2</sub>SO<sub>4</sub> acid catalyst for overnight.

## APPENDIX 4

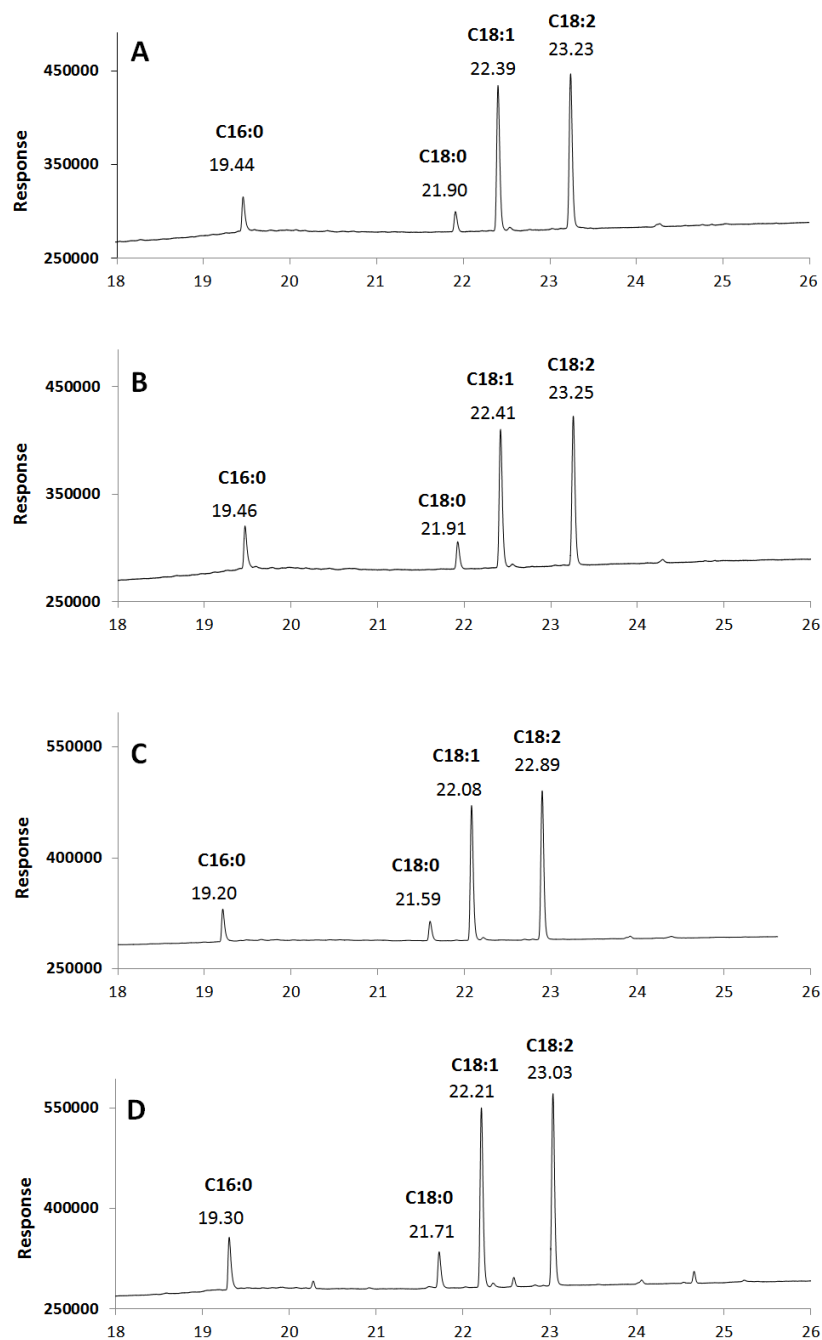


**FIG A4-5** GC/FID traces for FAEE products for transesterification reaction of sesame seed oil at room temperature and conditions using: (A) SM at flow rate of 0.3  $\mu\text{L}/\text{min}$ , (B) MSF at flow rate of 0.3  $\mu\text{L}/\text{min}$ , (C) commercial lipase beads (Novozyme 435) for 5 h in stirring-reactor, (D)  $\text{H}_2\text{SO}_4$  acid catalyst for overnight.

## APPENDIX 4

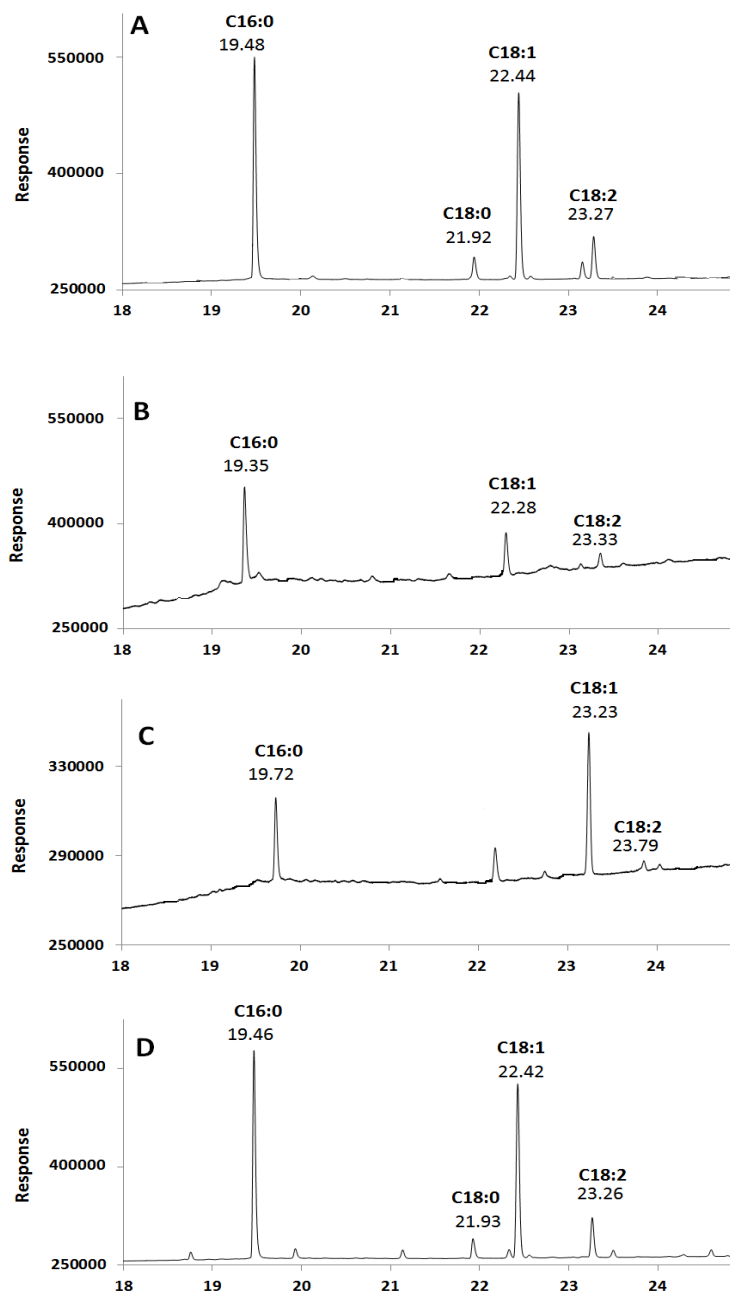


**FIG A4-6** GC/FID traces for FFAE products for transesterification reaction of rbd-palm oil at room temperature and conditions using: (A) SM at flow rate of 0.3  $\mu\text{L}/\text{min}$ , (B) MSF at flow rate of 0.3  $\mu\text{L}/\text{min}$ , (C) commercial lipase beads (Novozyme 435) for 5 h in stirring-reactor, (D)  $\text{H}_2\text{SO}_4$  acid catalyst for overnight.



## APPENDIX 5

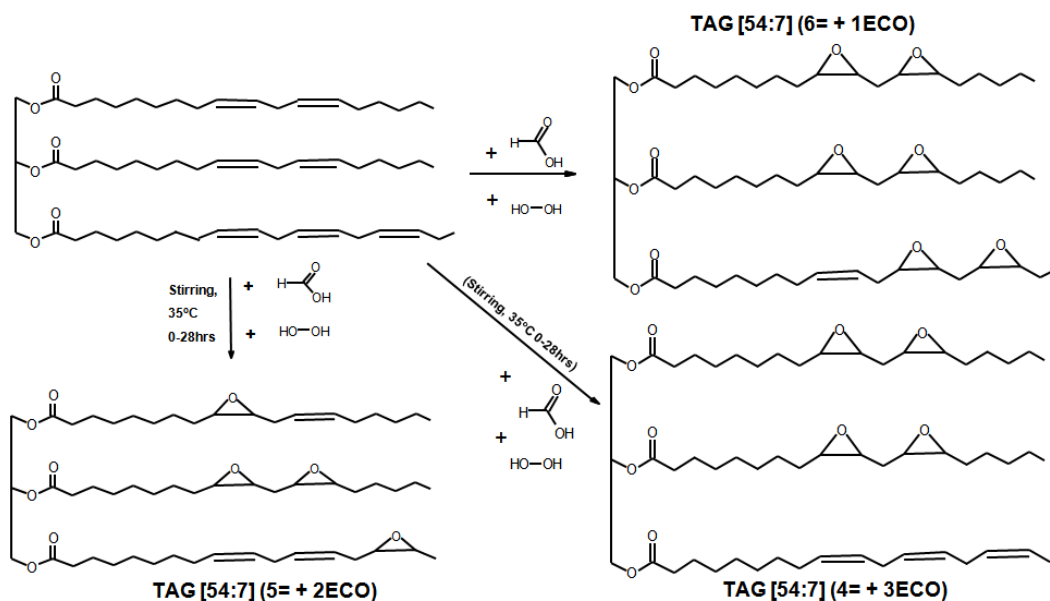


**FIG A5-1** Example showing canola oil with 3 double bonds (3=) or more (4=; 5=; 6; 7=) anywhere consist of 54 carbon total (54C) which had undergone partial epoxidation to give oxine ring(s) and remaining double bonds.

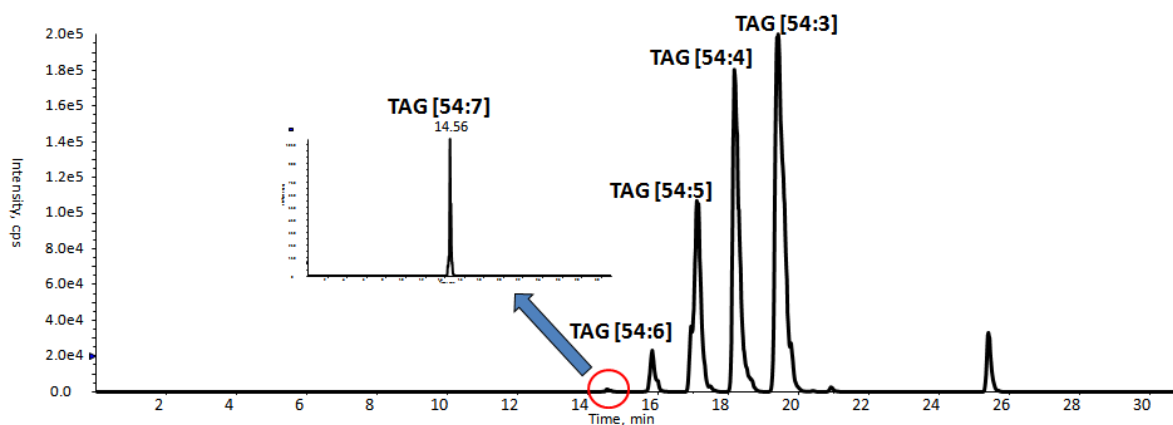


**FIG A5-2** A non-aqueous reversed phase liquid chromatography coupled to electrospray mass spectrometry (NARP-LC/ESI-MS) separation of TAGs in canola oil (starting material), consisting of TAGs 54C with 3-7 double bonds (TIC  $m/z$  range 500-1500).

## APPENDIX 5

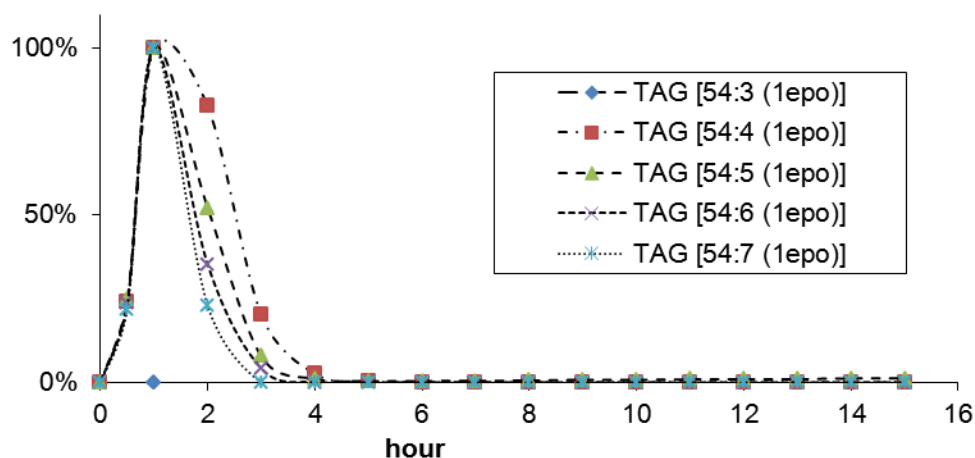


**FIG A5-3** The formation of mono-epoxy intermediates from TAG (54C) containing 3-7 double bonds (normalized).

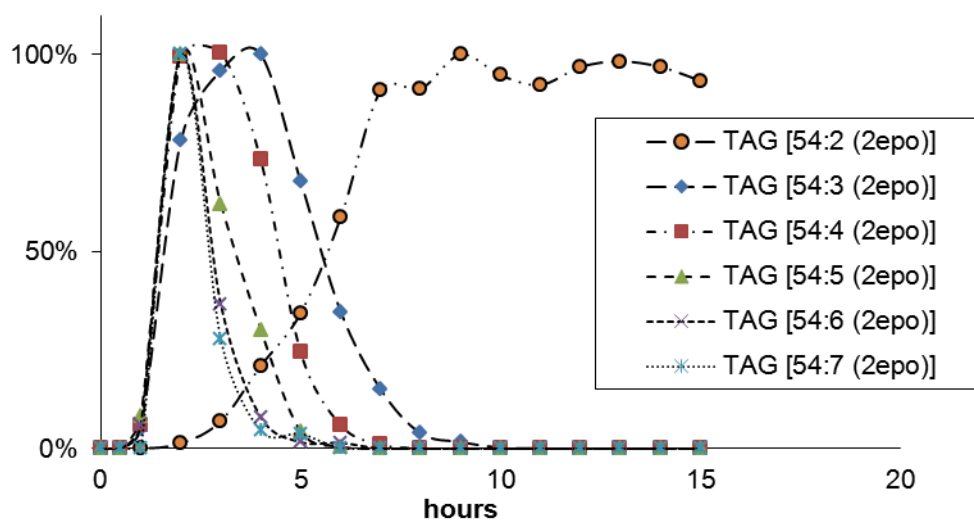


**FIG A5-4** The formation of di-epoxy intermediates and product from TAG (54C) containing 3-7 double bonds (normalized).

## APPENDIX 5

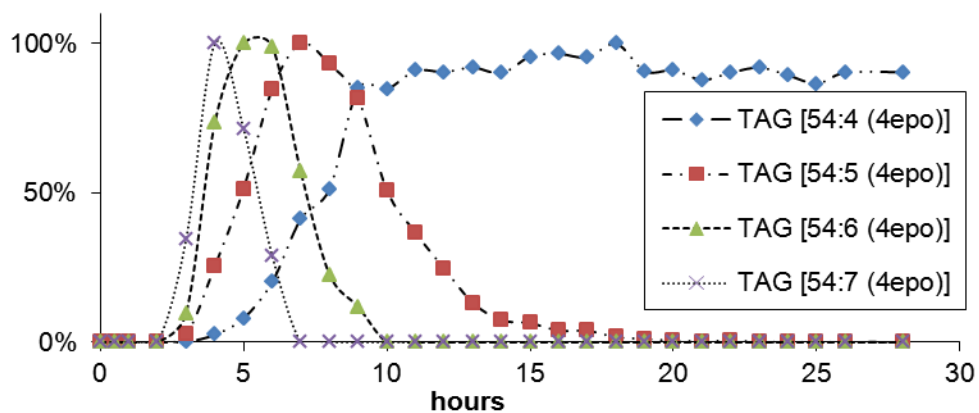


**FIG A5-5** The formation of 4-epoxy intermediates and product from TAG (54C) containing 4-7 double bonds (normalized).

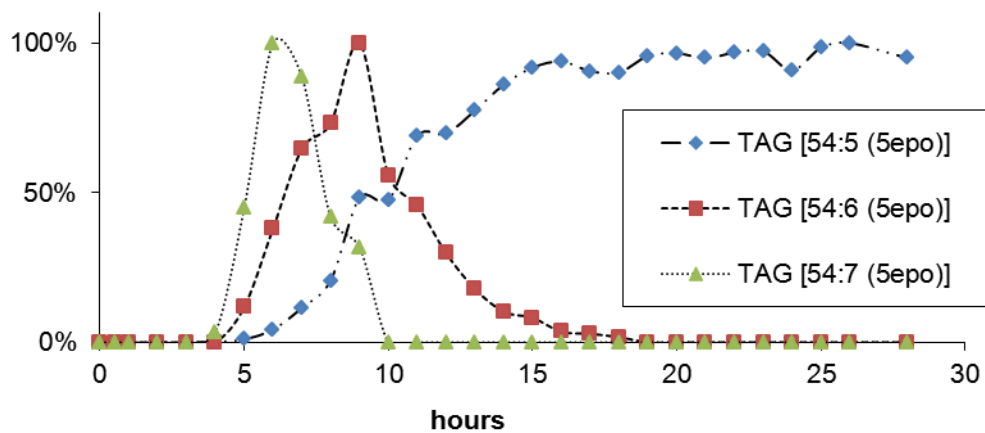


**FIG A5-6** The formation of 5-epoxy intermediates and product from TAG (54C) containing 5-7 double bonds (normalized).

APPENDIX 5

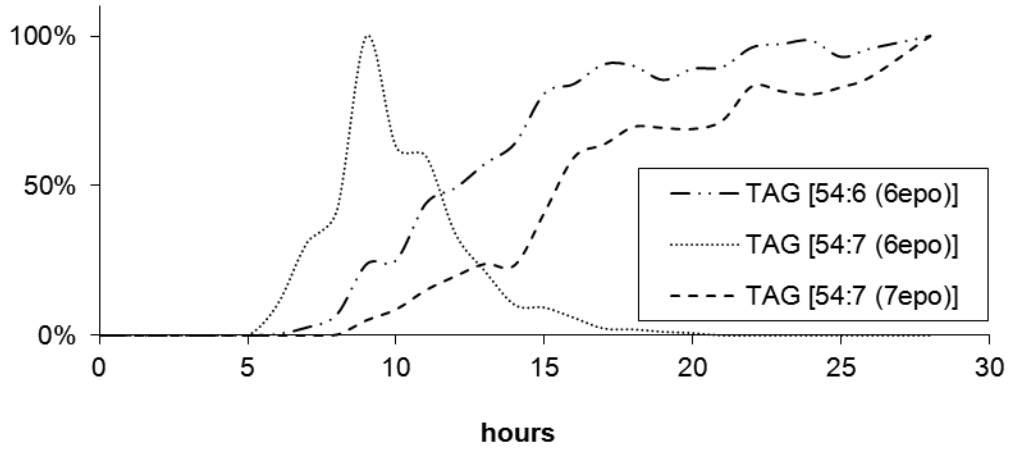


**FIG A5-7** The formation of 6-epoxy and 7-epoxy intermediate and products from TAG (54C) containing 6-7 double bonds (normalized).

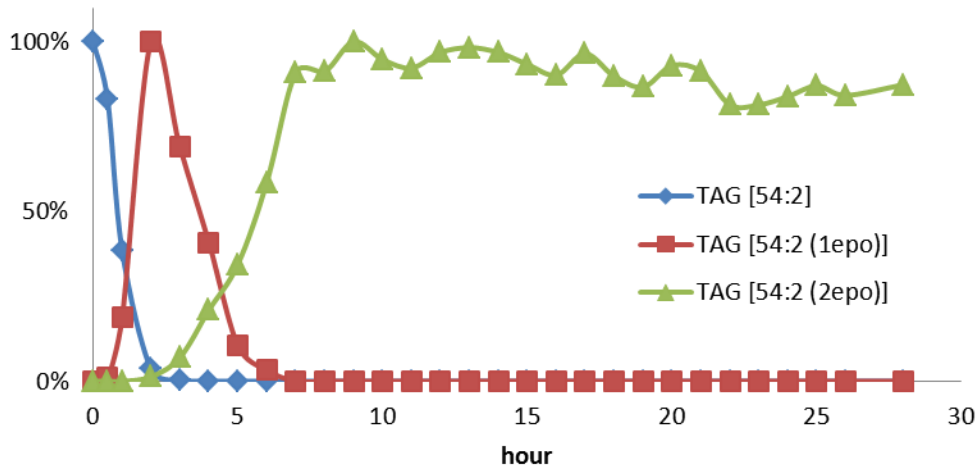


**FIG A5-8** The epoxidation of TAG [54:2] from canola oil plotted as a function of time (normalized intensities).

APPENDIX 5

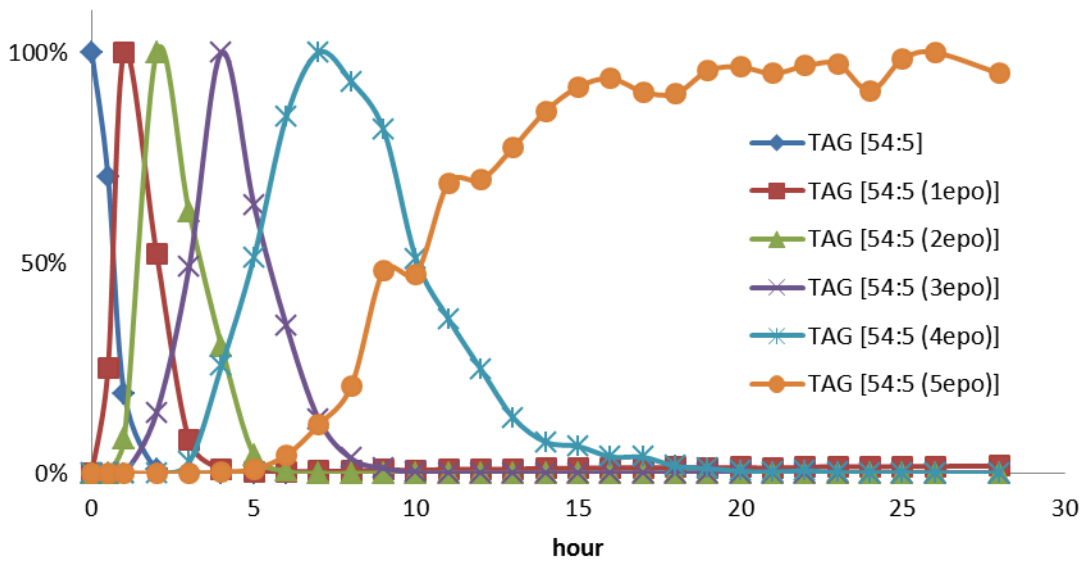


FIG A5-9 The epoxidation of TAG [54:5] from canola oil plotted as a function of time (normalized intensities).

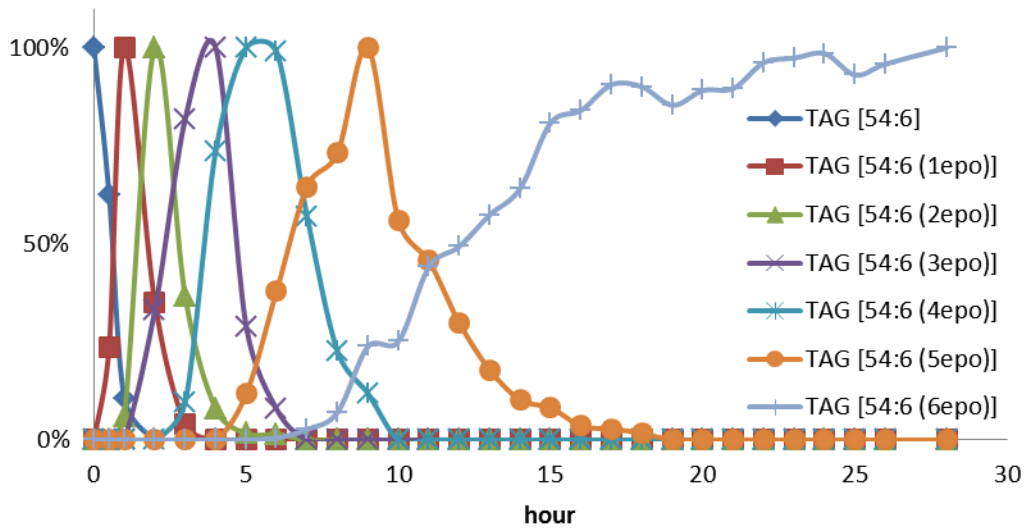


FIG A5-10 The epoxidation of TAG [54:6] from canola oil plotted as a function of time (normalized intensities).

APPENDIX 5

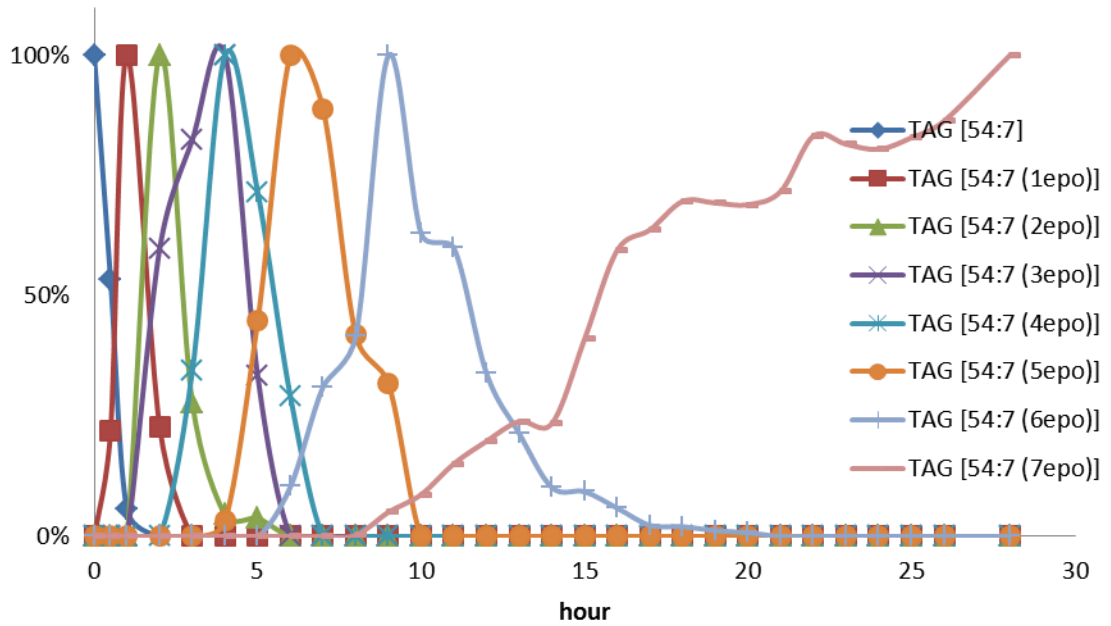


FIG A5-11 The epoxidation of TAG [54:7] form canola oil plotted as a function of time (normalized intensities).

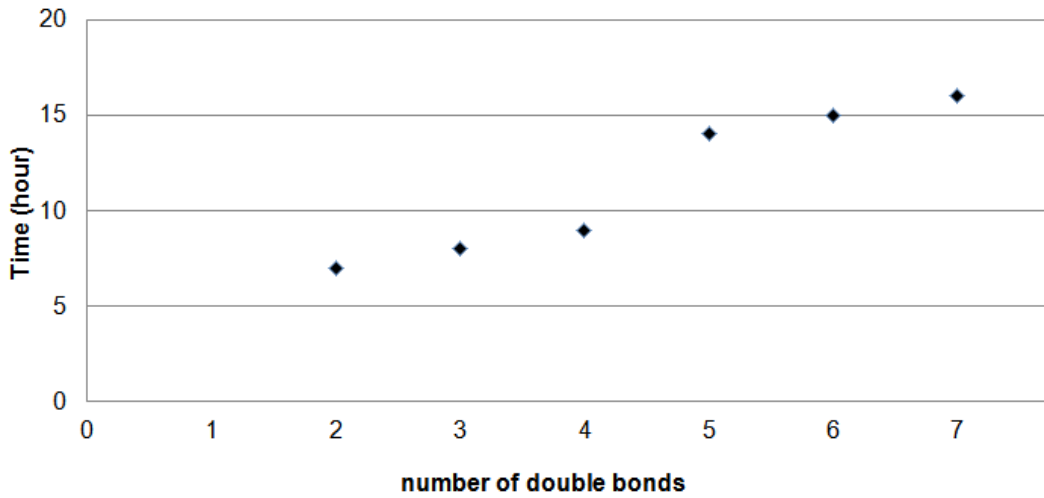


FIG A5-12 Time complete formation of epoxy (end product) for TAG (54C) containing 3-7 double bonds.